Fabrication of TiO$_2$ Nanoparticles by Microbial, Green and Hydrothermal Methods and their Possible Role in Developing Novel Restorative Material for Dental Caries

A thesis submitted in fulfillment of requirements for the degree
of
Doctor of Philosophy
in
Microbiology

By
Dr. Afsheen Qamar

Department of Microbiology

Faculty of Biological Sciences

Quaid-i-Azam University, Islamabad, Pakistan
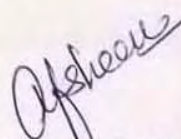
2023

بِسْمِ اللهِ الرَّحْمَنِ الرَّحِيمِ

DEDICATION

To my caring and loving Father, Mother and Husband and kids for their unhinged moral/ physical support and unfaltering trust in me, besides their affection, conviction and constant and encouragement and off-course my adorable kids, because without their support this project would not have been possible.

Author's Declaration

I **Ms. Afsheen Qamar** hereby state that my Ph.D. thesis titled **"Fabrication of TiO2 Nanoparticles by Microbial, Green and Hydrothermal Methods and their Possible Role in Developing Novel Restorative Material for Dental Caries"** is my own work and has not been submitted previously by me for taking any degree from Quaid-i-Azam University, Islamabad, Pakistan.

At any time if my statement is found to be incorrect even after I Graduate, the University has the right to withdraw my Ph.D. degree.

Ms. Afsheen Qamar
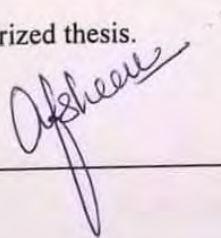Date: <u>11-08-2023</u>

Plagiarism Undertaking

"**Fabrication of TiO2 Nanoparticles by Microbial, Green and Hydrothermal Methods and their Possible Role in Developing Novel Restorative Material for Dental Caries**" is solely my research work with no significant contribution from any other person. Small contribution / help wherever taken has been duly acknowledged and that complete thesis has been written by me.

I understand the zero tolerance policy of the HEC and Quaid-i-Azam University towards plagiarism. Therefore I as an Author of the above titled thesis declare that no portion of my thesis has been plagiarized and any material used as reference is properly referred/cited.

I undertake that if I am found guilty of any formal plagiarism in the above titled thesis even after award of Ph.D degree and that HEC and the University has the right to publish my name on the HEC/University Website on which names of students are placed who submitted plagiarized thesis.
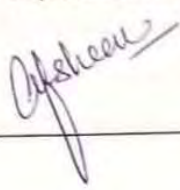
Student / Author Signature:_____

Name: **Ms. Afsheen Qamar**

Certificate of Approval

This is to certify that the research work presented in this thesis, entitled titled "Fabrication of TiO2 Nanoparticles by Microbial, Green and Hydrothermal Methods and their Possible Role in Developing Novel Restorative Material for Dental Caries" was conducted by **Ms. Afsheen Qamar** under the supervision of **Dr. Asif Jamal** and Co-supervision of **Dr. Shahab-ud-Din.** No part of this thesis has been submitted anywhere else for any other degree. This thesis is submitted to the Department of Microbiology, Quaid-i-Azam University, Islamabad in partial fulfillment of the requirements for the degree of Doctor of Philosophy in field of **Microbiology.**
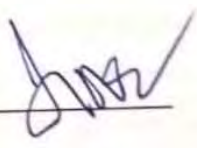
Student Name: **Ms. Afsheen Qamar**　　　　　Signature:_____

Examination Committee:

a) External Examiner 1:　　　　　　　　　　　Signature:_____

Dr. Allah Nawaz
House No. 667, Street No. 18,
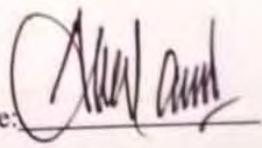Sector 1-8/2, Islamabad

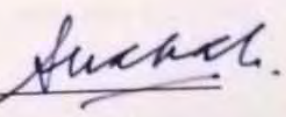b) External Examiner 2:　　　　　　　　　　　Signature:_____

Dr. Jehangir Arshad Khan
House No. 68, Street No. 51,
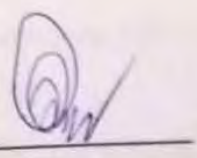Sector F-11/3, Islamabad.

Supervisor Name: **Dr. Asif Jamal**　　　　　Signature:_____

Co-Supervisor Name: **Dr. Shahab-ud-Din**　　Signature:_____
BDS, MSC, PhD,
SZABMU. SOD, Islamabad

Name of HOD: **Prof. Dr. Naeem Ali**　　　　Signature:_____

ACKNOWLEDGEMENTS

First and for most I am thankful to almighty Allah, my parents and family members who supported me whole heartedly in the completion of my PhD. program.

My greatest appreciation goes to my supervisor Dr. Asif Jamal for his unconditional availability, caring support, encouragement and his desire to share his knowledge at all times. His excellent insight into the subject has been a source of guidance where as his expert advises have shaped my academic development throughout my PhD studies. I could not find a better program director and mentor then Dr. Asif Jamal. I will always have my deepest gratitude for his willingness and unconditional help. His qualities are invaluable as a person and as a professional. This thesis would not have been possible without his endless support and effort.

It was a great privilege to have Dr Shahab Ud Din, Vice Principal from School of Dentistry, SZABMU as my co-supervisor because he always kept his door open for my questions, queries and concerns. His personal experience and advice gave me encouragement to continue in my process towards this PhD degree.

Thank you to Dr Yaqoob Khan, from Nanoparticles Department in National College of Physics, NCP and Dr Salman , Dr Masroor, Dr Nighat from Virology Department in National Institute of Health, NIH who has contributed into the project by providing me his constant support and taught me to handle and rectify mistakes and human errors.

A special gratitude goes to Dr Syed Mujtaba-Ul-Hassan from Department of Metallurgy and Materials Engineering, PIEAS and Dr. Bashir Ahmed from Department of Biotechnology, Islamic International University for extending his kind encouragement and extra time for the completion of my project.

Further, I would also like to thank Dr. Atta Ullah Shah and Dr. Uzma Asjid from Department of National Institute of Lasers and Optronics, Nilope for helping me in carrying out my preliminary experiments.

Special thanks to Dr Mazhar Mehmood, Director of Department of Metallurgy and Materials Engineering, PIEAS , Dr Yaqoob Khan from Nanoparticles Department in National College of

Table of Contents

List of Figures

List of Tables

List of Abbreviations

Serial	Name	Abbreviations
1.	Titania/Titanium oxide nanoparticles	TiO_2-Nps
2.	Nanoparticles	Nps
3.	X-Ray diffraction pattern spectroscopic analysis	XRD
4.	UV/VIS diffuse reflectance spectroscopic analysis	DRS
5.	Atomic force microscopic analysis	AFM
6.	Scanning electron microscopic analysis	SEM
7.	Dynamic light scattering spectroscopic analysis	DLS
8.	Energy dispersive x-ray analysis	EDX
9.	Fourier transmission infrared spectroscopic analysis	FTIR
10.	Band gap energy	Eg
11.	Glass ionomer cement	GIC
12.	*Staphylococcus aureus*	*S. aureus*
13.	*Enterococcus fecalis*	*E. faecalis*
14.	*Enterococcus faecium*	*E. faecium*
15.	*Lactobacillus acidophilus*	*L. acidophilus*
16.	*Pseudomonas aeuroginosa*	*P. aeuroginosa*
17.	*Escherichia coli*	*E. coli*
18.	*Streptococcus mutans*	*S.mutans*
19.	*Candida albicans*	*C.albicans*
20.	Vicker's microhardness	VHN
21.	Standard Error	S.E
22.	Weight percentage	Wt%
23.	Nanometer	nm
24.	Millimeter	mm
25.	Titanium oxide induced glass ionomer cements	TiO_2GIC
26.	Atomic percentage	At%
27.	Resin modified glass ionomer cement	RMGIC
28.	Nicotinamide adenine dinucleotide dehydrogenase	NADH

29.	Reactive oxygen species	ROS
30.	Colony forming unit/millimeter	CFU/ml
31.	Deoxyribonucleic acid	DNA
32.	Transmission electron microscopic analysis	TEM
33.	Hydroxyethyl methacrylate	HEMA
34.	Field emission scanning electron microscopic analysis	FSEM
35.	High resolution scanning electron microscopic analysis	HR-SEM
36.	Hydroxyl radicals	OH^-
37.	Hydrogen peroxide	H_2O_2
38.	Superoxide ions	O_2
39.	Mega pascals	Mpa
40.	Joint committee on powder diffraction standards	JCPDS
41.	Phosphate buffered saline	PBS
42.	Microgram/millilitre	ug/ml
43.	Dimethyl sulfoxide	DMSO
44.	American type culture collection	ATCC
45.	Revolutions per minute	Rpm
46.	Titanyl hydroxide	$Ti(OH)_2$
47.	Milligram	mg
48.	Millilitre	ml
49.	Titanium tetrachloride	$TiCl_4$
50.	Titanium oxide	O-Ti-O
51.	Gram	gm
52.	Dulbeccos modified eagle's medium	DMEM
53.	Electron volt	Ev
54.	Standard deviation	S.D
55.	Significance value	P value
56.	Greater than	>
57.	Lesser than	<
58.	Carbon	C

59.	Oxygen	O
60.	Fluorine	F
61.	Aluminium	Al
62.	Silicone	Si
63.	Strontium	Sr
64.	Phosphorus	P
65.	Sulphur	S
66.	Titanium	Ti

Abstract:

Globally, dental caries has been increasing with the passage of time despite the recent technological advancements in the field of dentistry. Nanotechnology has created new opportunities for the development of innovative materials with desirable strength, longevity and better efficacy. The current study was designed to produce and characterize the titanium oxide nanoparticles (TiO_2Nps) using biological and hydrothermal methods. Furthermore, the prepared TiO_2Nps were evaluated for their antimicrobial activity and suitability in developing innovative glass ionomer cement (TiO_2GIC) for dental caries treatment.

During first phase, TiO_2Nps were synthesized via three routes including *Bacillus coagulans*, *Mentha spicata* and *Conventional hydrothermal heating*. The synthesis of Nps was carried out under different process temperatures based on material's sensitivity. The change in yellow color of *Bacillus coagulans* culture solution, green color of *Mentha spicata* leaf extract and black color of titanium tetrachloride solution in the flasks to white color confirmed the formation of TiO_2Nps. In the second phase, these TiO_2Nps were characterized for their size, shape, phase form, surface roughness, morphology, topography, elemental composition, band gap energy and functional groups by utilizing standard techniques such as X-ray diffraction analysis (XRD), Scanning electron microscopic analysis (SEM), Atomic force microscopic analysis (AFM), UV/Vis diffuse reflectance spectroscopic analysis (DRS), Energy dispersive x-ray spectroscopic analysis (EDS), Fourier transform infrared spectroscopic analysis (FTIR), Dynamic light spectroscopic analysis (DLS) and Raman spectroscopic analysis (Raman). The TiO_2Nps synthesized by *Bacillus coagulans* were found to have spherical shape with diameter of 21.84 nm size and showed 100% pure anatase phase with no impurity. The TiO_2Nps prepared by *Mentha spicata* depicted slightly irregular spherical shaped particles having a size of about 37.60 nm in diameter and showed100% pure anatase phase form with no impurity in elemental composition however, carbon dixide was detected as a trace impurity. On the other hand,TiO_2Nps fabricated by *Conventional hydrothermal heating* manifested particle size of about 52.28nm in diameter, 82% anatase and 18% rutile phase without any impurity in its elemental composition. Thenitro-compounds and carbon dioxide was observed in their functional groups as trace impurities.

The third phase antimicrobial activity of TiO_2Nps synthesized by all the three routes against *Escherichia coli* (ATCC®35218[TM]), *Lactobacillus acidophilus* (ATCC®314[TM]), *Enterococcus faecalis* (ATCC®29212[TM]), *Enterococcus faecium* (ATCC®51559[TM]), *Staphylococcus aureus* (ATCC®25923[TM]) *and Pseudomonas aeruginosa* (ATCC®27853[TM]) was determined with the help of agar disc diffusion test. The antimicrobial activity of *Bacillus coagulans* TiO_2Nps against *E. coli* (27 mm $\pm$ 0.70), *L .acidophilus* (26 mm $\pm$ 0.70), *E. faecalis* (26 mm $\pm$ 0.70)*, (ATCC®51559[TM]) (13 mm $\pm$ 1.58), *S. aureus* (21 mm $\pm$ 1.58) *and P. aeruginosa* (25 mm $\pm$ 0.70) was comparatively higher from the TiO_2Nps prepared by *Mentha spicata* and *Conventional hydrothermal heating* (*P-value*< 0.05). The fourth phase investigated the biocompatibility of TiO_2Nps synthesized by all the three routes via MTT assay. The *Bacillus coagulans* drived TiO_2Nps depicted highest level of biocompatibility against fibroblast cell lines at all of the serial dilutions (99.57%, 97.43%, 95.51% and 93.00%) in comparison to TiO_2Nps prepared by *Mentha spicata i.e.* (99.35%, 95.82,92.09% and 90.79%). In case of TiO_2Nps fabricated by *Conventional hydrothermal heating* displayed least biocompatibilty of 98.92%, 94.43%, 9188% and 87.15%, and found to be mildly cytotoxic (*P-value* < 0.05). The

fifth phase incorporated the most suitable and biocompatible TiO_2 Nps in the dental restorative material named glass ionomer cement in order to test its mechanical properties. The *Bacillus coagulans* TiO_2 Nps were comparatively biosafe, biocompatible and acceptable to be incorporated in conventional dental glass ionomer cement (GIC) in the percentages of 0%, 3%, 5%, 7% and 10% in order to generate an innovative TiO_2GIC dental restorative material. The different percentages of TiO_2GIC dental restorative material was tested for its mechanical strength properties such as micro-hardness, compressive strength, flexural strength, shear bond strength, and surface morphology.

The current study concluded that microbial synthesis was much better choice for making nanoparticles with better strength and antimicrobial properties. The 5% TiO_2GIC dental restorative material was not only found to be biosafe and biocompatible but possessed the maximum mechanical strength properties such as micro-hardness, compressive strength, flexural strength, shear bond strength (*P-value* < 0.05). Moreover, 5% TiO_2GIC dental restorative material revealed the minimum crack formation and porosity. The magnified strength displayed by this innovative restorative material would be capable of bearing the excessive masticatory stresses in the oral cavity without undergoing any distortion in order to escalate its longevity, extra-stability and ideal shelf life. Therefore, the incorporation of TiO_2NPs proved to be better candidate for developing the long lasting dental restorative materials to treat the dental caries and could be used for commercial preparations conveniently and more feasibly in the current era.

Key Words: *Bacillus coagulans*, Dental Caries, Glass Ionomer Cement (GIC), Restoration, Titania Nanoparticles (TiO_2 Nps).

Graphical Abstract:
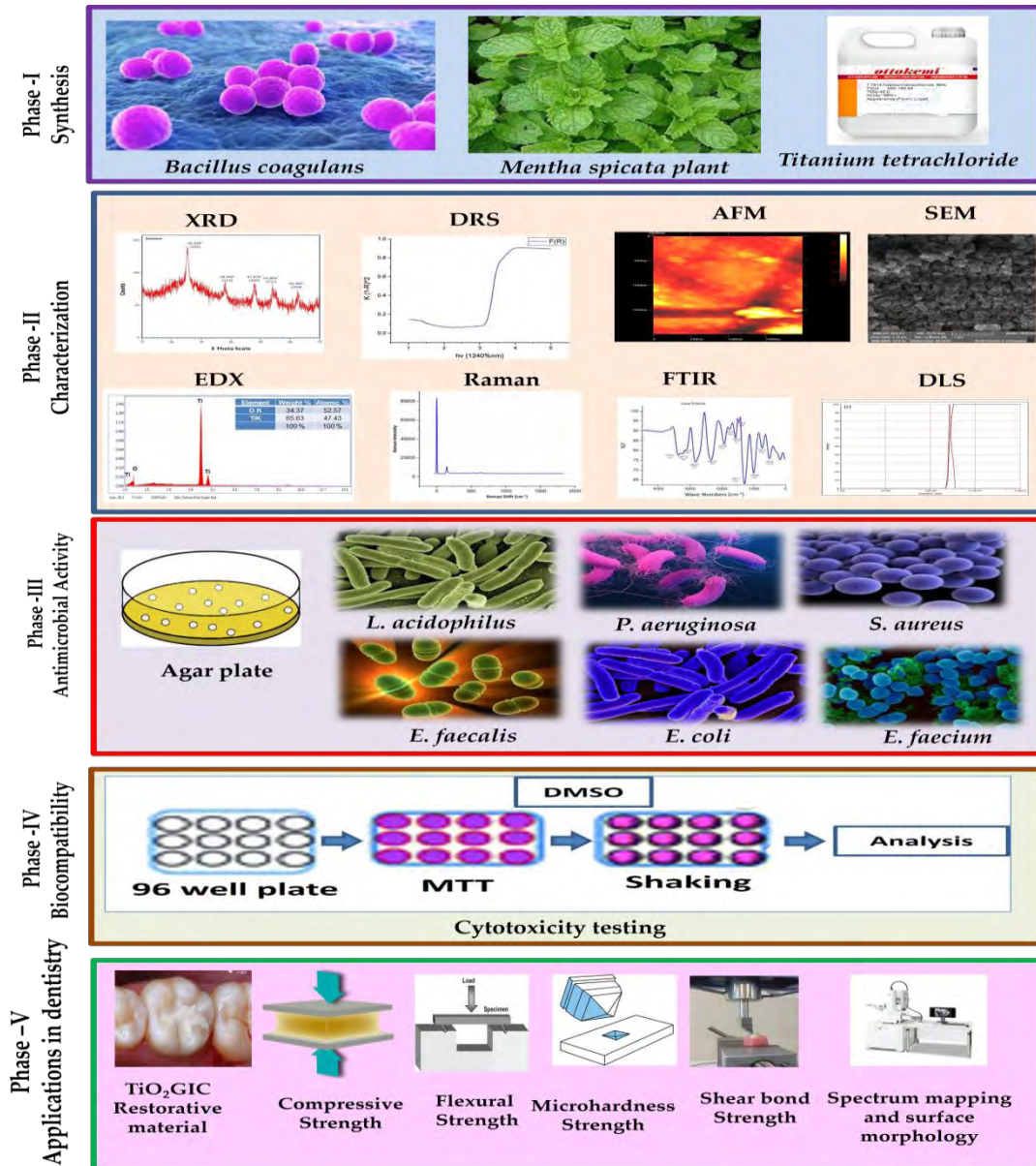
Publications:

1. Mansoor A, Mehmood M, Hassan SMU, Ali MI, Badshah M and Jamal A, 2023. Anti-bacterial effect of titanium-oxide nanoparticles and their application as alternative to antibiotics. Pak Vet J, 43(2): 269-275. http://dx.doi.org/10.29261/pakvetj/2023.039 (Published Impact factor: 2.3)

2. Mansoor, A.; Khurshid, Z.; Khan, M.T.; Mansoor, E.; Butt, F.A.; Jamal, A.; Palma, P.J. Medical and Dental Applications of Titania Nanoparticles: An Overview. *Nanomaterials* 2022, *12*, 3670. https://doi.org/10.3390/nano12203670(Published in Nanomaterials Impact factor: 5.07).

3. Mansoor A, Mehmood M, Ishtiaq M, Jamal A. Synthesis of TiO2 nanoparticles and demonstration of their antagonistic properties against selected dental caries promoting bacteria. Pak J Med Sci. 2023;39(5):---------. doi: https://doi.org/10.12669/pjms.39.5.7851 (Published on-line in Pakistan journal of medical sciences Impact factor: 2.34).

Chapter-1

Introduction:

The prevalence of dental caries has been increasing over the time despite recent technological advancements in the field of dentistry [1]. According to reliable statistics, 97.1 % of Pakistani population is affected by dental caries. The reasons behind this high incidence rate have been attributed to the poor health care system, low education status, non-availability of dental specialist in remote areas, cost of treatment and other socio-economic factors [2]. Dental caries is a multi-microbial disease subsequently, leads to the loss of tooth. Since years, restorative materials are commonly employed for treating carious teeth such as ceramics, amalgams, resin composites, and glass ionomer cements [3]. The glass ionomer cement is the most preferred restorative material because of its ability to release fluoride, good adhesion to tooth surface, acceptable aesthetic effects, biocompatibility and anti-microbial properties [4]. However, application of the glass ionomer cement (GIC) presents some technical limitations like compromised mechanical properties and moisture sensitivity posing a negative impact on overall quality of restorative material in terms of its stability, sustainability, longevity and shelf life [5]. Various attempts have been made to improve the mechanical properties of aforementioned materials to gain the desirable results; however, these formulations are associated with cytotoxic effects [6]. Another limitation is the high cost of additives which further restrict their applications besides being unsafe. Therefore, development of cost effective, non-toxic, biocompatible and mechanically improved restorative material is the need of the time. One of the important contemporary approaches to design such improved formulations is the addition of Nps in the parent material. It has been suggested that addition of metal oxide Nps could be very effective for enhancing the mechanical properties of the filling materials without leaving any negative effect. So far biologically produced Nps has not yet been characterized for their suitability and application in the glass ionomers cements. Keeping in view these limitations, current study was designed to develop cost effective glass ionomer cement restorative material having desired properties with the addition of biologically prepared Nps.

According to World Health Organization (WHO) dental caries is considered as a critical health issue for most of countries in world [7]. This is due to the fact that this disease has affected about 3.58 billion population around globe, irrespective of age, gender and culture. The data provided by WHO depicts that 60-90% children (486 million) and 35% adults around world are still suffering from dental caries disease [8]. Although, caries index has reduced in developed countries but it poses serious concerns in other countries, particularly Asia where incidence rate of dental caries is about 60-90% [9]. As previously stated, the onset of dental caries is highest in Pakistani population as compared to the other Asian countries because of various socio-economic problem including unavailability of dentists in the remote settings, low education status and less income [2]. Additional contributing factors responsible for causing dental caries includes unhygenic environment, poor eating habits, casual behavior, insufficient fluoride intake and oral hygiene [1]. The prevalence of dental caries globally has been displayed in Figure-1.1.
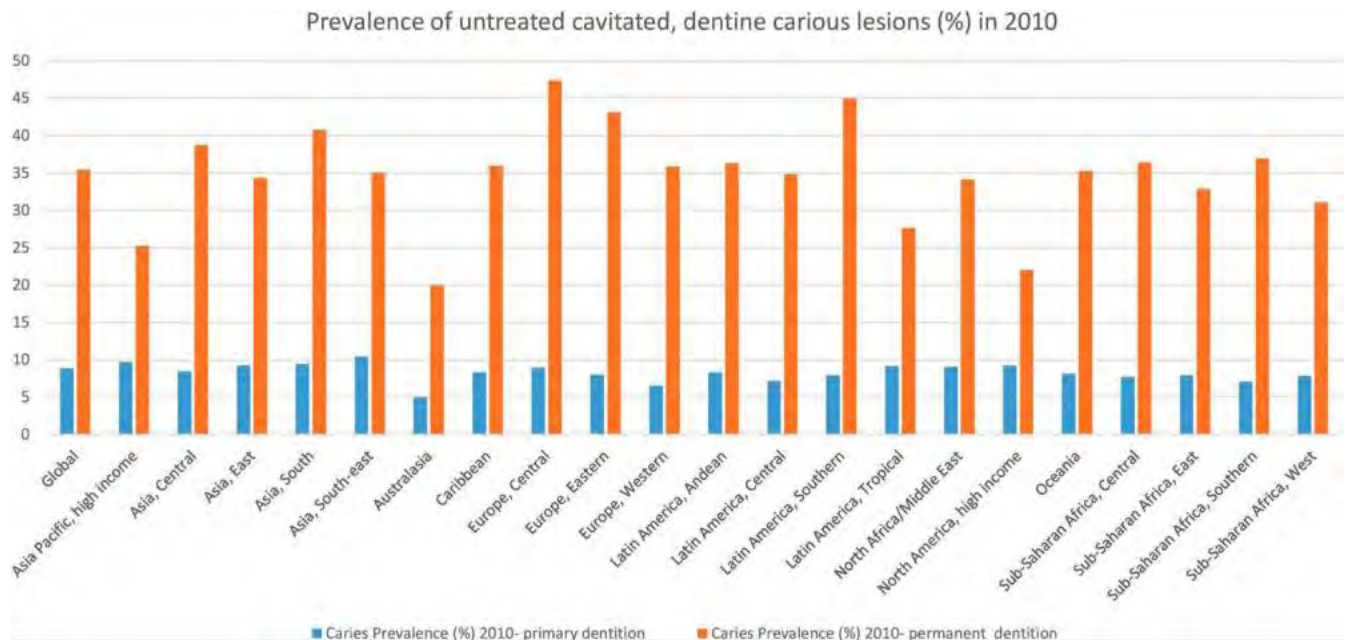
Figure-1.1: Prevalence of dental caries in different countries around the world [10]

Dental caries has been considered as a major disease of oral cavity having profound clinical significance. It develops by the transition of a healthy oral microbiome to acidogenic microbial community owing to multiplex intrinsic and extrinsic factors. The oral cavity contains a rich diversity of microbiomes including bacteria, fungi, protozoans and viruses. So far 700 microbial species have been identified from the human oral cavity. In functional perspectives, these microbiomes establish colonization on the tooth surface and oral mucosa in the form of biofilm, thereby, maintains a complex ecosystem with precise equilibrium. The onset of the disease is caused by the transition of oral microbiota towards more acidogenic microbial communities breaking the normal state of equilibrium. Various factors contribute in this transition such as poor oral hygiene which leads to the selective multiplication of pathogenic microorganisms in the oral cavity creating shift in the existing oral ecosystem. In addition, the dietary sugar intake provides competitive advantage to the pathogenic microorganisms to grow more rapidly and dominate the healthy microbial communities. As a consequence of greater sugar intake and increased population of acidogenic microorganisms in the oral cavity, the pH of the oral cavity turned acidic leaving a white spot on the tooth. Furthermore, insufficient amount of food, low fluoride and supplement intake deteriorate healthy oral microbiota by reducing the self-immunity resulting enhanced adhesion of these acidogenic communities on the surfaces of teeth in the form of biofilm. Consequently, this establishes dental caries with profound negative health effect. In technical terms, dental caries is a multi-microbial disease in which initial biofilm on tooth surface is formed by *Steptococcusmutans,* followed by dental caries initiation by variety of pathogenic caries promoting bacteria present in the oral cavity such as*Escherichia coli*, *Lactobacillus acidophilus* , *Enterococcus faecalis, Enterococcus faecium*, *Staphylococcus aureus and Pseudomonas aeruginosa* [8]. It has been reported that these species metabolize carbohydrates into organic acids through Embden-Meyerhof and related pathways causing onset of biofilm and dental caries as shown in Figure-1.2.
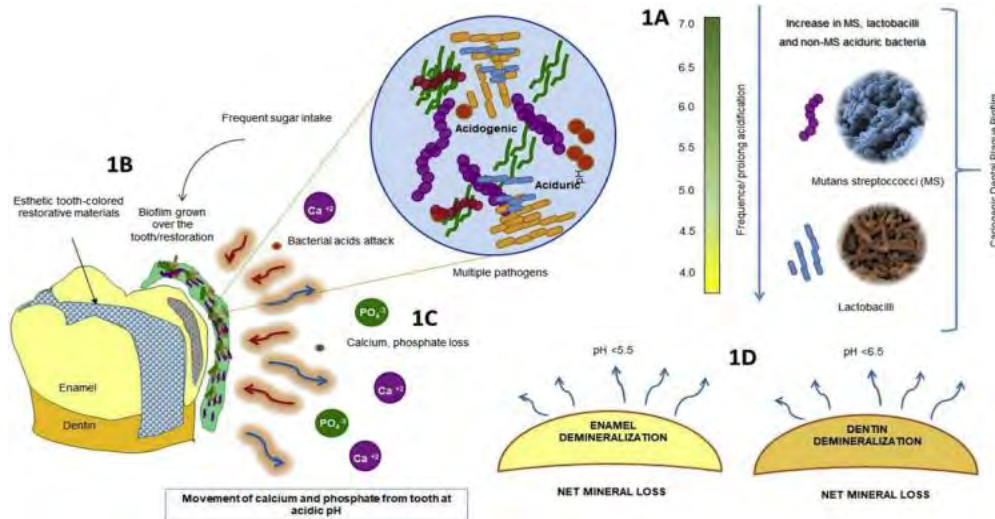
Figure-1.2: Pathways causing initiation of biofilm formation and dental caries [11]

Biofilm is a highly organized, dynamically co-ordinated and complex matrix of microbial communities established on the teeth surfaces embedded in extracellular polysaccharides (EPS) [12]. The dietary sucrose serves as substrate that facilitates biosynthesis of extracellular polysaccharides by selective oral microorganisms and help establishment of biofilm leading to diminishing the tooth structure.The tooth structure damaged by dental caries is irreversible and lead to deeper aspects resulting in loss of entire tooth. In order to prevent the entire tooth loss followed by dental caries, it is highly recommended to repair salvageable tooth structures with cost-effective, bio-compatible restorative dental materials having enhanced mechanical strength, longevity and shelf-life to sustain heavy masticatory loads in oral cavity. The initial attack of dental caries is on outermost acellular structure of tooth called enamel which can be easily repaired by restorative dental materials [8]

The only treatment of dental caries is restoration or filling of carious tooth after the removal of carious lesion from it in order to restore structure, function and aesthetics. Since years, some restorative materials commonly employed for treating carious teeth are ceramics, amalgams, resin composites, and glass ionomer cements [3]. The ceramic filling materials are not recommended any more due to lack of their aesthetics, physical, chemical and mechanical properties. The amalgam filling materials have lost their importance because of excessive tooth cutting, poor aesthetics and mercury toxicity [3,13]. The composite restorations are failed due to insufficient moisture control, poor isolation, poor proximal contact, insufficient tooth-preparation, highly sensitive nature, time-consuming and extremely expensive which hinders their usage [14]. The glass ionomer cement is the most preferred restorative material because of it's ability to release fluoride, good adhesion to tooth surface, acceptable aesthetic effects, biocompatibility and anti-microbial properties [15,16]. These desirable properties of GIC have been attributed to presence of ion leachable glass-powder and polymeric water soluble- acid in its formulation [5].

The major drawbacks of glass ionomer cement (GIC) on large scale are its extensively compromised mechanical properties and moisture sensitivity which poses a negative impact on quality of restorative material [5]. The mechanical properties of glass ionomer cement (GIC) that are adversely affected include toughness, wear-resistance, compressive - strength, fracture

strength, and tensile strength [14]. The use of glass ionomer cement filling material is greatly limited because it cannot sustain the masticatory pressures exerted by teeth in posterior regions of oral cavity [17]. There is an essential need to address these limitations of GIC in view of improving shelf-life, longevity, sustainability and durability of contemporary tooth restoring practices. Thus, glass ionomer cement can be effectively used for both short-term and long-term restorations in dental practice only and only if their mechanical strength and properties are enhanced [3]. In order to improve mechanical properties of glass ionomer cement, multiple fillers have been incorporated into it such as metals and non-reactive glass particles but still, achieving desired mechanical properties is a major challenge in field of dentistry [18]. Besides various claims, commercial modified forms of glass ionomer cements including glass carbomers and resin modified glass ionomer cements with improved properties have been introduced but they produced cytotoxic side-effects [6]. Thus, these filling materials are no more recommended and used in dentistry because of their non-biocompatibility.

Since start of this millennium, dendritic growth forms have been evidenced in fields of nanoscience and technology. The design principles and architecture of innovative nano materials such as carbon nanorods, nanospheres, nanotubes, and metal-Nps have changed traditional out-look of materials in science and nano-material based products and processes have started growing on rapid pace. The word ‚NANO' is derived from a greek-word ‚nano' meaning ‒dwarf" because it works at an atomic and molecular level where size range is between 1-100 nm [18]. In this epoch, nanotechnology has swiftly acquired significance in different areas of basic health care and biomedical sciences. Moreover, it involves diagnosis, treatment and prevention of dental diseases by relieving pain, preservation and improvement of dental health with nano-materials [19]. Recently, it has been discovered that Nps incorporating various elements can become the main feature that could enhance performance of restorative materials by providing promising results. The incorporation of Nps in materials have fascinatingly enhanced their certain properties such as optical, magnetic, physical, chemical, surface energy, biological and mechanical properties. Currently, metal oxide Nps have become focus of recent researches specifically in field of nano-technology, nano-science and material-sciences because of their ability to control morphology, size, shape, composition and structure of materials [20].

The Titania (TiO_2 Nps) has good biological reaction with human tissues, which is the sole reason for their utilization in medicine and dentistry with great success [21]. Additionally, these Nps are cost-effective and highly active against various pathogenic species responsible for oral diseases especially dental caries in teeth [8,22]. The Titania (TiO_2 Nps) are considered ideal for restorations in the oral cavity because of their compelling characteristics including: high electrical conductivity, chemical stability, low thermal conductivity, extremely white, increased malleability, and resistance against corrosion, scratches, wear, attrition's, fatigue, erosion, adfraction and abrasion [23]. These Nps have lower tendency of allergy and toxicity due to stability of alloy, restricted ion release and their effects [12,13,24].

Although, Titania (TiO_2 Nps) are least toxic but still they pose hazardous effects in nanometer-size [25]. The Titania (TiO_2 Nps) has been declared as suspicious possible carcinogenic compound that may be responsible for causing cancer [26]. The toxicity of these Nps depend on multiple factors such as route of synthesis, type of Nps, surface coating, aggregation, dissolution, interaction-mode with cells, hydrophobicity, ion-release by Nps, medium's pH,

route, concentration and time of exposure. Similarly, physical and chemical properties of Nps are also significantly responsible for inducing toxicity e.g: charge, shape, phase, size, band gap energy, surface morphology, texture, crystalline structure, elemental composition, functional groups and reducing agents during synthesis [27]. Recently, different attempts have been made to enhance mechanical strength of glass ionomer cements restorative materials by employing commercially available Titania (TiO_2 Nps). These Titania (TiO_2 Nps) may be non-biocompatible due to their size, composition, shape, phase, functional groups and route of synthesis [28,29]. However, researches done to-date have reported that size, shape, phase-form, and surface characteristics are principle parameters responsible for causing cytotoxicity in Nps [30,31].

The most significant characteristic that plays key role not only in estimating toxicity of Nps but also controlling all other properties are synthesis protocols of Nps. The most common methods used for production of Nps are conventional (physical, chemical) and biological (microbes, plants) methods. Previously, chemical methods involving toxic solvents were used for synthesis of Nps which offers limitations due to high temperature and pressure, costly nature, ecotoxicity, high-energy and environmental sustainability. Thus, synthesis of Nps by using chemical routes is not highly recommended. The latest innovations in biosynthesis of metal Nps point to new biotechnological procedures including natural biological resources such as algae, plants, bacteria, viruses and fungi both intracellularly as well as extracellularly [32,33].

The biological synthesis is considered as the most suitable choice for safe production of metallic Nps [34]. This is possible due to reason that these Nps are environmentally friendly, biocompatible, clean, and cost-effective [35]. In recent years, microorganisms are the most effective and eco-friendly nanofactories, with strong potential to control shape and size of Nps [36]. Thus, research has shifted from typical conventional synthesis methods to specific biogenic procedures, in which microorganisms can be easily used to synthesize these special Nps. There is a lack of available data on biogenic synthesis of metal oxide Nps [37]. The limitation of counterparty investigations is the availability of super fine dental restorative material with desirable properties. Therefore, finding a cost effective alternative for tooth problems has been a subject of current research in the area of dentistry. Current study was focused to develop a smart and innovative, glass ionomer cement restorative material with enhanced biocompatibility and antimicrobial activity to treat dental caries. The mechanical strength and properties of newly formulated glass ionomer cement restorative material were reinforced with Titania (TiO_2 Nps) and evaluated its suitability for possible use in future.

Aim:

The aim of the present study was to fabricate TiO_2 nanoparticles by microbial, green and electrochemical methods and their possible role in developing an innovative restorative material for dental caries.

Objectives:

The objectives of the current study were:-

1. Synthesis of Titania (TiO_2 Nps) by using *Bacillus coagulans*, *Mentha spicata* and *Conventional hydrothermal heating* methods.
2. Characterization of Titania (TiO_2 Nps) synthesized by *Bacillus coagulans*, *Mentha spicata* and *Conventional hydrothermal heating*.
3. Evaluation of antibacterial activity of Titania (TiO_2 Nps) synthesized via all these three routes.
4. In vitro evaluation of biocompatibility of Titania (TiO_2 Nps) synthesized by these three routes.
5. In vitro evaluation of mechanical properties of innovative TiO_2GIC restorative material at different percentages to be used as perfect restorative material in clinical dentistry.

Chapter-2

Background and Review of Literature:

Dental caries is one of the most important oral issues with profound clinical and health significance. It is a complex oral disease caused by various intrinsic and extrinsic factors specifically transformation of healthy oral microbiome and selective growth of pathogenic communities in the oral cavity. Current review will provide a comprehensive understanding of dental caries, its contributing factors, health effects, treatment options, recent advancement in the dental procedures and microbial and plant driven synthesis of Nps and use of nanotechnology in developing innovative restorative materials.

2.1. *Dental caries: A persistent global issue:*

The World Health Organization (WHO) reported that dental caries has been one of the most common oral dental diseases worldwide particularly in the developing countries. Despite significant improvements being carried out in public health sector, dental caries is still considered as a critical problem. Dated back in 5000 BC, prevalence of dental caries had been reported in the historical manuscripts as "Tooth worm". However, this myth was technically corrected by Pierre Fauchard who suggested that tooth decay is a main factor responsible for initiating dental caries and accumulation of several pathogenic bacteria in oral cavity [38]. Dental caries is a complicated oral disease with a very little understanding of its underlying mechanism [39]. The development of caries occurs in a series of complex processes which involves a) initiation of dental plaque biofilm formation b) reduction in pH of saliva and c) demineralization on surface of tooth's structure. Eventually, slow and gradual loss of tooth's enamel, dentine and cementum leading to sensitivity, pain, discomfort with entire tooth destruction [1]. The incidence of dental caries initiates in childhood and reaches its peak in the adulthood. According to the WHO, it is more dominant in low income countries as compared to high income countries which has been seriously increasing with the passage of time [8]. The incidence of caries is different in low income and high income countries have been revealed in the Figure-2.1.
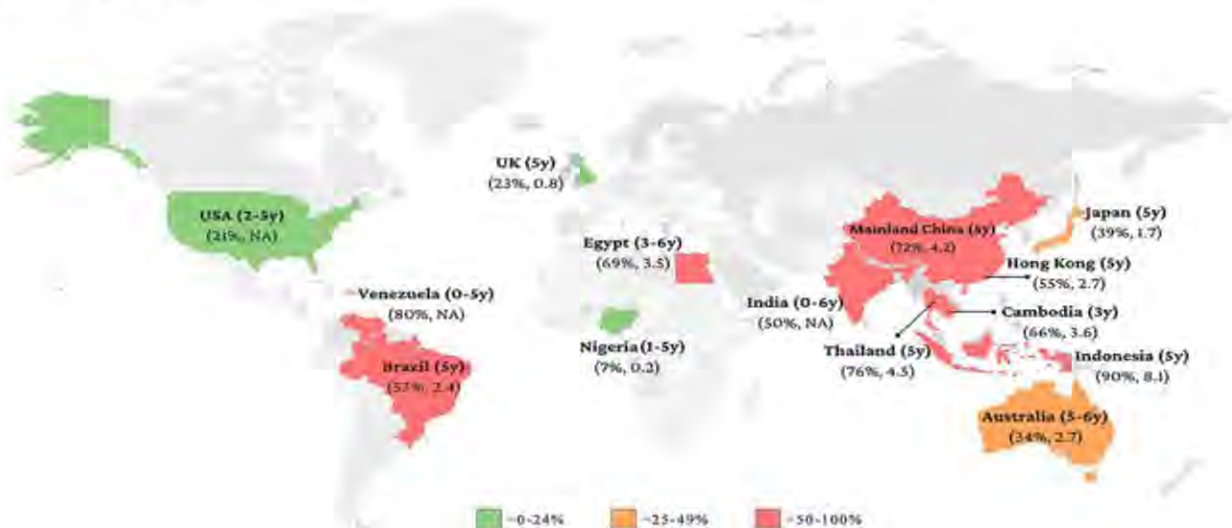
Figure-2.1: Incidence of dental caries in low income and high income countries [10].

2.1.1 *Source of cariogenic microorganisms:*

From mother to children, establishment of oral microbiome follows vertical transmission mode on birth and subsequently during feeding [40]. It has been witnessed that when microbial level in mother's saliva reaches 105 or more CFU/ml, rate of transmission of dental caries associated bacteria increase manifold in infants [41]. *Streptococcus* has been the main causative agent of forming the biofilm for caries initiation and is found in saliva of an individual including both adults and infants [42]. The microbiome of both adults and infants varies greatly and an imbalance between these microbes leads onset of the disease. Generally, the oral cavity of the infants contains *Granulicatella, Neisseria, Rothia, Veillonella, Hemophilus, Gemella, Rothia, Leptotrichia* and *Fusobacter.* However, in *adults Oribacter, Neisseria, Fusobacter, Haemophilus, Veillonella, Actinomycetes, Lactobacillus acidophilus, Staphylococcus aureus, Escherichia coli, Enterococcus faecalis, Enterococcus faecium, Staphylococcus aureus and Pseudomonas aeruginosa, Candida albicans, Rothia,* and *Trponema* species predominantly establish colonies in the oral cavity. The transformation from healthy microbiome to the onset of the disease has been associated with over dominance of the some pathogenic oral bacteria following their rapid multiplication and breaking the microbial community equilibrium in the oral cavity. Most commonly *L .acidophilus, S. aureus, E. coli, E. faecalis, E. faecium, S. aureus, P. aeruginosa,* and *C. albicans* areconsidered as the commonly caries promoting bacteria in the human oral cavity [8,43].

Oral cavity is composed of keratinized and non-keratinized stratified squamous epithelium on tongue, gingiva, periodontium, tooth's mucosa, hard and soft palate. These places constitute independent ecological niche that promote the development of unique microbial communities. This microbiome changes as the environment of oral cavity alters with aging process but still remain in stable state giving rise to microbial stability which is also referred as microbial homeostasis. There are certain factors that cause transient alterations in the stability of oral microbiome ecosystem such as dietary changes, temperature, salivary flow, salinity, long term antibiotics usage, pH conditions, redox potential, exposure to oxygen and nutrients affect the oral ecosystem resulting in accumulation of bacterial species that controls composition of biofilm [44,45].

2.1.2 *Correlation between microbial homeostasis and dental caries:*

The microbial homeostasis in the oral cavity controls the integrity of host defense. The direct relation between the oral environment and host defense is well established suggesting any participation may lead towards the onset of the disease. Various contributing factors play role in the changing healthy paradigm in which diet composition and salivary flow are considered determinant [46]. The sucrose and carbohydrates in the food promotes the rapid growth of microorganisms in the oral cavity particularly on the surfaces of teeth in the form of a oral biofilm. In addition to the dietary sugars, various factors of the saliva also contribute in the microbial attachment on the solid surfaces. These factors include lactoferrin, lysozyme, lactoperoxidase, stantine, mucin, immunoglobulin's and praline rich glycoproteins. The rapid microbial growth in the oral cavity, the balance between microorganisms and host defense is lost [47,48]. Furthermore, the pH of saliva drops as a result of increased number of acidogenic and acidophilic microorganisms on teeth's surface and deteriorate this situation. These microbes produce acids such as lactic-acid, formic-acid, acetic acid and propionic-acid. These

acids drop pH level of saliva below critical value of about 5.0-5.5 leading to demineralization of tooth's enamel structure followed by remineralization [49,50]. This demineralization and remineralization occurs in two phases: First phase of demineralization involves initial acid attack by bacteria, proteolytic destruction of tooth, loss of calcium phosphate and carbonate from enamel surface with formation of cavity and initiation of caries. During the second phase of remineralization, repair and recrystallization of tooth naturally by calcium, phosphate, proteins and fluoride present in saliva but to a lesser extent [50].

In the literature, two theories regarding dental caries has been proposed namely ―Specific plaque hypothesis" and ―Non-specific plaque hypothesis". The ―Specific plaque hypothesis" elaborates that only few microorganisms are responsible for dental caries which can be easily controlled by preventive measures. On the other hand, ―Non-specific plaque hypothesis" concludes that mixture of heterogeneous microorganisms play dominant role in development of caries. Eventually, the current dental caries hypothesis named as ―Ecological plaque hypothesis" has proposed that carbohydrate intake, low pH group of bacteria, *S.mutans*, *L .acidophilus, S. aureus, E. coli, E. faecalis, E. faecium, P. aeruginosa , C.albicans* play significant role in dental caries [8,51]. Dental caries in tooth's structure appear as white spot at initial stage which turns to black/brown spot at an advanced stage [52]. The microbial flora that establishes an acidic environment at different sites in oral cavity responsible for enhancing the chance of cariogenicity is illustrated in Table-2.1.

Table – 2.1 Microorganisms implicated in the human dental caries.

Groups	Microorganisms	References
Gram positive cocci	*Streptococcus mutans, Streptococcus mitis, Streptococcus salivarus, Streptococcus sanguis, Streptococcus intermedius, Streptococcus vestibularis, Staphylococcus aureus, Atopobium* spp, *Peptostreptococcus* spp, *Enterococcus fecalis.*	[53]
Gram positive rods	*Actinomyces odontolyticus, Actinomyces naeslundii, Actinomyces viscosus, Actinomyces israelii, Lactobacillus fermentum, Lactobacillus acidophillus, Bifiodobacterium dentium, Propionibacterium* spp.	[54]
Gram negative cocci	*Veillonella parvula, Nesseria* spp	[55]
Gram negative rods	*Bacteriodes denticola, Bacteriodes melaninogenicus,* *Fusobacterium necrophorum, Fusobacterium mortiferum, Escherishia coli, Klebsiella pneumoniae, Enterobacter aerogens, Citrobacter freundi, Pseudomonas fluorescence, Haemophilus* spp, *Prevotella* spp, *Leptotrichia* spp.	[56]
Yeasts	*Candida albicans, Candida tropicalis, Candida glabrata.*	[57]

2.1.3 *Dental plaque, quorum sensing and dental caries:*

Dental plaque is one of the first structures formed on tooth surface by bacteria commonly referred as biofilm. Biofilm has been defined as highly specialized, coordinated and well structured aggregation of microbial communities. In the oral cavity, particularity tooth surface, a complex polysaccharides matrix supports adhesion of microorganisms in the form of biofilm [58]. There are two patterns of biofilms produced by microorganisms on the tooth surfaces i.e supragingival plaque and sub gingival plaque. Former (supragingival plaque) is produced by gram positive bacteria including *Streptococcus species* predominantly *S. mutans,* that are involved in biofilm formation together with *Streptococcus gracillis,* and *Streptococcus salivarius* whereasdental caries initiates with the invasion of *L. acidophilus, E. coli, S. aureus, E. faecalis, E. faecium, P. aeruginosa,* and *C.albicans.* The later (sub gingival plaque) has been known to be produced by gram negative bacteria such as *Campylobacter, Actinobacillus, Porphyromonas gingivalis* and *Fusibacterium nucleatum.* It has been suggested that supragingival microbiomes are more likely related to dental caries and subgingival microbiota causes gingivitis and other periodontal diseases [8,59].

The development of biofilm has been carried out in three main steps; a) bacterial attachment to the enamel surfaces b) co-adhesion, colonization, production of extracellular polysaccharides and co-aggregation of other microorganism increasing biofilm biomass and c) detachment of bacteria from biofilm into the oral cavity resulting in dental caries [48]. Different forces such as Van-der Waals, electrostatic, and hydrophobic make the microorganisms adhere reversibly to each other during formation of biofilm. This accumulation of microorganisms in biofilm is very fast and quick eventually, leading to aggregation of new bacterial species with already colonized microorganisms [48,49]. Recent studies have indicated that establishment of the biofilm is based on the complex inter-species interactions and chemical communication between oral micro biome technically referred as quorum sensing. In this process microorganisms secretes diffusible signals ─autoinducers" which causes activation of the genetic switches by regulating the metabolic activity of cells in turn inducing the microbial film formation with elevated virulence.

The bacteria in the biofilm have the ability to communicate with each other and regulate metabolic processes. It has been reported that Quorum Sense (QS) signals represent signaling pathways activated in response to cell density and also regulates biofilm formation [60,61]. *Streptococcus* is a metabolically diverse bacteria having excellent adaptation profile in the host as compared to the other bacteria. Oral *Streptococcus* uses a small quorum sensing peptide pheromone as a stress-induced "alarm agent" to synchronize gene expression in specific cell populations, thereby coordinating important biological activities. [58]. Gram-positive bacteria produce heterogeneous group of short chain peptides molecules called as auto inducer peptides (AIPs), during quorum sensing. These peptides are ribosomal products which at the later stages of biosynthesis undergo post-translational modifications, thus attaining activation. These molecules are released via membrane associated ABC cassettes operated in an ATP dependent manor [62]

With the increase in bacterial population density, the auto inducer concentration also increases in the surrounding environment. After achieving a certain threshold level, the binding of oligopeptides to appropriate receptor in the bacterial membrane causing activation of receptor

kinase via phosphorylation of its histidine residue. In the next stages, phosphoryl group is transferred from receptor kinase to activate the response regulator molecule. As a result, activated response regulator regulates transcription of various target genes of the QS pathway. In *S. mutans, comepence stimulating peptides driven* quorum sensing (CSP-QS) system has been studied with relation to the involvement of *comCDE, comAB*, and *comX* andgenes. These genes are linked in a series. The precursor of the peptides are encoded by *comC* genewhich arefurnished and transported via ABC-transporter. The ABC membrane bounded transporter are product of *comAB* gene. In addition, *comDE* gene is also responsible to produce a two-component signal transduction system which initiate response upon recognition of competence stimulating peptides in *S. mutans*. Next in que, *Com*X encodes sigma factor for the regulation of various genes including autophosphorylation of ComE protein in collaboration with CSP and histidine kinase receptor encoded by ComD gene. Consequently, P-ComE activates *comCDE, comAB*, and *comX* genes and generate a positive feedback QS system. The classification of different QS systems is based upon their underlying mechanisms and genes involved. However, besides differences in various QS systems, the molecular machines of these systems follow same pattern of regulation specifically in establishment of biofilm. Figure 2.2 describes the QS system in *S. mutants* and its molecular switches during biofilm formation.
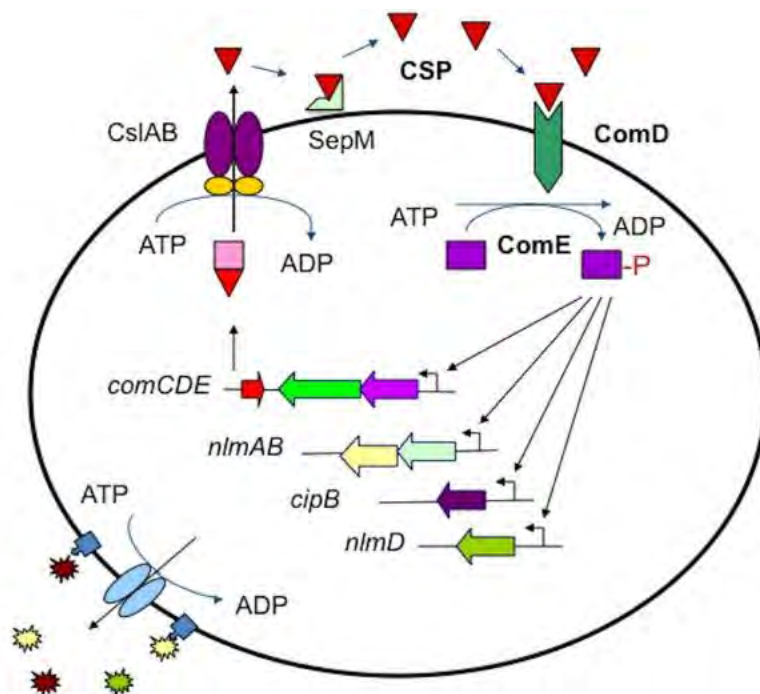
***Figure 2.2: QS system in the gram positive bacteria leading to the biofilm formation* [63].**

The microbial layer formation is a dynamic process where adhesion, growth, removal and reattachment occurs as a response of activation of QS system in the bacteria in the oral cavity. This biofilm flora may reach a thickness of 300-500 cells on the surface of human tooth. In addition, mature biofilm releases single cells in a row which joins together extending the biofilm to other parts of oral cavity. Dental plaque biofilms are potently strong enough to resist the antibiotic penetration into them in order to inhibit adverse effects of bacteria [64].

2.2. Contemporary approaches for the treatment of dental caries:

Human-civilizations have revealed that certain different materials including teeth, sea-shells, gold, wood, silver and bones were mostly used in an ancient era to replace and repair living natural tissues. Chinese used amalgam to repair lost tooth structures in 659.A.D [65]. The main reason for restoring the tooth cavity is to seal it and facilitate mechanical removal of dental plaque from restored tooth surface in order to prevent the further extension of dental caries [66]. The most common types of filling materials used until start of 20th century were zinc oxide eugenol, zinc phosphate and silicate-cement [67]. These restorative materials are utilized in dentistry since years but none of them reached the positive perfection due to lack of their performance properties [68]. Later on, conventional GIC filling material was introduced which was advanced by altering the concentration and ratio of powder-liquid used in its formulation but all the advanced forms produced certain adverse effects [1,69]. Still today, glass ionomer cement (GIC) is highly preferred filling material because it can retain most of the desired characteristics of filling materials required for treatment of dental caries. Therefore, this filling material has become a sensation in modern dentistry because of the possibility of various advancements that can be easily made into it [70]. The comparison among different filling materials are illustrated in Table-2.2

Table-2.2: Advantages and disadvantages of different conventional restorative materials.

Conventional Materials	Advantages	Disadvantages	Refrences
Amalgam	- Enhanced Durability. - Corrosion-resistant. - Easily manipulated. - Easily handled. - Bacterial leakage prevention. - Long shelf life. - Economical.	- Disruption of tooth structure. - Compromised aesthetics. - Allergic response. - Mercury toxicity. - Discoloration. - Microleakage.	[71]
Nickel or cobalt chrome alloys	- Resistance to decay. - Long term effectivity. - No fracture under stress - Needs minimum tooth removal. - Leakage resistance.	- Bad aesthetics. - Tissue irritation. - Tooth sensitivity. - Heat and cold conduction. - Expensive. - Toxicity.	[72]
Glass Ionomer	- Aesthetically perfect. - Fluoride release for caries	- Enhanced roughness. - Mechanical strength	[73]

	- prevention. - Minimum tooth removal. - Long-term durability. - Antimicrobial effects. - Cost-effectiveness. - Easy manipulation. - Both deciduous and permanent teeth.	- deduction. - Low antimicrobial properties. - Micro-leakage. - Surface wear. - Disintegration.	
Gold alloy	- Decay resistance. - Durability. - No fracture under stress. - Good fit. - Least tooth loss.	- Yellowish color. - Tooth sensitivity. - Highly expensive. - Micro-leakage.	[72]
Ceramics	- Excellent resistance to decay. - Resistant to surface wear. - Resistant to leakage.	- Weak material - Breaks easily - costly material. - Minimal tooth sensitivity.	[74]
Ceramic-fused metals	- Resistance to decay. - Durable. - No sensitivity of tooth. - Resists leakage.	- Excessive tooth removal. - Higher cost.	[64]
Resin ionomer	- Good aesthetics. - Prevents decay by releasing fluoride. - Minimum tooth removal. - Used for primary restoration of teeth. - Provide resistance against leakage. - Low rate of dental sensitivity.	- Very costly. - Wears fastly. - Enhanced toxicity.	[73]
Composite resin	Strongly durable.	Moderate tooth-sensitivity.	[74,75]

	• Tooth coloured. • Maximum tooth preservation. • No decay further. • Resistant to masticatory force.	• Most costly. • Time dependent shrinkage. • Temperature-sensitivity. • Micro-leakage over time. • Enhanced deterioration.	

2.2.1 *Glass ionomer cement (GIC) an ideal restorating material:*

2.2.1.1 *Composition:*

The GIC filling material is a mixture of glass powder and ionomer acid, which is a liquid. The composition of GIC powder and liquid ratio is listed in Table-2.3 [70].

Table-2.3: Ratio of basic powder and liquid in composition of general glass ionomer cement.

Powder			Liquid
Silica	-	41.9%	Polyacrylic acid (Itaconic acid,maleic acid) - 40- 55%
Alumina	-	28.6%	Tartaric acid - 6-15%
Aluminum fluoride	-	1.6%	Water - 30%
Calcium fluoride	-	15.7%	
Sodium fluoride	-	9.3%	
Aluminum phosphate	-	3.8	

2.2.1.2 *Structure and setting reaction of GlC restorative material:*

The main structure of conventional GIC is prepared by reaction between fluoro-aluminosilicate glass powder and aqueous solutions of polyacrylic-acid and/or other polyalkenyl-acids. The structure of GIC filling material is greatly affected by its setting reaction which in turn reduces the overall strength of this filling material. The factors responsible for affecting the structure of GIC filling includes acid-base reaction, water sorption, pH changes, too quick or too slow hardening, long storage duration and less water during mixing. The acid-base setting reaction takes place after mixing GIC powder and its acidic polymer liquid which decomposes the acidic polymer and sets GIC filling material quickly [17].

The setting reaction of GIC filling material undergoes three distinct phases: Stage-I, Stage-II and Stage-III. The decomposition of glass ionomer takes place in Stage-I in which polyacrylic acid impregnates GIC particles and tooth substrate. The acid neutralizes and precipitates both GIC particles and tooth substrate. As pH rises, poly acrylic acid ionizes and gets negatively

charged which sets up a diffusion gradient. This draws cations out of glass and tooth substrate resulting in dissociation of polymers along with increase in viscosity (Figure-2.3 a)TheStage-II is known as gelation and precipitation stage where pH increases and concentration of calcium, aluminium, and fluoride increases where insoluble poly acrylate precipitate resulting in formation of poly anions. These poly anions have carboxylate groups where cations bind them and form a gel matrix which sets in five minutes. The GIC absorbs moisture and the moistened chains gets degraded leading to loss of strength and mechanical properties. The GIC got dehydrated making the cracks appear in its structure followed by porosity. The Stage-III is referred as maturation stage which occurs after twenty four hours. The less stable calcium polyacrylate chains are replaced by aluminium polyacrylate which allows calcium to join fluoride and phosphate followed by diffusion in tooth. The presence of enough polysalts yields a physically stronger matrix and vice-versa (Figure-2.3 b) [76].
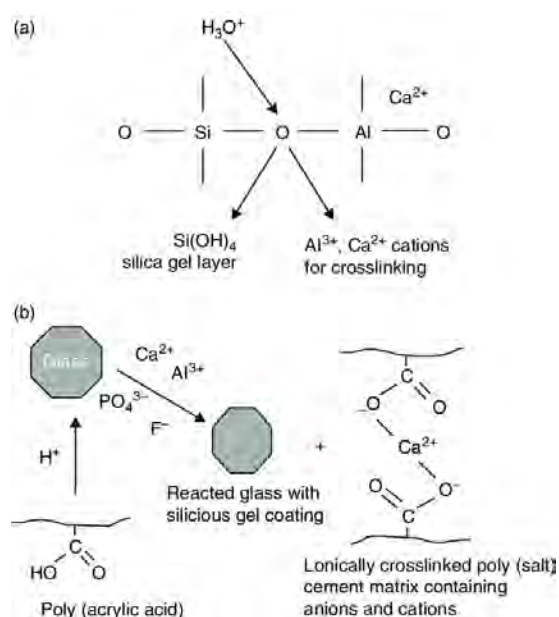
Figure-2.3: Setting reaction phases of GIC filling material showing: (a) acid degradation of alumino-silicate network, (b) setting reaction in GIC [77].

2.2.1.3 *Advantages of GIC restorative materials:*

The glass ionomer cements are potent dental materials clinically because they have certain special properties that make them suitable as restorative materials and important tool for preventing dental caries. The GIC restorative materials have additional qualities including biocompatibility, reduced toxicity, anti-cariogenic potency due to fluoride release, adhesion to moist tooth structure, compatibility with tooth enamel and long term sealing. Moreover, this filling is particularly advantageous in patients with high caries index as it prevents extension of dental caries which makes it a material of choice for restoration [78].

2.2.1.4 *Disadvantages of GIC restorative materials:*

There exists a chemical bond between GIC filling material and tooth structure due to presence of phosphate ion in tooth enamel and dentin which reacts with carboxylic acids in GIC. This chemical adhesion of GIC filling material can be strongly improved if different acids are used

as surface modifiers especially polycarboxylic acid, citric acid and phosphoric acid. These agents reduces the chemical adhesion of GiC filling material to tooth dentine by removing smear layer from its surface which is a drawback and needs attention. On the other hand, chemical adhesion of GIC filling material to tooth enamel is more stronger because of strong interaction of polycarboxylic acid and hydroxyapatite in tooth enamel which is an advantage [78]. The main disadvantage of GIC filling material includes its severely low mechanical strength and toughness. Previously, a study revealed that main causes of failed fillings in oral cavity are marginal as well as overall fracture. The basic mechanical standard properties that determine the quality of a filling material includes its fracture strength, elastic modulus, fracture toughness and surface-hardness. Additionally, flexural strength and compressive strength are considered as the most important parameters to test filling material's strength [79,80]. The compromised mechanical properties of GIC filling material is due to its moisture absorbing capacity in oral cavity which is a key drawback. This moisture absorption results in discoloration and decomposition of GIC filling material resulting in its deterioration in no time. The mechanical properties of GIC filling material must be enhanced in order to bear great stresses in oral cavity. There are certain qualities of GIC filling materials that make them an ideal materials in clinical dentistry but they pose severe limitations in terms of mechanical strength and properties to bear the masticatory loads in oral cavity without undergoing distortion [80].

2.2.1.5 *Modification of GIC filling material with resins:*

The HEMA and Bis-GMA are liquid resins potent enough to improve mechanical properties of GIC filling materials when added in small amounts. The hydrophilic resin monomer (HEMA) when added in GIC filling material produced resin modified glass ionomer cement (RMGIC) with certain enhanced mechanical properties [78].

The main drawback of this RMGIC filling material is its enhanced susceptibility to abrasive wear in oral cavity due to weak filler matrix coupling which reduces the stability and durability of this filling material. The biocompatibility of RMGIC filling material is significantly compromised after addition of HEMA monomer as it is released in different amounts from RMGIC filling material in first 24 hours making it cytotoxic [81]. The HEMA can absorb into human dentin producing cytotoxic effects to dental pulp cells [82]. There is a dire need of an ideal restorative material that should have multiple desired properties which includes aesthetics, anti-cariogenicity, biocompatibility, cost-effectiveness, bonding and adhesion [68,80].

2.3 *Epoch of nanotechnology:*

Nanotechnology has recently opened a new door for latest research which involves synthesis, characterization and manipulation of particle's structure one-dimensionally in nano-scale range of about 1-100 nanometers. The term ―nano‖ has been taken from greek language term ―Nanos‖, meaning ―dwarf‖ because it works at atomic and molecular level. Currently, nanotechnology has also gained popular status in health care systems quite rapidly because of its unique properties [83]. It is an emerging field utilized for diagnosis, treatment and prevention of oral dental diseases with certain nano structured materials [19].

2.3.1 *Factors affecting properties of Nps:*

The term "nanotechnology" was first used by Norio Taniguchi in 1974, although it had not been widely known [4,5]. Three main components had been considered essential for defining technology as nanotechnology [84].

1. The technology could change at the nano-scale dimensions.

2. The new fabricated structure must exhibit periodic repetition (ie, the nanoparticle should repeat itself periodically along one or more directions)

3. Although they are found in nano-scale dimensions their innovative characteristics, features and functions are nanometers, they should be similar to or better than the parent body.

The Nps depict advanced biological, physical and chemical properties as compared to their corresponding bulk materials from which they are fabricated. The huge diversity in size, shape, surface modification, morphology, chemical nature, dispersion state and dispersion medium of Nps from micro-scale to nano-scale has further enhanced their efficacy in diagnosis, treatment and prevention of diseases [4].

2.3.2 *Classification of the Nps:*

The Nps are generally classified into carbon based, organic and inorganic illustrated in Figure-2.4. The carbon base Nps are entirely made of carbon. The organic Nps are found to be non-toxic, biodegradable and ideal for drug delivery. The Nps that do not consume carbon during their synthesis are called inorganic Nps such as metal and metal oxide based Nps. The metal-oxide Nps have extraordinary properties e.g sizes (ranging between 10-100 nm), shapes (spherical, cylindrical etc) surface characteristics (pore size, high surface area to volume ratio, surface charge dentistry, surface charge), structures (crystalline, amorphous), color and sensitivity to various environmental factors (heat, air sunlight, moisture etc) [85].
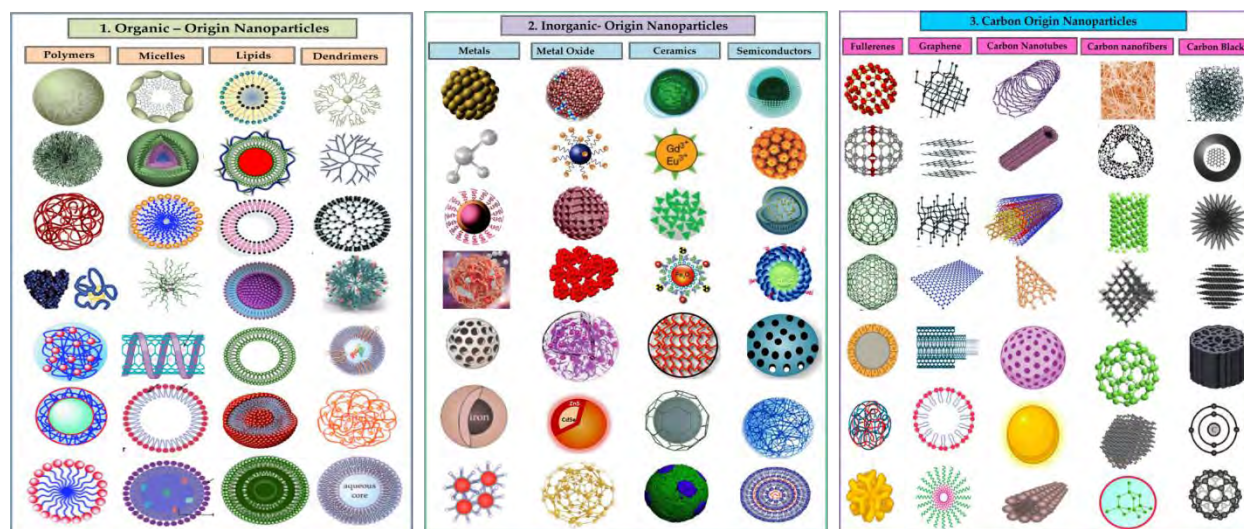
Figure-2.4: Classification of the Nps :(1) Organic-origin Nps, (2) Inorganic-origin Nps, (3) Carbon origin Nps.

2.3.3 *Nano-Titania or Titania (TiO₂ Nps):*

Nano-Titania or Titania (TiO$_2$ Nps) are Nps of metal oxides which exists mainly in powder or thin film form [21]. There are four crystal forms of Titania (TiO$_2$ Nps) which is depicted in Figure-2.5 [86]. Under normal conditions, Titania (TiO$_2$ Nps) are insoluble in water, and has a high refractive index of n=2.4 thus, making them absolutely extra white with enhanced properties [21].
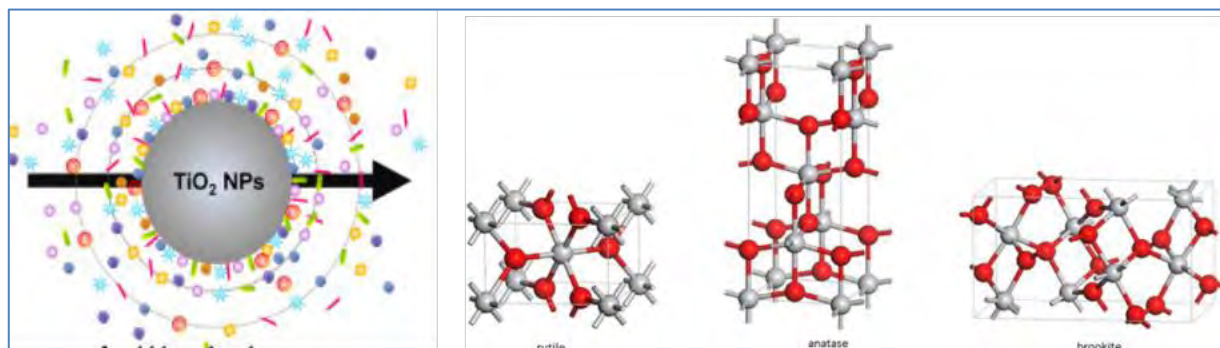
Figure-2.5: Different Crystal forms and phases of Titania (TiO₂ Nps).

Titanium has become material of choice as a result of its highly dominant biological [19], dental [14,59] and mechanical properties [59]. These Titania (TiO$_2$ Nps) are preferred due to low toxicity, fatigue resistance, low allergic potential, potent antimicrobial properties and above all biocompatibility. Moreover, Titania (TiO$_2$ Nps) are naturally occurring, non-expensive as compared to other metal-oxide Nps which are highly expensive and extensively toxic [87,88]. These Nps possess long-terms stability, durability and are powerful to great extent. The Titania (TiO$_2$ Nps) are light weight having low elastic modulus and enhanced strength [59]. The potently unique characteristics of Titania (TiO$_2$ Nps) include their corrosion resistance [59], highly active nature, physical and chemical stability, semi conductance and abrasion (Scratches) resistance. In addition, pure titanium can be bent in any shape because of its malleability which makes it a superior choice. These Nps have the capability to prevent attrition, abrasion, erosion, wear, tooth abrasion and galvanic pain in the tooth [18]. The Titania (TiO$_2$ Nps) are approved by ―American food and drug administration" (FDA) to be utilized in products related to food and drugs. The Titania (TiO$_2$ Nps) are commonly used in various dental appliances e.g: implants, mouth washes, implants, tooth pastes, sealers, orthodontic wires, crowns, bridges and endodontic instruments [89]. Thus, Titania (TiO$_2$ Nps) have been highly recommended and preferred to be used in dental restorations as they can withstand high level of mastication loads applied on the restorations in the oral cavity due to their enhanced strength [18].

2.3.3.1. *Phase-I: Synthesis protocols of the Titania (TiO₂ Nps):*

They are two common methods used for synthesis of Nps that are named as ni ―Top-Down method" and ―Bottom-Up method" [90]. The large bulk sized materials are converted to nano-sized particles in "Top-Down" method which includes common conventional methods such as physical and chemical methods. The main limitation of conventional methods involve origin of defects in surface, structure and morphology of new materials which adversely affects their

chemical and physical properties. The small sized particles like atoms or molecules are converted to nano-sized particles through redox reactions in "Bottom-Up" method which involves biological routes such as biogenic and green methods. These Nps are very stable, cost-effective and easily attained as a result of utilizing natural biological mediators such as proteins, enzymes, phytochemical etc [91]. The schematic presentation of different routes used for the synthesis of Nps are shown in Figure-2.6.
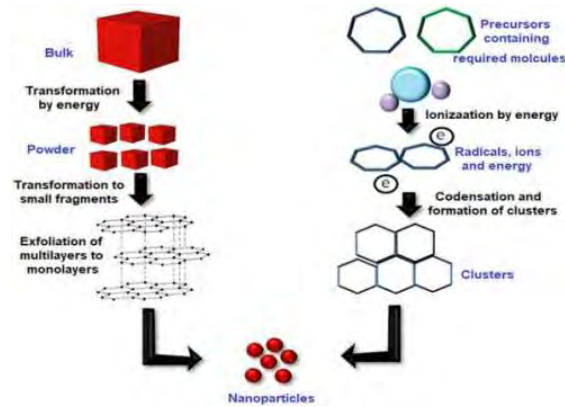
Figure 2.6: Schematic representation of protocol employed for synthesis of Nps [92].

(a) Conventional synthesis protocols of Titania (TiO₂ Nps):

The conventional methods for synthesis of Nps are widely used but these methods also offers limitations because of their high maintenance costs, expensive chemicals, high temperature, high pressure, ecotoxicity, high energy, environmental sustainability, time-consuming process and limited mass production. Currently, the main disadvantage of these Nps is their enhanced cytotoxic effects reported by researchers [33,93].

Furthermore, chemicals used in conventional methods pose damage to environment and eventually causing health hazards in humans reported by Boccaccini et al., in 2010 [94]. This is possible because chemicals increase complexity of reactions and produce impurities [95]. Different conventional methods along with their advantages and disadvantages are listed in Table-2.4.

Table-2.4: Advantages and disadvantages of different conventional methods of synthesis of Nps.

	Advantages	Disadvantages	Reference
Sol-gel method	• Excellent adhesion between substrate and top layer. • Protection against corrosion. • Sintering at low temperatures i.e 200-600°C. • Simple, economical and efficient. • High purity product.	•High Contraction occurs. •Residual hydroxyl and carbon groups are formed. •Long processing time. •Fine pores • Cytotoxity.	[96]
Gas condensation	• Production of ultrafine nanocrystalline metals and alloys.	• Need special devices. • Extremely slow.	[97]

Conventional hydrothermal method	• Substances formed are unstable near melting point. • High quality large crystals .	• Highly costly equipment. • Cytotoxity.	[98,99]
Laser ablation	• High-purity Nps production.	• Need special devices. • Difficult to control size, agglomeration, and crystal structure.	[100]
Chemical reduction	Cost-effective. Good production rate.	Application of toxic agents. • Hazardous by product formation. Cytotoxicity.	[101]

(b) Biological synthesis protocols of Titania (TiO$_2$-Nps):

Recently, environmentally friendly methods have gained more and more attention in production of Nps. These methods are referred as biogenic and green nanotechnology which is used to synthesize both metal and metal-oxide Nps. The microbial synthesis makes use of variety of bacteria, yeast, and fungi while plant utilizes roots, leaves, extracts and seeds [93].

(c) Differences between conventional and biological synthesis protocols for Nps:

There are reported adverse effects of conventional methods utilized in certain medical applications [102]. The biogenic and green synthesis protocols are extensively preferred because of their reliability, high yield production, eco-friendly and environmentally safe nature but above all their strong control over size, shape and morphology of newly formed Nps [33,102,103]. The comparative differences between biogenic, green and conventional synthesis of Nps are listed in Table-2.5 [102].

Table-2.5:*Comparative differences between biogenic, green and conventional synthesis of Nps.*

Properties	Conventional	Biological	Reference
Nature	• Expensive. • Toxic.	• Cost effective. • Nontoxic.	[91]
Reducing agents used	**Chemicals:** • Dimethylformamide, • N,N-dimethyformamide Ethylene glycol • Hydrazine hydrate • Sodium borohydride Polyol • Sodium citrate	**Biomolecules:** • Phenolics. • Polysaccharides • Flavones • TerpenoidS • Alkaloids • Proteins • Amino acids • Enzymes-nitrate reductase	[103]
Methodology	Chemical stabiliser (surfactant) is added.	No need to add a stabiliser (surfactant).	[104]

Environmental impact	• Environmental pollution • Energy-intensive	• Environmentally safe • No energy consumption	[103]
Antibacterial activity	Lower antimicrobial activity against pathogenic bacteria	Better antimicrobial activity against pathogenic bacteria	[104]
Stability	Not stable	Highly stable	[91]
Byproducts formation	Harmful by-products formed	No harmful byproducts formed	[91]
Biocompatible coating formation	No biocompatible coating is formed	Biocompatible coating formed on surface of Nps providing an additional effective surface area for interaction in biological environment	[91]
Process	Non-economical	Economical	[91]

(d) Factors controlling the biological synthesis protocols of Nps:

There are multiple factors that control synthesis, characterization and applications of Nps which involve total synthesis time, environmental conditions, temperature, synthesis protocols, solution's pH, concentration of extracts and concentration of raw materials. The factors contributing in biogenic and green synthesis are demonstrated in Figure-2.7 [102,105].
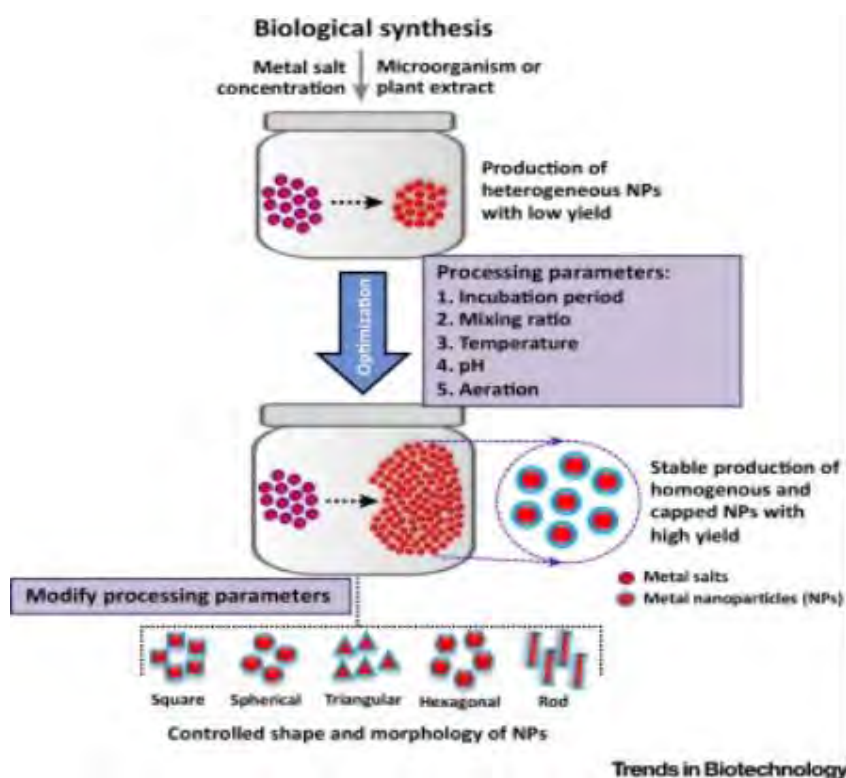
Figure-2.7: Factors controlling biogenic and green synthesis protocols of Nps [102,105].

(i) Solution's medium pH:

The pH of solution's medium used during synthesis of biogenic and green plays an essential role in affecting their size, shape, surface and texture. Previously, significant effect of pH on size and shape of silver (Ag) Nps has been reported by researchers [102,105].

(ii) Temperature:

Temperature of medium is also an essential parameter controlling the synthesis of Nps where highest temperature (>350°C) is required by physical methods and temperature (below 350°C) is used by chemical methods while ambient temperature (below 100°C) is used during biogenic and green synthesis [102,105].

(iii) Pressure:

The pressure enforced on reaction medium has strong influence on size and shape of biogenic and green Nps. The reduction rate of metal ions is more fast at ambient pressure due to usage of natural biological agents in biogenic and green synthesis is an additional advantage [102,105].

(iv) Time:

The incubation time period of reaction medium strongly influences the type and quality of biogenic and green synthesis of Nps. Additionally, light-exposure, synthesis-process and storage-conditions positively affects the characteristics of Nps. The long term storage of these Nps result in particle aggregation in turn enhancing their potency and shelf life without any adverse effects [102,105].

(v) Melting point:

The melting point of reaction medium during synthesis plays a key role in influencing the properties of Nps especially their shape and size. The low melting point of reaction medium indicates the conversion of Nps in range of nanometer scale. The stable Nps are formed quite easily who display different configuration and similar energy levels. These properties in turn adversely affect their numerous chemical properties [102,105].

(vi) Environment:

The characteristics of Nps are greatly influenced by surrounding environment as well. The biogenic Nps are thicker and large in size due to formation of coating around them due to oxidation or reduction reactions in their environment. These environmental reactions might be responsible for developing potent characteristics of Nps. In a study, zinc-sulphide Nps changed their crystalline-nature instantly with change in environment from wet to dry. In another study, cerium-nitrate Nps changed their chemical properties when peroxide was used in their suspension-medium [102,105].

(e) Mechanisms of biological synthesis or biosynthesis of Nps:

The mechanism behind biogenic and green synthesis of Nps has so far been seldom studied. Similarly, Garneson et al., reported in a study that microorganisms or plants consumed in

biogenic and green synthesis of Titania (TiO_2 Nps) being in-expensive are easily and readily available, grown easily and safely operated [106]. The microorganisms are easily available from air, soil, food crops and water while, plants are taken from soil in different seasons. Thus, phytochemicals produced by plants and enzymes or proteins secreted by microorganisms lead to production of relatively high quality of Nps [107].

(i) Proposed mechanisms of bacteria-derived biogenic synthesis of Nps:

Bacteria synthesizes Nps either by extra-cellular methods or intra-cellular methods. The extra-cellular methodology constitutes of enzyme secretion, bio-reduction and capping of Nps where nitrate-reductase is well known for playing the key role in synthesis. The intra-cellular methodology comprises of trapping, bio-reduction and capping of Nps through ion-transportation, electrostatic interactions between metal ions and microbial cells for synthesizing Nps [108]. The recommended method for synthesis of Nps is extra-cellular due its convenient and cheap availability, easy purification and down-streaming as well as less time-consuming protocols as compared to intra-cellular synthesis as shown in the Figure-2.8 [18].
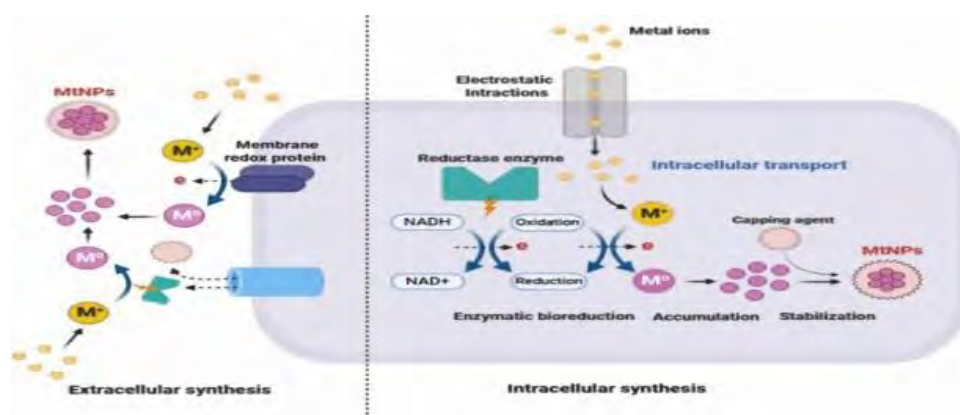
Figure-2.8: Extracellular and intracellular synthesis of Nps [20].

The bacteria is considered as momentous candidates for synthesis of metallic Nps as a result of their higher capability of reducing metal ions, high growth rate, flexibility, cost-effectiveness, large-scale production, biocompatibility, easy manipulation, culturing and handling properties [109,110]. This is due to reason that bacteria have developed certain defense mechanisms including extracellular precipitation, intra-cellular sequestration, metal ion concentration changes and efflux pumps which enhance their efficiency for synthesis [111]. Additionally, they have adopted certain activities of complex formation, dissimilar oxidation, precipitations as well as reduction of metal ions so as to combat the metal toxicity on large scale [111]. The NADH- dependent nitrate reductases solely play a notable role in bio-reduction of metal ions to produce metallic Nps due to their capability of transferring electrons to and / or from metal ions. This enzyme transfer allows only one electron from NADH to metal atoms for oxidation or reduction purpose. Bacteria synthesize Titania (TiO_2 Nps) in two different steps: In first step, metal ions are captured inside bacteria or outside on its surface while in second step, enzymatic action reduces the arrested TiO_2 metallic ions into metal Nps through NADH (nicotinamide adenine di-nucleotide). The metal ions in solution enter inside bacteria and break into titanium anions (Ti^{2-}) and titanium cations (Ti^{2+}). The release of electron ($\bar{e}$) from NADH occurs by reduction and it becomes NAD. This electron ($\bar{e}$) is taken by titanium cations (Ti^{2+})

inside bacteria as it gets electron deficient. The titanium cations (Ti^{2+}) is reduced to neutral titanium ions (Ti^0) which then accepts electrons resulting in formation of Titania (TiO_2 Nps). This occurs through Nucleation, Growth, Stabilization and Capping. (i) Nucleation is process of initial growth where nuclei act as templates for crystal growth. (ii) Growth involves spontaneous combination of larger and smaller particles through Ostwald ripening process or aggregation. (iii) Stabilization is the process where capping agents such as proteins, functional groups and enzymes forms a stable outer layer on Titania (TiO_2 Nps) surfaces. (iv) Capping of Titania (TiO_2 Nps) gives them stability in this step [112]. The schematic representation of the mechanism used for the synthesis of Nps is illustrated in the Figure -2.9.
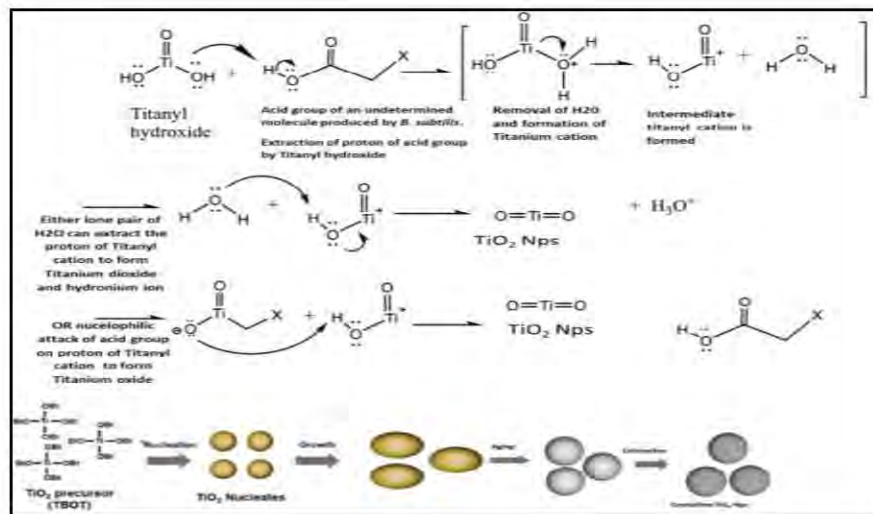
Figure-2.9: Mechanism of synthesis of Titania (TiO_2 Nps)using bacteria adapted from He and co-workers [112].

The chemical reaction elaborating the synthesis of Titania (TiO_2 Nps) is shown in the Figure-2.10.
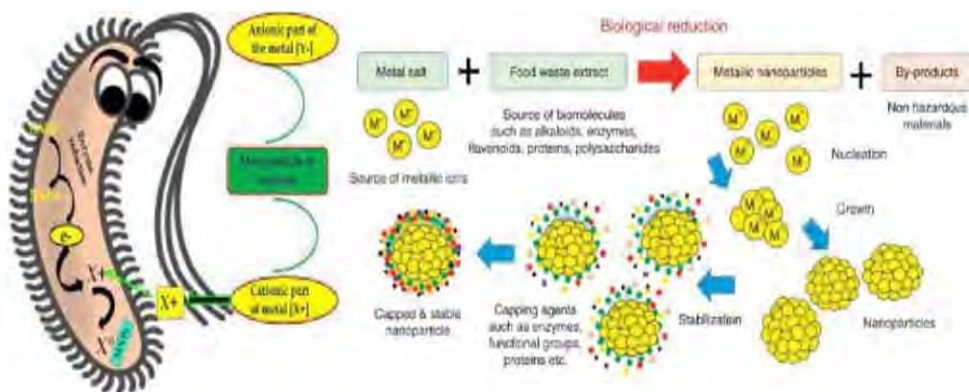
Figure-2.10: Chemical reaction depicting the synthesis of Titania (TiO_2 Nps).

Various previous studies revealed that use of bacteria in synthesis of metal Nps has attracted widespread attention because of its easy culturing and manipulation [91]. This biogenic route

involving microbes is cheap, eco-friendly, simple, fast, with antibacterial activity and anti-biofilm formation [113]. Furthermore, it is easy and highly reproducible as it does not require expensive chemicals, high temperature and pressure. This biogenic synthesis technique is simple with significantly enhanced multiple advantages [114]. This biogenic synthesis of Titania (TiO$_2$.Nps) from different microbes is listed in table-2.6.

Table 2.6: Titania (TiO$_2$.Nps) synthesized from different microbial species.

S.no	Bacterial species	Shape	Size (nm)	Characterization	Ref
1.	*Bacillussubtilis*	Spherical	11-32nm	SEM, TEM	[115]
2.	*Lactobacillus sp.*	Spherical	~ 24.6 nm	SEM, TEM	[116]
3.	*Propionibacterium jensenii*	Spherical	15–80	FSEM	[117]
4.	*Aeromonashydrophilia*	Spherical	28-54	XRD, and SEM	[118]
5.	*Bacillus subtilis*	Spherical	10–30	FTIR, UV, XRD and SEM, TEM.	[119]

(ii) Proposed mechanisms of plant-derived biological synthesis of Nps:

Different plant species exhibit different mechanisms when synthesizing Nps. The reduction ability of plants as well as reduction potential of ions play key role in production of Nps which further depends on type and quantity of biomolecules present in plants. The mechanism of fabrication of metallic oxide Nps by plants and their extracts is more complex as well as not fully understood. It is observed that generally, three phases are involved in synthesis of metallic Nps from plants. The activation phase involves bio-reducing metallic salts and ions by phytochemicals present in plant extract. The nucleation of already reduced metallic ions takes place in this phase. The growth phase comprises of spontaneous combining of larger and smaller Nps. The Ostwald ripening process is responsible for this purpose. The termination phase incorporates final shaping of metallic Nps. The newly formed Nps attain thermodynamic stability. This phase is strongly influenced by ability of plant extracts to stabilize metal Nps. The mechanism of green synthesis is displayed in Figure-*2.11* [120].

These three phases greatly affect characteristics of newly formed Nps such as increased duration of growth phase results in aggregation of Nps with irregular shape. The high surface energy exhibited by Nps make them less stable. The possible mechanism of bioreduction by titanyl hydroxide was investigated by Nasrollahzadeh and Sajadi illustrated in *Figure- 2.11* [121]. They confirmed that hydroxyl group of phenolic substances present in root extract of E. Heteradena Jaub has reduced Ti(OH)$_2$ to Titania (TiO$_2$.Nps). There is close interaction of phytochemicals with its relevant sites because polyphenols may be adsorbed on surface of Nps, during green synthesis. The bimolecular components such as polyphenols, flavonoids, terpenes, alkaloids, polysaccharides and heterocyclic compounds play an important role in reducing, capping, stabilizing, and preventing aggregation of highly mono-dispersed Nps. These biomolecules can coat Nps efficiently thereby, inducing strong synergistic effects in

biomedical applications [122]. The schematic diagram revealing the synthesis of Nps with the help of plants is given in the *Figure-2.11.*
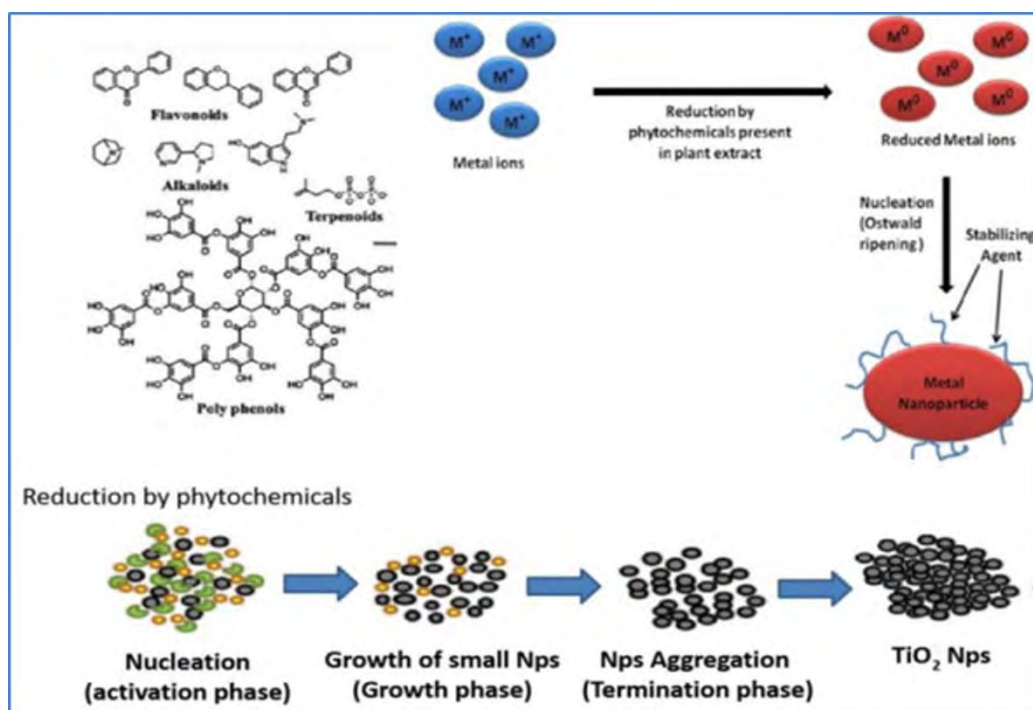
Figure-2.11: Mechanisms for the synthesis of Titania (TiO₂-Nps by plants).

The possible chemical reaction for the synthesis of Titania (TiO$_2$-Nps) by plants is given in the *Figure-2.12.*
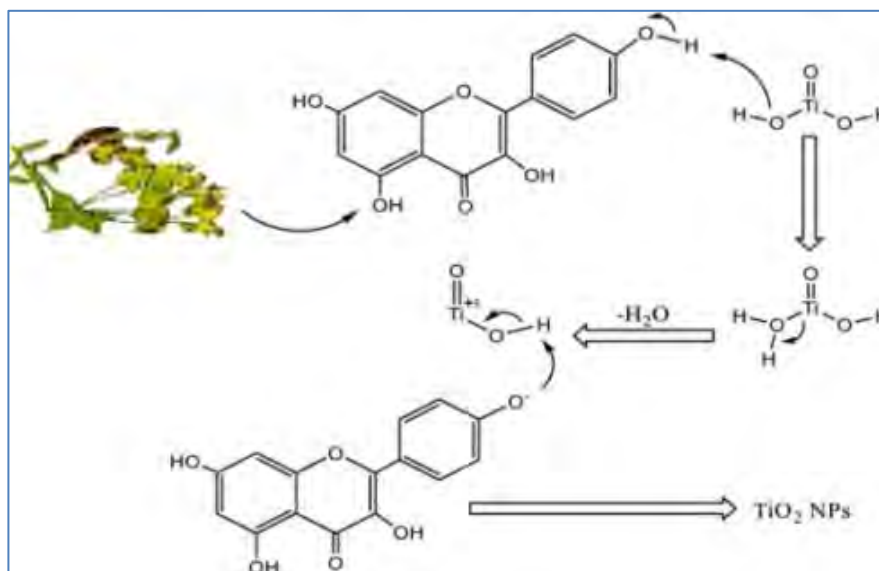
Figure-2.12: Possible chemical reaction mechanism of Titania (TiO₂-Nps) synthesis [121].

Previously, Titania (TiO$_2$-Nps) produced from leaf extract were elaborated as cheap, time-saving, environmentally friendly and simple. Therefore, green synthesis of Titania (TiO$_2$-Nps)

is considered as safe, eco-friendly, and energy-saving [123]. Many plants and their extracts have been used to synthesize various shapes of Titania (TiO$_2$ Nps) listed in *table-2.7.*

Table2.7: Titania (TiO$_2$ Nps) synthesized from different plants species.

Ser	Plant	Shape	Size(nm)	Characterization	Ref
1.	*Azadirachta indica leaves*	Spherical	25-87	FSEM	[124]
2.	*Psidium guajava leaves*	–	32.58	FSEM	[125]
3.	*Vitex negundo linn leaves*	Spherical	26-35	TEM	[126]
5.	*Orange peel extract*	Spherical	20-50	SEM	[127]
6.	*Trigonellafoenum-graecum* L.	Spherical	20–90	HR-SEM	[128]

They are four possible drawbacks with green synthesis utilizing plants which are as follows: Firstly: plant extracts are isolated from plants which are collected in different seasons from different geographical locations. This influences composition of plant extracts and alters its characteristics such as size, shape, morphology and properties of Nps. Secondly: leaf extract is rich source of metabolites such as, phenols, amides, flavones, ketones, carboxylic acids, sugars aldehydes, ascorbic acids and terpenoids. These components reduce metallic salts to metallic Nps. These phytochemicals work efficiently individually, additionally and synergistically. These phytochemicals are present in large amounts which makes these Nps poisonous [129].

Thirdly: The amino-acids i.e peptides cannot undergo complete bioreduction of metal ions to their metal Nps. This is due to two reasons: (i) Metal ions induces very strong chelation of peptides which inhibits their bio-reduction by reducing amino acids.(ii) Peptides weakly bind to metal ions due to proline, leucine & phenylalanine in their composition. These plant metabolites are not effective in reducing tetra-chloroauric acid anions, because they cannot retain metal ions close to reduction areas and sites. Metal ions are not reduced properly and desired yield couldn't be obtained. Fourthly: The amino acid sequence of proteins affect shape, size, morphology and number of newly-formed Nps. The C-terminal and N-terminal amino acid residues in peptide will slowly reduce metal ions to metal Nps thus, slowing down reduction reaction. The formation of large sized Nps adversely affects their characteristics and total yield ultimately [130]. These might be responsible for producing cytotoxic effects in plants.

2.3.3.2. *Phase-II: Standard Characterization techniques of Titania (TiO$_2$ Nps):*

The characterization of Titania (TiO$_2$ Nps) is carried out by different characterization techniques atomic-force microscopic analysis, UV/VIS Diffuse reflectance spectroscopic analysis , scanning electron microscopic analysis, elemental composition analysis, x-ray diffraction spectroscopic analysis, dynamic light scattering analysis and fourier transform infrared spectroscopic analysis. These techniques are used to depict size, shape, texture, phase form, structure, surface morphology, surface roughness, chemical composition, functional groups and compounds [131].

2.3.3.3 Phase-III: Antimicrobial activity of Titania (TiO$_2$ Nps):

The Titania (TiO$_2$ Nps)have shown potent antimicrobial, antifungal, antiviral and antiparasitic activities. This may be possible due to their better efficacy and negligible side-effects [132]. The Titania (TiO$_2$ Nps) have demonstrated antimicrobial activity against pathogenic micro-organisms responsible for causing dental caries [26]. The Titania (TiO$_2$ Nps) have displayed significant antimicrobial activity against both gram-negative as well as gram-positive bacteria [133]. The cell walls of both Gram-positive and Gram-negative bacteria have negative charge whereas metal Nps have positive charge on them. It is speculated that this feature affects interaction between bacterial cell wall and Nps or ions released from them. Thus, this interaction between negative (bacterial cell wall) charge and positive (metal Nps) charge facilitate entrance of released ions from metal Nps into bacterial cells resulting in destruction of pathogenic bacteria [16].

The mechanisms responsible for exhibiting antibacterial activity in Nps is (i) destroying the integrity of bacterial cell membranes, (ii) inducing oxidative stress through free radical formation , (iii) mutagenesis, (iv) Protein and DNA damage, (v) inhibition of DNA replication by binding to DNA, and (vi) respiratory chain damage . The Titania (TiO$_2$ Nps) mainly trigger production of reactive oxygen species (ROS) against pathogenic microbial cells and eventually kills them [91,134]. The mechanism adopted by the Nps for the antimicrobial activity is given in *Figure -2.13*.
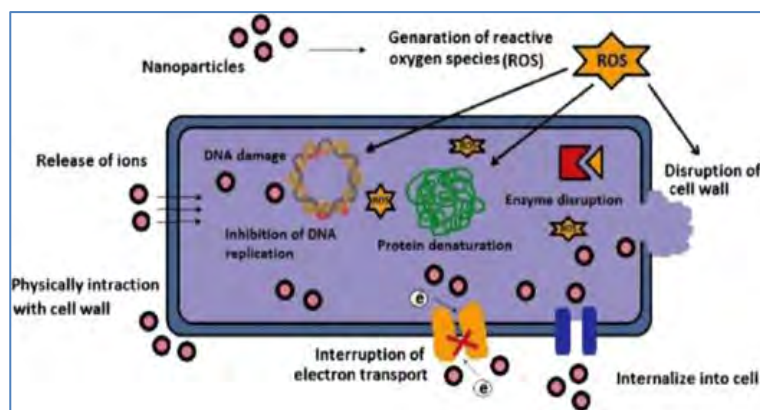
Figure-2.13: Mechanism showing the antimicrobial activity of the Titania (TiO$_2$ Nps) [134]

Both biologically and conventionally synthesized Titania (TiO$_2$ Nps) kill microorganisms but better antibacterial activity is perceived by biologically synthesized Nps. Their excellent antibacterial potential is attributed to capping agent provided by microbes and/or plant extracts. Moreover, microbially synthesizedTitania (TiO$_2$ Nps) have potent anti-microbial activity as compared to plants. This is possiblebecause of significant differences in chemical composition of same plants collected from habitats in different regions thereby, producing differences in results [135]. The anti-microbial activity of metal oxide Titania (TiO$_2$ Nps) against different pathogens is listed in *Ttable-2.8*.

Table-2.8: Antimicrobial activity of Titania (TiO$_2$ Nps) against various pathogens.

Target Organisms	Size (nm)	Shape and phase	Reference
S.pneumonia, S. aureus, B.subtilis, P.vulgaris, E. coli, P.aerugonisa, C.albicans	6nm, 25.8nm,33nm	Spherical Anatase, Rutile, mixed Anatase-Rutile	[136]
E. coli	10-25	Spherical Anatase	[137]
F. coli	10-25	Spherical Anatase	[138]
P. aeruginosa	10-25	Spherical Anatase	[139]
Fusobacterium nucleatum	10–70	Spherical Anatase	[136]
Bacillus subtilis	10-25	Spherical Anatase	[138]
Aquatic Biofilm	11-32nm	Spherical Anatase	[115]
S. aureus, E. coli	~ 24.6 nm	Spherical Anatase-rutile	[116]
S. aureus, E. coli	15–80	Spherical Anatase-rutile	[117]
S. aureus, S. pyogenes	28-54	Spherical Anatase	[118]
P. aeruginosa	10–30	Spherical Anatase	[119]
S.typhi, E. coli, K. pneumoniae	25-87	Spherical Anatase-rutile	[124]
S. aureus, E. coli	32.58	Spherical Anatase-rutile	[125]
S. aureus, E. coli	26-35	Spherical Anatase	[126]
S. aureus, E. coli and P. aeruginosa	20-50	Spherical Anatase	[127]
S. aureus, B.subtilis, P.vulgaris, C.albicans, P.aerugonisa, E. coli, E. faecalis, S. facalis, Y. enterocolitica, K. pneumoniae	20–90	Spherical Anatase	[128]

(a) Factors Affecting the Anti-microbial Activity of Titania (TiO$_2$ Nps):

The multiple powerful activities of metal-oxide Nps are possible only because of their exceptional physical, biological and chemical properties [140]. The important properties contributing to enhanced anti-microbial activities include concentration, surface morphology [141], structure, shape, size and interaction pattern of Nps with surface of micro-organisms [91,134].

(i) Size & concentration:

The effects of size and concentration have been analyzed in many different types of metal-oxide Nps. The large-sized Titania (TiO$_2$ Nps) (particle size: 62-74 nm) reported maximum

antimicrobial activity as compared to small-sized nanoparticles (particle size: 21 nm) against pathogenic microorganisms [142].

(ii) Chemical composition:

The metal-oxide Nps show enhanced antimicrobial qualities because chemical composition is the basis for various activities. Therefore, titanium oxide, silicon oxide and zinc oxide Nps revealed 90% antimicrobial activity against various micro-organisms [143].

(iii) Shape:

The shape of metal oxide Nps also displayed great impact on antimicrobial activity as reported in a previous study [144].

(iv) Target microorganisms:

The metal-oxide Nps have shown significant anti-microbial activity against both gram-negative and gram-positive bacteria [145]. The zinc oxide Nps revealed strong anti-microbial activity against both gram positive and gram negative bacteria [143].

(v) Synthesis methodology:

The synthesis method**s** have great impact on anti-microbial activity of metal-oxide Nps. The biologically synthesized Nps have potent anti-microbial activity as compared to Nps synthesized by conventional methods that utilize toxic stabilizing agents during their synthesis, thereby rendering less antimicrobial activity [32,33].

(vi) Phase form:

The 100% pure anatase Titania (TiO_2 Nps)produced by various methods depicted better anti-microbial activity in comparison to the mixed antase-rutile phases and pure rutile phases. This is possible to the highly active and reactive nature of the anatase phase in comparison to the rutile phase which is more stable comparatively thus, reduces the antimicrobial activity [136].

2.3.3.4 Phase-IV: Biocompatibility of Titania (TiO_2 Nps):

The Nps can enter the body through four distinct routes such as: skin, lungs, oral cavity and gastrointestinal tract. The cells and tissues of these human organs maintain a continuous contact with external environment. The Nps can enter human body through ingestion, inhalation and skin. After entering the human body Nps pass through circulatory and lymphatic systems. Eventually these Nps reach distinct human organs and tissues where they are adsorbed e.g: brain, bone-marrow, spleen, heart, kidney, liver, kidney, and nervous system. Thus, poor absorption of Nps in these human organs contribute to reduced biocompatibility [146].

There is an urgent need to evaluate human health and environmental safety regarding use of Nps. The biocompatibility of commercial Nps including silica, titanium oxide, silver, chrysotile and carbon nanotubes have been studied where these Nps have shown cytotoxicity in different cell-lines. There is dire need to investigate the toxicity before utilizing them biomedical implications [147]. These Nps are toxic to human tissues and cell-culture, leading to inflammatory cytokine production, increased oxidative-stress, and cell-death. The Nps may

also cause DNA mutations which will induce major structural damage to mitochondria eventually, leading to cell death [148]. Certain different Nps with their purpose, advantages and toxic effects are listed in *Table-2.9.*

Table 2.9: Purposes, advantages and toxic side effects of different Nps.

Material name	Purpose of use	Advantage of this material	Toxic side effects	Reference
Carbon nanotubes	• Tooth-filling. • Tooth-coating.	• Large surface-area. • Active agent. • Easy tooth adherence.	• High reactivity. • Inflammation. • Fibrotic reactions. • Cross membrane barriers. • Toxic (size & shape based).	[149]
Graphene	• Teeth-coating. • Implantation. • Biofilm reduction.	• Cost-effectiveness. • Fracture-resistant. • Proper crystal lattice. • Treat bacterial biofilm.	• Toxic (shape & size based). • Oxidative stress. • Metallic impurities.	[150]
Hydroxyapatite (HAp)	• Reduce Hypersensitiviy. • Tooth-filling. • Retard auxiliary demineralization. • Repair enamel.	• Easy tooth integration. • Similar tooth & bone composition. • Biocompatible • Tooth enamel adsorption. • Enamel protective layer. • Periodontal reformation.	• Protein-particle complexes killed by macrophages in tissues. • Dispersion into lungs, spleen, and liver by blood. • Inflammatory responses. • Oxidative stress. • Signalling pathway damaged. • Severe toxicity .	[151]
Zirconia	• Reduced tooth-bacterial adhesion. • Anticariogenic. • Effective polishing agent.	• Similar mechanical properties • Aesthetics. • Low cytotoxicity. • Slightly biocompatible. • High fracture resistance.	• Substantial DNA damage in human T-cells. • Apoptosis. • Iinhibition of cell proliferation in various cell lines. • Cellular oxidative stress . • Cell death. • Cross physiological barriers and produce adverse effects.	[151]
Silica	• Tooth filling. • Tooth polishing. • Anticariogenic. • Antibacterial. • Prevent hypersensitivity.	• Slightly Biocompatible. • Low toxicity . • Low density. • Significant adsorption ability. • Cost-effectiveness. • Reduced tooth surface roughness .	• Toxicity (Entry route and physio-chemical characters dependent). • Silicosis. • Lung cancer. • Severe cytotoxicity. • Oxidative stress. • Apoptosis (size & dose dependent). • Several genotoxicity & immunotoxicity. • DNA damage. • Gene Irregulation. • Autophagy.	[152]
Silver	• Antimicrobial .	• Inhibit bacterial	• Cytotoxicity.	[153]

	• Restorative material. • Dental prosthetic. • Dental implant.	colonization. • Easy bacterial penetration . • Slightly biocompatible. • Long-term antibacterial activity.	• Argyria. • Excessive ROS . • Oxidative stress. • Genotoxicity. • Lysosomal AcP activation. • Actine disruption. • Hemocyte phagocytosis. • Na-K-ATPase inhibition.	
TiO$_2$ Nps	• Antimicrobial agent. • Restorative material. • Dental prosthetics. • Reduced tooth-bacterial adhesion . • Provide protection against dental caries. • Bleaching agents. • Dental implants. • Orthodontics.	• Long term effect on dental implant. • Surface modification. • Less bacterial adhesion. • Improved hardness strength. • Biocompatible. • Low-toxic effect. • Chemically stable. • Low density. • Cost-effective. • Strong antimicrobial activity . • Enhanced mechanical properties. • Extraordinary functionality. • Long term stability. • Durability. • Fatigue resistant. • High mechanical resistance. • Corrosion and wear resistance. • Low thermal conductivity. • High electrical conductivity. • Versatile & adaptable material due to its strength and lightness. • Large spectrum of activity against microorganisms including Gram-negative and Gram-positive bacteria and fungi. • Scratch & abrasion resistant.	• Toxicity depends on route of exposition method of synthesis & physicochemical characteristics. • Cause cancer. • Cytotoxic effects of different concentrations (1-20) mg/cm^2 after oral administration. • Allergic reactions. • Capturing & absorption of TiO2 from GIT into blood, different internal organs, and urine resulting in cytotoxicity.	[154, 155]

(i) Mechanism of toxicity of the Nps:

The diversity in physical and chemical parameters of metal-oxide nanoparticle play key role in developing toxicity which includes particle-size, shape, morphology, crystalline structures, phase form, surface area, routes of synthesis, element composition, functional compounds,

texture, surface-coating and functionalization. Similarly, different factors responsible for promoting toxicity of nanoparticle promote toxicity involve oxidative stress, inflammation, chemical reactions, genetic damage which leads to inhibition of cell-division followed by cell-death [30,31]. The reactive oxygen species (ROS) and free radicals produced during oxidative stress is associated with cytotoxicity of metal-oxide nanoparticle. Subsequently, this causes damage to proteins, membranes and DNA of cells. Previously, various researches reported cytotoxic effects of Titania (TiO_2-Nps) by overproduction of reactive oxygen species (ROS) (such as O^{2-} (superoxide anion), OH (hydroxyl radical) and H_2O_2 (non-radical hydrogen peroxide)) with increased protein, lipid, and DNA peroxidation leading to cell death [156].

(ii) Properties of Nps causing toxicity:

There is strong direct relationship between physical and chemical properties of nanoparticles and cytoxicity. The dominant properties responsible for causing cytotoxicity are size, shape, structure, surface morphology, texture, surface roughness, phase form, chemical composition, synthesis protocols, dose, concentration, crystalline structure, functional compound, surface coating, functionalization and aggregation [157,158].

(a) Dose-dependent toxicity:

 The dose of Nps is directly related to cytotoxicity of these Nps. The genotoxic and cytotoxic effects of mixed anatase-rutile phased Titania (TiO_2-Nps)were reported with the increase in dose concentrations [159]. Previously, a study revealed cytotoxic effects of Titania (TiO_2-Nps)when exposed to large-sized Nps (80-110 nm diameter) at different doses [160].

(b) Size-dependent toxicity:

Size has been considered as one of the most important parameter responsible for inducing toxic effects. There exists a strong direct co-rrelation between Titania (TiO_2-Nps)size and level of DNA damage [157,158]. A study conducted by Savi. et. al. confirmed the severe toxic effects of large sized Titania (TiO_2-Nps) ($\leq$ 50nm) when administered in single low dose (2mg/kg) [161]. In another study, Titania (TiO_2-Nps) in small size (20-30nm) did not produce any toxic effect [162].

(c) Surface area-dependent toxicity:

Toxicity is greatly affected by crystalline structure, surface-area, and chemical composition. The smaller sized Nps have greater surface-area coming in contact with the cell surfaces that might lead to production of reactive oxygen species (ROS), oxidation [163], and DNA damage that might reduce the cell viability.

(d) Shape-dependent toxicity:

The shape of Nps also play a dominent role in determining their toxicity. There exists a direct co-relation between shape of NPs and cytotoxicity [163]. Different shapes of Nps display different cellular uptake, subcellular localization and production of reactive oxygen species [164]. Previously, researchers revealed that non-spherical nanoparticle (rod-shaped particles) is more cytotoxic as they are easily and quickly absorbed on cell surfaces in comparison with other Nps (spherical-shaped particles) [165].

(e) Crystalline structure-dependent toxicity:

The Titania (TiO$_2$-Nps)have anatase, rutile and brookite phases in their basic crystal structures and debye scherrer's formula displays its crystalline size which is smaller than its particle size. The chemical reactivity of anatase is high as compared to other phases [166]. A study reported that mixed anatase-rutile phase resulted in severe cytotoxic reactions resulting in apoptosis and oxidative stress [167]. In another study, pure 100% anatase Titania (TiO$_2$-Nps)reported slight induction in the cytotoxic effects [168]. The commercially available Titania (TiO$_2$-Nps)having large percentage of anatase (P-25 73-85% anatase, 14-17% rutile and 2-13% amorphous) were responsible for producing cytotoxic effects [169].

(f) Surface coating and functionalization:

The Nps without surface coatings result in initiation of toxicity after coming in contact with cells. Still, even less harmful particles can also be converted to highly toxic by using different techniques.The utilization of surfactants to form surface-coatings for Nps can greatly change their physical and chemical properties leading to cytotoxicity [170]. The reactive oxygen-species (ROS) are produced due to oxygen, oxygen free radicals and transition metals [163] on surface of Nps which causes inflammation. Previously, a study concluded that cytotoxicity of Nps is due to reactive oxygen species and surface free radicals [160].

(g) Routes of synthesis:

The route of synthesis of Nps is responsible for rendering them cytotoxic on larger extent. Certain synthesis pathways play an important role in toxicity of Nps. The conventional synthesis methods of Titania (TiO$_2$-Nps) require expensive and toxic chemicals whereas biological synthesis methods involve simple eco-friendly routes which show multiple advantages over conventional methods [171,172]. It is also worth knowing that formation of anatase or rutile phase is affected by synthesis conditions [91].

2.4 Phase-IV: Mechanical strength and properties of GIC restorative material:

Although conventional Titania (TiO$_2$-Nps)in GIC restorative material might have increased antimicrobial activity along with mechanical properties to some extent but might become responsible for producing cytotoxicity with the passage of time. The possible reason might be the nano-size of titanium oxide which have reported unknown hazardous side-effects [25]. Furthermore, previously a research concluded that titanium oxide is a possible carcinogenic compound in when used in Nps form. Currently, conventional Titania (TiO$_2$-Nps)have been classified as suspicious substances that cause cancer [21].

According to literature there are many combinations of conventionally available Titania (TiO$_2$-Nps) used in dental field. The researchers named Schmalz and Browne reported that biocompatibility of dental materials must be performed in oral environment to confirm that there is no adverse reaction of dental material because these materials are used in oral cavity and toxicity could be the only reason for their non-biocompatibility. Currently, glass ionomer cement (‗GIC') is one of the most successfully running restorative material in smart clinical practice [173]. The problems associated with GIC restorative material is its compromised mechanical strength and physicochemical properties in addition to water moisture with passage of time which adversely affects its durability and shelf life [15,16]. The incorporation of

conventional Titania (TiO_2 Nps) in GIC restoration enhanced the mechanical strength and physicochemical properties but induced pro-inflammatory effects in oral cavity [174]. This pro-inflammatory effect in oral cavity due to TiO_2 GIC restoration might lead to cytotoxicity with passage of time.

Table-2.10: *Effect of the incorporation of various Nps on the mechanical strength of GICs.*

Nanoparticle Type	Strength Type	Effect	Significance	References
Zinc oxide Nps	Compressive strength & Shear Strength	No effect with 3 wt%	-No improvement in mechanical characteristics - Not suitable for restorations	[175]
Zinc oxide Nps	Flexural strength	No effect with 5 wt%	- No improvement in mechanical characteristics - Not suitable for restorations	[176]
Ytterbium fluoride and barium sulphate	Compressive strength	Decreased with 1 wt%	- No improvement in mechanical characteristics - Not suitable for restorations	[177]
TiO_2 Nps	Flexural strength and Compressive strength	Increased with 3–5 wt% Decreased with 7 wt%	- Improvement in mechanical characteristics - Suitable for restorations	[178]
Chlorhexidine Hexameta phosphate Nps	Diametral tensile strength	Decreased with 10–20 wt%	- No improvement in mechanical characteristics - Not suitable for restorations	[179]

2.4.1 *Vicker's micro-hardness analysis of Titania (TiO_2 Nps) in GIC restoration (innovative TiO_2 GIC):*

The most important test used to evaluate of resistance of material's surface to penetration of load is commonly referred as Micro hardness testing [180]. Several studies have been conducted to investigate micro hardness of GIC restorative material containing Titania (TiO_2 Nps). In an in vitro study, it has been revealed that GIC restorative material incorporated with conventional Titania (TiO_2 Nps) have significantly increased Vicker's micro-hardness as compared to GIC restorative material without Titania (TiO_2 Nps) [18,181].

2.4.2 *Compressive strength analysisof Titania (TiO₂ Nps) in GIC restoration (innovative TiO₂GIC):*

The most important masticatory forces in oral cavity are compressive forces which are investigated by compressive strength analysis [180]. The compressive strength of 125 Mpa and 100 Mpa can withstand masticatory forces in adult and prime posterior dentition. The mechanical properties of GIC restorative material modified with conventional Nps have been investigated on large extent. Previously, several researchers reported an increase in GIC restorative material incorporated with conventional Titania (TiO₂ Nps) in comparison to GIC restorative material without Titania (TiO₂ Nps) [18,181]. The compressive-strength of different types of GIC restorative materials modified with conventional Titania (TiO₂ Nps) has increased to a great extent but toxicity may occur in these modified restorative materials in oral cavity. This might be due to utilization of conventional Titania (TiO₂ Nps) that are synthesized by conventional processes.

2.4.3 Flexural strength analysis *of Titania (TiO₂ Nps) in GIC restoration (innovative TiO₂GIC):*

The strength of GIC filling material can be best tested with the help of flexural strength analysis. It is considered as an appropriate method of testing strength of filling materials reported by Prosser H. et. al. Various researchers concluded that flexural strength of GIC restorative material incorporated with conventional Titania (TiO₂ Nps) has shown significant improvement in comparison to conventional GIC restorative material without Titania (TiO₂ Nps) [182]. However, there is a need to conduct more researches regarding flexural strength of GIC restorative material modified with Titania (TiO₂ Nps) to ensure their biocompatibility in oral cavity.

2.4.4 Shear bond strength analysis *of Titania (TiO₂ Nps) in GIC restoration (innovative TiO₂GIC):*

The structure of tooth and chemical bonding between them plays a significant key role in affecting bond strength of different components of tooth such as enamel and dentine [183]. Multiple studies have been carried out to estimate both enamel and dentine shear bond strength of tooth with GIC restorative material modified by incorporating conventional Titania (TiO₂ Nps). The improvement in shear-bond strength of both enamel and dentin portions of tooth with GIC restorative material containing conventional Titania (TiO₂ Nps) was revealed as compared to GIC restorative material without Titania (TiO₂ Nps) where shear bond strength was low [181,116]. The structure of tooth and chemical bonding between them plays a significant key role in affecting bond strength of both enamel and dentine [183]. The enamel has increased bond strength as compared to dentine.This is because enamel is outer most part of tooth with higher surface energy. This leads to increased chemical bonding between enamel and TiO₂GIC restorative material leading to enhanced shear bond strength. Similarly, dentine is inner part of tooth having lower surface energy [184]. The declined chemical bonding exists between dentine and TiO₂GIC restorative material leading to lower shear bond strength in comparison to enamel. The enamel is outermost hardest part of tooth which is more extensively exposed to harsh oral environment as compared to dentin, thereby requires further researches to be carried out in order to increase shear-bond strength of tooth enamel to GIC restorative material with Titania (TiO₂ Nps) to withstand excessive distortive forces in mouth.

2.4.5 *Spectrum mapping and surfacemorphologyof Titania (TiO$_2$Nps) in GIC restoration (innovative TiO$_2$GIC):*

There are two standard methods for analyzing the surface morphology of tooth enamel and dentin. These methods include qualitative and quantitative analysis where, performance of qualitative analysis by scanning electron microscope, and quantitative analysis by energy dispersive X-ray spectroscopy with spectrum mapping has been carried out [185].

Chapter-3

Materials and methods

The current study was designed for producing Nps and their applications in the dental restorative materials. The following describes overall study design, protocols of experiments and analytical tools used in this research. The study was conducted in the Department of Microbiology, Quaid-I-Azam University, Islamabad, Pakistan Institute of Engineering and Applied Sciences, Islamabad and National Institute of Health, Islamabad, Pakistan.

Study design:
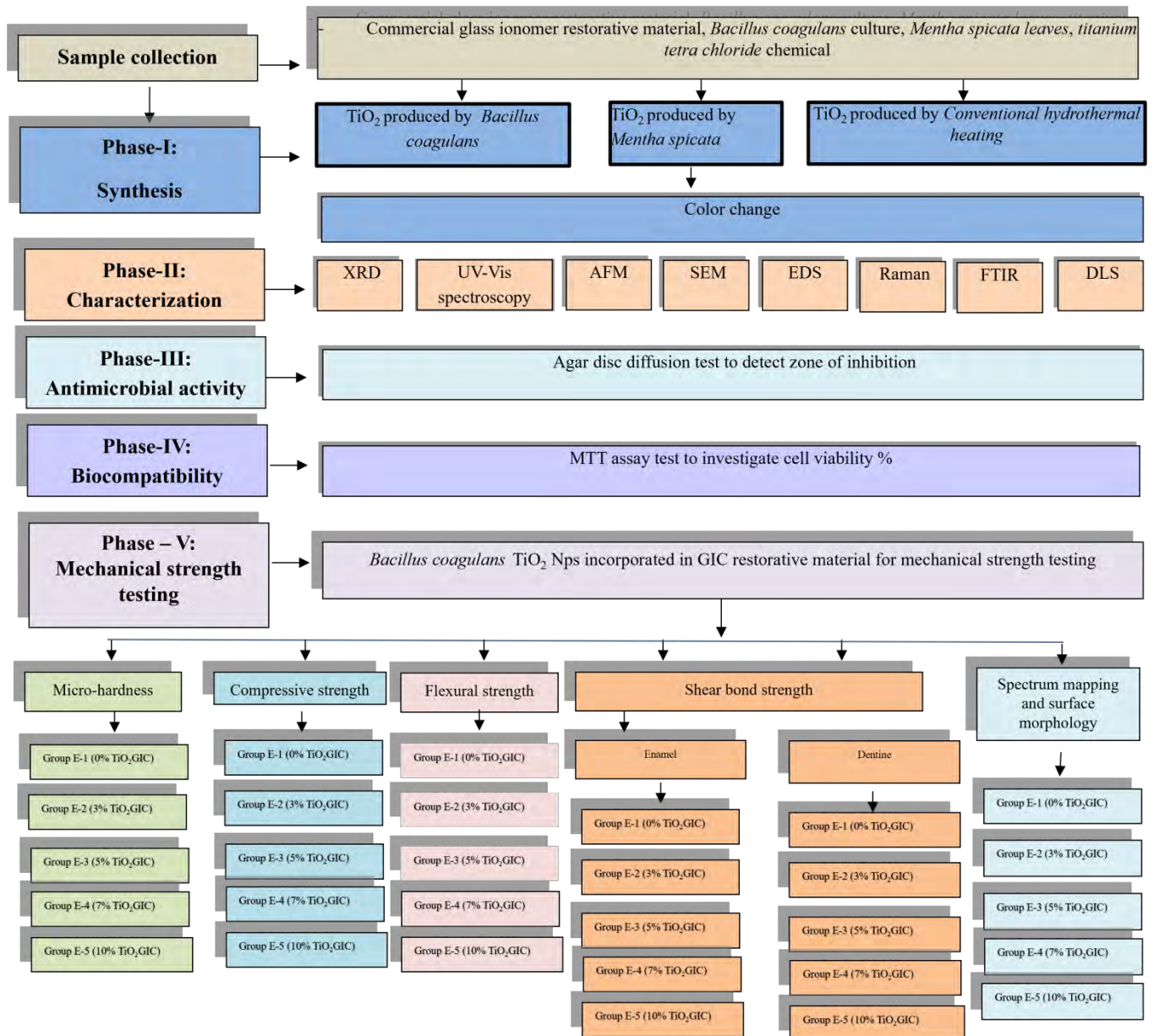
Figure 3.1: Methodology of the current study.
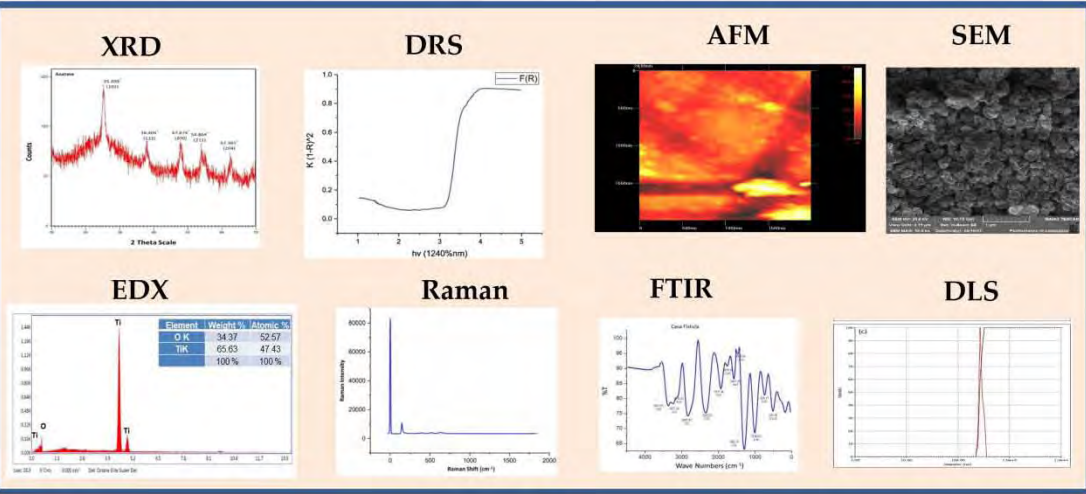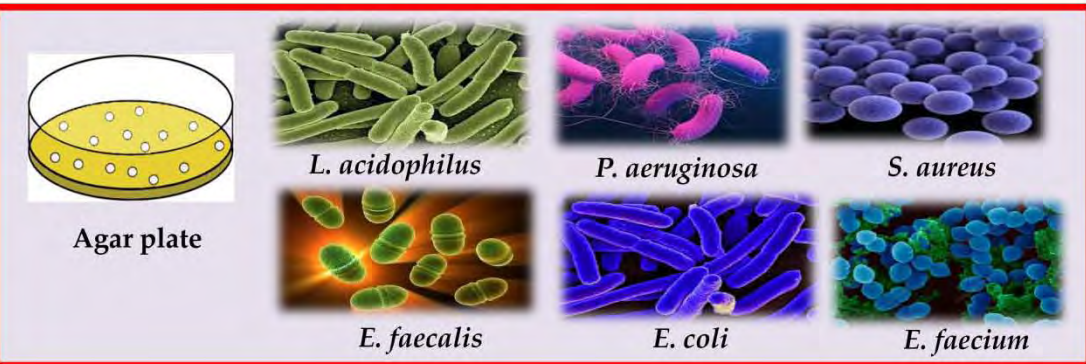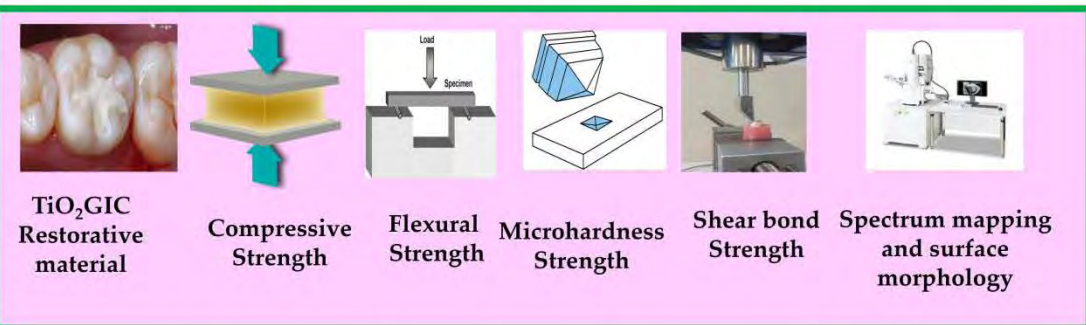
Figure-3.2: Graphical abstract of the current study.

3.1 *Phase-I: Synthesis of Titania (TiO$_2$ Nps):*

The Titania (TiO$_2$ Nps)were prepared by *Bacillus coagulans* in order to compare their efficacy in relation with the conventional methods. The schematic representation of the synthesis of Titania (TiO$_2$ Nps) by biogenic method using *Bacillus coagulans* is given in Figure-3.3.
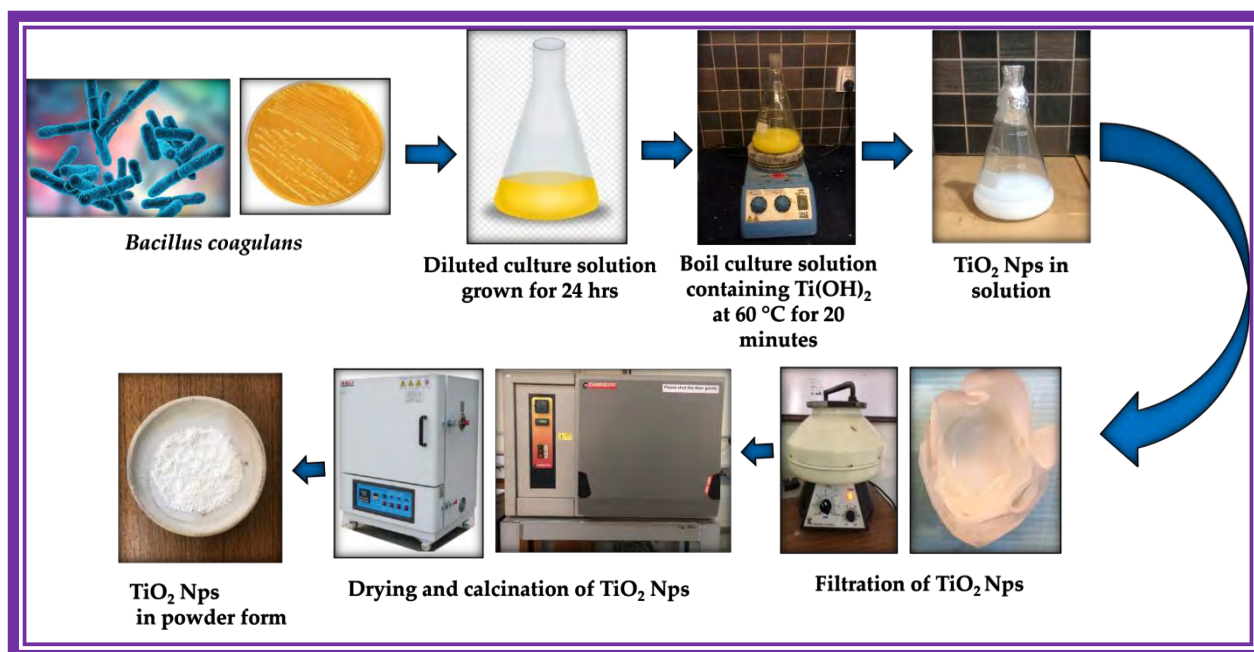
Figure-3.3: Schematic representation elaborating the synthesis of Titania (TiO$_2$ Nps) by Bacillus coagulans.

3.1.1 *Synthesis of Titania (TiO$_2$ Nps) by Bacillus coagulans:*

The experimental techniques used in present work comprised of Titania (TiO$_2$ Nps)synthesis by using *Bacillus coagulans* (Accession No:ATCC®7050^{TM}, Catalog No: 0596P Thermo Fisher Scientific, USA) taken from the National Institute of Health (NIH), Islamabad.

3.1.1.1 *Preparation of bacterial Inoculum:*

The *Bacillus coagulans* strain was freshly cultured on nutrient agar plates and incubated for 24 hrs in an incubator under 37°C. After that, 100 mL of the nutrient broth was prepared by mixing strains of freshly cultured *Bacillus coagulans* into Erlenmeyer flask. The flask was then incubated for the next 24 hours by placing them in shaking incubator (Memart, Germany) at 28°C and 150 rpm. After that, all content of flask was subjected to centrifugation at 10,000 rpm for 10 min in order to obtain the cell free filtrates.

3.1.1.2 *Biosynthesis of Titania (TiO$_2$ Nps):*

The supernatant was separated and 20 mL of 00.025 M Ti(OH)$_2$ solution (American Elements, 10884-Weyburn Ave, Los Angeles, CA, USA) was added to the 80 mL bacterial culture solution and it was heated on steam bath up to 60°C for 20 min until white deposition started to appear at the bottom of flask, indicating the initiation of transformation, followed by formation of Titania (TiO$_2$ Nps). The culture solution was cooled and allowed to incubate at room

temperature in laboratory ambience. After 12–48 h, culture solution was observed to have distinctly markable coalescent white clusters deposited at the bottom of flask [186].

3.1.1.3 *Harvesting of final product Titania (TiO$_2$ Nps)*:

Finally, solution containing Titania (TiO$_2$ Nps) was passed through centrifuge machine (centrifuge model MOD-800) twice so as to get completely pure Titania (TiO$_2$ Nps) without any sort of impurity left. After passing through centrifuge machine (Healtho, centrifuge model MOD-800 Beijing, China) ampules containing water solutions were kept still in stand to allow Titania (TiO$_2$ Nps)to settle down. When Titania (TiO$_2$ Nps) settled down in ampules water solution was thrown and these Nps were collected. These Titania (TiO$_2$-Nps) obtained were eventually, annealed in furnace (thermo electron LED GmbH, HERAEUS ACUTHERM, D-83505, langenselbold, Germany) for 2 hours at 80°C for proper drying. After drying, Titania (TiO$_2$ Nps)were calcinated in furnace at 500°C for 3 hours to attain fine powdered form of Titania (TiO$_2$ Nps).

3.1.2 *Synthesis of Titania (TiO$_2$ Nps) by Mentha spicata plant*:

The Titania (TiO$_2$ Nps)were prepared by *Mentha spicata* in order to compare their efficacy in relation with conventional methods. The schematic representation of synthesis of Titania (TiO$_2$ Nps)by green method using *Mentha spicata* is given in Figure-3.4.
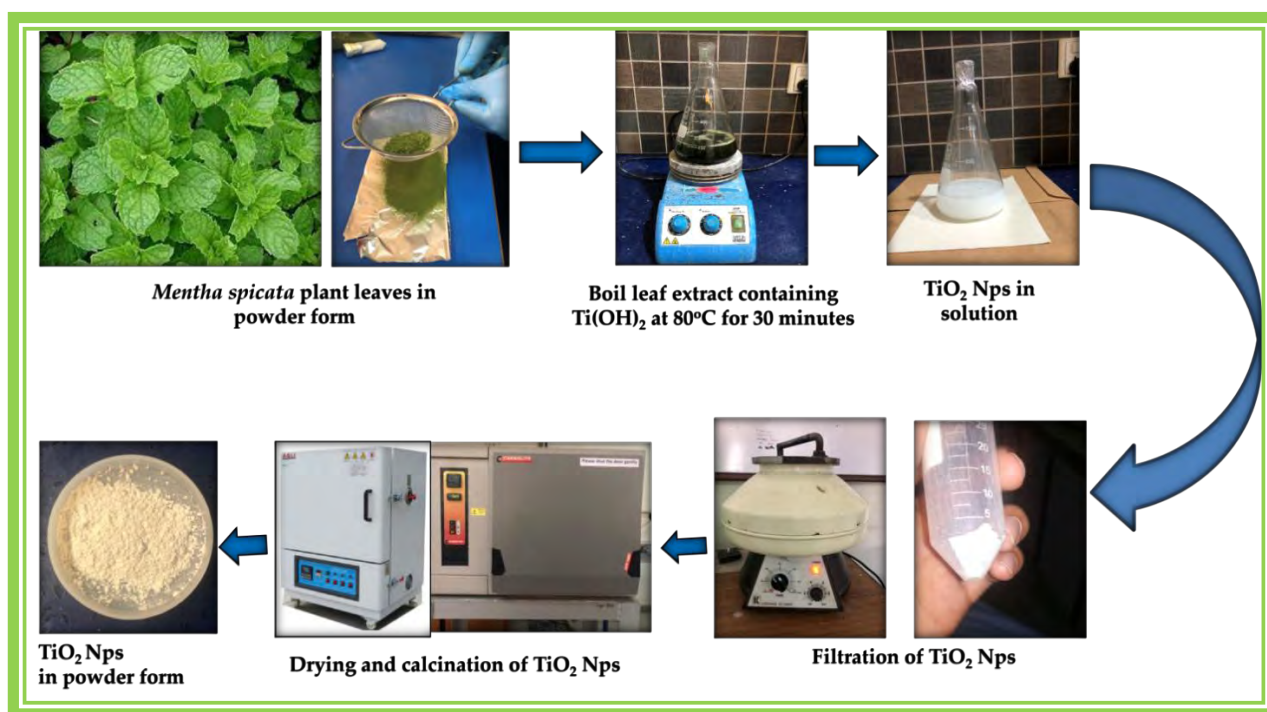
Figure-3.4: Schematic representation elaborating synthesis of Titania (TiO$_2$ Nps)by Mentha spicata plant.

3.1.2.1 Preparation of *Mentha spicata* powder:

Fresh *Mentha spicata* leaves were collected and then washed firstly with normal water to remove dust particles. Then, they were washed with distilled water to remove any other impurity. Leaves were kept at normal room temperature for drying. After few days they got dried and were crushed in powder form with the help of grinder. Following grinding, they were passed through 20 mesh sieve or whatmann N-1 filter paper so that very fine powder was obtained eventually [187].

3.1.2.2 *Preparation of plant extract:*

1 Mg of dried, finely ground plant powder was weighed in weighing balance (Lambart, Kern & Sohn Traders Model: BM-320, Germany) and was dissolved in 100 mL of distilled water in flask. The biomass and distilled water in flask was shook vigorously to get uniform mixture of plant extract solution (liquid form). Then, plant extract solution was heated and boiled at 100°C for 10 minutes as boiling helped in disintegrating cell wall of plant due to which biological agents came out. After 10 minutes, mixture in flask was left to cool down for some time. Then, mixture was passed through whatmann N-1 filter paper to get the biomass-free pure plant extract solution and stored at 4 °C.

3.1.2.3 *Preparation of Ti (OH)$_2$stock solution:*

1 ml of Ti(OH)$_2$(American Elements, 10884-Weyburn Ave, Los Angeles, CA, USA) was measured and then added into 80 ml of distilled water in flask. Then, solution was shaken vigorously to get Ti(OH)$_2$ properly and completely dissolved in distilled water to get a Ti(OH)$_2$ salt stock solution. Afterwards, 20 ml of biomass free pure plant extract solution prepared initially was added to Ti(OH)$_2$ salt stock solution.

3.1.2.4 *Preparation of Titania (TiO$_2$ Nps):*

This finally prepared solution in flask constituting of 20 mL plant extract solution and 80 mL Ti(OH)$_2$ salt stock solution was heated at 80°C for 30 minutes at 800rpm.Color changes were observed i.e from green to milky white. After 24 hours, solution was washed repeatedly with water and ethanol to remove any impurity if available.

3.1.2.5 *Harvesting of the final product:*

Finally, solution containing Titania (TiO$_2$ Nps)was passed through centrifuge machine (Healtho, centrifuge model MOD-800 Beijing, China) twice so as to get completely pure Titania (TiO$_2$ Nps)without any impurity left. After passing through centrifuge machine, ampules containing water solutions were kept still in a stand to allow the Titania (TiO$_2$ Nps)to settle down. When Titania (TiO$_2$ Nps)settled down in ampules, water solution was thrown and these Nps were collected. These Titania (TiO$_2$ Nps)obtained were finally annealed in furnace (thermo electron LED GmbH, HERAEUS ACUTHERM, D-83505, langenselbold, Germany) for 1 hours at 100°C for proper drying. These Nps were then calcinated at 500 °C for 3 hours to get fine powdered form [187,188].

3.1.3 *Synthesis of Titania (TiO₂ Nps)* by *Conventional hydrothermal heating* **method:**

The Titania (TiO₂ Nps) were prepared by *Conventional hydrothermal heating* methods in order to compare their efficacy in relation with biological methods. The schematic representation of synthesis of Titania (TiO₂ Nps)by *Conventional hydrothermal heating* method (Figure- 3.5).
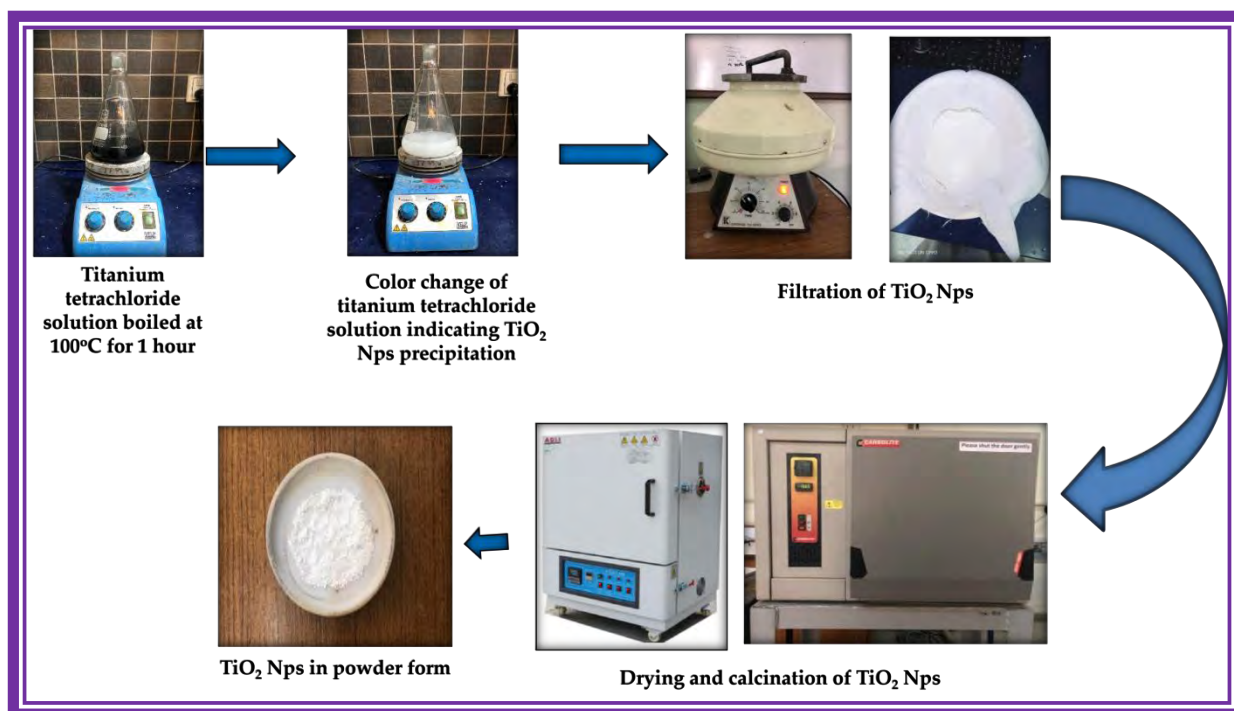
Figure-3.5: Schematic representation elaborating synthesis of Titania (TiO₂ Nps) by Conventional hydrothermal heating.

3.1.3.1 *Preparation of TiCl₄ stock solution:*

1 mL TiCl₄ salt (Sigma-Aldrich, Merck KGaA, Darmstadf, Germany) was taken and then dissolved in 100 ml of de-ionized water to make 1 molar salt solution of TiCl₄ .Then, 1 molar solution of TiCl₄ salt was put in flask and placed on hot plate (WITEG. Model: MSH-20A.P/N:DH.WMH03120,MA, Burma). Metallic stirrer was put in flask for uniform mixing. Then, flask containing Ticl₄ salt solution was heated at 100°C until, precipitates of Titania (TiO₂ Nps)were obtained. Heating was continued until color of solution containing Titania (TiO₂ Nps)was changed initially from black to dark purple. After sometime, it changed its color to blue and then finally, to white which confirmed the presence of Titania (TiO₂ Nps).These Npswere filtered with help of whatman N-1 filter paper using deionized water.

3.1.3.2 *Harvesting of the final product:*

Finally, Titania (TiO₂ Nps)were repeatedly centrifuged with de-ionized water and ethanol until white jelly like cake was formed.

3.1.3.3 *Calcination of Titania (TiO₂ Nps) :*

The harvested product was in the form of jelly like cake that was then placed in heating oven at 110 °C for 2 hours in order to get powdered form of the final product. This heating completely

dried jelly like cake which was calcinated at 500°C for 3 hours into fine powdered form Titania (TiO$_2$-Nps)with help of morter and pestle [189].

3.2 *Phase-II: Standard Characterization of Titania (TiO$_2$-Nps):*

Characterization of Titania (TiO$_2$-Nps)synthesized by different routes i.e microbe (*Bacillus coagulans*), plant (*Mentha spicata*) and chemical (*Conventional hydrothermal heating)* methods were individually characterized by utilizing standard protocols. The characterization of these different types of Titania (TiO$_2$-Nps) was conducted with X-Ray powder diffraction analysis (XRD), UV-VIS diffuse reflectance spectroscopic analysis (DRS), atomic force microscopic analysis (AFM), scanning electron microscopc analysis (SEM), energy dispersive x-ray spectroscopic analysis (EDX), fourier transmission infrared spectroscopic analysis (FTIR), dynamic light scattering spectroscopic analysis (DLS) and Raman spectroscopic analysis [131,186,187]. The antimicrobial activity of these synthesized Titania (TiO$_2$-Nps) was carried out by agar disc diffusion test [187]. The biocompatibility of these Titania (TiO$_2$-Nps)was scrutinized by MTT assay to check cell viability % (cytotoxicity) of Nps exposed to fibroblast cell lines [8]. The regime of characterization of Titania (TiO$_2$-Nps)synthesized by *Bacillus coagulans, Mentha spicata* and *Conventional hydrothermal heating* is listed in Figure-3.6.
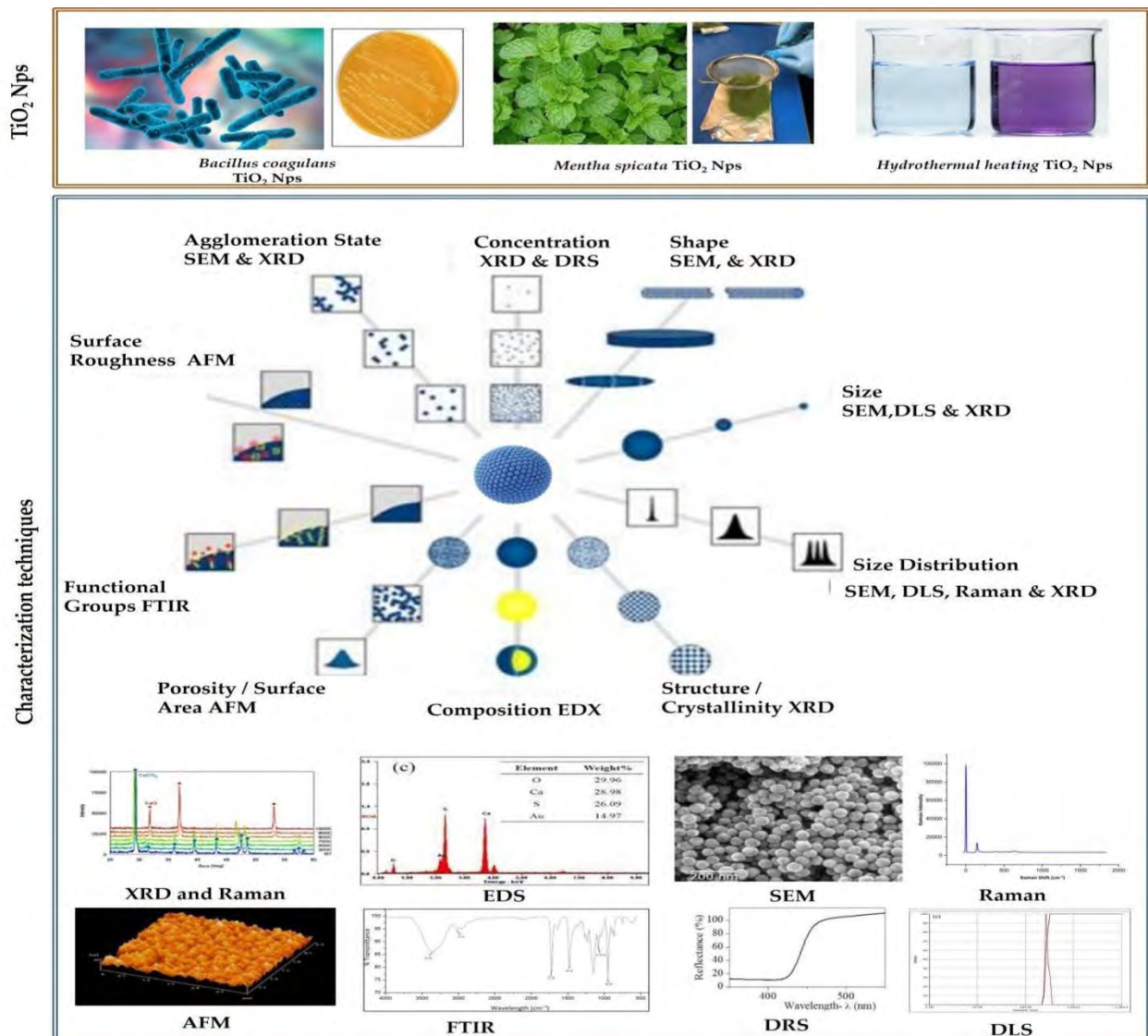
Figure-3.6: Characterization techniques performed for Titania (TiO₂Nps) synthesized by Bacillus coagulans, Mentha spicata and Conventional hydrothermal heating.

3.2.1 *XRD analysis of Titania (TiO₂Nps) for crystalline size and phase:*

X-ray powder diffraction analysis was carried out by using XRD diffractor (DP-MAXZ 2400/ Diffractometer, Rigaku Corporation, Akishima, Tokyo, Japan) to identify the crystalline size and phase form of Nps. Measurements were established at room temperature hence utilizing the current of 150mA and voltage of 40 kV at angles of 2Ө i.e 20°- 80° having step size= 0.02°, nickel filtered Cu Kα; (λ = 1.54, Å) radiation' and solid state germanium detector with cooled liquid nitrogen. The Joint Committee Powder Diffraction Standards Card; (JCPDS) was used to formulate and compare spectral plots for data analysis [187,188].

3.2.2 *DRS analysis of Titania (TiO₂Nps) for confirmation of crystalline size :*

UV-Vis Diffuse reflectance spectrophotometer (Perkin Elmer, UV/VIS/NIR Spectrometer Lambda 950 Waltham, MA, USA) was used to detect the crystalline size of Nps by calculating their band gap energy in the reflectance mode and confirmed the formation of Titania (TiO₂-Nps) at wavelength range between 200-800 cm^{-1} [186,187].

3.2.3 *AFM analysis of Titania (TiO₂Nps) for size shape and surface topography :*

The size, shape and surface topography of Titania (TiO₂Nps)samples prepared by three different methods was studied by using atomic force microscopy (Quesant Universal SPM, Ambios Technology, Santa Cruz, CA,USA) which was then evaluated by AFM images using software (Nanoscope, IIIa, Digital Instruments). The suspensions of Titania (TiO₂Nps)were prepared by dissolving 1mg of Titania (TiO₂Nps)in 1ml of ethanol. One drop from each suspension of Titania (TiO₂Nps)was placed on glass slide and dried by evaporation. Once dried, Titania (TiO₂Nps) on glass slab were covered with another glass slab and placed under cantilever tip of AFM to generate topographic map for each and every sample. [186,187].

3.2.4 *SEM analysis of Titania (TiO₂Nps) for particle size and shape:*

Scanning Election microscope (Nova nanosem 430; Fei company 4022 261 49391-S column F&G stron prep, Hillsboro, OR, USA) was employed to detect particle shape, size and morphology of Titania (TiO₂Nps) synthesized by *Bacillus coagulans, Mentha spicata* and *Conventional hydrothermal heating* methods. The suspensions of Titania (TiO₂Nps)were prepared by dissolving 1mg Titania (TiO₂Nps)in 1mL of ethanol for all types. After sonicating, suspensions of Titania (TiO₂Nps)for 15 minutes, a drop from each type of suspension was placed on carbon stub and dried by evaporation. After drying, Titania (TiO₂Nps)on carbon stub were sputter coated for 1minute in sputtering coater machine (Emitech, ks550x,USA). SEM was performed at different magnifications in order to perceive morphology [186,187].

3.2.5 *EDS analysis of Titania (TiO₂Nps) for elemental composition:*

Energy dispersive x-ray spectroscopic analysis (nova nanosem 430; fei company, 4022 261 49391-S column FEG Siron Prep, Hillsboro, OR, USA) was done for elemental compositional analysis of Titania (TiO₂Nps)prepared by *Bacillus coagulans, Mentha spicata* and

Conventional hydrothermal heating methods. The EDS helped to identify particular elements along with their atomic and weight percentages. The EDS generated x-ray spectrum in entire scan area of SEM and energy of x-ray was characteristic of element from which x-ray was emitted [186,187].

3.2.6 *FTIR analysis of Titania (TiO$_2$ Nps) for the presence of functional groups:*

FTIR (JASCO FT/IR-6600, Ultrech-Amsterdam, AMS, Netherlands) analysis was carried out to ascertain the functional groups present in the Titania (TiO$_2$ Nps)synthesized by three different methods such as *Bacillus coagulans, Mentha spicata* and *Conventional hydrothermal heating*. These functional groups were recorded in the range of 400-4000cm^{-1} to identify chemical compounds present on the surface of the Titania (TiO$_2$ Nps)[186,187].

3.2.7 *DLS analysis of Titania (TiO$_2$ Nps) for the hydrodynamic size in suspension:*

DLS (Zeta sizer-nano Z-S Apparatus, ZEN-36000, Malvern panaLytical, Malvern-UK) was used to confirm the hydrodymic size of Nps in the suspension at submicron level less than 1nm. The hydrodynamic size of Titania (TiO$_2$ Nps)synthesized by *Bacillus coagulans, Mentha spicata* and *Conventional hydrothermal heating* were carried out [186,187].

3.2.8 *Raman analysis of Titania (TiO$_2$ Nps) for size and shape:*

The phase form and size of the Titania (TiO$_2$-Nps) by raman spectroscopy (MST- 4000A, DONGWO, OPTRON, Gyeonggi-do, Korea) was conducted between 200 cm^{-1} and 800 cm^{-1} [190]. There are six main peaks for distinguishing the phase form in raman active modes including 1 peak at A_{1g}, 2 peaks at B_{1g} and 3 peaks at E_g. The presence of three peaks i.e 1 peak at A_{1g} ,1 peaks at B_{1g} and 1 peak at $E_g$confirms the phase of Nps. The active modes of B_{1g} peak represents symmetric bending, E_g peak shows symmetric stretching and A_{1g} elaborates O-Ti-O anti-symmetric bending vibration in its spectrum.The large particle size of Nps shows reduced intensity of raman peak and vice versa [191].

3.3 *Phase-III: Determination of antimicrobial activity of Titania (TiO$_2$ Nps) for zone of inhibition:*

The antimicrobial activity of Titania (TiO$_2$ Nps)synthesized by *Bacillus coagulans, Mentha spicata* and *Conventional hydrothermal heating* was carried out by standard agar disc diffusion test [187]. The schematic representation of antimicrobial activity of Titania (TiO$_2$ Nps) is illustrated in Figure-3.7.
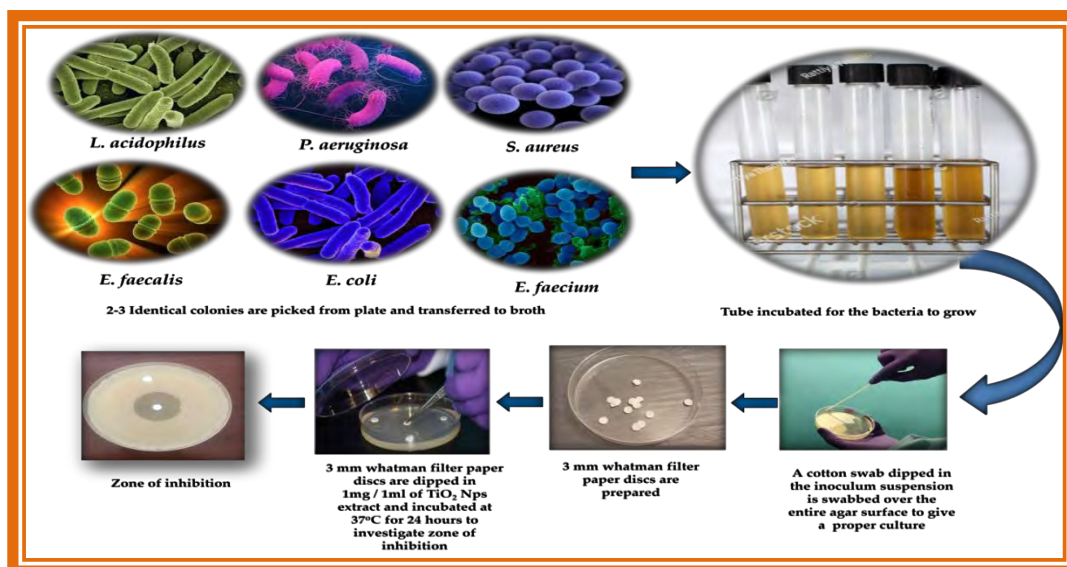
Figure:3.7: Representation of agar disc diffusion test to investigate the zone of inhibition formed by Titania (TiO₂ Nps) against dental caries promoting pathogenic bacteria.

3.3.1 Agar disc diffusion test:

3.3.1.1 Preparation of media:

1.5 gm of agar was added to 100 ml of distilled water in flask to prepare nutrient agar media. The solution in flask was vigorously shaken and then glucose was added to it. The mouth of flask was tightly closed with thick cotton pellet and then covered with aluminum foil. This media was sterilized in an autoclave for about 45 minutes followed with cooling at room temperature. When media was properly cooled then, about 15-20 mL of it was poured into petri dishes in a laminar flow. The petri dishes were kept and allowed to cool down so that media could undergo solidification [187].

3.3.1.2 Analysis of antimicrobial activity:

Antimicrobial property of Titania (TiO₂ Nps)was carried out by utilizing agar disc diffusion analysis. This procedure was carried out against certain caries promoting bacteria including both gram positive as well as gram negative bacteria such as *E. coli* (ATCC®35218^TM), *L .acidophilus* (ATCC®314^TM), *E. faecalis* (ATCC®29212^TM)*, E. faecium* (ATCC®51559^TM), *S. aureus* (ATCC®25923^TM) *and P. aeruginosa* (ATCC®27853^TM). These bacteria were cultured by using Lysogenic broth agar medium. Freshly prepared overnight bacterial culture was utilized and 15 mL of Lysogenic broth agar was poured in disposable petri dishes which were initially autoclaved. Bacterial cultures were spread uniformly on petri dishes. The Titania (TiO₂ Nps)synthesized by three different routes were diluted in PBS solution at concentration of 1mg / ml and was placed in sonicator for 15 minutes to get uniformly mixed stock solutions of different types of Titania (TiO₂ Nps). Then, Whatman filter paper was cut into small rounded shape to form 3mm diameter discs, which were dipped, in each type of prepared Titania (TiO₂ Nps)stock solutions. All these three filter paper discs of about 3mm in diameter carrying different types of Titania (TiO₂ Nps)were placed in petri dish containing LB agar along with one filter paper dipped in water used as a control group. These three different types of Titania (TiO₂ Nps)on filter paper discs were tested against the aforementioned caries promoting

pathogenic bacteria. The tests plates containing different types of Titania (TiO$_2$ Nps)were incubated at about 37 °C for at least 24 hours. The result was predicted by measuring zone of inhibition in mm or cm to find out type of Titania (TiO$_2$ Nps) that had the most enhanced antimicrobial activity [187].

3.4 Phase-IV: Testing of Biocompatibility of Titania (TiO$_2$ Nps) for cell viability %:

The biocompatibility (cell viability %) testing of Titania (TiO$_2$ Nps)synthesized by *Bacillus coagulans, Mentha spicata* and *Conventional hydrothermal heating* was carried out by standard MTT assay test [192]. The schematic representation of biocompatibility (cell viability %) analysis of Titania (TiO$_2$ Nps)is illustrated in Figure-3.8.
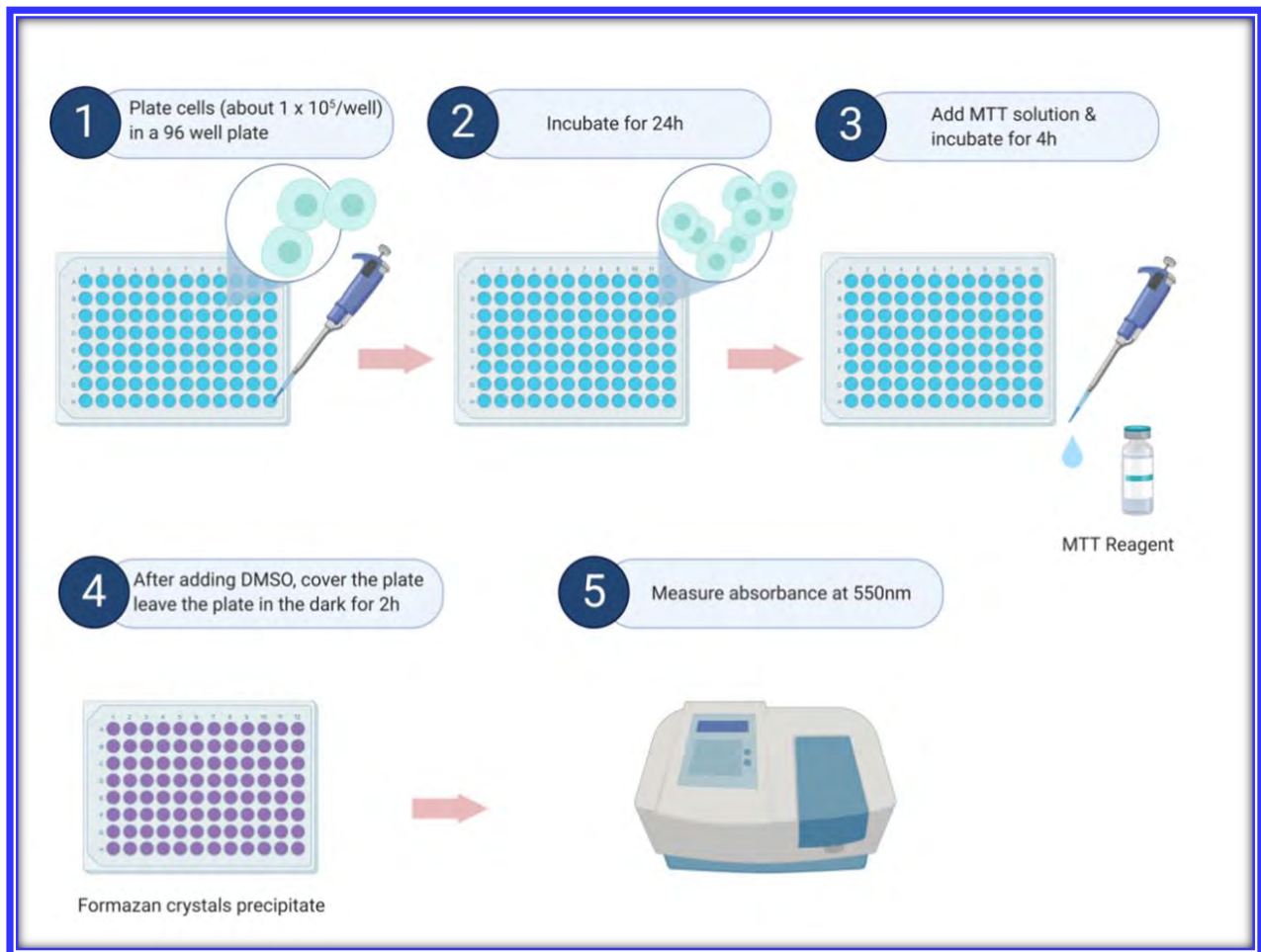
Figure-3.8: Schematic representation of MTT assay for biocompatibility (cell viability%) analysis against Titania (TiO$_2$ Nps) synthesized by Bacillus coagulans, Mentha spicata and Conventional hydrothermal heating .

3.4.1 Biocompatibility (cell viability %) assessment
3.4.1.1 Cell culture:
3.4.1.1.1 Cells utilized in the current study:
Cells utilized in the current study were L929 mouse fibroblast, purchased from American Type Culture Collection (ATCC, Manassas, VA, USA) [193]. These cell lines were obtained through the National Institute of Health (NIH), Islamabad.

3.4.1.1.2 *Preparation of cell culture:*

Cell culture is a technique used to investigate the characteristics and properties of alive cell lines which can't be performed in a living creature.L929 mouse fibroblast cells obtained from NIH institute were placed in flasks and were maintained in standard culture conditions i-e DMEM (Dulbeccos Modified Eagle's medium, USA) supplemented with 10% fetal bovine serum (HyClone Lab, Logan, Utah), 100ul/mL penicillin, 2.5ug/ml streptomycin for complete removal of cryoprotective DMSO-dimethyl sulfoxide (Sigma, Prod.No.D2650, USA). The cells were regularly monitored every 24 hours. The culture media was changed regularly twice a week and were incubated in a humidified atmosphere of 5% CO_2 at 37°C [193].

3.4.1.1.3 *Determination of cell splitting:*

The splitting was initiated when cells in flask were multiplied and absence of any bacteria, virus or fungus was determined. After cultured cells were allowed to proliferate, their adherence at a logarithmic phase was detached by a process called trypsinization (0.02% trypsin in 0.25% EDTA) [194]. The cells were microscopically observed that they had splitted from base and floated.

3.4.1.1.4 *Cell culturing in standard 96-well plate:*

The cells were counted in hemacytometer after trypsinization. When cells reached a certain amount of number the cell suspension was made in 10% DMEM containing 1×10^4 cells. Then, 100 µL was taken and seeded in each well of standard 96-well plate used. Again, seeded 96-well plate was incubated for 24-48 hrs (Depends on type of cell) with 5% CO_2 in incubator at 37°C. After this, 96-well plate was then examined by an inverted microscope to observe the culture confluency [193].

3.4.1.2 *Preparation of Titania (TiO$_2$ Nps)stock solution and serial dilutions of low and high dose:*

Different types of Titania (TiO$_2$ Nps)prepared by *Bacillus coagulans, Mentha spicata* and *Conventional hydrothermal heating* methods were added as 1mg/ml concentration of stock solution for each type of Titania (TiO$_2$ Nps). These three types of Titania (TiO$_2$ Nps)were placed in sonicator for about 15 minutes so as to get uniformly mixed stock solutions of Titania (TiO$_2$ Nps). The pipette was used to take out 4×10^{-3} ml from 1mg/ml TiO$_2$ stock solution and poured into 8 ml PBS (0.5 µg/8ml) to make high dose serial dilution of initial concentration for all types of synthesized Titania (TiO$_2$ Nps).Other low serial dilutions for all types of synthesized Titania (TiO$_2$ Nps) were prepared from 4 ml PBS (0.063µg/4ml, 0.125µg/4ml and 0.25µg/4ml). The low and high dose of serial solutions for synthesized Titania (TiO$_2$ Nps) from all the three routes was illustrated in the table-3.1[193]. The working solution of this concentration was prepared by using the following standard formula:

$C_1 x V_1 = C_2 \times V_2$

Where,

C_1= Concentration of Stock Solution.

C_2= Concentration of Serial Dilution

V_1= Desired volume of Stock Solution.

V_2= Desired volume for Serial Dilution

Therefore, the calculations were done by:-

$$V_1 = \frac{C_2\,V_2}{C_1}$$

This formula was valid and used when required dose was in molar units or in g/ml. The PBS solution was used to prevent removal of porphyrin from cultured cells. All the required stock solutions and serial dilutions for different types of Titania (TiO_2 Nps)utilized in this experiment were freshly prepared just 3 hrs prior to the initiation of experiment to avoid any bias.

Custom protocol for Molarity calculations of Titania (TiO_2 Nps)from mass & Volume:

Mass = 0.005 grams
Formula weight (daltons) = 79.87
Volume = 5 milliliter
Molarity = 12.5203 milliliter
Calculate serial dilution using = Initial concentration and dilution factor
Stock solution name = TiO_2
Diluent name = PBS
Concentration of stock solution = 1 mg/ml
Serial dilution initial concentration = 0.5 µg/ml
Dilution factor = 2
Final volume for each dilution = 4 ml
Number of dilutions = 4

Table-3.1: Custom protocol for preparation of low and high dose serial dilutions of TiO_2 with PBS solvent.

Dilutions	Stock solutions of TiO_2 Nps(ml)	PBS (ml)	TiO_2 (µg/ml)
1	4 x 10-3 (from 1 mg/ml stock)	8	0.5
2	4 (from dilution 1)	4	0.25
3	4 (from dilution 2)	4	0.125
4	4 (from dilution 3)	4	0.063

3.4.1.3 Analysis of MTT assay for cell viability % (cytotoxicity):

The cells were cultured in 96 well plates at density of 45000 cells/ml cells per well in 200 µl culture medium. The cells were exposed to Titania (TiO_2 Nps) after 70-80% of confluence. Finally, cultures were exposed to TiO_2 extracts i.e 50 ul/well. This means that 50ul/well from all the serial dilution concentrations (0.063µg, 0.125µg, 0.25µg and 0.5µg)from all types of Titania (TiO_2 Nps)prepared were poured in columns of 96-well plate directly. Water was used as control group and was also poured in columns of 96-well plate. The 28 microliters of MTT dye 2mg/ml was added to each well, and plates were incubated at 37 °C in 5% CO_2/air for 2 hours. The medium was then carefully removed, and purple products were dissolved in 130µL dimethyl sulfoxide (DMSO).The plates were shaken for 10 min [195] to prevent the Nps from interfering with this assay. After incubation period, fluorescence of each well was measured at wavelength of 490nm with a fluorescence reader BIORAD (Thermo Fisher New York USA). Three different readings for each sample was recorded [192].

The mathematical equation used to calculate cell viability was given as follows [196];

Cell viability % = $\dfrac{\text{Mean Optical Density of Test Group}}{\text{Mean Optical Density of Control Group}}$ x 100%

The cytotoxicity of Titania (TO$_2$ Nps) was categorized as: noncytotoxic (cell viability: >90%); mildly cytotoxic (cell viability: 60-90%); moderately cytotoxic (cell viability; 30-60%) and severely cytotoxic (cell viability: 30%-less) [197].

3.5 Phase-V: *Determination of mechanical strength and properties of GIC restorative material:*

3.5.1 *Standard composition of conventional GIC:*

Glass-ionomer cement (GICs) mainly composed of a basic glass powder and an acidic polymer which would set by an acid-base reaction between these components [196]. The standard commercial brand composition of GIC used is listed in table-3.2.

Table-3.2: Standard composition of glass ionomer cements filling material.

Powder			Liquid
Silica	-	41.9%	Polyacrylic acid (Itaconic acid, maleic acid) - 40- 55%
Alumina	-	28.6%	
Aluminum fluoride	-	1.6%	
Calcium fluoride	-	15.7%	Tartaric acid - 6-15%
Sodium fluoride	-	9.3%	Water - 30%
Aluminium phosphate	-	3.8	

3.5.2   *Preparation of different combinations of GIC and Titania (TiO$_2$ Nps):*

The conventional GIC filling material was purchased from local vendor of Islamabad. The group divisions, group compositions of different synthesized Titania (TiO$_2$ Nps)and company name of commercial GIC filling material is shown in *Table*-3.3[197].

Table- 3.3: Group names and compositions of TiO$_2$GIC cement samples pertaining different concentrations.

Ser	Group divisions	Group Compositions	Company name
1	Control group (E-1)	GIC + 0 wt% TiO$_2$	Universal Restorative Cement-2
2	Experimental group (E-2)	GIC + 3 wt% TiO$_2$	Universal Restorative Cement-2
3	Experimental group (E- 3)	GIC + 5 wt% TiO$_2$	Universal Restorative Cement-2
4	Experimental group (E-4)	GIC + 7 wt% TiO$_2$	Universal Restorative Cement-2
5	Experimental group (E- 5)	GIC + 10 wt% TiO$_2$	Universal Restorative Cement-2

3.5.3 *Concentration of Titania (TiO$_2$ Nps)in GIC restorative material:*

The different concentrations of Titania (TiO$_2$ Nps) and GIC filling material employed in the current study are shown in table-3.4.All different concentration of Titania (TiO$_2$ Nps) and GIC

powder (GC universal restorative cement 2) were vigorously mixed in vortex for at least complete one minute so as to get precise measurements [198].

Table-3.4: Standard mixing of different concentrations of GIC and Titania (TiO$_2$Nps)to make TiO$_2$GIC powder.

Ser	Group percentages	GIC Powder Concentration	Titania (TiO$_2$-NPs) concentration	Total Concentration of TiO$_2$GIC
1	E-1 (0% TiO$_2$GIC)	5 gm	0% w/w (0 gm)	5 gm TiO$_2$GIC
2	E-2 (3% TiO$_2$GIC)	5 gm	3% w/w (0.15 gm)	5.15 gm TiO$_2$GIC
3	E-3 (5% TiO$_2$GIC)	5 gm	5% w/w (0.25 gm)	5.25 gm TiO$_2$GIC
4	E-4 (7% TiO$_2$GIC)	5 gm	7% w/w (0.35 gm)	5.35 gm TiO$_2$GIC
5	E-5(10% TiO$_2$GIC)	5 gm	10% w/w (0.50 gm)	5.50 gm TiO$_2$GIC

3.5.4 *Mixing of Titania (TiO$_2$Nps)with GIC Cement:*

The Titania (TiO$_2$-Nps)synthesized by *Bacillus coagulans, Mentha spicata* and *Conventional hydrothermal heating* were obtained as white powder. The balancing machine (Sigma-Aldrich, St. Louis, MO, USA) was used to get accurate measurements of different concentrations of Titania (TiO$_2$-Nps)and GIC powder. The TiO$_2$GIC powder at different concentrations was mixed with mortar and pestle to get a uniform mixture.

3.5.4.1 *Sample size distribution for mechanical strength and properties testing:*

A total of 250 samples having different concentrations of Titania (TiO$_2$-Nps)were used testing of mechanical properties. The groups included were conventional control group E-1 (0% TiO$_2$GIC), experimental group E-2 (3% TiO$_2$GIC), experimental group E-3 (5% TiO$_2$GIC), experimental group E-4 (7% TiO$_2$GIC) and experimental group E-5 (10% TiO$_2$GIC) having n=10 in each group is shown in Table-3.3. These prepared samples were used for testing micro-hardness (n=10), flexural strength (n=10), compressive strength (n=10) and shear bond strength to enamel (n=10) and dentin (n=10) component of tooth structure shown in Table-3.5. The surface morphology of these samples (n=10) was tested under SEM after the compressive strength testing was done.

Table 3.5: Sample size distribution for mechanical strength testing (N = 250).

Flexural Strength	Compressive Strength and SEM	Shear Bond Strength		Micro-hardness
		Enamel	Dentin	
Group1=10	Group1=10	Group1=10	Group1=10	Group1=10
Group 2=10	Group 2=10	Group 2=10	Group 2=10	Group 2=10
Group 3=10	Group 3=10	Group 3=10	Group 3=10	Group 3=10
Group 4=10	Group 4=10	Group 4=10	Group 4=10	Group 4=10
Group 5=10	Group 5=10	Group 5=10	Group 5=10	Group 5=10
50	50	50	50	50

3.5.4.2 *Basic regime for mechanical strength and properties testing:*

The basic regime for carrying out different tests for enhancing mechanical strength of concentrations of TiO$_2$GIC is shown in Figure-3.9.
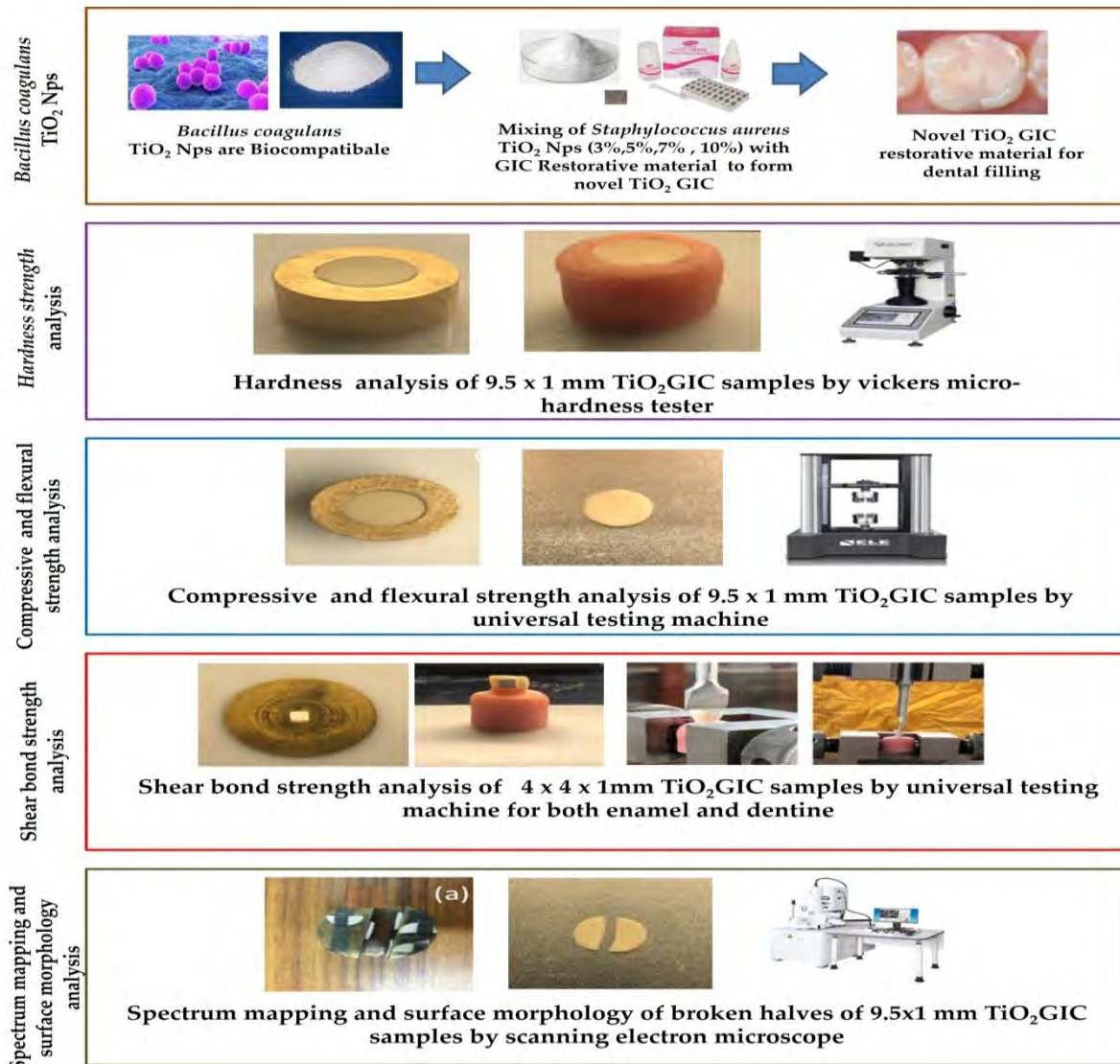
Figure-3.9: Schematic representation of mechanical properties testing of innovative TiO$_2$GIC restorative material synthesized by Bacillus coagulans at different percentages.

3.5.5 *Evaluation of mechanical strength and properties of TiO$_2$GIC cement samples at different concentrations:*
3.5.5.1 *Preparation of mould:*

Electronic vernier calliper (NSK, Tochigi, Japan) was used for accurately measuring dimensions of Metal moulds prepared for testing hardness of TiO$_2$GIC powder used as filling material in common dental practices. The metal mold of about 9.5X1mm was prepared for testing Vicker's micro-hardness, Flexural strength, Compressive strength, and Surface morphology (scanning electron microscopy). The metal blocks of 4x4 x 1mm were made for carrying out shear bond strength on both enamel and dentin portions of tooth [198].

3.5.5.2 *Preparation of sample:*

TiO_2GIC cement circular samples measuring 9.5 x 1mm (n=50) for all different concentrations i.e groups such as conventional control E-1 (0% TiO_2GIC), experimental group E-2 (3% TiO_2GIC), experimental group E-3 (5% TiO_2GIC), experimental group E-4 (7% TiO_2GIC) and experimental group E-5 (10% TiO_2GIC) were made in Metal molds according to manufacturer's instructions. All concentrations of powder samples were mixed with poly-acrylic acid to get soft and creamy mixture which was loaded into cylindrical metal mold. The hardened TiO_2GIC cement circular blocks (9.5X1mm) of different concentrations were obtained after sometime which were removed from metal mold. Then, these different concentrations of TiO_2GIC samples were placed in epoxy mounting die to carry out cold mounting of these samples at room temperature for about 20-30 minutes to get completely dried TiO_2GIC cement samples.The silicon carbide paper grits of different sizes (1000, 2400 and 4000) and diamond pastes of 1-6 microns was used in grinding machine (PN: zl01244575.4 Nanjing: Scientific, Instrument Measurement & Control Co; Ltd, China) to carry out smothering and polishing of samples. The total of 50 samples were made ready to perform Vicker's micro-hardness test out of which, 10 TiO_2GIC cylinders belonged to conventional control group E-1 (0% TiO_2-Nps), 10 TiO_2GIC cement samples of experimental group E- 2 (3% TiO_2-Nps), 10 TiO_2GIC cement samples of experimental group E- 3 (5% TiO_2-Nps), 10 TiO_2GIC cement samples of experimental group E- 4 (7% TiO_2-Nps) and 10 TiO_2GIC cement samples of experimental group E- 5 (10% TiO_2-Nps) [198].

3.5.5.3 *Testing of Vicker's micro-hardness of TiO_2GIC cement samples at different concentrations:*

The ISO: 9001:2008 certified diamond Indentor having 300 gm or 3N force was used to Perform Vicker's micro-hardness test on prepared cicular blocks. The Vicker's hardness tester (Model: 401 Mud, S/N: 414, Wolpertw group, Atlanta, USA) was used. The Vicker's hardness tester was attached to a microscope (Nikon- 514770, Tokyo, Japan) for complete visualization of indents as well as diagonal lengths such as d1 and d2. The 3 indentations on each specimen were employed for 15 seconds. The Vicker's micro-hardness test is utilized under ISO 9917-1:2007 and preferred because it can measure errors more accurately even on small and rounded surfaces [198].

3.5.5.4 *Testing of compressive strength of TiO_2GIC cement samples at different concentrations:*

The two flat metal disks in universal testing machine (Shenzhen SANS: testing machine co; Ltd,. Tokyo, China) was used for compressive strength testing, of prepared TiO_2GIC cement samples at all different concentrations. These TiO_2GIC cement samples were subjected to compressive load at cross speed of about 1mm/min mpa. This load wasn't stopped for a moment and was continued to apply till entire TiO_2GIC cement samples broke. This procedure was repeated for all 10 TiO_2GIC cement samples at different concentrations and finally results and measurements were recorded and obtained [198].

3.5.5.5 *Testing of flexural strengthof TiO$_2$GIC cement samples at different concentrations:*

The TiO$_2$GIC circular blocks (9.5 x 1mm) of different concentrations such as as conventional control group E-1 (0% TiO$_2$GIC), experimental group E-2 (3% TiO$_2$GIC), experimental group E-3 (5% TiO$_2$GIC), experimental group E-4 (7% TiO$_2$GIC) and experimental group E-5 (10% TiO$_2$GIC) were used for flexural strength testing having n= 10 for each group. The three points bending was performed in Universal Testing Machine (Shenzhen SANS: Testing machine Co; Ltd. Tokyo, China)to test flexural strength of prepared TiO$_2$GIC cement samples. Then, each prepared TiO$_2$GIC cement sample was placed in cylinder having opening of about 10 mm in diameter. Afterwards, total load with slow increase at cross speed of 1mm/min mpa was applied and ensured. When TiO$_2$GIC cement sample broke and divided into two completely equal parts, load application was immediately stopped.This procedure was repeated for all 10 TiO$_2$GIC cement samples at different concentrations and finally results and measurements were recorded and obtained [198].

3.5.5.6 *Testing of shear bond strength of TiO$_2$GIC cement samples at different concentrations:*

100 freshly extracted, human anterior teeth were stored in 0.1% thymol solution and were used for measurement of shear bond strength to both enamel and dentin part of the human tooth. The teeth for enamel and dentin shear bond testing were mounted in the epoxy resin. These teeth were divided into 10 different subgroups i.e 5 for measuring enamel bond strength with conventional control group E-1 (0% TiO$_2$GIC), experimental group E-2 (3% TiO$_2$GIC), experimental group E-3 (5% TiO$_2$GIC),experimental group E-4 (7% TiO$_2$GIC) and experimental group E-5 (10% TiO$_2$GIC) and in same manner they were divided into 10 different subgroups for measuring dentinal bond strength with conventional control group E-1 (0% TiO$_2$GIC), experimental group E-2 (3% TiO$_2$GIC), experimental group E-3 (5% TiO$_2$GIC),experimental group E-4 (7% TiO$_2$GIC) and experimental group E-5 (10% TiO$_2$GIC). Each subgroup of both enamel and dentin contained 10 teeth each initially these samples of TiO$_2$GIC cement samples at different concentrations i.e 0% TiO$_2$GIC, 3% TiO$_2$GIC, 5% TiO$_2$GIC, 7% TiO$_2$GIC, and 10% TiO$_2$GIC, for testing both enamel and dentin shear bond strength were fixed in depoxi steel resin (magic depoxi steel) after labeling them. These TiO$_2$GIC cement sample blocks of about 4x4 x1mm at different concentrations were developed in metal mold as per manufacturer's recommendations. The enamel labial surfaces of all teeth were properly finished and polished with 400 and 800 silicon carbide abrasive paper in metallographic polishing machine (PN: zl01244575.4 Nanjing: Scientific, Instrument Measurement & Control Co; Ltd, Tokyo, China). Following, this all 4x4x1mm blocks of different concentrations of TiO$_2$GIC cement samples were attached to enamel labial surfaces of all teeth and cleaned in an ultrasonic cleaning machine (Branson; Smith Kline Company; C.A, USA) for at least one minute is this was carried out for enamel bond strength testing.

The labial surface of tooth was reduced to almost 1.5 mm with high speed diamond bur to get dentine part of tooth. Then, tooth surface was prepared, finished and polished with 400 as well as 800 silicon carbide abrasive paper in metallographic polishing machine having a frequency converter (PN: zl01244575.4 Nanjing: Scientific, Instrument Measurement & Control Co; Ltd, Tokyo, China). Then, all 4x4 x1mm blocks of different concentrations of TiO$_2$GIC cement samples were attached to dentinal surfaces of all teeth and cleaned in an ultrasonic cleaning

machine (Branson; Smith Kline Company; C.A, USA) for at least one minute. The shear bond strength testing for both enamel and dentine was held in Universal Testing Machine (Shenzhen SANS: Testing Machine Co; Ltd, Tokyo, China) with cross speed of 1mm/min mpa which meant that all TiO$_2$GIC cement sample blocks at different concentrations were attached to enamel and dentin surfaces which were held tightly in mounting jig prepared. Then, force was applied at interface of TiO$_2$GIC cement sample blocks attached to both enamel and dentin, using metal pin. After application of force, all TiO$_2$GIC cement sample blocks got detached from dental surfaces of both enamel and dentin. The bond between TiO$_2$GIC cement sample blocks and dental surfaces (both enamel and dentine) broke at interface followed by stopping the force ultimately. Finally, all details were recorded and measured. [198].

3.5.5.7 *Scanning electron microscopic analysis and spectrum mapping for compositional analysis of TiO$_2$GIC cement samples at different concentrations:*

The broken parts of TiO$_2$GIC cement sample blocks (9.5x1 mm) for all different concentrations of groups such as conventional control group E-1 (0% TiO$_2$GIC), experimental group E-2 (3% TiO$_2$GIC), experimental group E-3 (5% TiO$_2$GIC), experimental group E-4 (7% TiO$_2$GIC) and experimental group E-5 (10% TiO$_2$GIC), after compressive strength testing were finished as well as polished with 400; 1000; 1500; silicon carbide abrasive paper in metallographic polishing machine having frequency converter (PN: zl01244575.4 Nanjing: Scientific, Instrument Measurement & Control Co; Ltd, Tokyo, China). Later, all these, TiO$_2$GIC cement sample blocks were cleaned in ultrasonic cleaning machine (Branson; Smith Kline Company; C.A, USA) with completely pure distilled water for about five minutes. These were then, stuck tightly with carbon conductive tape on aluminum stub in a sequence. All TiO$_2$GIC cement sample blocks were sputter coated in sputter coating machine (Quorum: technologies; ltd. ashford, ken; England) for at least 30 minutes. Then, all these TiO$_2$GIC cement sample blocks were kept tight in specimen holder of SEM (Nova; Nanosem; 430; FEI Company, 4022 261 49391-S Column feg SIRON Prep, Austin, Texas, USA) and cross-section of all TiO$_2$GIC cement sample blocks were observed with flow of secondary electrons at different magnifications. This was carried out for compositional analysis by spectrum mapping and surface morphology by SEM [198].

3.6 *Statistical analysis:*

The SPSS version 24.00 (IBM's Corporations, Armonk-s, N.Y; USA) was used to conduct the statistical analysis. One-way ANOVA test and POST HOC TUKEY test was used for single and multiple comparisons. The significance level for the current study was accounted at *P-value* < 0.05.

Chapter-4

Results:

Present study was designed to synthesize Titania (TiO$_2$ Nps) following three different routes by using *Bacillus coagulans, Mentha spicata* and *Conventional hydrothermal heating* process.These three types of TiO$_2$ Nps were then characterizsed by standard protocols using XRD, DRS, AFM, SEM, EDX, FTIR, DLS and Raman for size, shape, phase form, surface morphology, topography,functional compounds and elemental composition. These Nps were tested for their antimicrobial activity by agar disc diffusion test and were then investigated for their biocvompatibility via MTT Assay test. The Titania (TiO$_2$ Nps) displaying comparatively more antimicrobial activity and biocompatibility were induced in conventional GIC at different concentrations to produce an innovative Titania (TiO$_2$ Nps) based dental GIC restorative material. This innovative restorative material was tested for their mechanical properties such as micro-hardness, compressive strength, flexural strength, shear bond strength and surface morphology.

4.1 Phase-I: Synthesis of Titania (TiO$_2$ Nps):

4.1.1   Visual color change of Titania (TiO$_2$ Nps) by Bacillus coagulans:

The *Bacillus coagulans* culture solution was yellowish-cream in color initially which turned to white after the experiment indicating the formation of Titania (TiO$_2$ Nps) (Figure-4.1).

Figure-4.1: Synthesis of Titania (TiO$_2$ Nps) by Bacillus coagulans: (a) Bacillus coagulansculture solution, (b) Titania (TiO$_2$ Nps) in solution form , (c) Cake form of Titania (TiO$_2$ Nps) and (d) Fine powdered form of Titania (TiO$_2$ Nps) .

4.1.2 Visual color change of Titania (TiO$_2$ Nps) by Mentha spicata:

The *Mentha spicata* substrate solution was green in color before experiment and changed to white color after the experiment confirming the formation of Titania (TiO$_2$ Nps) (Figure-4.2).
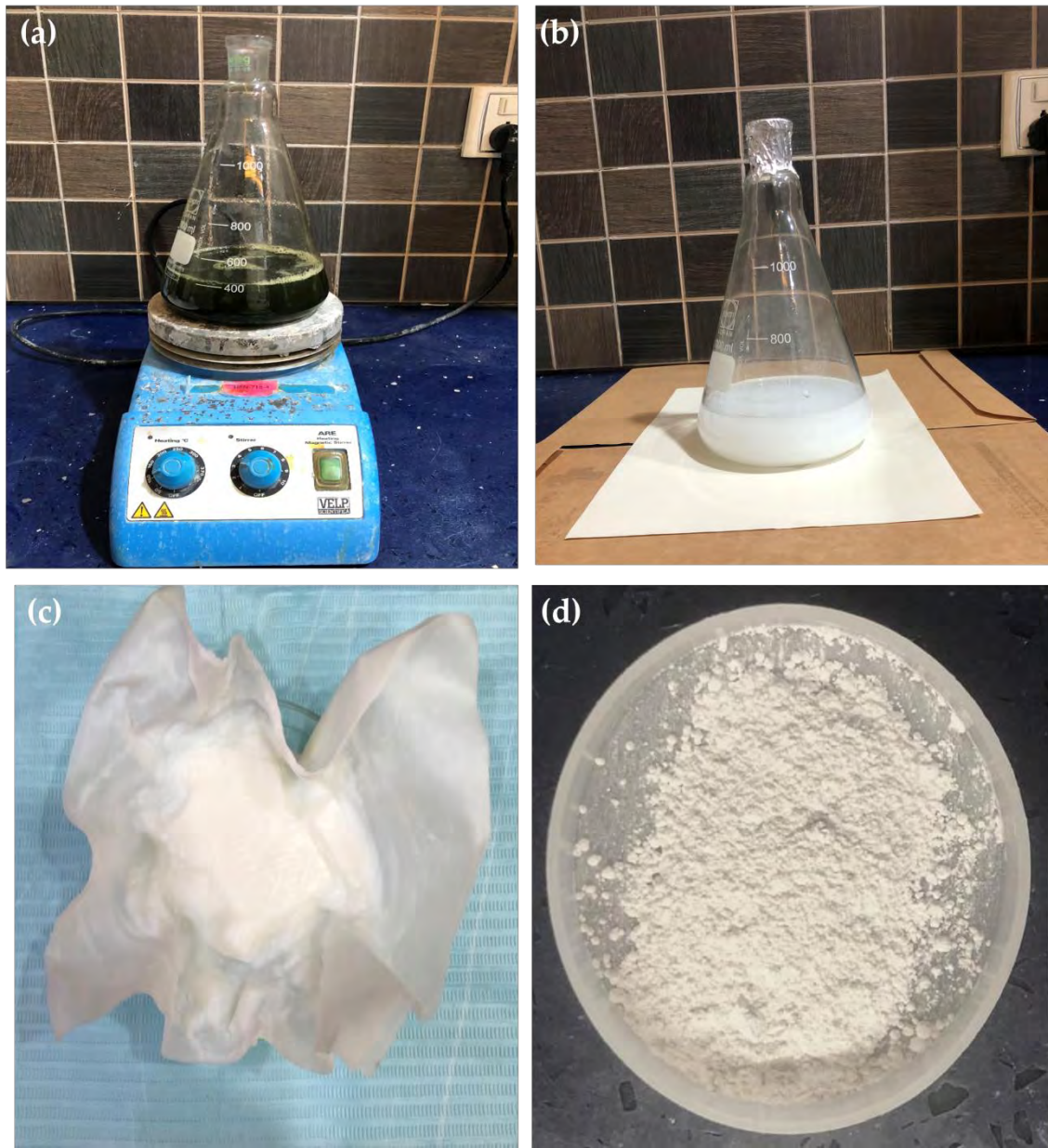
Figure -4.2: Synthesis of Titania (TiO$_2$ Nps) by Mentha spicata: (a) Mentha spicata substrate solution, (b) Titania (TiO$_2$ Nps) in solution form, (c) Cake form of Titania (TiO$_2$ Nps) and (d) Fine powdered form of Titania (TiO$_2$ Nps).

4.1.3 Visual color change of Titania (TiO$_2$ Nps) by Conventional hydrothermal heating:

The TiCl$_4$ substrate solution was black in color before the experiment and changed to white color after the experiment confirming the formation of Titania (TiO$_2$ Nps) (Figure-4.3).
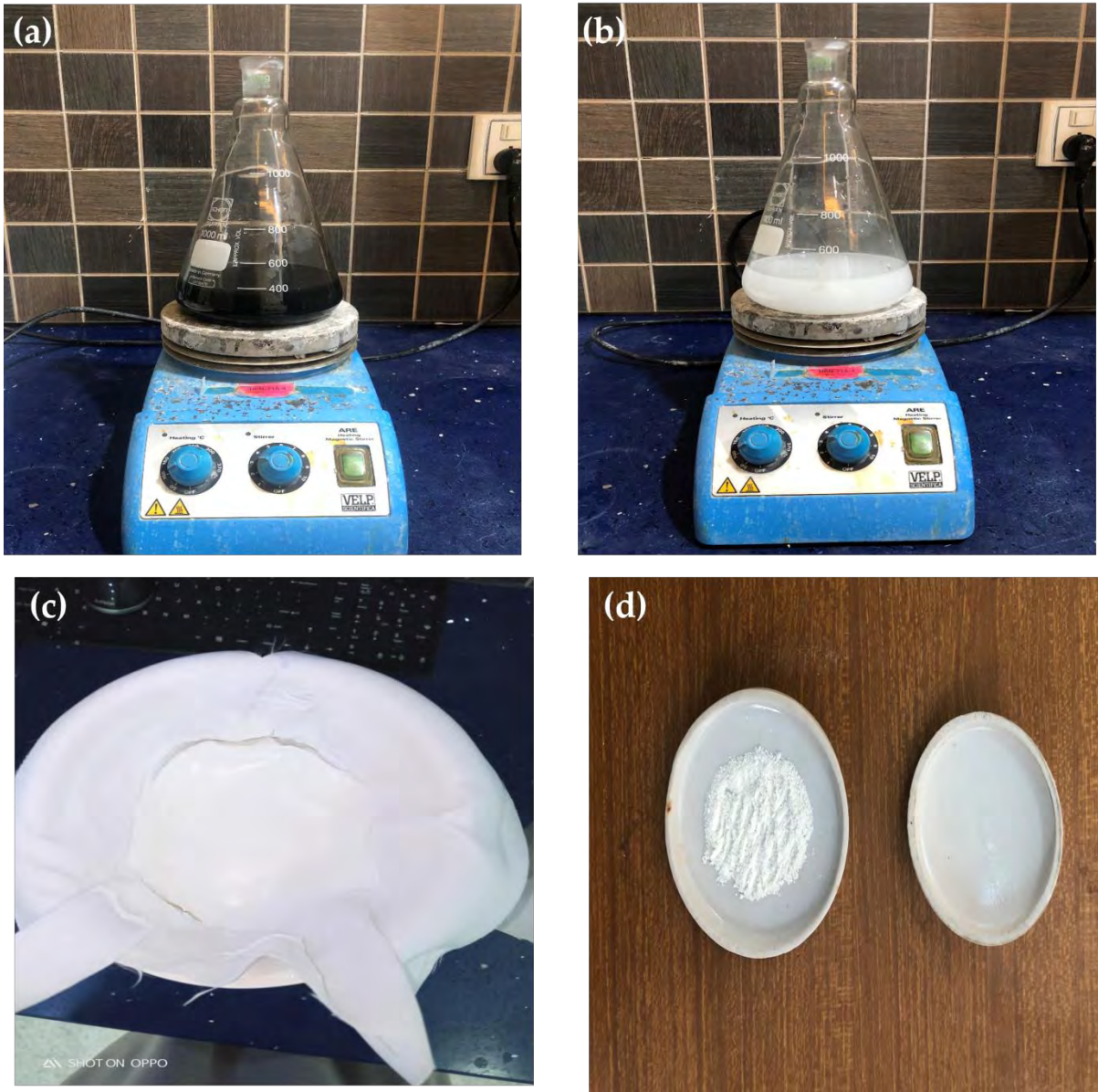
Figure-4.3: Synthesis of Titania (TiO₂-Nps)by Conventional hydrothermal heating: (a) Titanium tetrachloride substrate solution, (b) Titania (TiO₂-Nps) in solution form, (c) Cake form of Titania (TiO₂-Nps) and (d) Fine powdered form of Titania (TiO₂-Nps).

4.2 Phase-II: Characterization of Titania (TiO₂-Nps):

4.2.1 XRD analysis of Titania (TiO₂-Nps) for crystalline size and phase:

X-ray diffraction analysis was carried out to the ascertain size of crystalline size and phase of Titania (TiO₂-Nps) synthesized by *Bacillus coagulans, Mentha spicata* and *Conventional hydrothermal heating*. The fine powdered samples of all different types of Titania (TiO₂-Nps) were placed on XRD grid for analysis of different peaks at 2Θ to find out their phases i.e Anatase, Rutile or Brookite.

Crystalline size can be determined by Debye Scherrer's equation:

$$T = \frac{K\lambda}{B\,Cos\,\Theta}$$

1. *T* = grain-size of crystalline.
2. K = shape factor having constant value = 0.9.
3. λ = **x-raywavelength,** CuK_α=1.5406A°
4. *β* = full width at half maximum (**FWHM**) after subtracting instrumental line broadening, **radians**. It is denoted as Δ(2*Θ*) and *Θ* is **Bragg** angle.

4.2.1.1 XRD analysis of Titania (TiO₂ Nps) synthesized by Bacillus coagulans:

XRD pattern of Titania (TiO₂ Nps) synthesized by *Bacillus coagulans* was found to be in complete accordance with JCPDS card no: 01-071-1167 that showed main peak (101) of anatase phase predominantly at 2*Θ* = 25.38°. Other peaks were observed at (004) 37.98°, (200) 48.14°, (211) 54.12°, (213) 62.77°, (116) 68.59° and (301) 75.17°. The Titania (TiO₂-Nps) produced by *Bacillus coagulans* were found to be in 100% pure anatase phase (Figure -4.4).
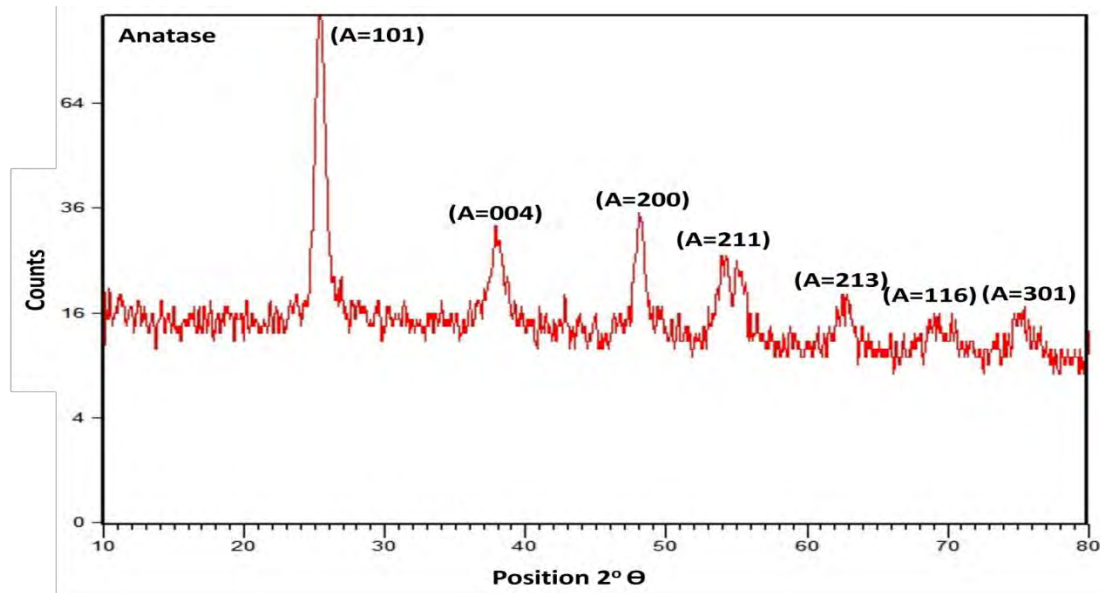
Figure-4.4: XRD pattern, of Titania (TiO₂ Nps) synthesized by Bacillus coagulans depicting various prominent peaks of anatase.

The crystalline size of these Titania (TiO₂ Nps) was calculated by Debye - Scherrer's formula which was found to be 21.84 nm (Table-4.1).

Table-4.1: *Crystalline size calculation of Titania (TiO₂ Nps) synthesized by Bacillus coagulans through Debye-Scherrer's equation.*

No.	B obs. [°2Th]	B std. [°2Th]	Peak pos. [°2Th]	B struct. [°2Th]	Crystalline size [Å]
1	0.669	0.008	25.38	0.661	123
2	0.629	0.008	37.98	0.621	135
3	0.472	0.008	48.14	0.464	188
4	0.629	0.008	54.12	0.621	144
5	0.629	0.008	55.2	0.621	144
6	0.944	0.008	62.77	0.936	99
7	0.152	0.008	75.175	0.144	696
					218.4285714 Å Size in nm = 21.84nm

4.2.1.2 *XRD analysis of Titania (TiO₂ Nps) synthesized by Mentha spicata plant :*

XRD pattern of Titania (TiO₂ Nps) synthesized by *Mentha spicata* was found to be in accordance with JCPDS Card no: 00-001-0562 that showed existence of main peak (101) of anatase phase basically at $2\Theta = 25.39°$. Other peaks observed were at (103) 37.89°, (200) 48.14°, (105) 53.97°, (213) 62.77°°, (116) 68.89°, (107) 75.37° The Titania (TiO₂ Nps) synthesized by *Mentha spicata* were observed to be lying in 100% pure anatase phase (Figure-4.5).
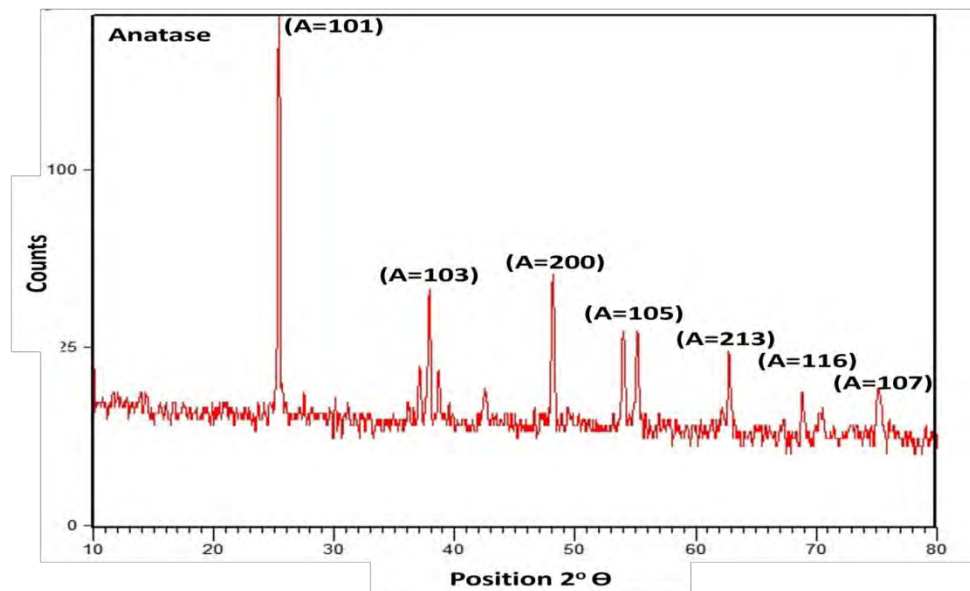
Figure-4.5: XRD pattern, of Titania (TiO₂ Nps) synthesized by Mentha spicata depicting various prominent peaks of anatase.

The crystalline size of Titania (TiO₂ Nps) synthesized by *Mentha spicata* was calculated by Debye - Scherrer's formula which was found to be 37.6 nm (Table-4.2).

Table-4.2:   *Crystalline size of Titania (TiO₂ Nps) synthesized by Mentha spicata through Debye- Scherrer's equation.*

No.	B obs. [°2Th]	B std. [°2Th]	Peak pos. [°2Th]	B struct. [°2Th]	Crystalline size [Å]
1	0.216	0.008	25.397	0.208	392
2	0.196	0.008	37.896	0.188	447
3	0.216	0.008	38.651	0.208	405
4	0.472	0.008	42.503	0.464	184
5	0.236	0.008	48.147	0.228	382
6	0.236	0.008	53.979	0.228	391
7	0.216	0.008	55.172	0.208	431
8	0.196	0.008	62.773	0.188	495
9	0.236	0.008	68.899	0.228	423
10	0.472	0.008	70.384	0.464	210
					376 Å Size in nm = 37.6nm

4.2.1.3 XRD analysis of Titania (TiO₂ Nps) synthesized by Conventional hydrothermal heating:

XRD pattern of Titania (TiO₂ Nps) synthesized by *Conventional hydrothermal heating* was found to be in complete accordance with JCPDS card no 01-071-1166 that completely showed main peak (101) of anatase phase predominantly at 2Θ = 25.32°. Other peaks were observed at (103) 37.00°, (004) 37.84°, (112) 38.61°, (200) 48.12°, (105) 53.98°, (211) 55.16°·, (213) 62.30°, (204) 62.82° and (116) 68.92°. The only rutile peak observed at 2Θ = 27.45° was in collaboration with JCPDS card no 00-077-0440. The Titania (TiO₂ Nps) produced by *Conventional hydrothermal heating* were found to be in 82% pure anatase phase and 18% rutile phase (Figure-4.6).
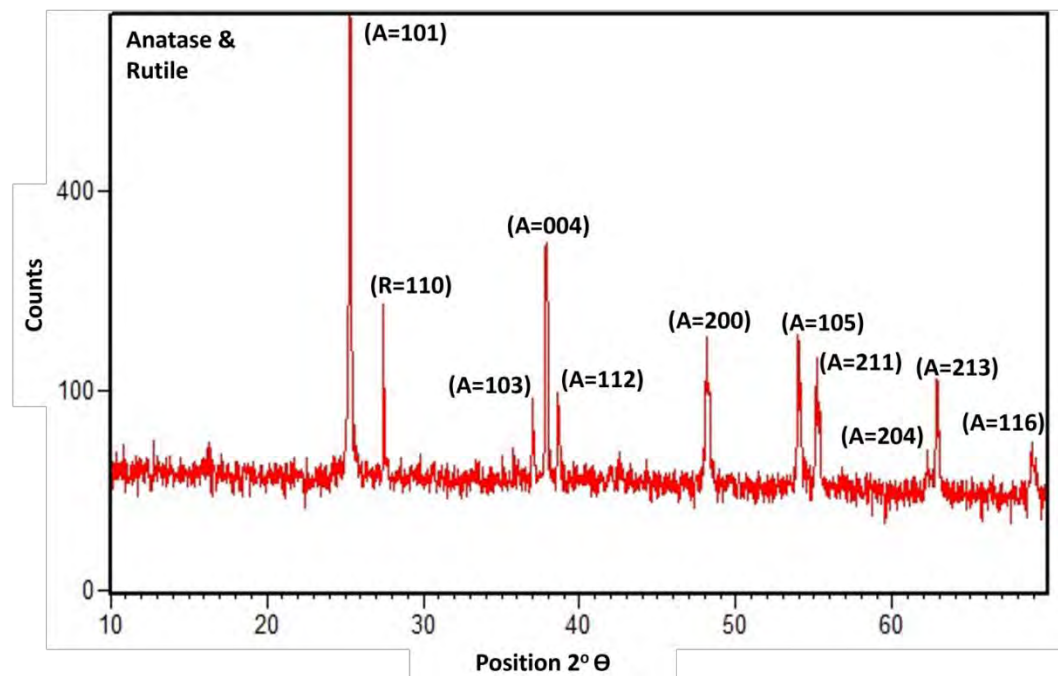
Figure-4.6: XRD pattern, of Titania (TiO₂ Nps) synthesized by Conventional hydrothermal heating depicting various prominent peaks of anatase with one rutile peak.

The crystalline size of Titania (TiO₂ Nps) synthesized by *Conventional hydrothermal heating* was calculated by the Debye - Scherrer's formula which was found to be 52.28 nm (Table-4.3).

Table-4.3: Crystalline size of Titania (TiO₂ Nps) synthesized by Conventional hydrothermal heating through Debye- Scherrer's equation.

No.	B obs. [°2Th]	B std. [°2Th]	Peak pos. [°2Th]	B struct. [°2Th]	Crystalline size [Å]
1	0.11	0.008	25.323	0.102	798
2	0.078	0.008	27.454	0.07	1168
3	0.59	0.008	37.004	0.582	144
4	0.59	0.008	37.849	0.582	144
5	0.59	0.008	38.613	0.582	145
6	0.59	0.008	48.123	0.582	149
7	0.59	0.008	53.985	0.582	153
8	0.12	0.008	55.168	0.112	800
9	0.288	0.008	62.301	0.28	332
10	0.096	0.008	62.823	0.088	1058

11	0.12	0.008	68.926	0.112	860
					522.8181818 Å Size in nm = 52.28 nm

4.2.1.4 Summary of XRD analysis Results for crystalline size and phase:

XRD pattern of Titania (TiO$_2$ Nps) synthesized by *Bacillus coagulans, and Mentha spicata* were found to be in 100% pure anatase phase. On the other hand, *Conventional hydrothermal heating* displayed 82% anatase phase and 18% rutile phase .The crystalline size of Titania (TiO$_2$ Nps) synthesized by *Bacillus coagulans were 21.84 nm* where asTitania (TiO$_2$ Nps) synthesized by *Mentha spicata* and *Conventional hydrothermal heating were 37.60 nm and 52.28 nm* (Figure-4.7)
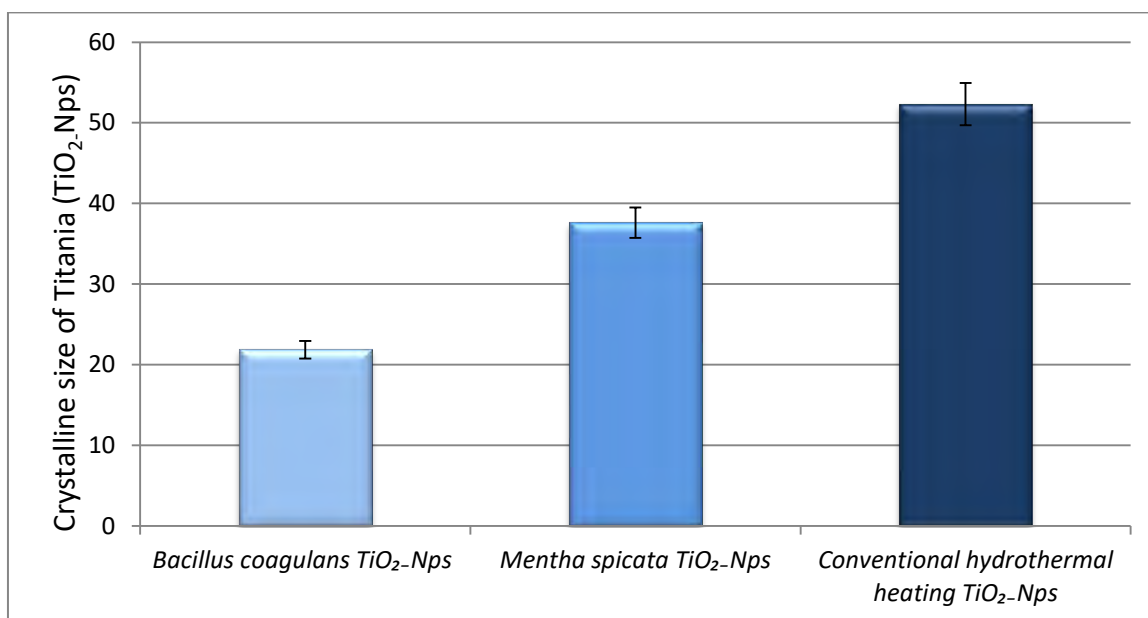
Figure-4.7: Differences in the crystalline size of Titania (TiO$_2$ Nps) synthesized by Bacillus coagulans, Mentha spicata and Conventional hydrothermal heating obtained after XRD analysis pattern.

4.2.2 DRS analysis of Titania (TiO$_2$ Nps) for confirmation of crystalline size:-

The Eg (band gap energy) for pure Titania (TiO$_2$ Nps) was taken from wave- length values corresponding to intersection points of horizontal and vertical areas in spectrum plotted from UV-Vis spectroscopy data in reflectance mode.The standard value for band gap energy (Eg =3.23 eV) was calculated by equation:

$$E (Eg) = hv = \frac{hc}{\lambda} \, eV$$

In this equation, h was plank's constant having value of 6.626 x 10^{-34} J/s and v was frequency.

Moreover, λ is wavelength where λ = c/v in which λ= 403 while c was speed of light with constant value of 3 x 10^8 m/s. By putting values:

$$E = \underline{6.6025 \times 10^{-34} \times 3 \times 10^8} \qquad = 3.23 \, eV$$

The band gap energy value verifies the crystalline size of the Titania (TiO$_2$ Nps). When the calculated band gap energy value is increased from the standard value of 3.23eV this confirms the smaller crystalline size of the Titania (TiO$_2$ Nps) formed but when the calculated energy band gap is decreased from the calculated value then larger crystalline size is of Nps is confirmed. Thus, inverse relationship exists between energy band gap and crystalline size. The absorbance mode in the DRS spectrum confirms the formation of Titania (TiO$_2$ Nps) between the wave length 200-600 cm^{-1}[199].

4.2.2.1 DRS analysis of Titania (TiO$_2$ Nps) synthesized by Bacillus coagulans:

The DRS spectrum confirmed the formation of Titania (TiO$_2$ Nps) by *Bacillus coagulans* at337nm wavelength. Theband gap energy calculated for Titania (TiO$_2$ Nps) synthesized by *Bacillus coagulans* was found to be 3.5 eV confirming that crystalline size of these Titania (TiO$_2$ Nps) was small (Figure-4.8).
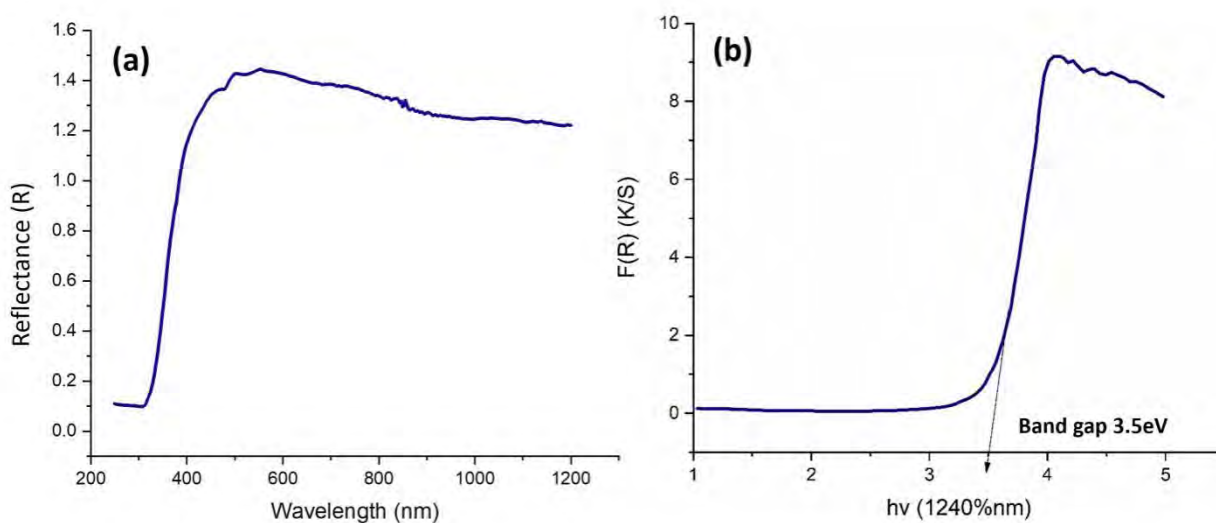
Figure-4.8: *DRS pattern scan of Titania (TiO$_2$ Nps) synthesized by Bacillus coagulans showing: (a) Formation at specific wave length, (b) Energy band gap confirming the small crystalline size of Titania (TiO$_2$ Nps).*

4.2.2.2 DRS analysis of Titania (TiO$_2$ Nps) synthesized by Mentha spicata plant:

The DRS spectrum confirmed the formation of Titania (TiO$_2$ Nps) by *Mentha spicata* at329 nm wavelength. Theband gap energy of Titania (TiO$_2$ Nps) synthesized by *Mentha spicata* was 3.2 eV attributing that crystalline size of these Titania (TiO$_2$ Nps) was medium (Figure-4.9).
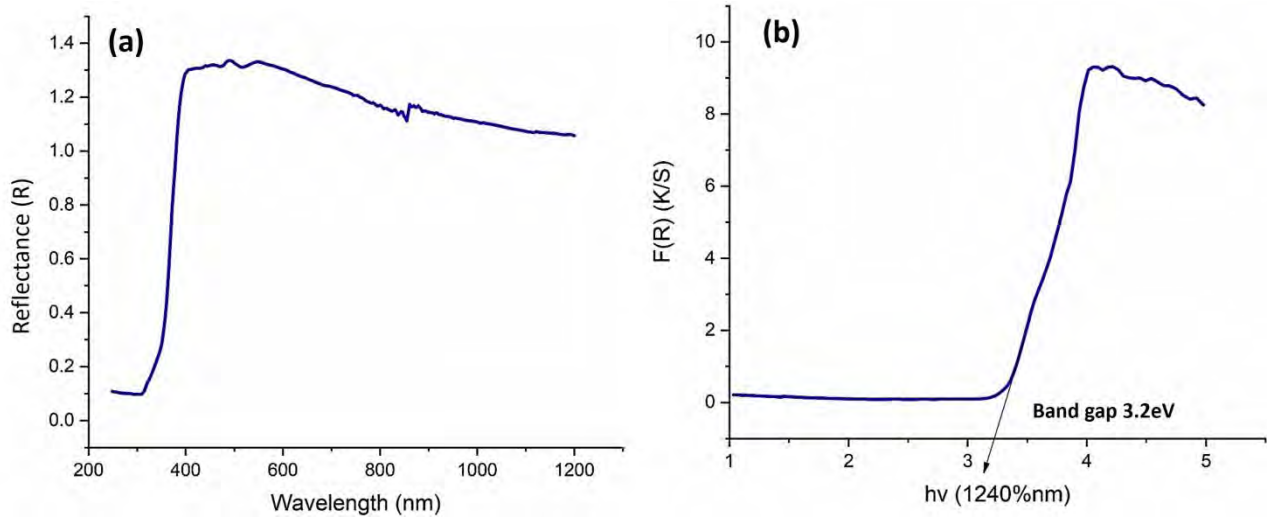
Figure-4.9: DRS pattern scan of Titania (TiO₂-Nps) synthesized by Mentha spicata showing: (a) Formation at specific wave length, (b) Energy band gap confirming the medium crystalline size of Titania (TiO₂-Nps).

4.2.2.3 DRS analysis of TiO₂-Nps synthesized by Conventional hydrothermal heating:

The DRS spectrum confirmed the formation of Titania (TiO₂-Nps) by *Conventional hydrothermal heating* at337 nm wavelength. TheTiO₂-Nps synthesized by *Conventional hydrothermal heating* calculated the band energy to be 2.9 eV. The crystalline size of these Titania (TiO₂-Nps) was comparatively the largest (Figure-4.10).
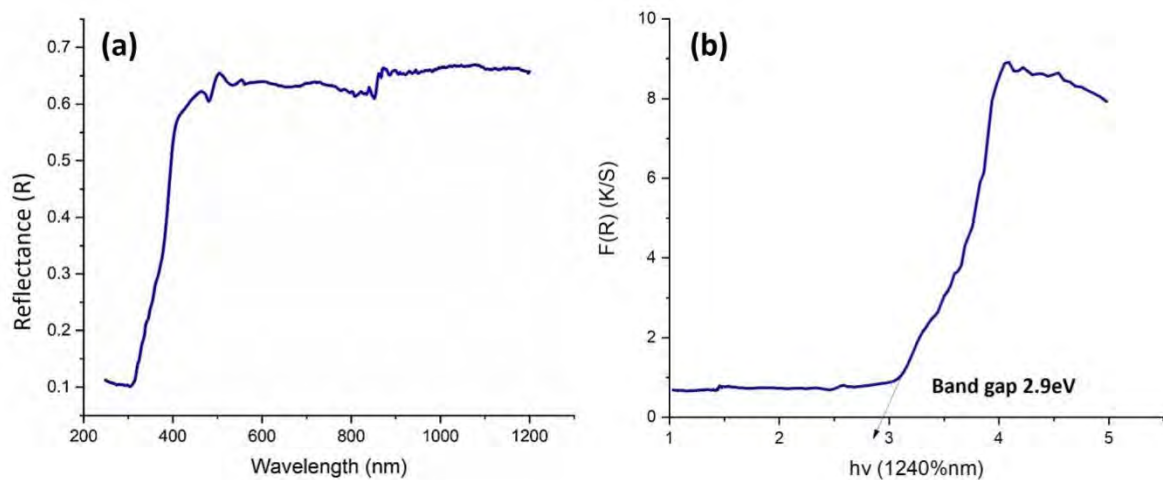
Figure-4.10: DRS pattern scan of Titania (TiO₂-Nps) synthesized by Conventional hydrothermal heating showing: (a) Formation at specific wave length, (b) Energy band gap confirming the larges crystalline size of Titania (TiO₂-Nps).

4.2.2.4 Summary of DRS analysis results for confirmation of crystalline size :

The band ga*P-value* s calculated by DRS spectrum for Titania (TiO₂-Nps) synthesized by different routes such as *Bacillus coagulans, Mentha spicata* and *Conventional hydrothermal heating* were observed to be at 3.5 eV, 3.2eV and 2.9 eV which verified that the crystalline size of Titania (TiO₂-Nps) synthesized by *Bacillus coagulans* was the smallest in comparison

to *Mentha spicata* and *Conventional hydrothermal heating* Titania (TiO_2-Nps) where crystalline sizes were found to be medium and larger comparatively (Figure-4.11).
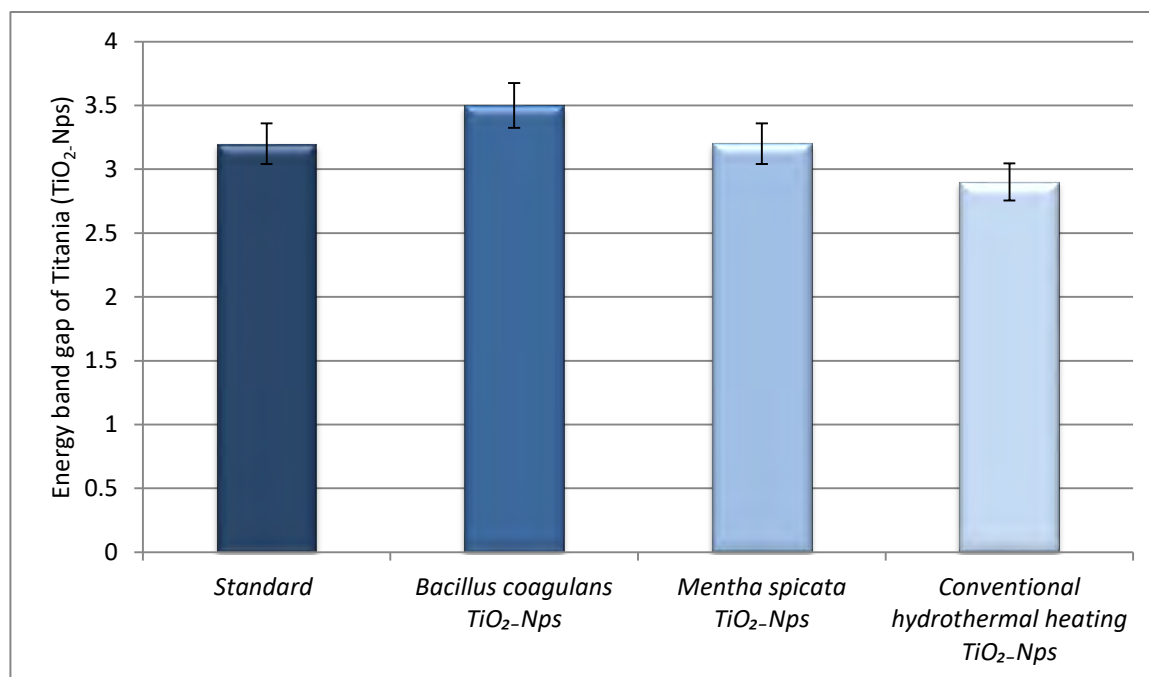
Figure-4.11: DRS pattern scan, comparing the energy band gap of Titania (TiO_2-Nps) synthesized by Bacillus coagulans, Mentha spicata and Conventional hydrothermal heating methods with the standard DRS value.

4.2.3 *AFM analysis of Titania (TiO_2-Nps) for the size, shape and surface topography:*

The AFM analysis was carried out to observe 3D topological map of surface of Titania (TiO_2-Nps) synthesized by *Bacillus coagulans, Mentha spicata* and *Conventional hydrothermal heating* methods for their size, shape, texture and roughness. The images of Titania (TiO_2-Nps) synthesized by *Bacillus coagulans, Mentha spicata* and *Conventional hydrothermal heating* were taken in tapping mode of AFM having scan rate of 0.5 Hz and scan resolution of 1024.

4.2.3.1 *AFM analysis of Titania (TiO_2-Nps) synthesized by Bacillus coagulans:*

The AFM scan of Titania (TiO_2-Nps) synthesized by *Bacillus coagulans* depicted predominantly spherical shape, small size, smooth surface having surface roughness of about Rms=4.485 (Figure-4.12).
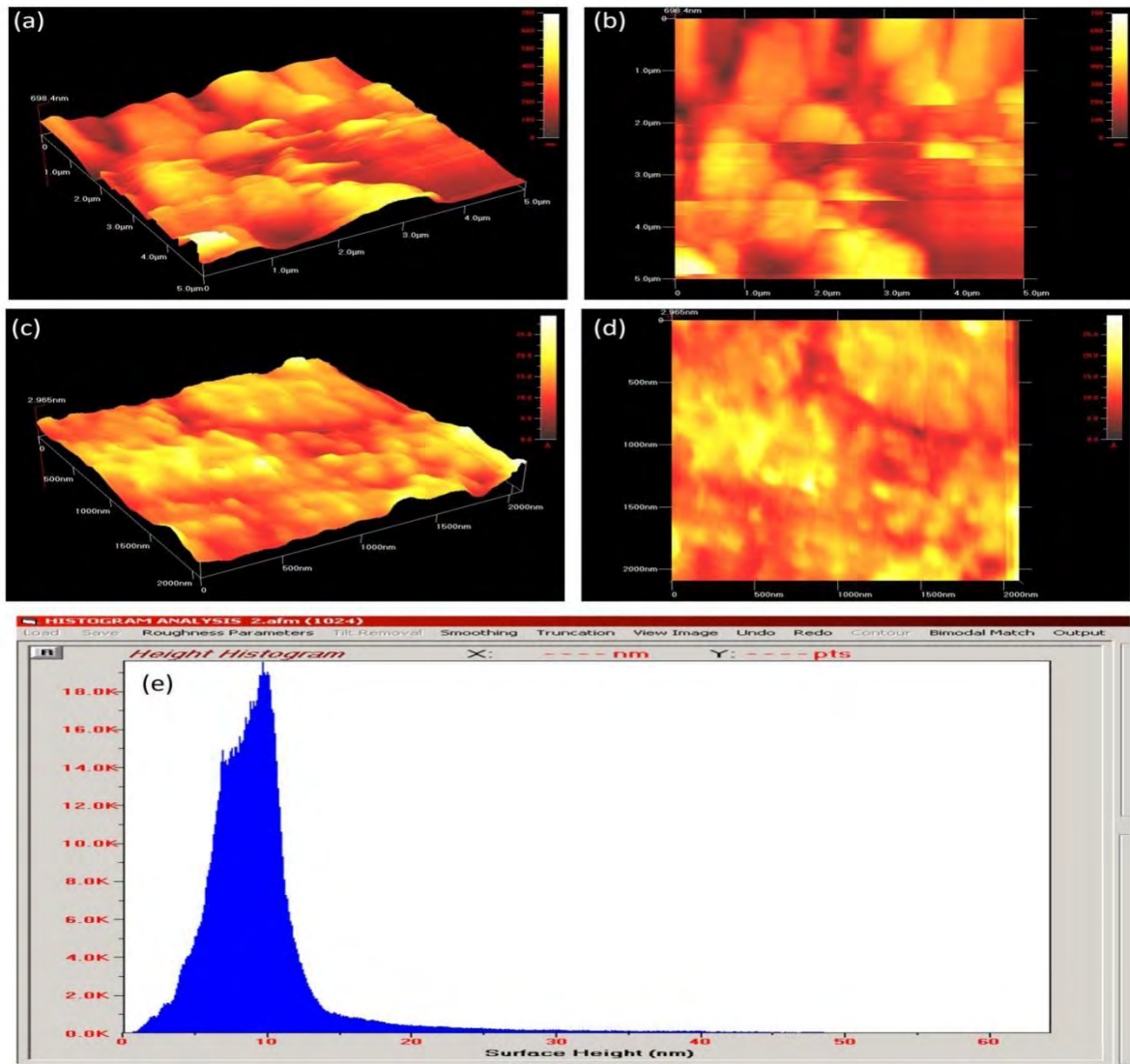
Figure-4.12: A three dimensional AFM image of Titania (TiO$_2$ Nps) synthesized by Bacillus coagulans showing : (a,b) Small size and spherical shape at low resolution, (c,d) Small size and spherical shape at high resolution and (e) Histogram showing minimum surface roughness value at highest peak intensity and lowest surface height confirming their smooth surface.

4.2.3.2 *AFM analysis of Titania (TiO$_2$ Nps) synthesized by Mentha spicata plant:*

The AFM scan of Titania (TiO$_2$ Nps) synthesized by *Mentha spicata plant* revealed their medium size having predominantly spherical shape with slightly irregular shaped particles. These Titania (TiO$_2$ Nps) were found to be less smooth having surface roughness of about Rms=5.693 (Figure-4.13).
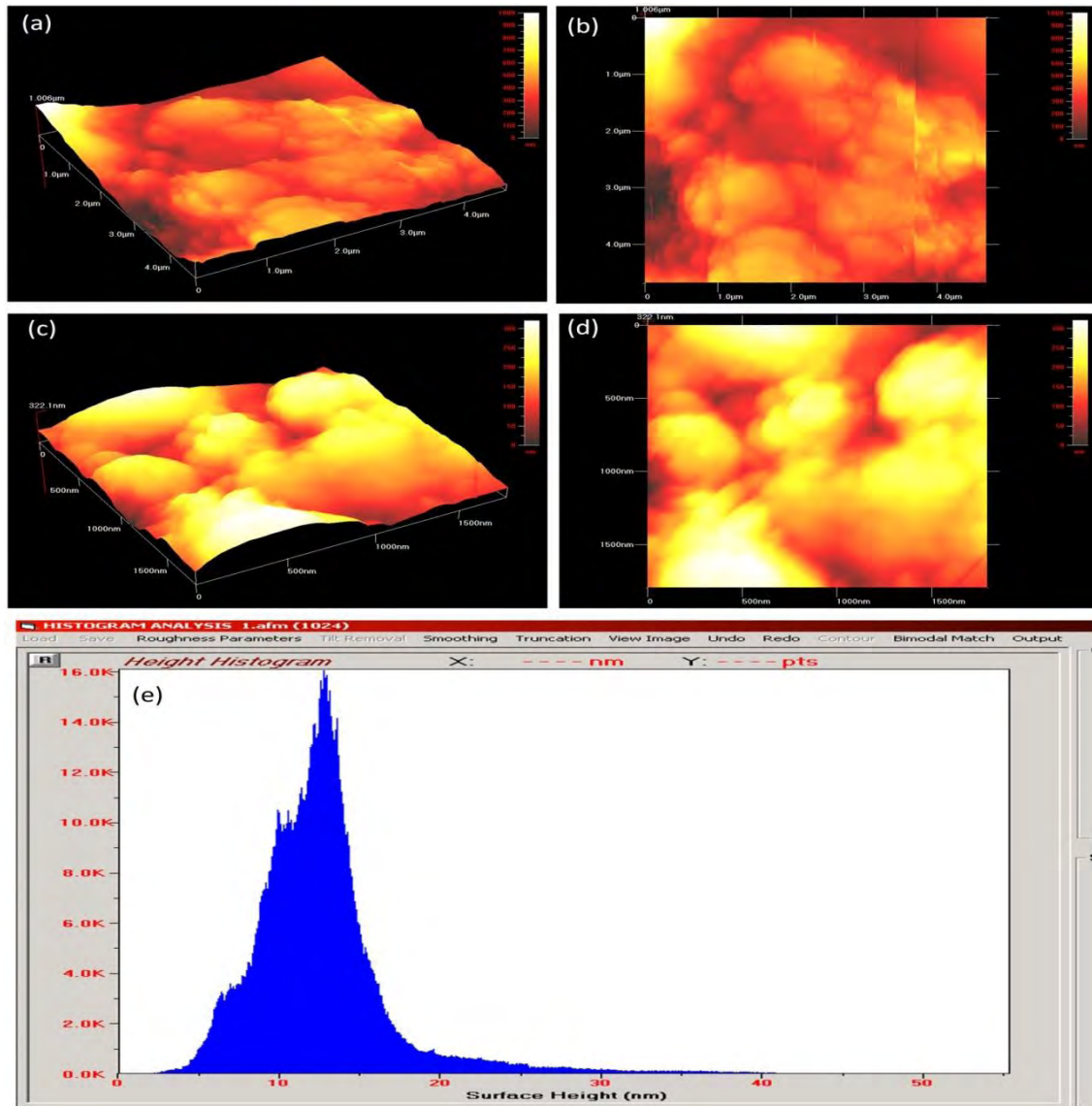
Figure-4.13: A three dimensional AFM image of Titania (TiO₂ Nps) synthesized by Mentha spicata showing: (a, b) Medium size and predominantly spherical shape with slightly irregular shaped particles at low resolution, (c, d) Medium size and predominantly spherical shape with slightly irregular shaped particles at high resolution and (e) Histogram showing medium surface roughness value at medium peak intensity and medium surface height confirming their less smooth surface.

4.2.3.3 *AFM analysis of Titania (TiO₂ Nps) synthesized by Conventional hydrothermal heating:*

The Titania (TiO₂ Nps) prepared by *Conventional hydrothermal heating* showed the large size having mixture of spherical with slightly more irregularly shaped particles in their AFM scan. The surface texture of these Nps was least smooth having surface roughness (Rms) value of about 8.275 respectively (Figure-4.14).
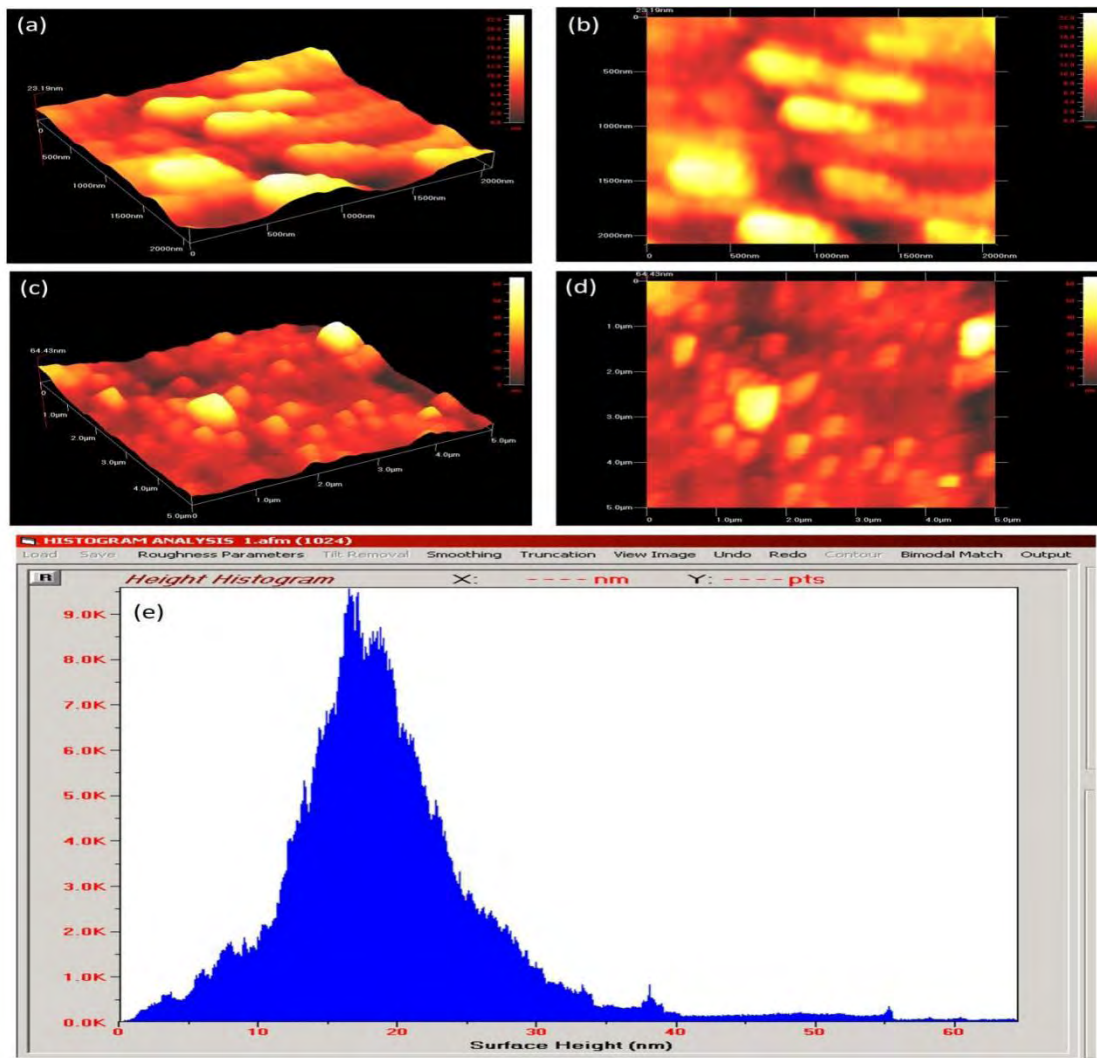
Figure-4.14: *A three dimensional AFM image of Titania (TiO₂ Nps) synthesized by Conventional hydrothermal heating showing: (a, b) Large size and predominantly spherical shape with slightly more irregular shaped particles at low resolution, (c, d) Large size and predominantly spherical shape with slightly more irregular shaped particles at high resolution and (e) Histogram showing maximum surface roughness value at lowest peak intensity and highest surface height confirming their least smooth surface.*

4.2.3.4 Summary of AFM analysis results for size, shape and surface topography:

The Titania (TiO₂ Nps) synthesized by *Bacillus coagulans* were found to be ideally small, predominantly spherical, highly smooth having surface roughness (Rms) value of 4.485. The Titania (TiO₂ Nps) formed by *Mentha spicata* revealedmedium size, predominately spherical with slightly irregular shaped particles, less smooth surface having surface roughness (Rms) value of 5.693. The Titania (TiO₂ Nps) synthesized by *Conventional hydrothermal heating* were of large size, predominantly spherical with slightly more irregular shaped particles, least smooth surface having surface roughness (Rms) values of about 8.275 respectively (Figure-4.15).
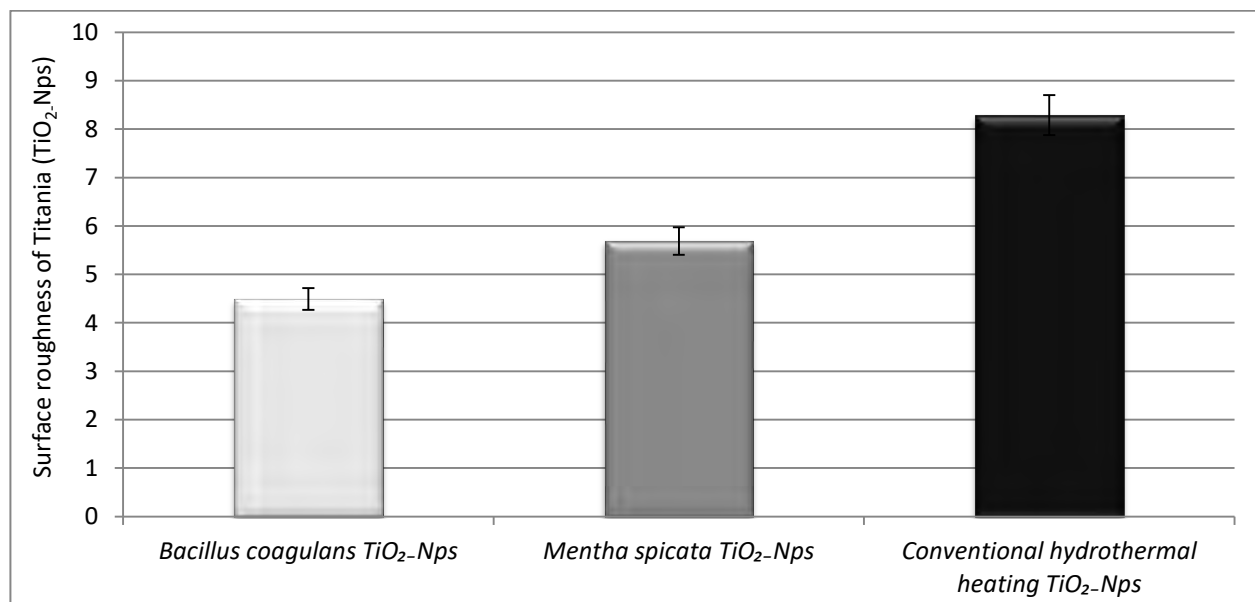
Figure-4.15: AFM analysis of Titania (TiO₂Nps) synthesized by Bacillus coagulans, Mentha spicata and Conventional hydrothermal heating confirming the surface roughness (RMS) values.

4.2.4 SEM analysis of Titania (TiO₂Nps)for particle size and shape:

All Titania (TiO$_2$ Nps) were investigated for surface morphology to calculate the size and shape utilizing scanning electron microscope (NOVA) Nanosem 430; FEI company, 4022 261 49391-S column FEG Siron Prep) at an accelerating voltage, 20.00 KV and working distance 15 mm.The particle size calculated by SEM is always greater than the crystalline size calculated by XRD.

4.2.4.1 *SEM analysis of Titania (TiO$_2$Nps) synthesized by Bacillus coagulans*:-

The SEM micrographs of Titania (TiO$_2$ Nps) synthesized by *Bacillus coagulans* displayed dominantly spherically shaped Nps found individually as well as in aggregates. The particle size of these Nps was found in the diameter of about 23 nm confirming their small size (Figure-4.16 a and b).
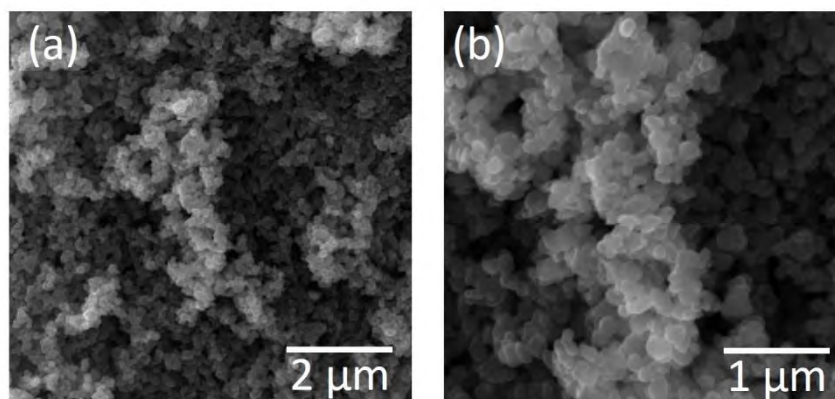
Figure-4.16: Scanning electron microscopic image of Titania (TiO$_2$Nps) synthesized by Bacillus coagulans showing small particle size and predominantly spherical shape at: (a) 2 kx ,(b) 1 kx .

4.2.4.2 *SEM analysis of Titania (TiO₂.Nps) synthesized by Mentha spicata plant:-*

The SEM micrographs of Titania (TiO₂.Nps) synthesized by *Mentha spicata* revealed presence of predominantly spherical shaped with slightly irregular shaped particles in an agglomerated manner. The particle size of these Nps was found to about 39 nm which confirmed their medium size (Figure-4.17a and b).
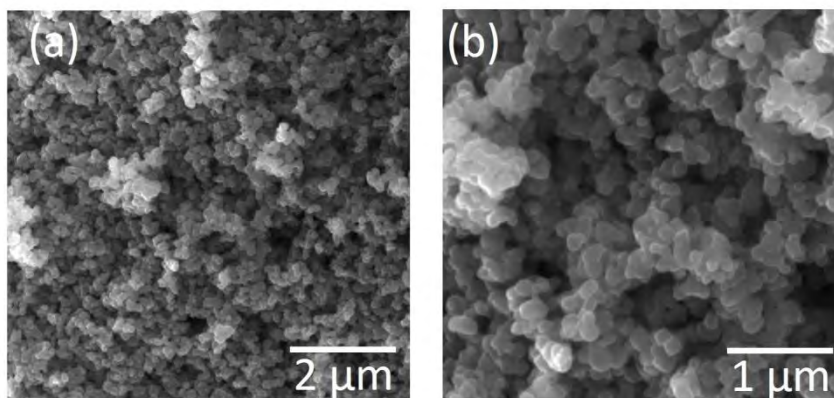
Figure-4.17: Scanning electron microscopic image of Titania (TiO₂.Nps) synthesized by Mentha spicata showing medium particle size and predominantly spherical with slightly irregular shaped particles at: (a) 2 kx ,(b) 1 kx.

4.2.4.3 *SEM analysis of Titania (TiO₂.Nps) synthesized by Conventional hydrothermal heating:-*

The SEM micrographs of Titania (TiO₂.Nps) synthesized by *Conventional hydrothermal heating* methods depicted predominantly spherical with slightly more irregular shaped particles in agglomeration form. The particle size of Titania (TiO₂.Nps) synthesized by *Conventional hydrothermal heating* was calculated to be 54 nm in diameter confirming their large particle size comparatively (Figure-4.18 a and b).
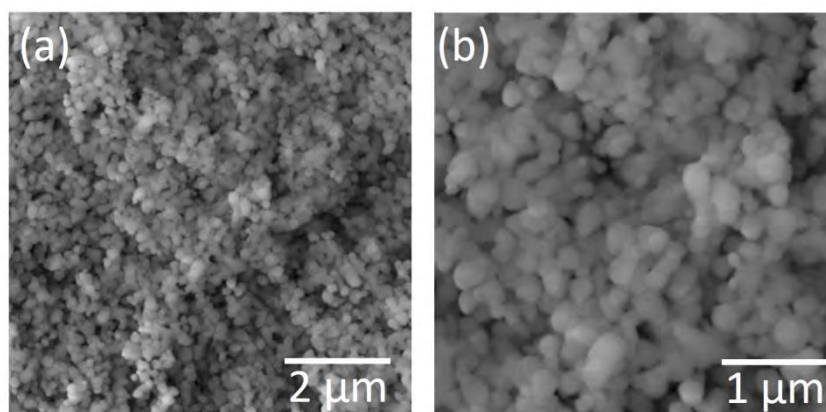
Figure-4.18: Scanning electron microscopic image of Titania (TiO₂.Nps) synthesized by Conventional hydrothermal heating showing large particle size and predominantly spherical with slightly more irregular shaped Nps at : (a) 2 kx ,(b) 1 kx .

4.2.4.4 *Summary of SEM analysis results for particle size and shape*:-

SEM micrographs displayed spherical shaped Titania (TiO$_2$-Nps) synthesized by *Bacillus coagulans* having smallest particle size of 23 nm. The Titania (TiO$_2$-Nps) synthesized by *Mentha spicata* revealed predominantly spherical with slightly irregular shaped Nps having medium particle size of about 39 nm. On the other hand, Titania (TiO$_2$-Nps) synthesized by *Conventional hydrothermal heating* demonstrated predominantly spherical with slightly more irregular shaped Nps having the large particle size of about 54 nm (Figure-4.19).
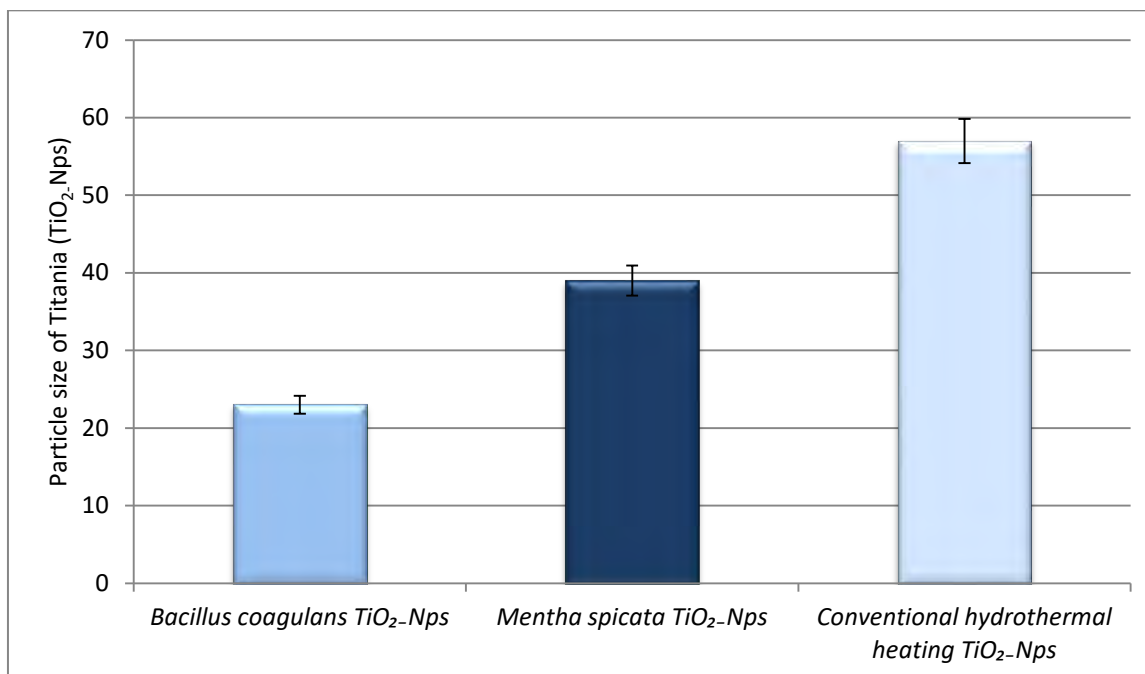
Figure-4.19:Scanning electron microscopic image of Titania (TiO$_2$-Nps) synthesized by Bacillus coagulans, Mentha spicata and Conventional hydrothermal heating methods showing their particle sizes.

4.2.5 *EDX analysis of Titania (TiO$_2$-Nps) for elemental composition in its spectrum*:-

The EDX spectrum Titania (TiO$_2$-Nps) synthesized by *Bacillus coagulans, Mentha spicata* and *Conventional hydrothermal heating* were investigated for the presence of their patent elemental composition along with any impurity if present.The weight% and atomic % of different elements in the spectrum of Titania (TiO$_2$-Nps) prepared by all the routes were calculated.

4.2.5.1 *EDX analysis of Titania (TiO$_2$-Nps) synthesized by Bacillus coagulans*:-

The EDX spectrum of Titania (TiO$_2$-Nps) synthesized by *Bacillus coagulans* revealed intense peak of titanium (Ti) and oxygen (O) in its spectrum. The weight % and atomic % of titanium in EDX spectrum was found to be 86.10% and 67.41% whereas Oxygen was 13.90% and 32.59% There was no additional peak observed in the EDX spectrum of these Nps (Figure - 4.20).
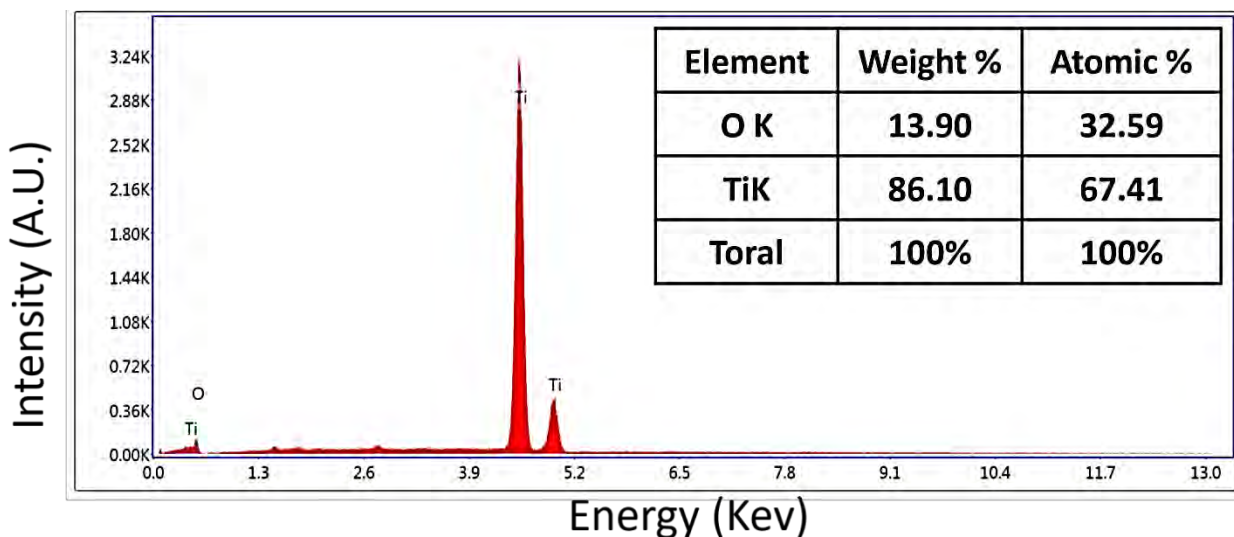
Figure-4.20: Energy dispersive x-ray spectroscopic analysis of Titania (TiO₂ Nps)
synthesized by Bacillus coagulans displaying the peaks of titanium and oxygen with weight
% and atomic %.

4.2.5.2 EDX analysis of Titania (TiO₂ Nps) synthesized by Mentha spicata:-

Intense peaks of titanium and oxygen were observed in EDX spectrum of these Titania (TiO₂ Nps) synthesized by *Mentha spicata plant*. The Titanium was available in 78.30 weight % and 54.65 atomic % while oxygen was in 21.70 weight % and 45.35 atomic %.There was no additional peak observed in the EDX spectrum of these Nps (Figure-4.21)
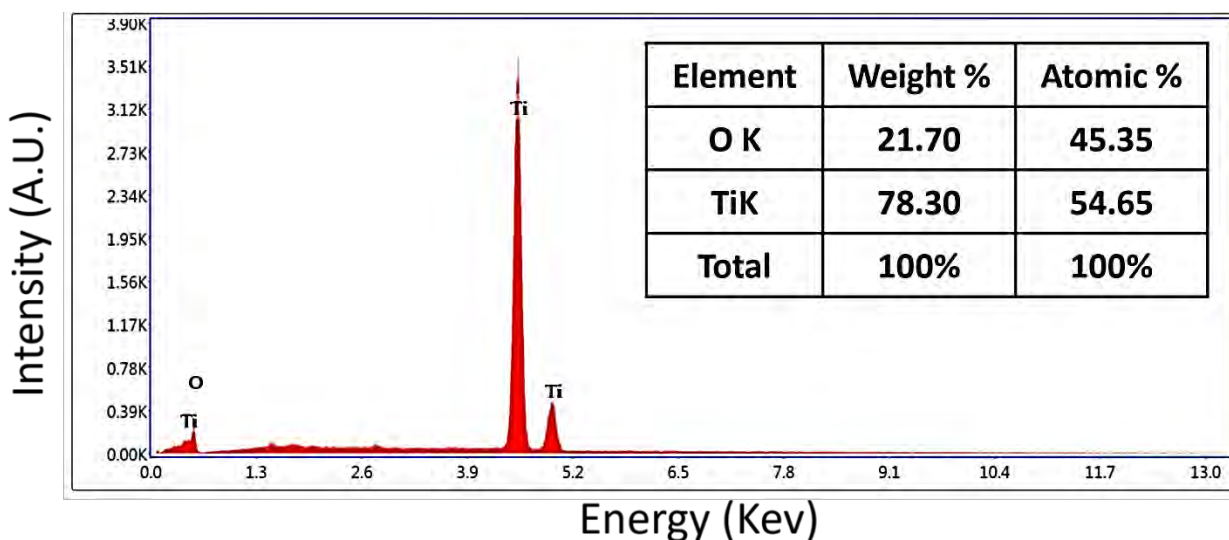
Figure-4.21: Energy dispersive x-ray spectroscopic analysis of Titania (TiO₂ Nps)
synthesized by Mentha spicatadisplaying the peaks of titanium and oxygen with weight %
and atomic %.

4.2.5.3 *EDX analysis of Titania (TiO$_2$ Nps) synthesized by Conventional hydrothermal heating:-*

The main peaks of tiatanium (Ti) and oxygen (O) were detected in EDX spectrum of Titania (TiO$_2$-Nps) synthesized by *Conventional hydrothermal heating*. The weight % and atomic % of main elements i.e Titanium was 76.28% and 51.79% whereas oxygen was 23.72% and 48.21% .There was no additional peak observed in the EDX spectrum of these Nps (Figure-4.22).

Element	Weight %	Atomic %
O K	23.72	48.21
TiK	76.28	51.79
Total	100%	100%
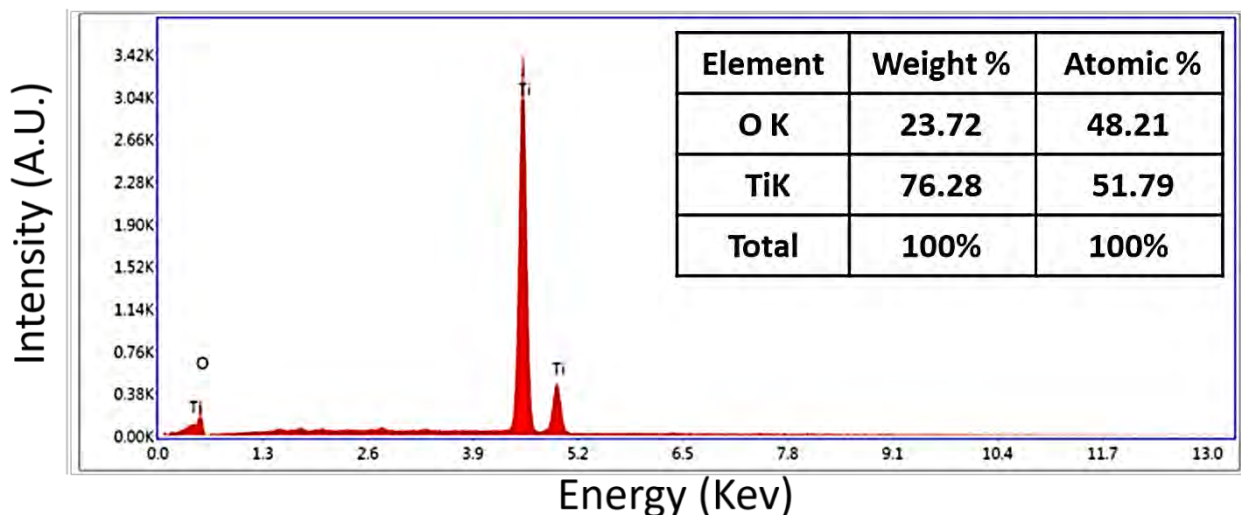
Figure-4.22. Energy dispersive x-ray spectroscopic analysis of Titania (TiO$_2$-Nps) synthesized by Conventional hydrothermal heatingdisplaying the peaks of titanium and oxygen with weight % and atomic %.

4.2.5.4 *Summary of EDX analysis results for elemental composition in its spectrum:-*

The EDX spectrum of Titania (TiO$_2$ Nps) synthesized by *Bacillus coagulans*, *Mentha spicata* and *Conventional hydrothermal heating* revealed prominent peaks of titanium and oxygen in weight % and atomic % with no other impurities in their spectrum. The amount of titanium in weight % and atomic% was found to be maximum in Titania (TiO$_2$ Nps) synthesized by *Bacillus coagulans* in comparison to Titania (TiO$_2$ Nps) synthesized by *Mentha spicata* and *Conventional hydrothermal heating* where weight % and atomic % of titanium was comparatively less (Figure-4.23).
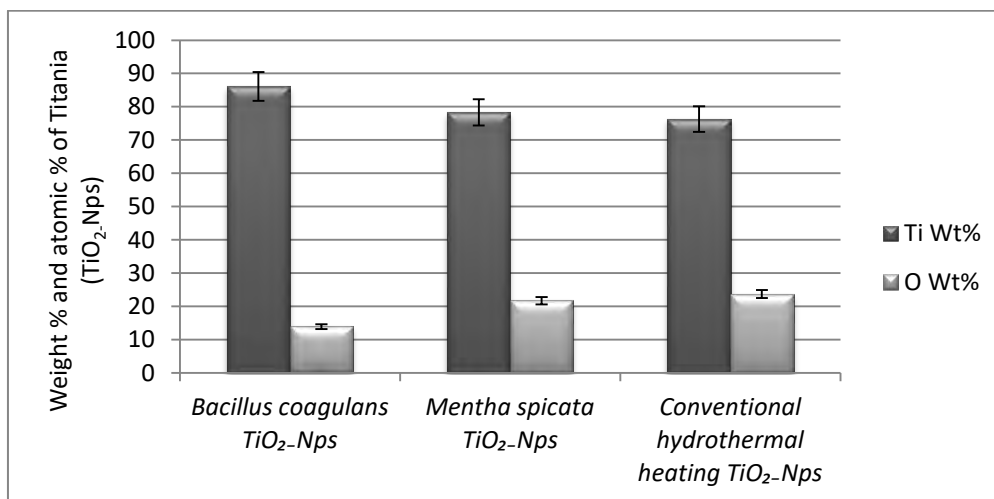
Figure-4.23:Energy dispersive x-ray spectroscopic analysis of Titania (TiO$_2$_Nps) synthesized by Bacillus coagulans, Mentha spicata and Conventional hydrothermal heating displaying the peaks of pure titanium and oxygen with weight % and atomic %in their spectrum.

4.2.6 *FTIR analysis of Titania (TiO$_2$_Nps) for the presence of functional groups*:-

The FTIR revealed functional compounds of Titania (TiO$_2$_Nps)synthesized by *Bacillus coagulans,Mentha spicata* and *Conventional hydrothermal heating* in broad band spectrum between 4000-100 cm^{-1}.

4.2.6.1 *FTIR analysis of Titania (TiO$_2$_Nps) synthesized by Bacillus coagulans*:-

In FTIR spectrum of Titania (TiO$_2$_Nps) synthesized by *Bacillus coagulans* salient and spectacular peak were recorded at 2925.51 cm^{-1}, 2791.09 cm^{-1}, 1649.07 cm^{-1} and 689.17 cm^{-1}respectively. The eminent wave at 2943.51 cm^{-1} was due to stretching of terminating (O-H) hydroxyl groups. The peaks at 2791.09 cm^{-1} employed C-H stretching corresponding to carboxyl group. Moreover, C=O stretching was evidenced at peak of 1649.07 cm^{-1}corresponding to group of amines. In addition, last peak was evident at 581.17 cm^{-1}for Ti-O-Ti bending ensuring formation of metal oxygen bonds resulting in synthesis of Titania (TiO$_2$_Nps).There was no additional peak observed in the FTIR spectrum of these Nps(Figure-4.24, Table-4.4).

Table-4.4: *Formation of peaks, peak intensities and groups at different wavelengths in spectrum of of Titania (TiO$_2$_Nps) synthesized byBacillus coagulans.*

Peaks	Peak Intensity (cm^{-1})	Groups	Wavelength (cm^{-1})
O-H	3419.23 cm^{-1}	Alcohol	4000-3000 cm^{-1}
C-H	2791.09 cm^{-1}	Aldehyde	3000-2500 cm^{-1}
C=O	1649.07 cm^{-1}	Amine	2000-1650 cm^{-1}
C-N	1318.23 cm^{-1}	Amines	1400-1000 cm^{-1}
Ti-O-Ti	581.17 cm^{-1}	Titanium Oxide	1000-400 cm^{-1}
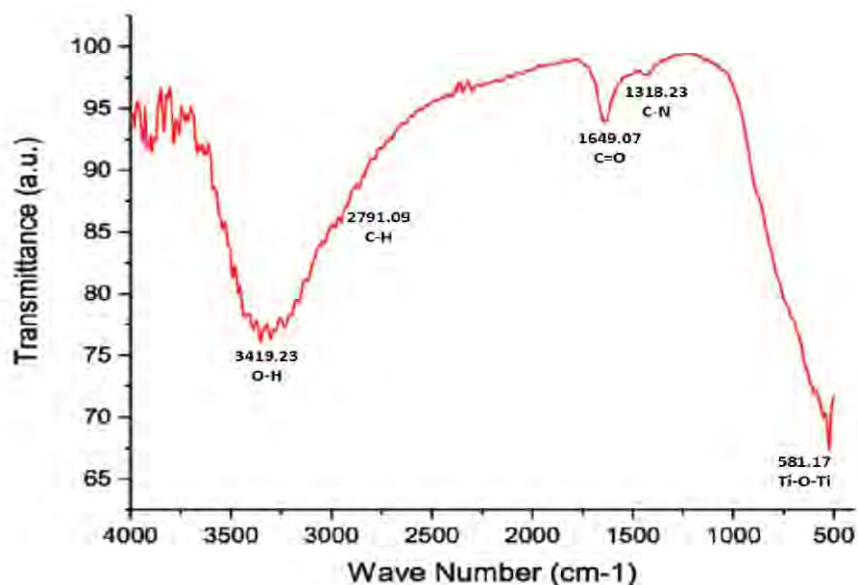
Figure -4.24: FTIR spectrum, of Titania (TiO₂-Nps) synthesized by Bacillus coagulans demonstrating various peaks of its patent functional groups with no additional peak.

4.2.6.2 *FTIR analysis of Titania (TiO₂-Nps) synthesized by Mentha spicata plant:-*

The characteristic peaks fabricated by FTIR of Titania (TiO₂-Nps) synthesized by *Mentha spicata* were 3667.21 cm^{-1}, 3654.09 cm^{-1}, 3361.36 cm^{-1}, 2729.43 cm^{-1}, 2663.75 cm^{-1}, 1996.56 cm^{-1}, 1703.69 cm^{-1}, 1656.11 cm^{-1}, 1546.93 cm^{-1}, 503.23 cm^{-1} and 464.17 cm^{-1} respectively. The peaks generated at 3667.2 cm^{-1}, 3654.09 cm^{-1} and 3361.36 cm^{-1}were due to stretching vibrations of O-H groups of alcohol. Therefore, peaks produced at 2729.43 cm^{-1}, 2663.75 cm^{-1} and 1996.56 cm^{-1} revealed stretching vibrations of C-H groups of alkynes and aldehydes. The peaks observed at 1703.56 cm^{-1}, 1656.11 cm^{-1} and 1546.93 cm^{-1} corresponded to bending vibrations of O-H groups of hydroxyl compounds. The peak at 1499.01 cm^{-1} was responsible for producing the O=C=O containing carbon dioxide. The peaks obtained at 503.23 cm^{-1} and 464.17 cm^{-1} attributed to stretching and bending vibrations of Ti-O-Ti groups. The carbon dioxide peak at 1499.01 cm^{-1}was an additional peak in its FTIR spectrum (Figure-4.25, Table-4.5)

Table-4.5: *Formation of peaks, peak intensities and groups at different wavelengths in spectrum of Titania (TiO₂-Nps) synthesized by Mentha spicata plant.*

Peaks	Peak Intensity (cm^{-1})	Groups	Wavelength (cm^{-1})
O-H Stretching	3667.21 cm^{-1}	Alcohol	4000-3000 cm^{-1}
O-H Stretching	3654.09 cm^{-1}	Alcohol	4000-3000 cm^{-1}
O-H Stretching	3361.36 cm^{-1}	Alcohol	4000-3000 cm^{-1}
C-H Stretching	2729.43 cm^{-1}	Alkynes	3000-2500 cm^{-1}
C-H Stretching	2663.75 cm^{-1}	Alkynes	3000-2500 cm^{-1}
C-H Stretching	1996.56 cm^{-1}	Aldehyde	3000-2500 cm^{-1}
C=O Bending	1703.69 cm^{-1}	Hydroxyl Compound	2000-1650 cm^{-1}
C=O Bending	1656.11 cm^{-1}	Hydroxyl Compound	2000-1650 cm^{-1}
C=O Bending	1546.93 cm^{-1}	Hydroxyl Compound	2000-1650 cm^{-1}

| O=C=O | 1449. 01 cm^{-1} | Carbon dioxide | 1450-1400 cm^{-1} |
| Ti-O-Ti | 503.23 cm^{-1} | Titanium Oxide | 1000-400 cm^{-1} |
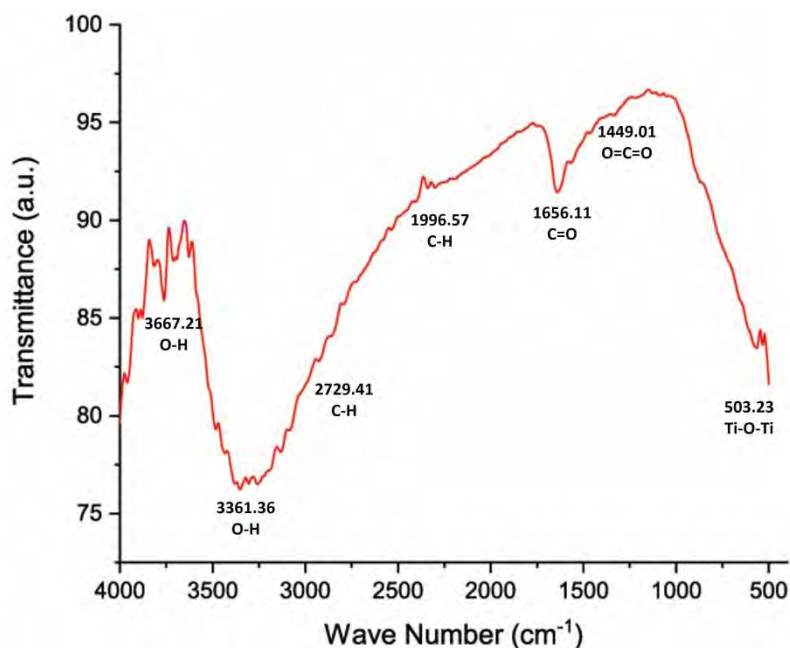
Figure -4.25: FTIR spectrum, of Titania (TiO$_2$ Nps) synthesized by Mentha spicata demonstrating various peaks of its patent functional groups with an additional peak of carbon dioxide at 1499.01 cm^{-1}.

4.2.6.3 *FTIR analysis of Titania (TiO$_2$ Nps) synthesized by Conventional hydrothermal heating:-*

The chief notable peaks generated by FTIR of Titania (TiO$_2$ Nps) synthesized by *Conventional hydrothermal heating* were 3491.23 cm^{-1}, 3277.19 cm^{-1}, 3113.41 cm^{-1}, 2900.97 cm^{-1}, 2363.75 cm^{-1}, 1937.49 cm^{-1}, 1679.13 cm^{-1}, 1621.07 cm^{-1}, 1557.91 cm^{-1}, 1453.71 cm^{-1}, 1018.23 cm^{-1}, 675.11 cm^{-1} & 540.52 cm^{-1} respectively. The peaks at 3491.23 cm^{-1}, 3277.19 cm^{-1}, 3113.41 cm^{-1} and 1679.13 cm^{-1} occurred because of O-H stretching vibrations of alcohol groups. The peaks at 2900.97 cm^{-1} revealed C-H stretching of organic compound while peaks at 2363.75 cm^{-1} and 675.11 cm^{-1} attributed to C-C stretching vibrations of alkyne groups. In addition, peaks at 1445.71 cm^{-1} demonstrated O=C=O showing carbon dioxide groups and C-N stretching vibrations of amines were recorded at 1018.23 cm^{-1}. Other peaks such as 1937.49 cm^{-1} revealed C-H bending of aromatic compound, 1679.13 cm^{-1} peak showed O-H bending of hydroxyl group, 1621.07 cm^{-1} peak revealed N-H bending of amine group, 1557.91 cm^{-1} peak observed N-O stretching of nitro-compound. The last peak was evident at 540.52 cm^{-1} ensuring Ti-O-Ti bending resulting in Titania (TiO$_2$ Nps) formation. The peaks at 1445.71 cm^{-1} and 1557.91 cm^{-1} for carbon dioxide and nitro-compounds were additional peaks in the FTIR spectrum of these Nps (Figure-4.26, Table-4.6)

Table-4.6: Formation of peaks, peak intensities and groups at different wavelengths in spectrum of Titania (TiO₂ Nps)synthesized by Conventional hydrothermal heating.

Peaks	Peak Intensity (cm⁻¹)	Groups	Wavelength (cm⁻¹)
O-H Stretching	3419.23 cm⁻¹	Alcohol	4000-3000 cm⁻¹
O-H Stretching	3277.19 cm⁻¹	Alcohol	4000-3000 cm⁻¹
O-H Stretching	3113.41 cm⁻¹	Alcohol	4000-3000 cm⁻¹
C-H Stretching	2900.97 cm⁻¹	Organic Compound	2400-2000 cm⁻¹
CΞC Stretching	2363.75 cm⁻¹	Alkyne	2400-2000 cm⁻¹
C-H Bending	1937.49 cm⁻¹	Aromatic Compound	2000-1650 cm⁻¹
O-H Bending	1679.13 cm⁻¹	Alcohol	2000-1650 cm⁻¹
N-H Bending	1621.07 cm⁻¹	Amine	1670-1600 cm⁻¹
N-O Stretching	1557.91 cm⁻¹	Nitro Compound	1600-1500 cm⁻¹
O=C=O	1445.71 cm⁻¹	Carbon oxide	1450-1400 cm⁻¹
C-N	1018.23 cm⁻¹	Amines	1400-1000 cm⁻¹
C=C	675.11 cm⁻¹	Alkane Bending	1000-650 cm⁻¹
Ti-O-Ti	544.52 cm⁻¹	Titanium Oxide	1000-400 cm⁻¹
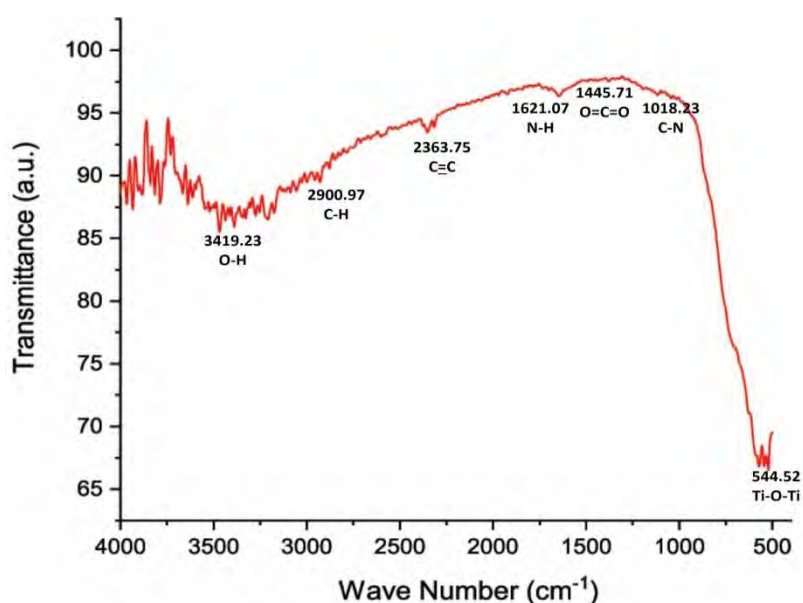
Figure -4.26: FTIR spectrum, of Titania (TiO₂ Nps) synthesized by Conventional hydrothermal heating demonstrating various peaks of its patent functional groups with additional peaks of carbon dioxide and nitro-compounds at 1445.71 cm⁻¹ and 1557.91 cm⁻¹.

4.2.6.4 *Summary of FTIR analysis results for the presence of functional groups*:-

The FTIR spectrum confirmed synthesis of Titania (TiO₂ Nps) by producing evident peaks between 800 cm⁻¹ – 400 cm⁻¹. The FTIR spectrum of Titania (TiO₂-Nps)synthesized by *Bacillus coagulans* revealed patent functional groups of O-H, C-H, C= O and Ti-O-Ti with no other additional groups. The FTIR spectrum of Titania (TiO₂ Nps) synthesized by *Mentha spicata* depicted functional groups of O-H, C-H, C= O and Ti-O-Ti with an additional peak of

carbon dioxide in its spectrum and Titania (TiO$_2$.Nps) synthesized by *Conventional hydrothermal heating* showed functional groups of O-H, C-H, C= O, C-O, N-H, N-O, C-N, C=C and C $\equiv$ C and Ti-O-Ti with other additional peaks of carbon dioxide and nitro-compounds in its spectrum respectively (Figure-4.27).
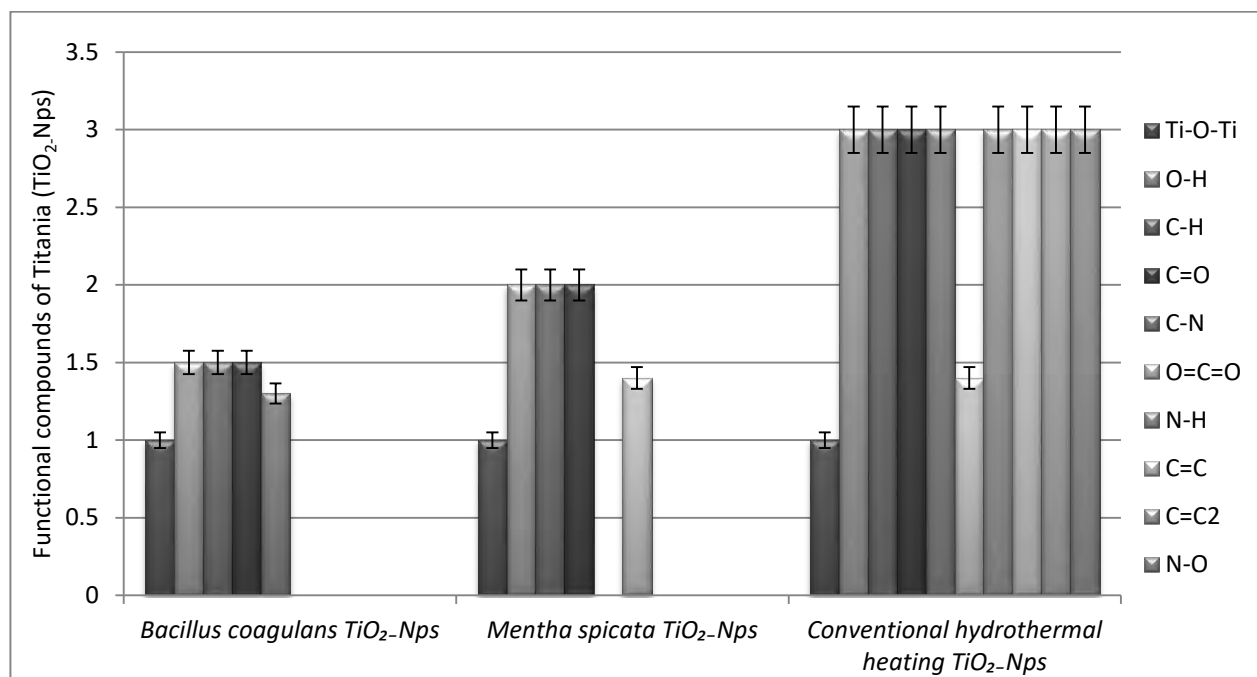
Figure-4.27: FTIR spectroscopy analysis of Titania (TiO$_2$.Nps) synthesized by Bacillus coagulans, Mentha spicata and Conventional hydrothermal heatingmethods displaying various patent peaks with the additional peaks.

4.2.7 *DLS analysis* **of** *Titania (TiO$_2$.Nps)for the hydrodynamic size in suspension:*

The DLS analysis was carried out to confirm the hydrodynamic particle size of Titania (TiO$_2$.Nps) in the suspension form. The standard shows that the hydrodynamic size calculated by DLS is greater in comparison to the crystalline size calculated by XRD and particle size investigated by SEM in comparison to the values obtained by XRD, and SEM analysis [200].

4.2.7.1 *DLS analysis of Titania (TiO$_2$.Nps) synthesized by Bacillus coagulans:-*

The DLS scan depicted the 34 nm particle size of Titania (TiO$_2$.Nps) synthesized by *Bacillus coagulans* which was greater than the crystalline size obtained by XRD analysis and particle size attained by SEM analysis for these Nps as per the DLS standard (Figure-4.28).
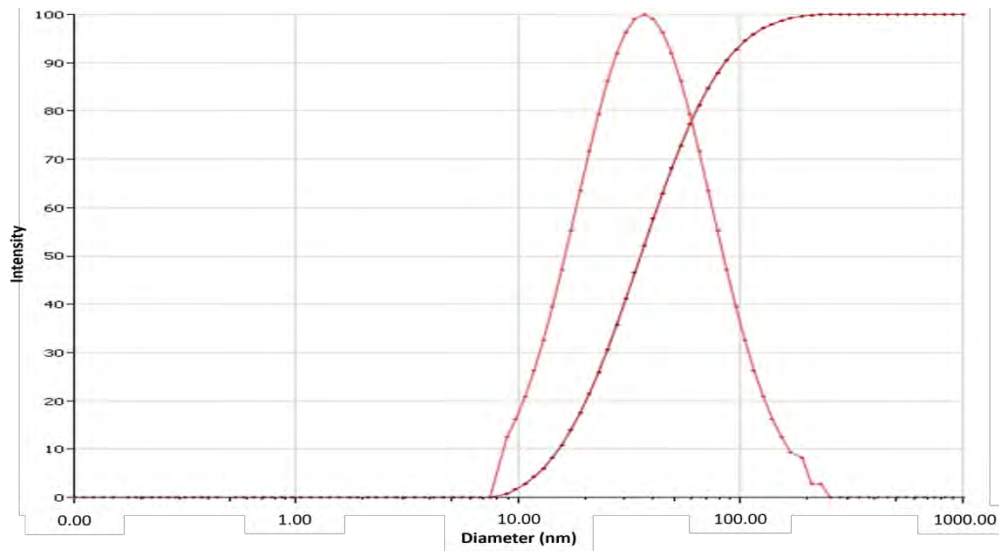
Figure -4.28: DLS spectrum, of Titania (TiO2 Nps) synthesized by Bacillus coagulans demonstrating the smallest hydrodynamic particle size.

4.2.7.2 DLS analysis of Titania (TiO2 Nps) synthesized by Mentha spicata plant:-

The DLS scan revealed 49 nm particle size of Titania (TiO2 Nps) synthesized by *Mentha spicata* which was slightly greater than the crystalline size obtained by XRD analysis and particle size attained by SEM analysis for these Nps as per the DLS standard (Figure-4.29).
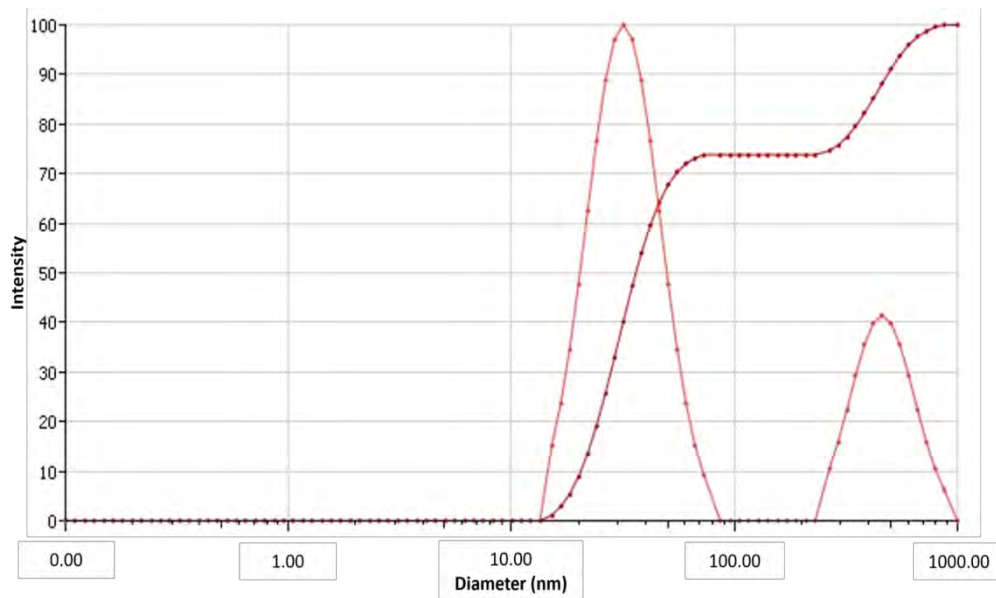
Figure -4.29: DLS spectrum, of Titania (TiO2 Nps) synthesized by Mentha spicata demonstrating the medium hydrodynamic particle size.

4.2.7.3 DLS analysis of Titania (TiO2 Nps) synthesized by Conventional hydrothermal heating:-

The DLS scan showed 58 nm particle size of Titania (TiO2 Nps) synthesized by *Conventional hydrothermal heating* which was greater than the crystalline size obtained by XRD analysis

and particle size attained by SEM analysis for these Nps as per the DLS standard (Figure-4.30).
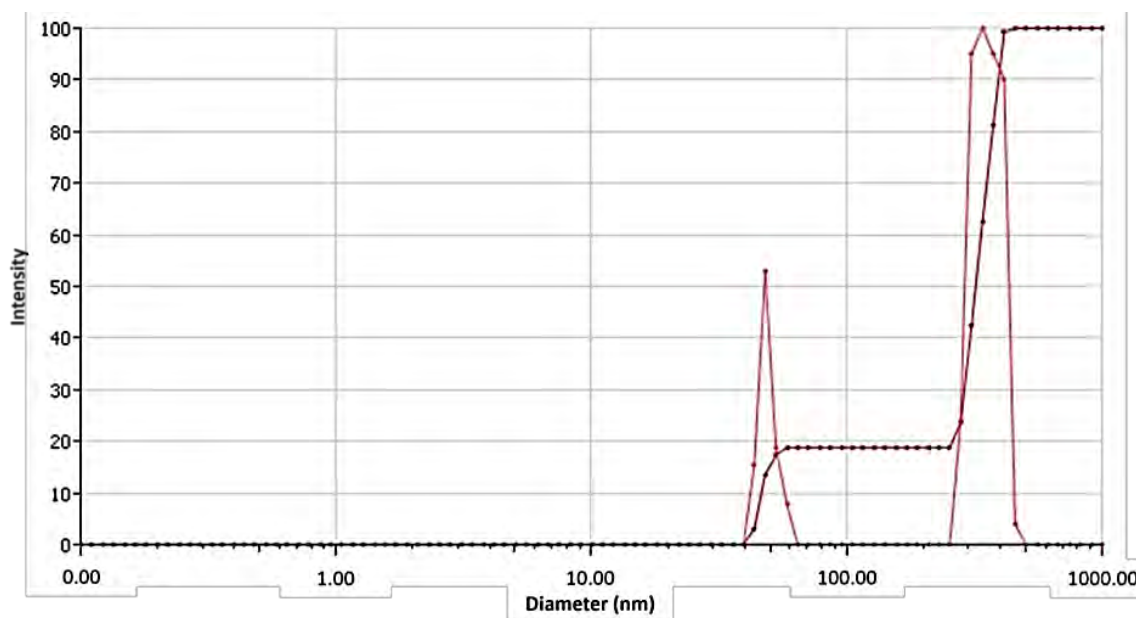
Figure -4.30: DLS spectrum, of Titania (TiO₂.Nps) synthesized by Conventional hydrothermal heating demonstrating the largest hydrodynamic particle size.

4.2.7.4 Summary of DLS analysis resultsfor the hydrodynamic size in suspension:-

The DLS scan revealed the hydrodynamic particle size of Titania (TiO_2.Nps) synthesized by *Bacillus coagulans, Mentha spicata* and*Conventional hydrothermal heating* which was found to be 34 nm, 49 nm and 58 nm. These hydrodynamic particle size values obtained for all these synthesized Nps were greater than the crystalline size obtained by the XRD analysis and particle size attained by the SEM analysis which was in collaboration with XRD, and SEM (Figure-4.31)
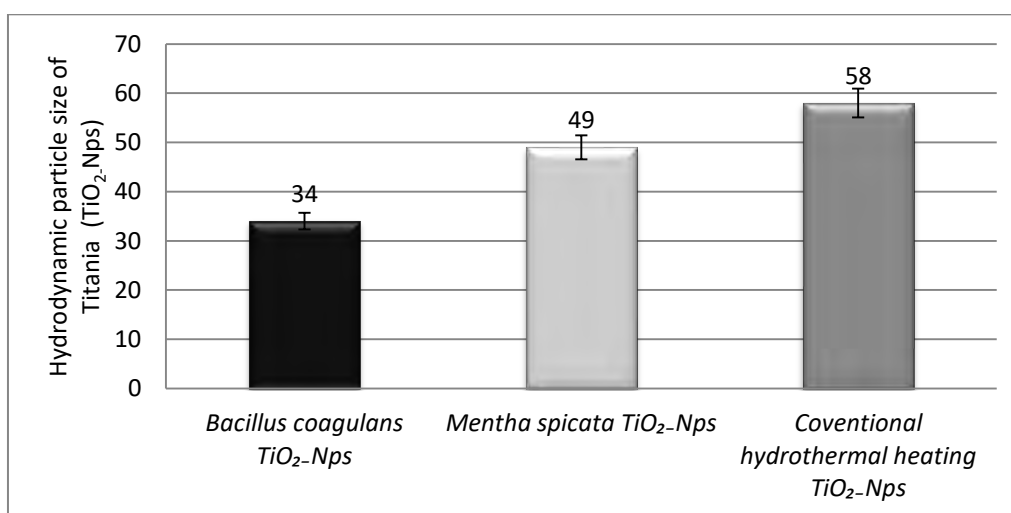
Figure-4.31: DLS spectroscopy analysis of Titania (TiO₂.Nps) synthesized by Bacillus coagulans, Mentha spicata and Conventional hydrothermal heatingmethods displaying their different hydrodynamic particle sizes.

4.2.8 *Raman Spectroscopic analysis of Titania (TiO₂ Nps) for size and phase:*

The confirmation of particle size and phase form of Titania (TiO₂ Nps) was carried out by raman spectroscopy accurately between 200 cm⁻¹ and 800 cm⁻¹ [190]. The factor group analysis is used to confirm the phase form of the Titania (TiO₂ Nps). There are six main peaks available in the active modes of raman for defining the phase of the Nps such as 1 peak at A_{1g}, 2 peaks at B_{1g} and 3 peaks at E_g. Out of these six peaks if only three peaks such as 1 peak at E_g, 1 peak at A_{1g}, and 1 peak at B_{1g} are present in the raman active modes then the phase of the Nps gets confirmed in the spectrum. The active modes of B_{1g} peak represents symmetric bending, E_g peak shows symmetric stretching and A_{1g} elaborates O-Ti-O anti-symmetric bending vibration in its spectrum and these three peaks are responsible for the formation of the main phase form of Titania (TiO₂ Nps). The particle size is calculated by the raman intensity in its spectrum. The larger raman intenisty shows the smaller particle size of Titania (TiO₂ Nps) whereas smaller raman intensity shows the larger particle size of these Nps [191].

4.2.8.1 *Raman Spectroscopic analysis of Titania (TiO₂ Nps) synthesized by Bacillus coagulans:* The active modes in raman scan of Titania (TiO₂ Nps)demonstrated E_g at 243 cm⁻¹, B_{1g} at 398cm⁻¹, A_{1g} at 517 cm⁻¹ and E_g at 643 cm⁻¹ which dominantly represented the anatase phase of the synthesized Titania (TiO₂ Nps). The raman intensity at 1,00,000 revealed the small size of Titania (TiO₂ Nps) which was in close association with the SEM and XRD (-4.32).
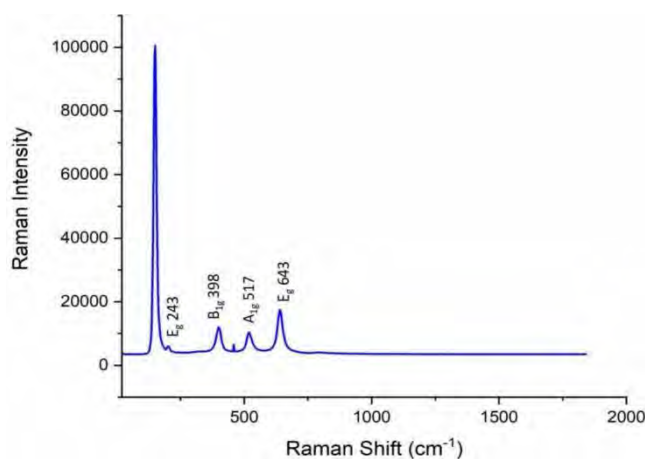
Figure 4.32: Raman spectroscopic scan image of Titania (TiO₂ Nps) synthesized by Bacillus coagulans, showing small size at highest raman intensity and pure peaks of anatase phase.

4.2.8.2 *Raman Spectroscopic analysis of Titania (TiO₂ Nps) synthesized by Mentha spicata plant:-*

The active modes in raman scan of Titania (TiO₂ Nps)demonstrated E_g at 243 cm⁻¹ , B_{1g} at 398 cm⁻¹, A_{1g} at 517 cm⁻¹ and E_g at 640 cm⁻¹ which showed the anatase phase of the synthesized Titania (TiO₂ Nps). The raman intensity at 98000 revealed the medium size of Titania (TiO₂ Nps) which was in collaboration with the SEM and XRD (Figure-4.33).
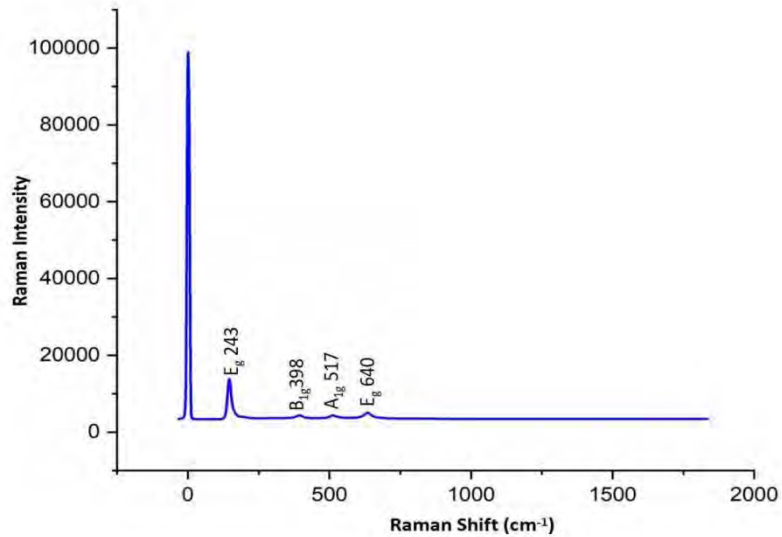
Figure-4.33: Raman spectroscopic scan image of Titania (TiO₂ Nps) synthesized by Mentha spicata, showing small size at medium raman intensity and pure peaks of anatase phase.

4.2.8.3 Raman Spectroscopic analysis of Titania (TiO₂ Nps) synthesized by Conventional hydrothermal heating:-

The active modes in raman scan of Titania (TiO₂ Nps)demonstrated E_g at 243 cm^{-1} , B_{1g} at 397 cm^{-1}, A_{1g} at 519 cm^{-1} and E_g at 641 cm^{-1} of which 243 cm^{-1}, 519 cm^{-1} and 641 cm^{-1} demonstrated the anatase phases while peak at at 397cm^{-1} revealed rutile phase of the synthesized Titania (TiO₂ Nps). The raman intensity at 97000 revealed the largest size of Titania (TiO₂ Nps) which is in accordance with the SEM and XRD (Figure-4.34).
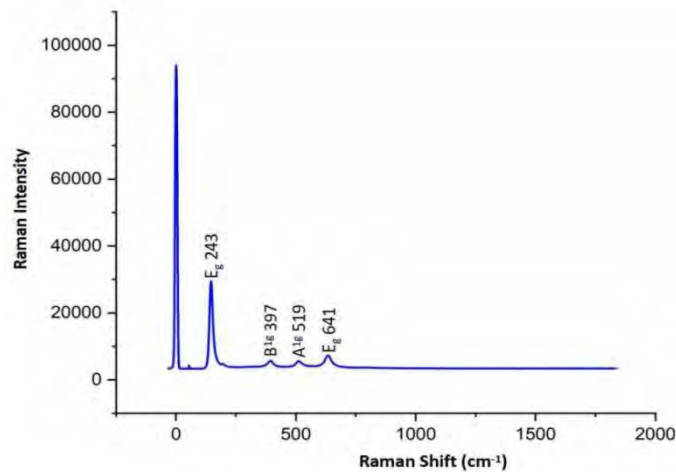
Figure-4.34: Raman spectroscopic scan image of Titania (TiO₂ Nps) synthesized by Conventional hydrothermal heating, showing large size at lowest raman intensity and pure peaks of anatase phase with one rutile peak.

4.2.8.4 Summary of Raman spectroscopic analysis results for size and phase:

The active modes of raman peaks in Titania (TiO₂ Nps) synthesized by *Bacillus coagulans* and *Mentha spicata* manifested pure anatase phase while Titania (TiO₂ Nps) produced by

Conventional hydrothermal heating showed the pure anatase phase with one rutile peak in its spectrum. The raman intensity at 100000 reveals the smallest size of Titania (TiO$_2$.Nps) synthesized by *Bacillus coagulans* whereas the raman intensity at 98000 reveals the medium size of Titania (TiO$_2$.Nps) fabricated by *Mentha spicata* plant. The Titania (TiO$_2$.Nps) produced by *Conventional hydrothermal heating* demonstrated the raman intensity peak at 97000 showing the largest size of these Nps (Figure-4.35)
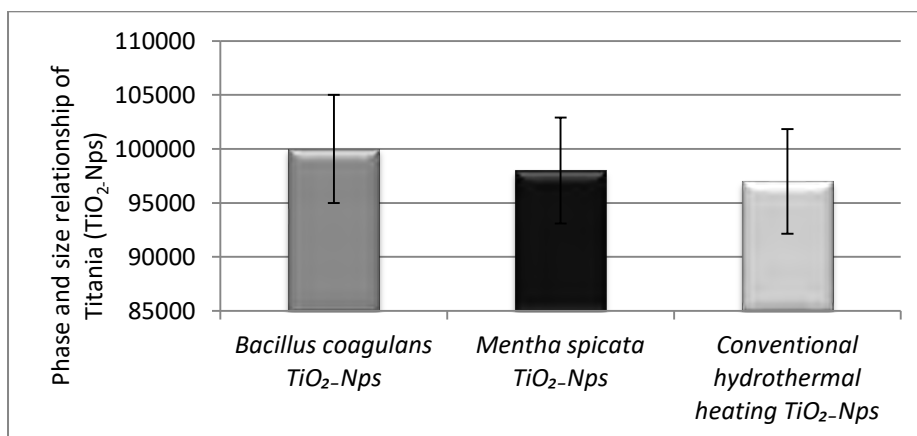
Figure-4.35: Summary of Raman spectroscopy analysis of Titania (TiO$_2$.Nps) synthesized by Bacillus coagulans, Mentha spicata and Conventional hydrothermal heating depicting the phase and size relationship associated with raman intensity.

4.3   Phase-III: *Antimicrobial activity of Titania (TiO$_2$.Nps) for zone of inhibition***:**

The antimicrobial activity of Titania (TiO$_2$.Nps) synthesized by *Bacillus coagulans* (n=5), *Mentha spicata* (n=5) and *Conventional hydrothermal heating* (n=5) were tested against several caries promoting bacteria in humans such as *E. coli* (ATCC®35218[TM]), *L .acidophilus* (ATCC®314[TM]), *E. faecalis* (ATCC®29212[TM]), *E. faecium* (ATCC®51559[TM]), *S. aureus* (ATCC®25923[TM]) *and P. aeruginosa* (ATCC®27853[TM]) (Figure-4.36).
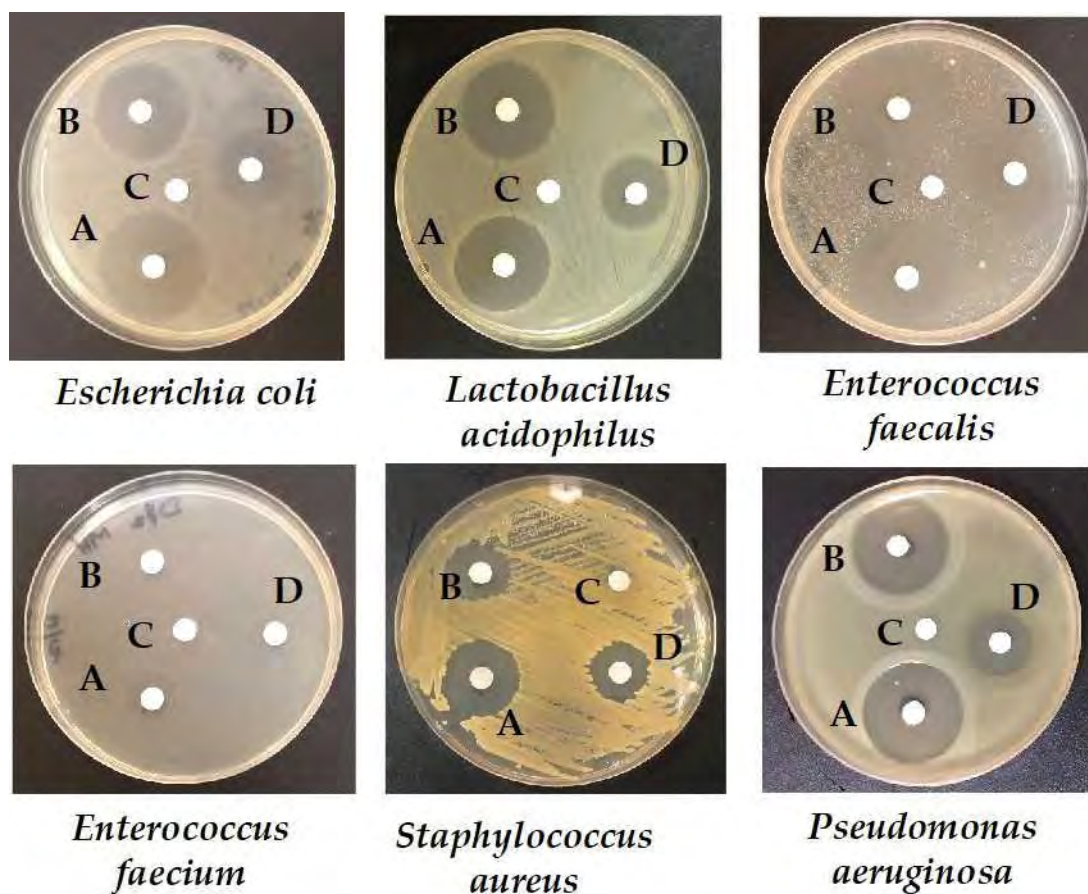
Figure-4.36: Zone of inhibition obtained by Titania (TiO₂ Nps) against E. coli, L .acidophilus, E. faecalis, E. faecium, S. aureus and P. aeruginosa : (A) control (water), (B)= Titania (TiO₂ Nps) synthesized by Bacillus coagulans, (C)= Titania (TiO₂ Nps) synthesized by Mentha spicata and (D)= Titania (TiO₂ Nps) synthesized by Conventional hydrothermal heating .

4.3.1 *Antimicrobial activity of Titania (TiO₂ Nps) synthesized by Bacillus coagulans:*

The Titania (TiO₂ Nps) synthesized by *Bacillus coagulans* exhibited maximum zone of inhibition against all the caries promoting pathogens (Figure-4.36, Table 4.7).

Table 4.7: *Zone of Inhibition (mm) produced byTitania (TiO₂ Nps) synthesized by Bacillus coagulansagainst E. coli, L .acidophilus, E. faecalis, E. faecium,S. aureus and P. aeruginosa with standard deviation (S.D) and standard error (S.E).*

Ser	Bacterial Strain	Zone of Inhibition (mm) produced by Titania (TiO₂ Nps) synthesized by *Bacillus coagulans* with S.D and S.E
1.	*E. coli*	27 mm $\pm$ 0.71 (0.41)
2.	*L .acidophilus*	26 mm $\pm$ 0.70 (0.41)
3.	*E. faecalis*	26 mm $\pm$ 0.71 (0.41)
4.	*E. faecium*	13 mm $\pm$ 1.59 (0.41)
5.	*S. aureus*	21 mm $\pm$ 1.58 (0.41)
6.	*P. aeruginosa*	25 mm $\pm$ 0.67 (0.41)

4.3.2 *Antimicrobial activity of Titania (TiO₂ Nps) synthesized by Mentha spicata:*

The Titania (TiO₂ Nps) synthesized by *Mentha spicata* manifested zone of inhibition against all the caries promoting pathogens but comparatively less than Titania (TiO₂ Nps) synthesized by *Bacillus coagulans*(Figure-4.36, Table 4.8).

Table 4.8: *Zone of Inhibition (mm) produced byTitania (TiO₂ Nps)* **synthesized by** *Mentha spicata plant against E. coli*, *L .acidophilus*, *E. faecalis, E. faeciumS. aureus and P. aeruginosa with standard deviation (S.D) and standard error (S.E).*

Ser	Bacterial Strain	Zone of Inhibition (mm) produced by Titania (TiO₂ Nps) synthesized by *Mentha spicata* with S.D and S.E
1.	*E. coli*	24 mm ± 0.73 (0.47)
2.	*L .acidophilus*	24 mm ± 1.03 (0.47)
3.	*E. faecalis*	23 mm ± 1.61 (0.47)
4.	*E. faecium*	Nil ± 0.00 (0.00)
5.	*S. aureus*	17 ± 1.58 (0.47)
6.	*P. aeruginosa*	24 mm ± 1.07 (0.47)

4.3.3 Antimicrobial activity of Titania (TiO₂ Nps) synthesized by Conventional hydrothermal heating:

The Titania (TiO₂ Nps) synthesized by *Conventional hydrothermal heating* method revealed minimum zone of inhibition against all the caries promoting pathogens in comparison to Titania (TiO₂ Nps) synthesized by *Bacillus coagulans* and *Mentha spicata* (Figure-4.36, Table 4.9).

Table 4.9: *Zone of Inhibition (mm) produced byTitania (TiO₂ Nps) synthesized by Conventional hydrothermal heating against E. coli*, *L .acidophilus*, *E. faecalis, E. faeciumS. aureus and P. aeruginosa with standard deviation (S.D) and standard error (S.E).*

Ser	Bacterial Strain	Zone of Inhibition (mm) produced by Titania (TiO₂ Nps) synthesized by *Conventional hydrothermal heating* with S.D and S.E
1.	*E. coli*	19 mm ± 1.58 (0.43)
2.	*L .acidophilus*	19 mm ± 1.58 (0.43)
3.	*E. faecalis*	20mm ± 1.58 (0.43)
4.	*E. faecium*	Nil ± 0.00 (0.00)
5.	*S. aureus*	16 ± 0.70 (0.43)
6.	*P. aeruginosa*	20 mm ± 1.58 (0.43)

The mean difference in the antimicrobial activity between the Titania (TiO₂ Nps) synthesized by all three routes was significant (*P-value* < 0.05). The antimicrobial activity of the Titania (TiO₂ Nps)synthesized by *Bacillus coagulans* was found to be maximumwhile moderate in the

Titania (TiO$_2$-Nps)synthesizedby *Mentha spicata* and minimum in the Titania (TiO$_2$-Nps) synthesizedby *Conventional hydrothermal heating* (*P-value* < 0.05) (Table 4.10).

Table: 4.10: *Mean difference in the antimicrobial activity of Titania (TiO$_2$-Nps) synthesized by Bacillus coagulans, Mentha spicata plant, and Conventional hydrothermal heating.*

S.No	TiO$_2$-Nps synthesized by different routes	Comparison of Antimicrobial activity between TiO$_2$-Nps synthesized by different routes	Mean Difference with standard error (S.E)	*P-value*
1.	TiO$_2$-Nps synthesized by *Bacillus coagulans*	TiO$_2$-Nps synthesized ced by Mentha spicata	4.33 (0.30)	0.001
		TiO$_2$-Nps synthesized by *Conventional hydrothermal heating*	7.33 (0.30)	0.001
2.	TiO$_2$-Nps synthesized by *Mentha spicata*	TiO$_2$-Nps synthesized by *Bacillus coagulans*	-4.33 (0.30)	0.001
		TiO$_2$-Nps synthesized by *Conventional hydrothermal heating*	3.00 (0.30)	0.001
3.	TiO$_2$-Nps synthesized by *Conventional hydrothermal heating*	TiO$_2$-Nps synthesized by *Bacillus coagulans*	-7.33 (0.30)	0.001
		TiO$_2$-Nps synthesized by Mentha spicata	-3.00 (0.30)	0.001

4.3.4 *Summary of antimicrobial activity results for zone of inhibition:*

The Titania (TiO$_2$-Nps) synthesized by *Bacillus coagulans* revealed maximum antimicrobial activity against all the dental caries promoting pathogens as compared to the Titania (TiO$_2$-Nps) produced by *Mentha spicata* and*Conventional hydrothermal heating* that displayed reduced antimicrobial activity comparatively (Figure-4.37).
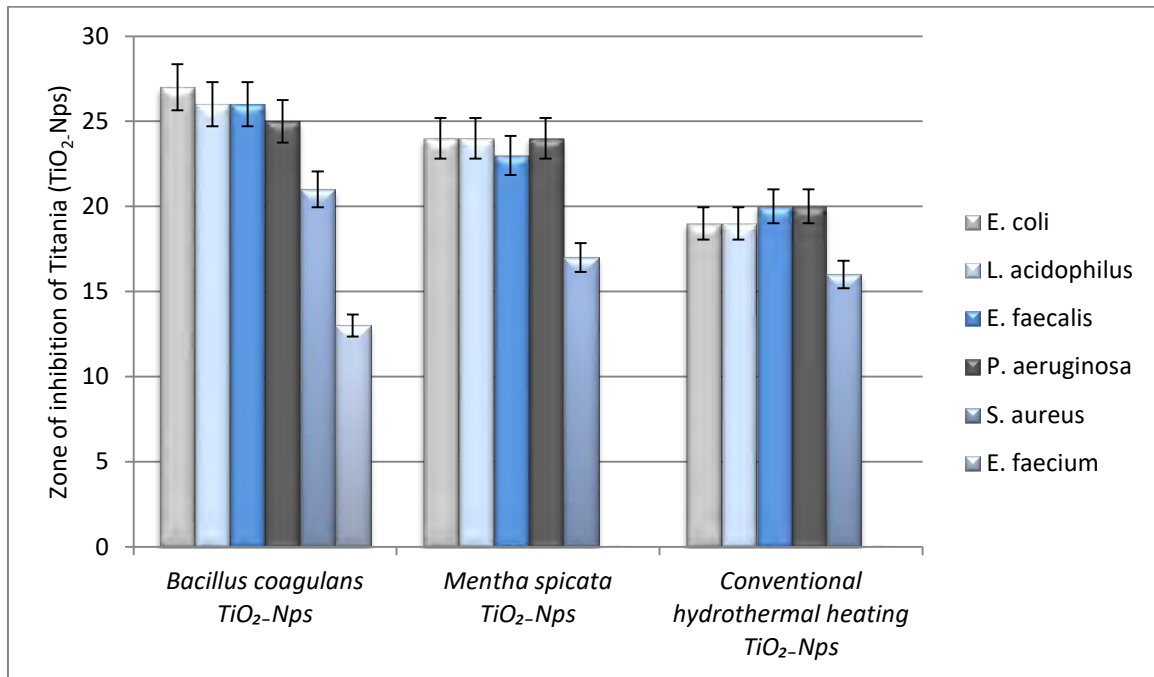
Figure-4.37: Antimicrobial activity of Titania (TiO₂Nps) synthesized by Bacillus coagulans, Mentha spicata plant, and Conventional hydrothermal heatingdepicting zone of inhibition against various dental caries promoting pathogens.

4.4   Phase-IV: Biocompatibility of Titania (TiO₂Nps) for the cell viability %:

4.4.1   Biocompatibility analysis (Cell viability %) of the Titania (TiO₂Nps):

The Titania (TiO₂Nps) synthesized by *Bacillus coagulans,Mentha spicata* and *Conventional hydrothermal heating* were evaluated for cell viability % after exposing to L929 mouse fibroblasts. These three types of Titania (TiO₂Nps)were compared with each other at different dilutions of 0.063 µg/ml, 0.125 µg/ml, 0.25 µg/ml, and 0.50 µg/mlfor their cell viability % to calculate their cytotoxic/ non-cytotoxic nature. The 0.063 µg/ml was the low dose and 0.50 µg/ml was the high dose in the current study for the synthesized Titania (TiO₂Nps) from all the three routes. The cell viability % or survival rate of fibroblasts was 100% against the control group. The Titania (TiO₂Nps) synthesized by *Bacillus coagulans* depicted an increased cell viability % or survival rate of fibroblast in comparison to the Titania (TiO₂Nps) formed by *Mentha spicata* and *Conventional hydrothermal heating* methods which was significant (*P-value* <0.05) at the end of the investigation.

The universally accepted standard used for detecting cytotoxicity-response of Nps was categorized as Noncytotoxic (cell viability, > 90%), mild cytotoxic (cell viability between 60 - 90 %), moderate cytotoxic (cell viability between 30-60%) and severe cytotoxic (between 30% - less) [201]. Cell viability was calculated by equation:-

$$\text{Cell viability \%} = \frac{\text{Mean optical density of test group}}{\text{Mean optical density of control group}} \times 100$$

The cell viability % or fibroblast cells survival rate against all the serial dilutions of Titania (TiO₂Nps) synthesized by *Bacillus coagulans* and *Mentha spicata* revealed no cytotoxic effect till the end of the investigation. On the other hand, cell viability % or fibroblast cells survival

rate against high dose serial dilution of Titania (TiO$_2$Nps) synthesized by *Conventional hydrothermal heating* showed mild cytotoxicity (Table-4.11).

Table- 4.11: *Cell viability % or fibroblast cells survival rate against different serial dilutions of Titania (TiO$_2$Nps)synthesized by Bacillus coagulans, Mentha spicata plant, and Conventional hydrothermal heating.*

Ser	Groups	Cell Viability % at serial dilution (0.063 µg/ml) with S.D &S.E	Cell Viability % at serial dilution (0.125 µg/ml) with S.D &S.E	Cell Viability % at serial dilution (0.25 µg/ml) with S.D &S.E	Cell Viability % at serial dilution (0.5 µg/ml) with S.D &S.E	Standard % for cytotoxicity detection in which the groups exist	Cytotoxicity status
1.	Control	100% + 0.00 (0.00)	100%+ 0.00 (0.00)	100% + 0.00 (0.00)	100% +0.00 (0.00)	100%	Non cytotoxic
2.	*Bacillus coagulans* TiO$_2$Nps	99.57% + 0.56 (0.32)	97.43% + 0.11 (0.06)	95.51%+ 2.27 (1.31)	93.14%+ 1.49 (0.86)	> 90%	Non cytotoxic
3.	*Mentha spicata* TiO$_2$Nps	99.35 + 0.29 (0.17)	95.82%+ 0.38(0.22)	92.09% + 0.22(0.13)	90.79%+0.34 (0.20)	> 90%	Non cytotoxic
4.	*Conventional hydrothermal heating* TiO$_2$Nps	98.92 + 0.23 (0.13)	94.43%+ 1.13 (0.65)	91.88%+0.27 (0.16)	^87.15% + 1.48(0.85)	> 90%	Non cytotoxic
						^60-90%	^Mildly cytotoxic

The mean differences in the cell viability % between control group and the Titania (TiO$_2$Nps)synthesized by *Bacillus coagulans,Mentha spicata* and *Conventional hydrothermal heating* exposed to L929 mouse fibroblasts was insignificant at low dose serial dilution (0.063 µg/ml)as there was not much difference in the cell viability % of control group with other groups showing their increased cell viability % or fibroblast cells survival rate (*P-value* >0.05). The cell viability % or fibroblast cells survival rate reduced with progress in the concentrations of the serial dilutions which was found to be significant among the inter groups such as control group and the Titania (TiO$_2$Nps)synthesized by *Bacillus coagulans,Mentha spicata* and *Conventional hydrothermal heating* at high dose serial dilution (0.5 µg/ml). The control group revealed 100% cell viability or fibroblast cells survival rate in comparison to other Titania (TiO$_2$Nps) groups investigated (*P-value* < 0.05). The mean differences of cell viability % or fibroblast cells survival between control group and the Titania (TiO$_2$Nps)synthesized by *Bacillus coagulans,Mentha spicata* plant and *Conventional hydrothermal heating* was significant (*P-value* < 0.05) but insignificant between *Mentha spicata* and *Conventional hydrothermal heating* groups(*P-value* > 0.05) at serial dilution (0.25 µg/ml). The mean differences of cell viability % or fibroblast cells survival between control group and Titania (TiO$_2$Nps)synthesized by *Bacillus coagulans,Mentha spicata* and *Conventional hydrothermal heating* was significant (*P-value* < 0.05) at high dose serial dilution (0.5 µg/ml). This

confirmed the non-cytotoxic nature of the Titania (TiO$_2$-Nps)synthesized by *Bacillus coagulans* and*Mentha spicata* but slightly cytotoxic nature of the Titania (TiO$_2$-Nps) synthesized by *Conventional hydrothermal heating* incomparison to the control group (Table-4.12).

Table-4.12: *Cell viability % analysis between control group and different types of Titania (TiO$_2$-Nps) with S.E (Standard Error) at different serial dilutions.*

Comparison of cell viability % at different serial dilutions	Control group and TiO$_2$-Nps synthesized by different routes	Cell viability% comparison between control group and TiO$_2$-Nps synthesized by different routes exposed to fibroblasts	Mean Difference with standard error (S.E)	*P-value*
At serial dilution **(0.063 μg/ml)**	Control group	*Bacillus coagulans* TiO$_2$-Nps	0.43 (0.27)	0.159
		Mentha spicata plant TiO$_2$-Nps	0.65 (0.27)	0.047
		Conventional hydrothermal heating TiO$_2$-Nps	1.08 (0.27)	0.005
	Bacillus coagulans TiO$_2$-Nps	Control group	-0.43 (0.27)	0.159
		Mentha spicata TiO$_2$-Nps	0.22 (0.27)	0.449
		Conventional hydrothermal heating TiO$_2$-Nps	0.65 (0.27)	0.047
	Mentha spicata TiO$_2$-Nps	Control group	-0.65 (0.27)	0.047
		Bacillus coagulans TiO$_2$-Nps	-0.22 (0.27)	0.449
		Conventional hydrothermal heating TiO$_2$-Nps	0.43 (0.27)	0.159
	Chydrothermal heating TiO$_2$-Nps	Control group	-1.08 (0.27)	0.005
		Bacillus coagulans TiO$_2$-Nps	-0.65 (0.27)	0.047
		Mentha spicata TiO$_2$-Nps	-0.43 (0.27)	0.159
At serial dilution **(0.125 μg/ml)**	Control group	*Bacillus coagulans* TiO$_2$-Nps	2.57 (0.49)	0.001
		Mentha spicata TiO$_2$-Nps	4.18 (0.49)	0.001
		Conventional hydrothermal heating TiO$_2$-Nps	5.57 (0.49)	0..001
	Bacillus coagulans TiO$_2$-Nps	Control group	-2.57 (0.49)	0.001
		Mentha spicata TiO$_2$-Nps	1.61 (0.49)	0.011
		Conventional hydrothermal TiO$_2$-Nps	3.00 (0.49)	0.001
	Mentha spicata TiO$_2$-Nps	Control group	-4.18 (0.49)	0.001
		Bacillus coagulans TiO$_2$-Nps	-1.61 (0.49)	0.011
		Conventional hydrothermal heating TiO$_2$-Nps	1.39 (0.49)	0.023
	Conventional hydrothermal heating TiO$_2$-Nps	Control group	-5.57 (0.49)	0.001
		Bacillus coagulans TiO$_2$-Nps	-3.00 (0.49)	0.001
		Mentha spicata TiO$_2$-Nps	-1.39 (0.49)	0.023
At serial dilution **(0.25 μg/ml)**	Control group	*Bacillus coagulans* TiO$_2$-Nps	4.49 (0.94)	0.001
		Mentha spicata TiO$_2$-Nps	7.91 (0.94)	0.001
		Conventional hydrothermal heating TiO$_2$-Nps	8.12 (0.94)	0.001
	Bacillus coagulans TiO$_2$-Nps	Control group	-4.49 (0.94)	0.001
		Mentha spicata TiO$_2$-Nps	3.42 (0.94)	0.007
		Conventional hydrothermal TiO$_2$-Nps	3.63 (0.94)	0.005
	Mentha spicata TiO$_2$-Nps	Control group	-7.91 (0.94)	0.001
		Bacillus coagulans TiO$_2$-Nps	-3.42 (0.94)	0.007

		Conventional hydrothermal heating TiO$_2$-Nps	0.21 (0.94)	0.829
	Conventional hydrothermal heating TiO$_2$-Nps	Control group	-8.12 (0.94)	0.001
		Bacillus coagulans TiO$_2$-Nps	-3.63 (0.94)	0.005
		Mentha spicata TiO$_2$-Nps	-0.21 (0.94)	0.829
At serial dilution (0.5 µg/ml)	Control group	Bacillus coagulans TiO$_2$-Nps	6.86 (0.87)	0.001
		Mentha spicata TiO$_2$-Nps	9.21 (0.87)	0.001
		Conventional hydrothermal heating TiO$_2$-Nps	12.85 (0.87)	0.001
	Bacillus coagulans TiO$_2$-Nps	Control group	-6.86 (0.87)	0.001
		Mentha spicata plant TiO$_2$-Nps	2.35 (0.87)	0.027
		Conventional hydrothermal heating TiO$_2$-Nps	5.99 (0.87)	0.001
	Mentha spicata TiO$_2$-Nps	Control group	-9.21 (0.87)	0.001
		Bacillus coagulans TiO$_2$-Nps	-2.35 (0.87)	0.027
		Conventional hydrothermal heating TiO$_2$-Nps	3.64 (0.87)	0.003
	Conventional hydrothermal heating TiO$_2$-Nps	Control group	-12.85 (0.87)	0.001
		Bacillus coagulans TiO$_2$-Nps	-5.99 (0.87)	0.001
		Mentha spicata TiO$_2$-Nps	-3.64 (0.87)	0.003

4.4.2 *Summary of Biocompatibility analysis (Cell viability %) of the Titania (TiO$_2$-Nps):-*

The cell viability % or survival rate of fibroblast cells against the Titania (TiO$_2$-Nps) synthesized by *Bacillus coagulans* and *Mentha spicata* revealed non-cytotoxic behavior (cell viability > 90%). The cell viability % or survival rate of fibroblast cells against the Titania (TiO$_2$-Nps) synthesized by *Conventional hydrothermal heating* confirmedmildly cytotoxic behavior (cell viability% between 60-90%) at the end of the investigation (*P-value* < 0.05) (Figure-4.38).
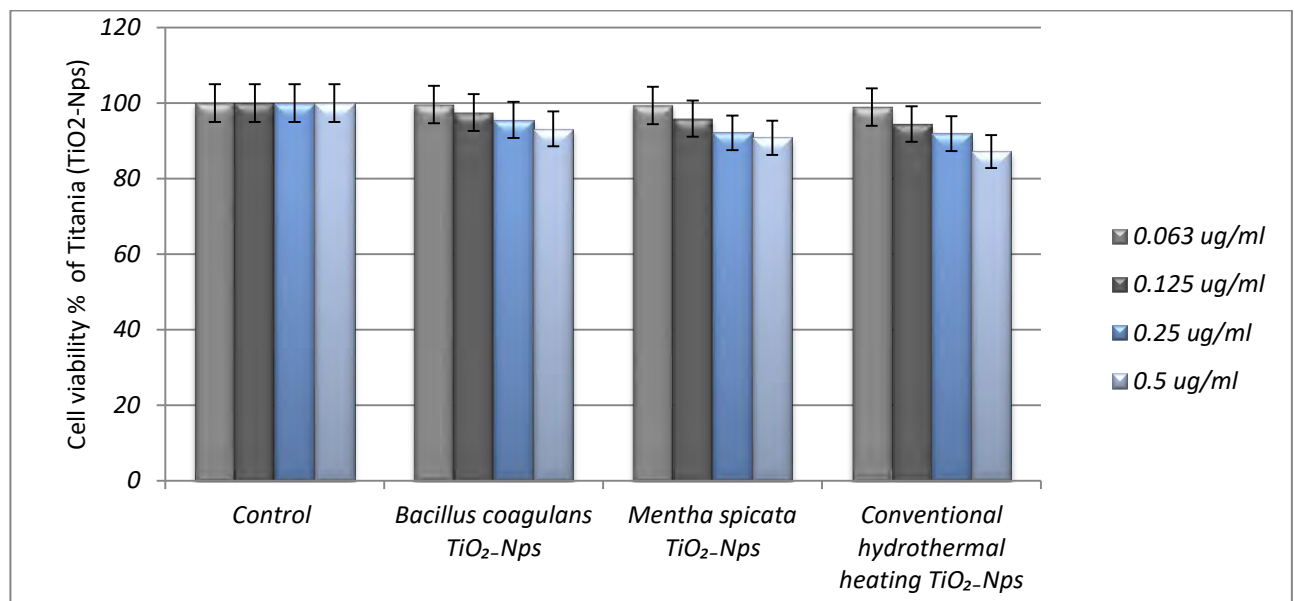
Figure-4.38: *Cell viability % or fibroblast cells survival rate against Titania (TiO$_2$-Nps)synthesized by Bacillus coagulans, Mentha spicata and Conventional hydrothermal heating in comparison to control group investigated at different serial dilutions.*

4.5   **Phase-V:** *Mechanical strength and properties of GIC restorative material:*

4.5.1   *Incorporation of Titania (TiO$_2$-Nps)in GIC (TiO$_2$GIC):-*

The Titania (TiO$_2$-Nps) synthesized by *Bacillus coagulans* were found to be most stable, safe and sustainable with enhanced antimicrobial activity and biocompatibility. Therefore, these Nps were induced in the glass ionomer filling material to develop an absolute filling material with enhanced mechanical properties.The mechanical properties of different concentrations of filling material groups such as conventional control group E-1 (0% TiO$_2$GIC), experimental group E-2 (3% TiO$_2$GIC), experimental group E-3 (5% TiO$_2$GIC), experimental group E-4 (7% TiO$_2$GIC) and experimental group E-5 (10% TiO$_2$GIC) were investigated to compare micro-hardness, compressive strength, flexural strength, shear bond strength of enamel and dentine with surface morphology.

4.5.2   *Mechanical strength and properties testing:*

4.5.2.1   *Vicker's micro-hardness analysis of TiO$_2$GIC cement samples at different concentrations***:**

The hardness strength of TiO$_2$GIC was investigated by Vicker's micro-hardness tester which revealed systematic increase in a linear pattern with increase in % of the Titania (TiO$_2$-Nps) in GIC up to 5% and linear pattern decrease in the Vicker's micro-hardness strength with increase in % of Titania (TiO$_2$-Nps) in GIC up to 10%. The conventional control group E-1 (0% TiO$_2$GIC) displayed minimum hardness strength whereas experimental group E-3 (5% TiO$_2$GIC) displayed maximum hardness strength. The differences in Vicker's micro-hardness strength among conventional control group E-1 (0%TiO$_2$GIC), experimental group E-2 (3%TiO$_2$GIC), experimental group E-3 (5%TiO$_2$GIC), experimental group E-4 (7% TiO$_2$GIC) and experimental groupE-5(10% TiO$_2$GIC) was significant (*P-value* < 0.05) (Table-4.13).

Table-4.13: Vicker's micro-hardness **(VHN)** *and standard error of various concentrations of TiO$_2$GIC cements.*

Control and TiO$_2$GIC Samples	Total Samples (n)	Vicker's micro-hardness (VHN) of control and TiO$_2$GIC Samples with standard deviation (VHN±S.D)	Standard Error (S.E)
Conventional control group E-1 (0% TiO$_2$GIC)	10	53.80 ± 1.26	0.39
Experimental group E-2 (3% TiO$_2$GIC)	10	62.40 ± 1.06	0.33
Experimental group E-3 (5% TiO$_2$GIC)	10	67.70 ± 0.46	0.15
Experimental group E-4 (7% TiO$_2$GIC)	10	59.10 ± 0.87	0.27
Experimental group E-5 (10% TiO$_2$GIC)	10	57.90 ± 1.08	0.34

The inter-group comparisons of TiO$_2$GIC at all percentages showed a significant difference in the Vicker's micro-hardness values (*P-value* <0.05) (Table-4.14).

Table-4.14:Intergroup comparisons of Vicker's micro-hardness of TiO₂GIC cements containing various concentrations of Titania (TiO₂.Nps).

Control and different concentrations of TiO₂GIC Samples	Comparison of Vicker's micro-hardness between control and different concentrations of TiO₂GIC samples	Mean Difference of Vicker's micro-hardness between control and different concentrations of TiO₂GIC samples with standard error (S.E)	*P-value*
Conventional control group E-1 (0% TiO₂GIC)	Vicker's micro-hardness of Experimental group E-2 (3% TiO₂GIC)	-8.60 (0.44)	0.001
	Vicker's micro-hardness of Experimental groupE-3 (5% TiO₂GIC)	-13.90 (0.44)	0.001
	Vicker's micro-hardness of Experimental group E-4 (7% TiO₂GIC)	-5.30 (0.44)	0.001
	Vicker's micro-hardness of Experimental group E-5 (10% TiO₂GIC)	-4.10 (0.44)	0.001
Experimental group E-2 (3% TiO₂GIC)	Vicker's micro-hardness of Conventional control group E-1 (0% TiO₂GIC)	8.60 (0.44)	0.001
	Vicker's micro-hardness of Experimental groupE-3 (5% TiO₂GIC)	-5.30 (0.44)	0.001
	Vicker's micro-hardness of Experimental group E-4 (7% TiO₂GIC)	3.30 (0.44)	0.001
	Vicker's micro-hardness of Experimental group E-5 (10% TiO₂GIC)	4.50 (0.44)	0.001
Experimental group E-3 (5% TiO₂GIC)	Vicker's micro-hardness of Conventional control group E-1 (0% TiO₂GIC)	13.90 (0.44)	0.001
	Vicker's micro-hardness of Experimental group E-2 (3% TiO₂GIC)	5.30 (0.44)	0.001
	Vicker's micro-hardness of Experimental group E-4 (7% TiO₂GIC)	8.60 (0.44)	0.001
	Vicker's micro-hardness of Experimental group E-5 (10% TiO₂GIC)	9.80 (0.44)	0.001
Experimental group E-4 (7% TiO₂GIC)	Vicker's micro-hardness of Conventional control group E-1 (0% TiO₂GIC)	5.30 (0.44)	0.001
	Vicker's micro-hardness of Experimental group E-2 (3% TiO₂GIC)	-3.30 (0.44)	0.001
	Vicker's micro-hardness of Experimental groupE-3 (5% TiO₂GIC)	-8.60(0.44)	0.001
	Vicker's micro-hardness of Experimental group E-5 (10% TiO₂GIC)	1.20 (0.44)	0.009
Experimental group E-5 (10% TiO₂GIC)	Vicker's micro-hardness of Conventional control group E-1 (0% TiO₂GIC)	4.10 (0.44)	0.001
	Vicker's micro-hardness of Experimental group E-2 (3% TiO₂GIC)	-4.50 (0.44)	0.001
	Vicker's micro-hardness of Experimental groupE-3 (5% TiO₂GIC)	-9.80 (0.44)	0.001
	Vicker's micro-hardness of Experimental group E-4 (7% TiO₂GIC)	-1.20 (0.44)	0.009

4.5.2.1.1 *Indentation evaluationof TiO$_2$GIC cement samples after Vicker's micro-hardness analysis:*

The images of indentations after the Vicker's micro-hardness analysis were taken under the inverted fluorescence microscope (Czech Republic) (Figure-4.39). The conventional control group E-1 (0% TiO$_2$GIC) displayed the largest indentation size (Figure-4.39a) confirming the minimum micro-hardness strength value (59.10 $\pm$ 0.87 VHN, S.E = 0.27). Similarly, linear pattern decrease in indentation size was recorded with the increase in the micro-hardness strength values up to 5% TiO$_2$GIC in the experimental group E-3 (5% TiO$_2$GIC) that revealed maximum Vicker's micro-hardness strength value (Figure -4.39c) (67.90 $\pm$ 0.48 VHN, S.E = 0.15). The experimental group E-4 (7% TiO$_2$GIC) showed slightly greater indentation size (Figure -4.39d) confirming reduction in Vicker's micro-hardness strength and experimental group E-5 (10% TiO$_2$GIC) revealed largest indentation size (Figure -4.39e) confirming the maximum declination in the Vicker's micro-hardness strength value (53.90 $\pm$ 0.88 VHN, S.E = 0.39) which was significant (*P-value* < 0.001) (Figure -4.39, Table-4.12).
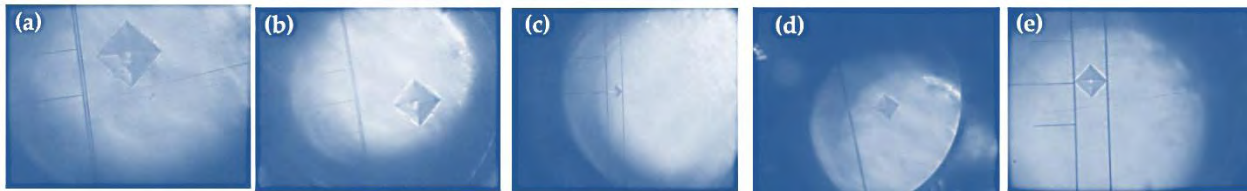
Figure-4.39: Indentations evaluation after the Vicker's micro-hardness analysis under the inverted fluorescence microscope for TiO$_2$GIC cement samples at different concentrations showing: (A) Conventional control group E-1(0% TiO$_2$GIC) showing greatest indentation size with smallest Vicker's micro-hardness strength value, (B) Experimental group E-2 (3% TiO$_2$GIC) showing smaller indentation size with slightly greater Vicker's micro-hardness strength value, (C)Experimental group E-3 (5% TiO$_2$GIC) showing smallest indentation size with greatest Vicker's micro-hardness strength value, (D) Experimental group E-4 (7% TiO$_2$GIC) showing greater indentation size with smaller Vicker's micro-hardness strength value, and (E) Experimental group E-4 (10% TiO$_2$GIC) showing more greater indentation size with slightly more smaller Vicker's micro-hardness strength value.

4.5.2.1.2 *SEM micrographs of TiO$_2$GIC cement samples for surface cracks after Vicker's micro-hardness analysis:*

SEM analysis of 9.5 x 1 mm of TiO$_2$GIC cylinders of all the samples was carried out after the Vicker's micro-hardness testing. These included the groups named conventional control group E-1 (0% TiO$_2$GIC), experimental group E-2 (3% TiO$_2$GIC), experimental group E-3 (5% TiO$_2$GIC), experimental group E-4 (7% TiO$_2$GIC) and experimental groupE-5 (10% TiO$_2$GIC). The increase in the concentration of TiO$_2$Nps in GIC depicted the linear pattern decrease of cracks in TiO$_2$GIC samples up to the experimental group E-3 containing 5% (Figure 4.40 a-c) and linear pattern increase in cracks in the group E-4 containing 7% TiO$_2$Nps and experimental group E-5having 10 % TiO$_2$Nps (Figure 4.40 d,e). The group conventional control group E-1 (0% TiO$_2$GIC) (Figure 4.40a) revealed maximum crack sites because of the least hardness strength as a result of absence of TiO$_2$Nps. The experimental group E-2 (3% TiO$_2$GIC) (Figure 4.40b) revealed slight deduction in cracks and this deduction in cracks became maximum in the experimental group E-3 (5% TiO$_2$GIC) (Figure 4.40c). Further

increase in the percentages of TiO_2 Nps greatly reduced the hardness strength and revealed moderate cracks in the experimental group E-4 (7% TiO_2GIC) (Figure 4.40d). The experimental group E-5(10% TiO_2GIC) (Figure 4.40e) depicted maximum crack sites because of the minimum hardness strength attained in this group.
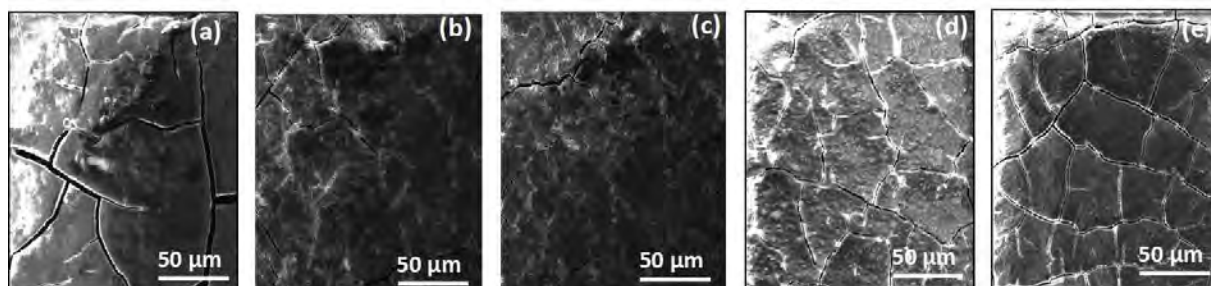
Figure 4.40. *SEM images of TiO$_2$GIC cement samples at low and high resolutions showing cracks of different concentrations of Titania (TiO$_2$ Nps) : (a) Conventional control group E-1 (0%TiO$_2$GIC) showing maximum cracks on its surface because of minimum hardness strength value, (b) Experimental group E-2 (3% TiO$_2$GIC) showing moderate cracks on its surface because of slightly increased hardness strength value, (c) Experimental group E-3 (5% TiO$_2$GIC) showing least cracks on its surface because of maximum hardness strength value, (d) Experimental group E-4 (7% TiO$_2$GIC) showing more cracks on its surface because of minimal hardness strength value, (e) Experimental group E-5 (10% TiO$_2$GIC) showing slightly more cracks on its surface because of more minimal hardness strength value.*

4.5.2.1.3 Summary of Vicker's micro-hardness analysis of TiO$_2$GIC cement samples at different concentrations:

The maximum value of Vicker's micro-hardness strength was found in the experimental group E-3 (5% TiO_2GIC) which was 67.90 ± 0.48 VHN, S.E = 0.15 as compared to the conventional control group E-1 (0% TiO_2GIC) which was 59.10 ± 0.87 VHN, S.E = 0.27 and other experimental groups E-2 (3% TiO_2GIC), E-4 (7% TiO_2GIC) and E-5 (10% TiO_2GIC) ($p.value < 0.05$) (Figure-4.41).
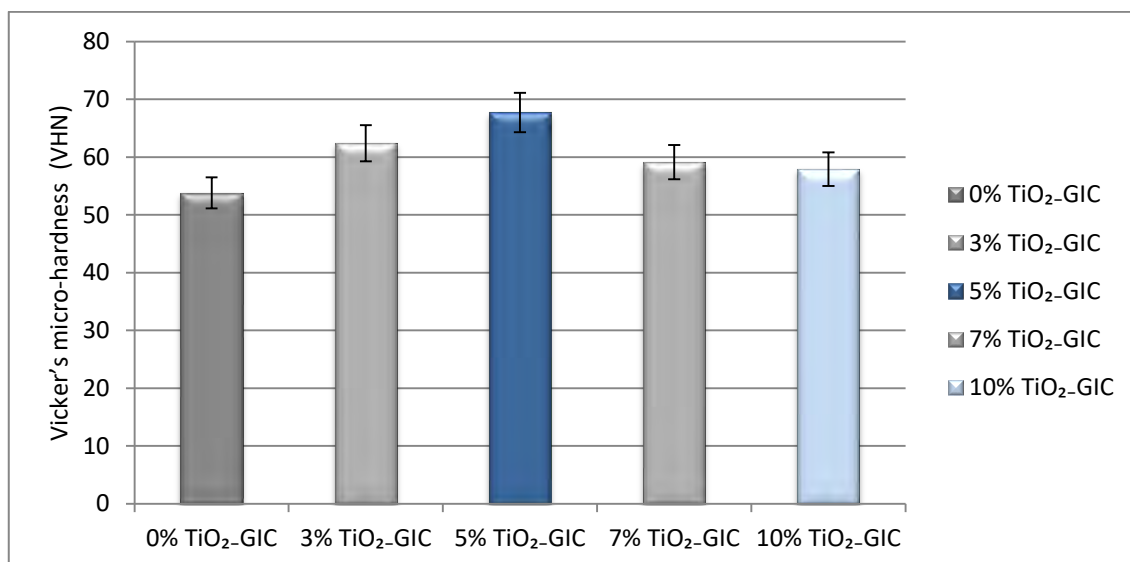
Figure-4.41: Mean differences in the Vicker's micro-hardness (VHN) of TiO₂GIC cement samples at different concentrations.

4.5.2.2 *Compressive strength analysis of TiO₂GIC cement samples at different concentrations***:**

The compressive strength of different percentages of Titania (TiO₂ Nps) added to GIC manifested linear pattern increase in the compressive strength of the conventional control group E-1 (0% TiO₂GIC), experimental group E-2 (3% TiO₂GIC) and experimental group E-3 (5% TiO₂GIC). The experimental group E-4 (7% TiO₂GIC) and experimental groupE-5(10% TiO₂GIC) revealed linear pattern decrease in the compressive strength which was also significant (*P-value* < 0.05) (Table-4.15).

Table-4.15: *Compressive strength and standard error of TiO₂GIC cement samples at different concentrations.*

Control and TiO₂GIC Samples	Total Samples (n)	Compressive Strength of control and TiO₂GIC Samples with standard deviation (MPa ±S.D)	Standard Error (S.E)
Conventional control group E-1 (0% TiO₂GIC)	10	9.11 ± 1.4	0.46
Experimental group E-2 (3% TiO₂GIC)	10	13.93 ± 1.3	0.43
Experimental group E-3 (5% TiO₂GIC)	10	19.51 ± 1.2	0.41
Experimental group E-4 (7% TiO₂GIC)	10	15.54 ± 0.5	0.18
Experimental group E-5 (10% TiO₂GIC)	10	11.61 ± 1.2	0.40

The mean differences in the inter-group TiO₂GIC samples at different concentrations elaborated maximum compressive strength in the experimental group E-3 (5% TiO₂GIC) and minimum in the experimental group E-5 (10% TiO₂GIC) which was also significant (*P-value* < 0.001) (Table-4.16)

Table-4.16: *Inter-group comparisons of compressive strength of TiO₂GIC cement samples containing various concentrations of Titania (TiO₂ Nps).*

Control and different concentrations of TiO₂GIC Samples	Comparison of compressive strength between control and different concentrations of TiO₂GIC samples	Mean Difference of compressive strength between control and different concentrations of TiO₂GIC samples with standard error (S.E)	*P-value*

Conventional control group E-1 (0% TiO$_2$GIC)	Compressive strength of Experimental group E-2 (3% TiO$_2$GIC)	-4.82 (0.55)	0.001
	Compressive strength of Experimental group E-3 (5% TiO$_2$GIC)	-10.40 (0.55)	0.001
	Compressive strength of Experimental group E-4 (7% TiO$_2$GIC)	-6.43 (0.55)	0.001
	Compressive strength of Experimental group E-5 (10% TiO$_2$GIC)	-2.50 (0.55)	0.001
Experimental group E-2 (3% TiO$_2$GIC)	Compressive strength of Conventional control group E-1 (0% TiO$_2$GIC)	4.82 (0.55)	0.001
	Compressive strength of Experimental group E-3 (5% TiO$_2$GIC)	-5.58 (0.55)	0.001
	Compressive strength of Experimental group E-4 (7% TiO$_2$GIC)	-1.61 (0.55)	0.006
	Compressive strength of Experimental group E-5 (10% TiO$_2$GIC)	2.32 (0.55)	0.001
Experimental group E-3 (5% TiO$_2$GIC)	Compressive strength of Conventional control group E-1 (0% TiO$_2$GIC)	10.40 (0.55)	0.001
	Compressive strength of Experimental group E-2 (3% TiO$_2$GIC)	5.58 (0.55)	0.001
	Compressive strength of Experimental group E-4 (7% TiO$_2$GIC)	3.97(0.55)	0.001
	Compressive strength of Experimental group E-5 (10% TiO$_2$GIC)	7.90 (0.55)	0.001
Experimental group E-4 (7% TiO$_2$GIC)	Compressive strength of Conventional control group E-1 (0% TiO$_2$GIC)	6.43 (0.55)	0.001
	Compressive strength of Experimental group E-2 (3% TiO$_2$GIC)	1.61 (0.55)	0.006
	Compressive strength of Experimental group E-3 (5% TiO$_2$GIC)	-3.97 (0.55)	0.001
	Compressive strength of Experimental group E-5 (10% TiO$_2$GIC)	3.93 (0.55)	0.001
Experimental group E-5 (10% TiO$_2$GIC)	Compressive strength of Conventional control group E-1 (0% TiO$_2$GIC)	2.50 (0.55)	0.001
	Compressive strength of Experimental group E-2 (3% TiO$_2$GIC)	-2.32 (0.55)	0.001
	Compressive strength of Experimental group E-3 (5% TiO$_2$GIC)	-7.90 (0.55)	0.001
	Compressive strength of Experimental group E-4 (7% TiO$_2$GIC)	-3.93 (0.55)	0.001

4.5.2.2.1 *Summary of Compressive strength analysis of TiO$_2$GIC cement samples at different concentrations:*

The compressive strength analysis revealed a systematic linear pattern increase in the compressive strength of TiO$_2$GIC samples with the increase in % of TiO$_2$ Nps in glass ionomer cement up to 5% and linear pattern decrease up to 10%. The maximum value of compressive strength was attained by the experimental group E-3 (5% TiO$_2$GIC) which was C.S = 19.51,

S.E = 0.55 while minimum value of compressive strength was attained by the experimental group E-5 (10% TiO$_2$GIC) which was C.S=11.61,S.E=0.55 when compared with the conventional control group E-1 (0% TiO$_2$GIC) where C.S= 9.11,S.E = 0.55 (*P-value* < 0.001) (Fig-4.42).
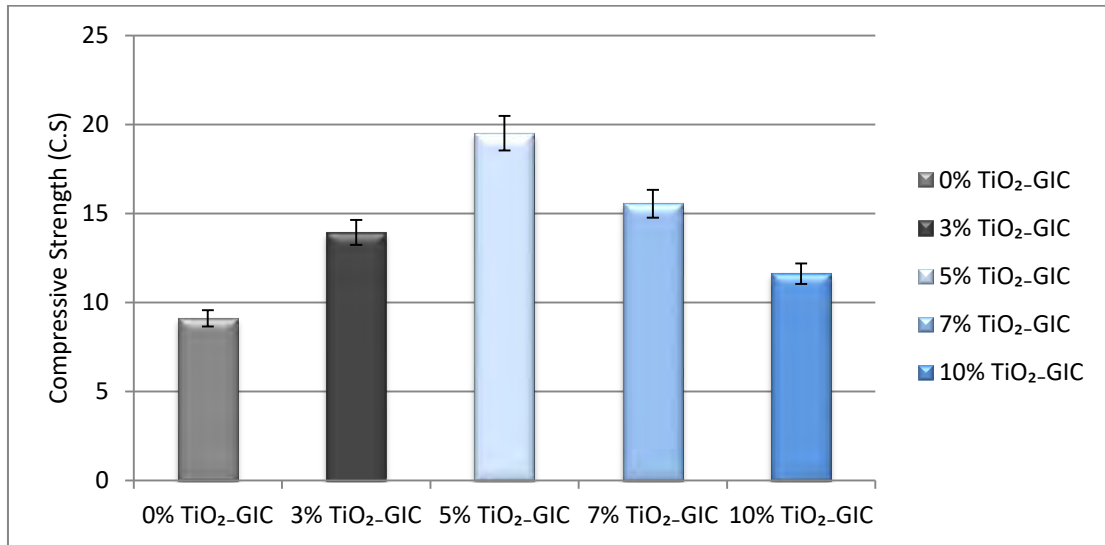
Figure-4.42: **Differences in Compressive Strength (C.S) of*TiO$_2$GIC* cement samples at different concentrations.**

4.5.2.3. *Flexural strength analysis of TiO$_2$GIC cement samples at different concentrations***:**

When Titania (TiO$_2$ Nps) were added to the GIC in different percentages, it fabricated a linear pattern increase in the flexural strength of the conventional control group E-1 (0% TiO$_2$GIC), experimental group E-2 (3% TiO$_2$GIC) and experimental group E-3 (5% TiO$_2$GIC). On the other hand, experimental group E-4 (7% TiO$_2$GIC) and experimental groupE-5(10% TiO$_2$GIC) notified decrease in the flexural strength in a linear pattern which was significant (*P-value* < 0.05) (Table-4.17)

Table-4.17: *Flexural strength and standard error of various concentrations of TiO$_2$GIC cement samples.*

Control and TiO$_2$GIC Samples	Total Samples (n)	Flexural Strength of control and TiO$_2$GIC Samples with standard deviation (MPa ±S.D)	Standard Error (S.E)
Conventional control group E-1 (0% TiO$_2$GIC)	10	19.31 ±0.9	0.31
Experimental group E-2 (3% TiO$_2$GIC)	10	24.17±1.4	0.45
Experimental group E-3 (5% TiO$_2$GIC)	10	31.29±1.1	0.37
Experimental group E-4 (7% TiO$_2$GIC)	10	26.15±1.8	0.58

Experimental group E-5 (10% TiO₂GIC)	10	21.93±2.4	0.77

The mean differences in the flexural strength of the inter-group TiO_2GIC cement samples revealed the maximum flexural strength in the experimental group E-3 (5% TiO_2GIC) and minimum flexural strength in the experimental group E-5 (10% TiO_2GIC) which was significant (*P-value* < 0.05) (Table-4.18).

Table-4.18: Inter-group comparisons of flexural strength of TiO₂GIC cement samples containing various concentrations of Titania (TiO₂ Nps).

Control and different concentrations of TiO₂GIC Samples	Comparison of flexural strength between control and different concentrations of TiO₂GIC samples	Mean Difference of flexural strength between control and different concentrations of TiO₂GIC samples with standard error (S.E)	*P-value*
Conventional control group E-1 (0% TiO₂GIC)	Flexural strength of Experimental group E-2 (3% TiO₂GIC)	-4.86 (0.74)	0.001
	Flexural strength of Experimental group E-3 (5% TiO₂GIC)	-11.98 (0.74)	0.001
	Flexural strength of Experimental group E-4(7% TiO₂GIC)	-6.84 (0.74)	0.001
	Flexural strength of Experimental group E-5 (10% TiO₂GIC)	-2.62 (0.74)	0.001
Experimental group E-2 (3% TiO₂GIC)	Flexural strength of Conventional control group E-1 (0% TiO₂GIC)	4.86 (0.74)	0.001
	Flexural strength of Experimental group E-3 (5% TiO₂GIC)	-7.12 (0.74)	0.001
	Flexural strength of Experimental group E-4 (7% TiO₂GIC)	-1.98 (0.74)	0.011
	Flexural strength of Experimental group E-5 (10% TiO₂GIC)	2.24 (0.74)	0.004
Experimental group E-3 (5% TiO₂GIC)	Flexural strength of Conventional control group E-1 (0% TiO₂GIC)	11.98 (0.74)	0.001
	Flexural strength of Experimental group E-2 (3% TiO₂GIC)	7.12 (0.74)	0.001
	Flexural strength of Experimental group E-4 (7% TiO₂GIC)	5.14 (0.74)	0.001
	Flexural strength of Experimental group E-5 (10% TiO₂GIC)	9.36 (0.74)	0.001
Experimental group E-4 (7% TiO₂GIC)	Flexural strength of Conventional control group E-1 (0% TiO₂GIC)	6.84 (0.74)	0.001
	Flexural strength of Experimental group E-2 (3% TiO₂GIC)	1.98 (0.74)	0.011
	Flexural strength of Experimental group E-3 (5% TiO₂GIC)	-5.14 (0.74)	0.001
	Flexural strength of Experimental group E-5 (10% TiO₂GIC)	4.22 (0.74)	0.001
Experimental group	Flexural strength of Conventional control group E-1 (0% TiO₂GIC)	2.62 (0.74)	0.001

E-5 (10% TiO$_2$GIC)	Flexural strength of Experimental group E-2 (3% TiO$_2$GIC)	-2.24 (0.74)	0.004
	Flexural strength of Experimental group E-3 (5% TiO$_2$GIC)	-9.36 (0.74)	0.001
	Flexural strength of Experimental group E-4 (7% TiO$_2$GIC)	-4.22 (0.74)	0.001

4.5.2.3.1 *Summary of flexural strength analysis of TiO$_2$GIC cement samples at different concentrations:-*

The flexural strength analysis revealed a systematic linear pattern increase in the flexural strength of TiO$_2$GIC cement samples with the increase in % of Titania (TiO$_2$-Nps) in the glass ionomer cement up to 5% and linear pattern decrease up to 10%. The maximum value of the flexural strength was attained by the experimental group E-3 (5% TiO$_2$GIC) which was F.S = 31.29, S.E = 0.37) while minimum value of the flexural strength was attained by the experimental group E-5 (10% TiO$_2$GIC) which was F.S=21.93,S.E=0.77 when compared with conventional control group E-1 (0% TiO$_2$GIC) where F.S= 19.31, S.E = 0.31 (*P-value* < 0.001) (Figure -4.43).
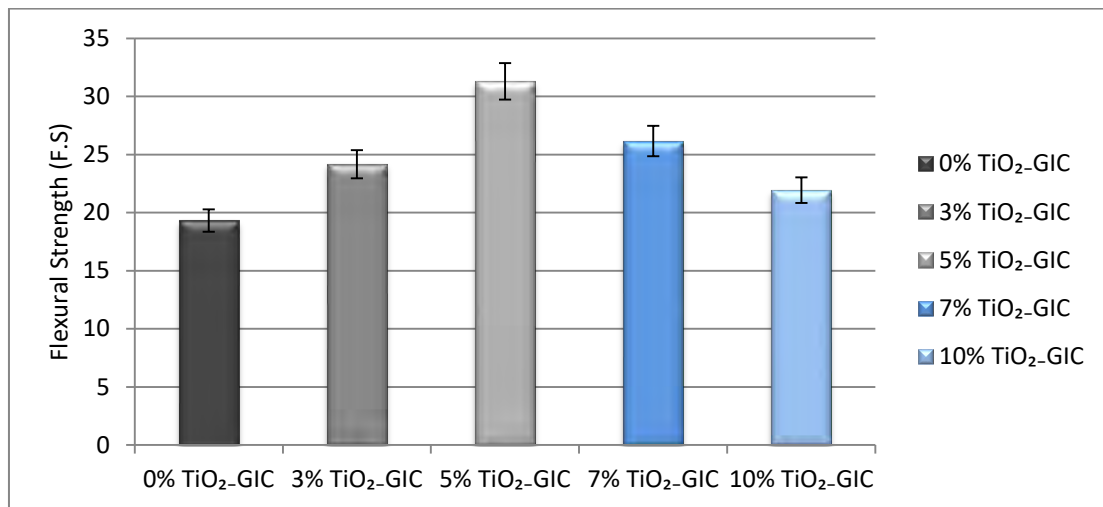
Figure-4.43: Differences in Flexural Strength (F.S) ofTiO$_2$GIC cement samples at different concentrations.

4.5.2.4 *Shear bond strength analysis of TiO$_2$GIC cement samples at different concentrations:*

Shear bond strength was carried out for both the enamel and dentine portions of the tooth by bonding all the samples of TiO$_2$GIC cement containing different percentages of Titania (TiO$_2$-Nps) first to the enamel and then to the dentin. In addition, enamel shear bond strength of all the samples of TiO$_2$GIC cements was greater than that of dentine shear bond strength comparatively, which was significant (*P-value* < 0.05).

4.5.2.4.1 *Enamel shear bond strength of TiO$_2$GIC cement samples at different concentrations:*

The enamel shear bond strength of TiO$_2$GIC cement samples illustrated a linear pattern increase with increase in the percentage of Titania (TiO$_2$-Nps) up to 5%. This increase in

enamel shear bond strength was demonstrated from conventional control group E-1 (0% TiO$_2$GIC), to experimental group E-2 (3% TiO$_2$GIC) and finally experimental group E-3 (5% TiO$_2$GIC). On the other hand, experimental group E-4 (7% TiO$_2$GIC) and experimental groupE-5(10% TiO$_2$GIC) revealed a linear pattern decrease with the increase in the percentage of Titania (TiO$_2$.Nps) which was significant (*P-value* <0.05) (Table-4.19).

***Table-4.19: Enamel Shear Bond strength** and standard error of various concentrations of* TiO$_2$GIC cement samples.

Control and TiO$_2$GIC Samples	Total Samples (n)	Enamel shear bond Strength of control and TiO$_2$GIC Samples with standard deviation (MPa ±S.D)	Standard Error (S.E)
Conventional control group E-1 (0% TiO$_2$GIC)	10	2.11 ±0.21	0.06
Experimental group E-2 (3% TiO$_2$GIC)	10	2.62±0.19	0.06
Experimental group E-3 (5% TiO$_2$GIC)	10	4.19±0.36	0.11
Experimental group E-4 (7% TiO$_2$GIC)	10	3.6±0.52	0.16
Experimental group E-5 (10% TiO$_2$GIC)	10	3.08±0.28	0.08

The mean differences between the inter-groups of TiO$_2$GIC cement samples at different percentages displayed maximum enamel shear bond strength in the experimental group E-3 (5% TiO$_2$GIC) but minimum enamel shear bond strength in the experimental group E-5 (10% TiO$_2$GIC) which was also significant (*P-value* < 0.05) (Table-4.20).

***Table-4.20: Inter-group comparisons of enamel shear bond strength of TiO$_2$GIC cement* samples containing various concentrations of Titania (TiO$_2$ Nps).**

Control and different concentrations of TiO$_2$GIC Samples	Comparison of enamel shear bond strength between control and different concentrations of TiO$_2$GIC samples	Mean Difference of enamel shear bond strength between control and different concentrations of TiO$_2$GIC samples with standard error (S.E)	*P-value*
Conventional control group E-1 (0% TiO$_2$GIC)	Enamel shear bond strength of Experimental group E-2 (3% TiO$_2$GIC)	-0.51 (0.15)	0.001
	Enamel shear bond strength of Experimental group E-3 (5% TiO$_2$GIC)	-2.08 (0.15)	0.001
	Enamel shear bond strength of Experimental group E-4 (7% TiO$_2$GIC)	-1.49 (0.15)	0.001
	Enamel shear bond strength of Experimental group E-5 (10% TiO$_2$GIC)	-0.97 (0.15)	0.001

	Enamel shear bond strength of Conventional control group E-1 (0% TiO$_2$GIC)	0.51 (0.15)	0.001
Experimental group E-2 (3% TiO$_2$GIC)	Enamel shear bond strength of Experimental group E-3 (5% TiO$_2$GIC)	-1.57 (0.15)	0.001
	Enamel shear bond strength of Experimental group E-4 (7% TiO$_2$GIC)	-0.98 (0.15)	0.001
	Enamel shear bond strength of Experimental group E-5 (10% TiO$_2$GIC)	-0.46 (0.15)	0.004
Experimental group E-3 (5% TiO$_2$GIC)	Enamel shear bond strength of Conventional control group E-1 (0% TiO$_2$GIC)	2.08 (0.15)	0.001
	Enamel shear bond strength of Experimental group E-2 (3% TiO$_2$GIC)	1.57 (0.15)	0.001
	Enamel shear bond strength of Experimental group E-4 (7% TiO$_2$GIC)	0.59 (0.15)	0.001
	Enamel shear bond strength of Experimental group E-5 (10% TiO$_2$GIC)	1.11 (0.15)	0.001
Experimental group E-4 (7% TiO$_2$GIC)	Enamel shear bond strength of Conventional control group E-1 (0% TiO$_2$GIC)	1.49 (0.15)	0.001
	Enamel shear bond strength of Experimental group E-2 (3% TiO$_2$GIC)	1.98 (0.15)	0.001
	Enamel shear bond strength of Experimental group E-3 (5% TiO$_2$GIC)	-0.59 (0.15)	0.001
	Enamel shear bond strength of Experimental group E-5 (10% TiO$_2$GIC)	0.52 (0.15)	0.001
Experimental *experimental group E-5* (10% TiO$_2$GIC)	Enamel shear bond strength of Conventional control group E-1 (0% TiO$_2$GIC)	0.97 (0.15)	0.001
	Enamel shear bond strength of Experimental group E-2 (3% TiO$_2$GIC)	0.46 (0.15)	0.004
	Enamel shear bond strength of Experimental group E-3 (5% TiO$_2$GIC)	-1.11 (0.15)	0.001
	Enamel shear bond strength of Experimental group E-4 (7% TiO$_2$GIC)	-0.52 (0.15)	0.001

4.5.2.4.1.1 *Summary of enamel shear bond strength of TiO$_2$GIC cement samples at different concentrations*:

The enamel shear bond strength analysis revealed a systematic linear pattern increase in the enamel shear bond strength of TiO$_2$GIC with the increase in % of Titania (TiO$_2$Nps) in glass ionomer cement up to 5% and linear pattern decrease up to 10%. The maximum value of enamel shear bond strength was attained by the experimental group E-3 (5% TiO$_2$GIC) where E.B.S = 6.91, S.E = 0.12 while minimum value of the enamel shear bond strength was attained by the experimental group E-5 (10% TiO$_2$GIC) where E.B.S=2.20, S.E=0.11 when compared with the conventional control group E-1 (0% TiO$_2$GIC) where E.B.S= 2.11,S.E = 0.06 (*P-value* < 0.001) (Figure -4.44).
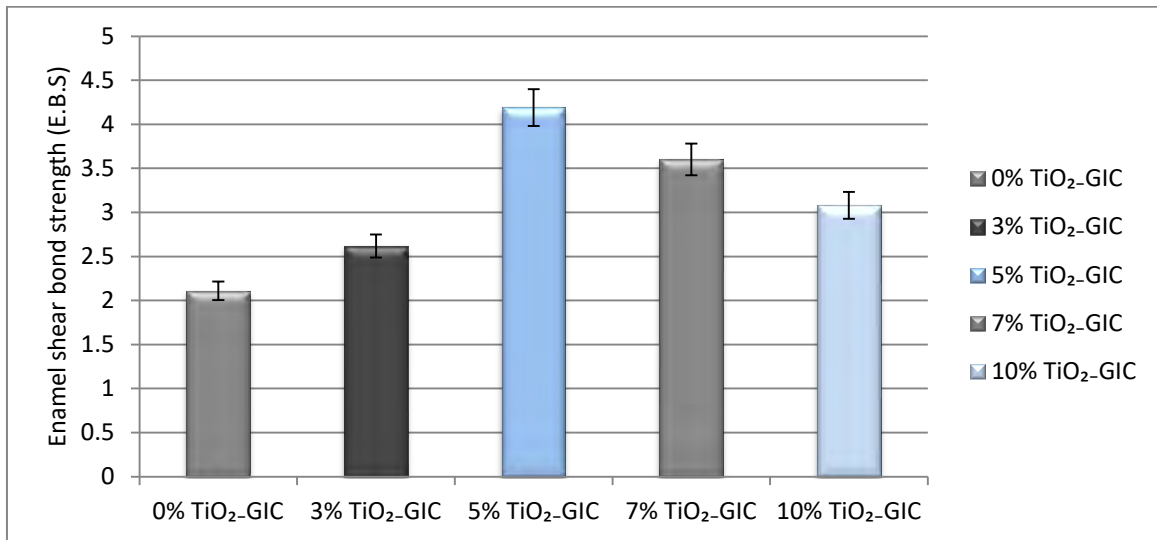
***Figure-4.44: Differences in the enamel shear bond strength (E.B.S) of*TiO₂GIC cement samples at different concentrations.**

4.5.2.4.2   *Dentin shear bond strength of TiO₂GIC cement samples at different concentrations*:

Dentin shear bond strength of TiO_2GIC cement samples demonstrated a linear pattern increase with the increase in the percentage of Titania (TiO_2 Nps) such as conventional control group E-1 (0% TiO_2GIC), experimental group E-2 (3% TiO_2GIC) and experimental group E-3 (5% TiO_2GIC). However, a systematic linear pattern decrease was notified in the experimental group E-4 (7% TiO_2GIC) and experimental group E-5 (10% TiO_2GIC) which was significant (*P-value* < 0.05) (Table-4.21).

Table-4.21: Dentin shear bond strength and standard error of various concentrations of TiO₂GIC cements.

Control and TiO₂GIC Samples	Total Samples (n)	Dentin shear bond Strength of control and TiO₂GIC Samples with standard deviation (MPa ±S.D)	Standard Error (S.E)
Conventional control group E-1 (0% TiO₂GIC)	10	1.98 ±0.19	0.06
Experimental group E-2 (3% TiO₂GIC)	10	2.25±0.22	0.07
Experimental group E-3 (5% TiO₂GIC)	10	3.67±0.32	0.10
Experimental group E-4 (7% TiO₂GIC)	10	3.10±0.21	0.06
Experimental group E-5 (10% TiO₂GIC)	10	2.51±0.21	0.06

The mean differences of the inter-groups TiO_2GIC cement samples at different percentages revealed maximum dentin shear bond strength in the experimental group E-3 (5% TiO_2GIC)

and minimum shear bond strength in the experimental group E-5 (10% TiO_2GIC) which was significant (P-value < 0.05) (Table-4.22).

Table-4.22: Inter-group comparisons of dentin shear bond strength of TiO_2GIC cement samples containing various concentrations of Titania (TiO_2Nps).

Control and different concentrations of TiO_2GIC Samples	Comparison of dentin shear bond strength between control and different concentrations of TiO_2GIC samples	Mean Difference of dentine shear bond strength between control and different concentrations of TiO_2GIC samples with standard error (S.E)	P-value
Conventional control group E-1 (0% TiO_2GIC)	Dentin shear bond strength of Experimental group E-2 (3% TiO_2GIC)	-0.27 (0.11)	0.015
	Dentin shear bond strength of Experimental group E-3 (5% TiO_2GIC)	-1.69 (0.11)	0.001
	Dentin shear bond strength of Experimental group E-4 (7% TiO_2GIC)	-1.12 (0.11)	0.001
	Dentin shear bond strength of Experimental group E-5 (10% TiO_2GIC)	-0.53 (0.11)	0.001
Experimental group E-2 (3% TiO_2GIC)	Dentin shear bond strength of Conventional control group E-1 (0% TiO_2GIC)	0.27 (0.11)	0.015
	Dentin shear bond strength of Experimental group E-3 (5% TiO_2GIC)	-1.42 (0.11)	0.001
	Dentin shear bond strength of Experimental group E-4 (7% TiO_2GIC)	-0.85 (0.11)	0.001
	Dentin shear bond strength of Experimental group E-5 (10% TiO_2GIC)	-0.26 (0.11)	0.019
Experimental group E-3 (5% TiO_2GIC)	Dentin shear bond strength of Conventional control group E-1 (0% TiO_2GIC)	1.69 (0.11)	0.001
	Dentin shear bond strength of Experimental group E-2 (3% TiO_2GIC)	1.42 (0.11)	0.001
	Dentin shear bond strength of Experimental group E-4 (7% TiO_2GIC)	0.57 (0.11)	0.001
	Dentin shear bond strength of Experimental group E-5 (10% TiO_2GIC)	1.16 (0.11)	0.001
Experimental group E-4 (7% TiO_2GIC)	Dentin shear bond strength of Conventional control group E-1 (0% TiO_2GIC)	1.12 (0.11)	0.001
	Dentin shear bond strength of Experimental group E-2 (3% TiO_2GIC)	0.85 (0.11)	0.001
	Dentin shear bond strength of Experimental group E-3 (5% TiO_2GIC)	-0.57 (0.11)	0.001
	Dentin shear bond strength of Experimental group E-5 (10% TiO_2GIC)	0.59 (0.11)	0.001
Experimental group	Dentin shear bond strength of Conventional control group E-1 (0% TiO_2GIC)	0.53 (0.11)	0.001

E-5 (10% TiO$_2$GIC)	Dentin shear bond strength of Experimental group E-2 (3% TiO$_2$GIC)	0.26 (0.11)	0.019
	Dentin shear bond strength of Experimental group E-3 (5% TiO$_2$GIC)	-1.16 (0.11)	0.001
	Dentin shear bond strength of Experimental group E-4 (7% TiO$_2$GIC)	-0.59 (0.11)	0.001

4.5.2.4.2.1 *Summary of dentin shear bond strength of TiO$_2$GIC cement samples at different concentrations:*

The dentin shear bond strength analysis revealed a systematic linear pattern increase in the dentin shear bond strength of TiO$_2$GIC with the increase in the % of Titania (TiO$_2$Nps) in glass ionomer cement up to 5% and linear pattern decrease up to 10%. The maximum value of dentin shear bond strength was attained by the experimental group E-3 (5% TiO$_2$GIC) where D.B.S = 5.64, S.E = 0.08 while minimum value of dentin shear bond strength was attained by the experimental group E-5 (10% TiO$_2$GIC) where D.B.S=1.92,S.E=0.11 when compared with the conventional control group E-1 (0% TiO$_2$GIC) where D.B.S= 1.98,S.E = 0.06 (*P-value* < 0.05) (Figure -4.45).
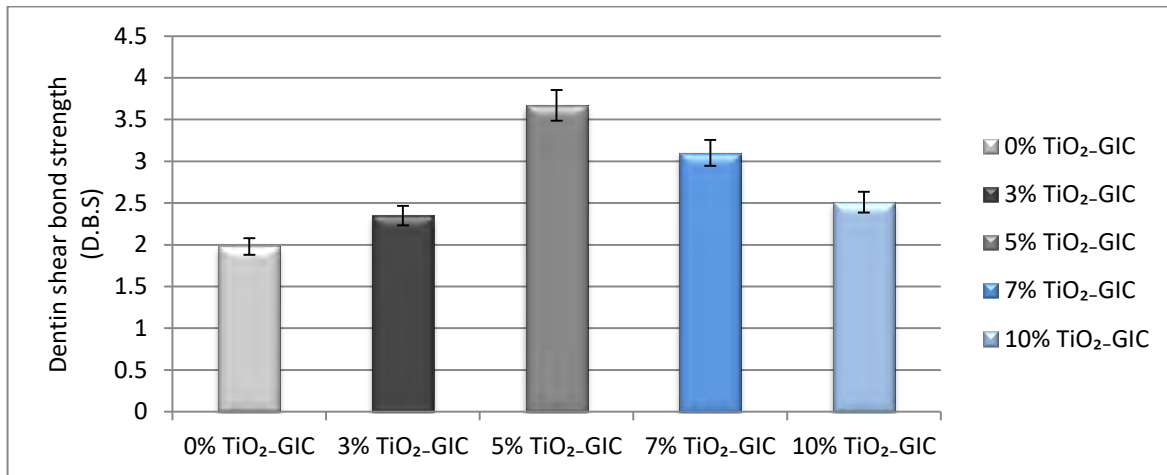
Figure-4.45: Differences in the dentin shear bond strength (D.B.S) ofTiO$_2$GIC cement samples at different concentrations.

4.5.2.6 *Scanning electron microscopic analysis for surface morphology and Spectrum mapping for compositional analysis:*

The spectrum mapping for compositional analysis of Conventional control group E-1 (0% TiO$_2$GIC) and experimental groups including E-2 (3% TiO$_2$GIC), E-3 (5% TiO$_2$GIC), E-4 (7% TiO$_2$GIC) and E-5 (10% TiO$_2$GIC) containing different concentrations of TiO$_2$Npsis given in the *Table*-4.23.

Table 4.23: Differences in the elemental composition of TiO$_2$GIC cement samples containing various concentrations of Titania (TiO$_2$Nps).

Sr	Elements	Conventional control group E-1 (0%TiO$_2$GI)	Experimental group E-2 (3%TiO$_2$GIC)	Experimental group E-3 (5%TiO$_2$GIC)	Experimental group E-4 (7%TiO$_2$GIC)	Experimental group E-2 (10%TiO$_2$GIC)
1.	Al	23.95%	23.89%	23.51%	22.02%	20.62%
2.	Si	20.07%	20.03%	20.01%	20.00%	19.71%
3.	C	14.93%	13.57%	12.03%	13.55%	13.02%
4.	O	14.55%	15.91%	16.21%	10.51%	14.01%
5.	F	2.04%	3.59%	6.46%	10.30%	10.34%
6.	Sr	22.60%	21.19%	20.57%	20.41%	19.14%
7.	P	1.70%	1.17%	0.33%	0.97%	0.59%
8.	S	0.16%	0.15%	0.09%	0.31%	0.11%
9.	Ti	0%	0.50%	0.79%	1.93%	2.45%

4.5.2.6.1   *Conventional Control group E-1 (0% TiO$_2$GIC):*

The SEM scans of Conventional control group E-1 (0% TiO$_2$GIC) showed maximum degradation sites having largest size of cracks and greatest number of voids in glass particles of GIC matrix at 50KX and 20KX magnifications due to absence of Titania Nps (Figure-4.46a and b).The compositional analysis revealed the presence of different percentages of elements in its composition without Titania Nps. The atomic % of elements present in it are C (14.93%), O (14.55%), F (2.04%) , Al (23.95%), Si (20.07%), Sr (22.60%), P (1.70%) and S (0.16%). The Al, Sr, Si, C and O were found in the maximum amounts whereas F, P and S were found in lesser quantities (Figure-4.46c, Table-4.23). The elemental mapping confirmed the presence of carbon, oxygen, fluorine, aluminum, silicon, strontium, phosphorus and sulphur in its spectrum (Figure- 4.46d).
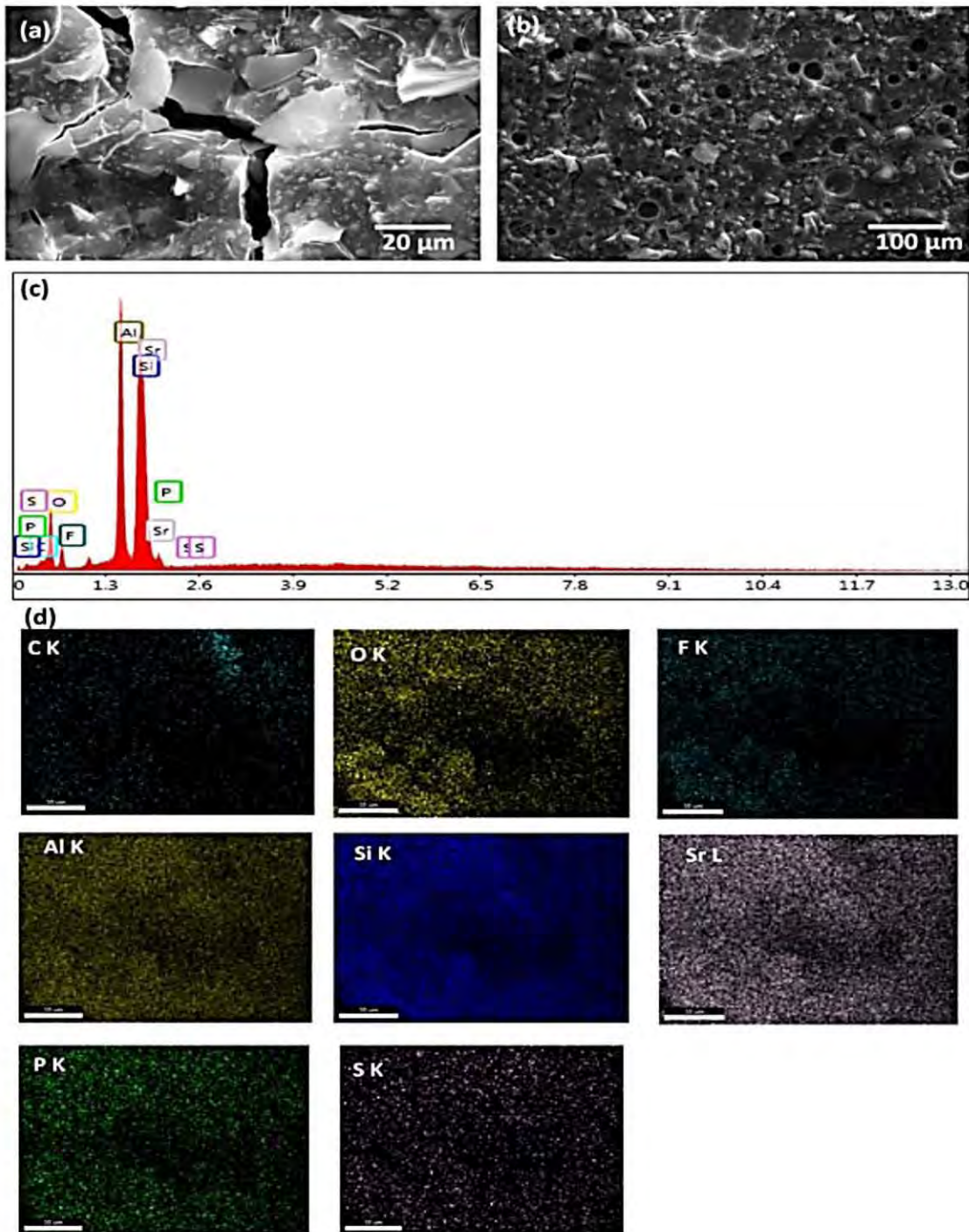
Figure-4.46: Spectrum mapping and Scanning electron microscopic analysis of Conventional control group E-1 (0% TiO$_2$GIC) displaying : (a,b) glass particles having disintegration sites with cracks and voids in its matrix without Titania Nps in the SEM image, (c) atomic % composition of elements in the EDX scan and, (d) Exact quantity of different constituents present in the elemental spectrum.

4.5.2.6.2   *Experimental group E-2 (3% TiO₂GIC):*

The SEM scans of experimental group E-2 (3% TiO$_2$GIC)displayed slight reduction in degradation sites having declined size of cracks and number of voids in glass particles with 3% Titania Nps in GIC matrix at 50KX and 20KX magnifications (Figure-4.47 a and b). The compositional analysis demonstrated the presence of C (13.57%), O (15.91%), Al (23.89%), Si (20.03%), Sr (21.19%), P (1.17%), S (0.15%), F (3.59%) and Ti (0.50%) in its composition by atomic %. The amounts of Al, Sr, Si, C, O, P and S were reduced whereas F was increased in comparison to the Conventional control group E-1 (0% TiO$_2$GIC) and presence of Ti was confirmed (Figure-4.47c). The presence of carbon, oxygen, fluorine, aluminum, silicon, strontium, phosphorus, sulphur and titanium were revealed in its composition by the elemental spectrum mapping (Figure-4.47d).
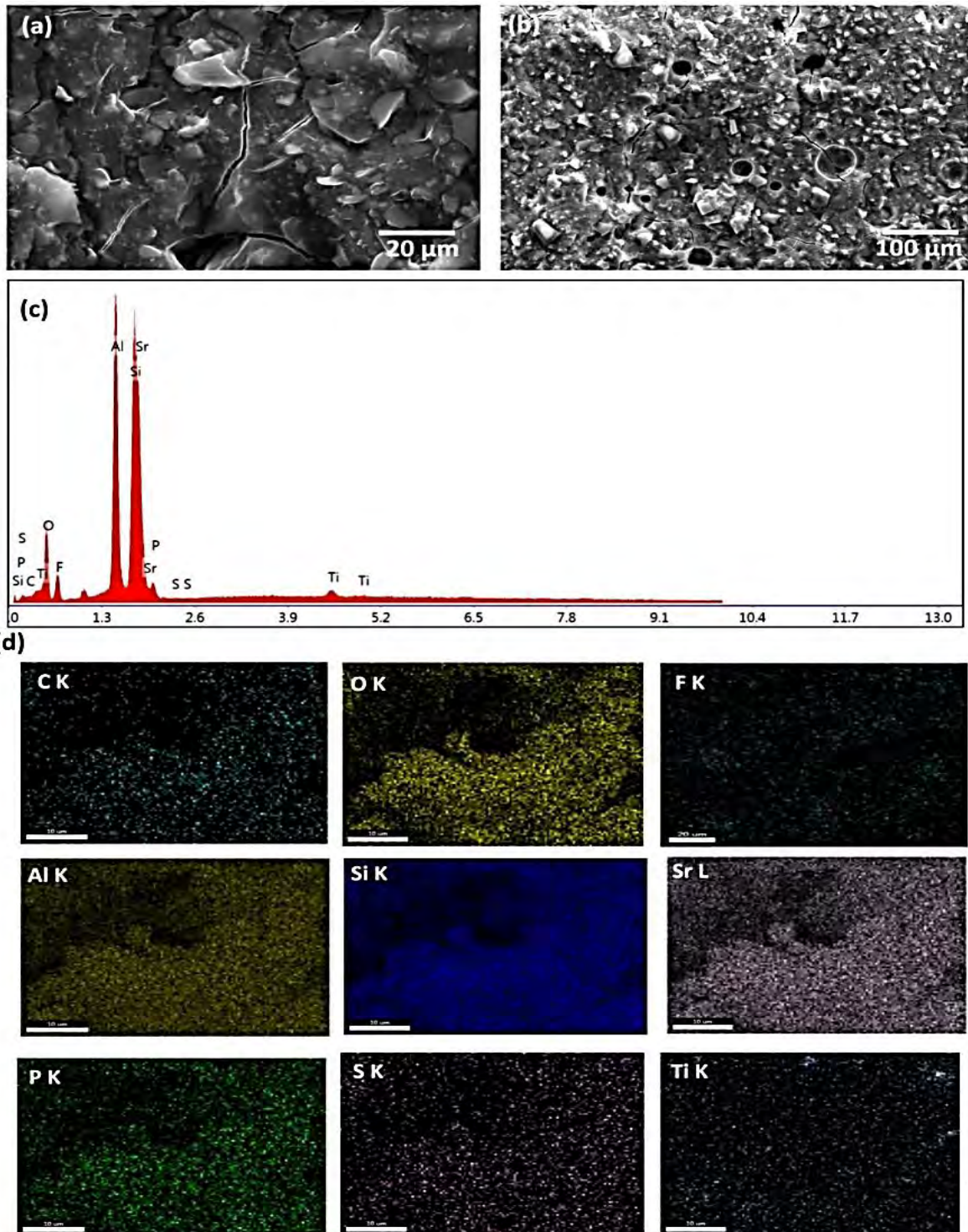
Figure 4.47 : Spectrum mapping and Scanning electron microscopic analysis of Experimental group E-2 (3% TiO$_2$GIC) displaying: (a) glass particles having slightly reduced disintegration sites with cracks and voids in its matrix with 3% Titania Nps in the SEM image, (c) atomic % composition of elements in the EDX scan and, (d) Exact quantity of different constituents present in the elemental spectrum .

4.5.2.6.3: *Experimental group E-3 (5% TiO$_2$GIC):*

The SEM scans of experimental group E-3 (5% TiO$_2$GIC)displayed maximum reduction in degradation sites having minimum cracks and no voids in glass particles with 5% Titania Nps in GIC matrix at 50KX and 20KX magnifications as compared to the experimental group E-2 (3% TiO$_2$GIC) and Conventional control group E-1 (0% TiO$_2$GIC) (Figure-4.48a and b). The compositional analysis demonstrated the presence of C (12.03%), O (16.21%), F (6.46%), Al (23.51%), Si (20.01%), Sr (20.57%), P (0.33%), S (0.09%) and Ti (0.79%) in its composition by atomic %.The amounts of Al, Sr, Si, P and S were reduced whereas F and Ti was increased in comparison to the Conventional control group E-1 (0% TiO$_2$GIC) and experimental group E-2 (3% TiO$_2$GIC). The maximum decrease in carbon content and maximum increase in O was observed in this group (Figure-4.48c). The presence of carbon, oxygen, fluorine, aluminum, silicon, strontium, phosphorus, sulphur with more titanium were evidenced in its composition by the elemental spectrum mapping (Figure-4.48d).
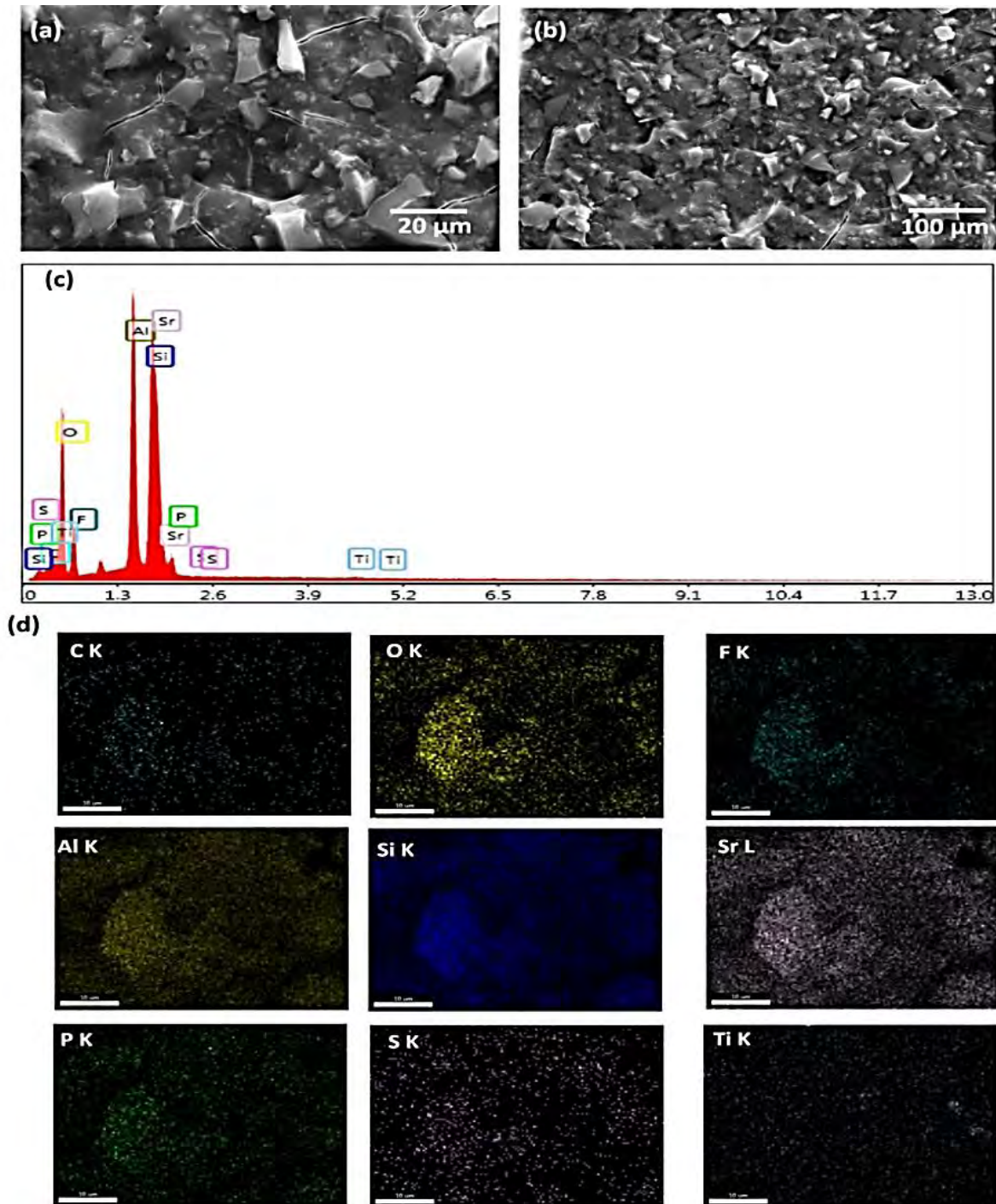
Figure 4.48: Spectrum mapping and Scanning electron microscopic analysis of Experimental group E-3 (5% TiO₂GIC) displaying: (a) glass particles having maximum reduction in disintegration sites without cracks and voids in its matrix with 5%Titania Nps in the SEM image, (c) atomic % composition of elements in the EDX scan and, (d) Exact quantity of different constituents present in the elemental spectrum.

4.5.2.6.4   *Experimental group E-4 (7% TiO$_2$GIC):*

The SEM scans of experimental group E-4 (7% TiO$_2$GIC) displayed reduction in degradation sites having cracks and voids in glass particles having more increased quantity of Titania Nps in the GIC matrix at 50KX and 20KX magnifications. These degradation sites having cracks and voids were more as compared to the experimental group E-2 (3% TiO$_2$GIC) and experimental group E-3 (5% TiO$_2$GIC) but lesser than Conventional control group E-1 (0% TiO$_2$GIC) (Figure-4.49a and b). The compositional analysis demonstrated the presence of C (13.55%), O (10.51%), F (10.30%), Al (22.02%), Si (20.00%), Sr (20.41%), P (0.97%), S (0.31%) and Ti (1.93%) in its composition by atomic %.The amounts of Al, Sr, Si, P, S and C were reduced in comparison to Conventional control group E-1 (0% TiO$_2$GIC) and experimental group E-2 (3% TiO$_2$GIC) whereas F and Ti was increased further, when compared with Conventional control group E-1 (0% TiO$_2$GIC) and experimental group E-2 (3% TiO$_2$GIC).The content of P, S, C and F in this group was greater than experimental group E-3 (5% TiO$_2$GIC) but O, Al, Sr, and Si were lesser comparatively (Figure-4.49c). The presence of carbon, oxygen, fluorine, aluminum, silicon, strontium, phosphorus, sulphur and titanium were confirmed in its composition by the elemental spectrum mapping (Figure-4.49d).
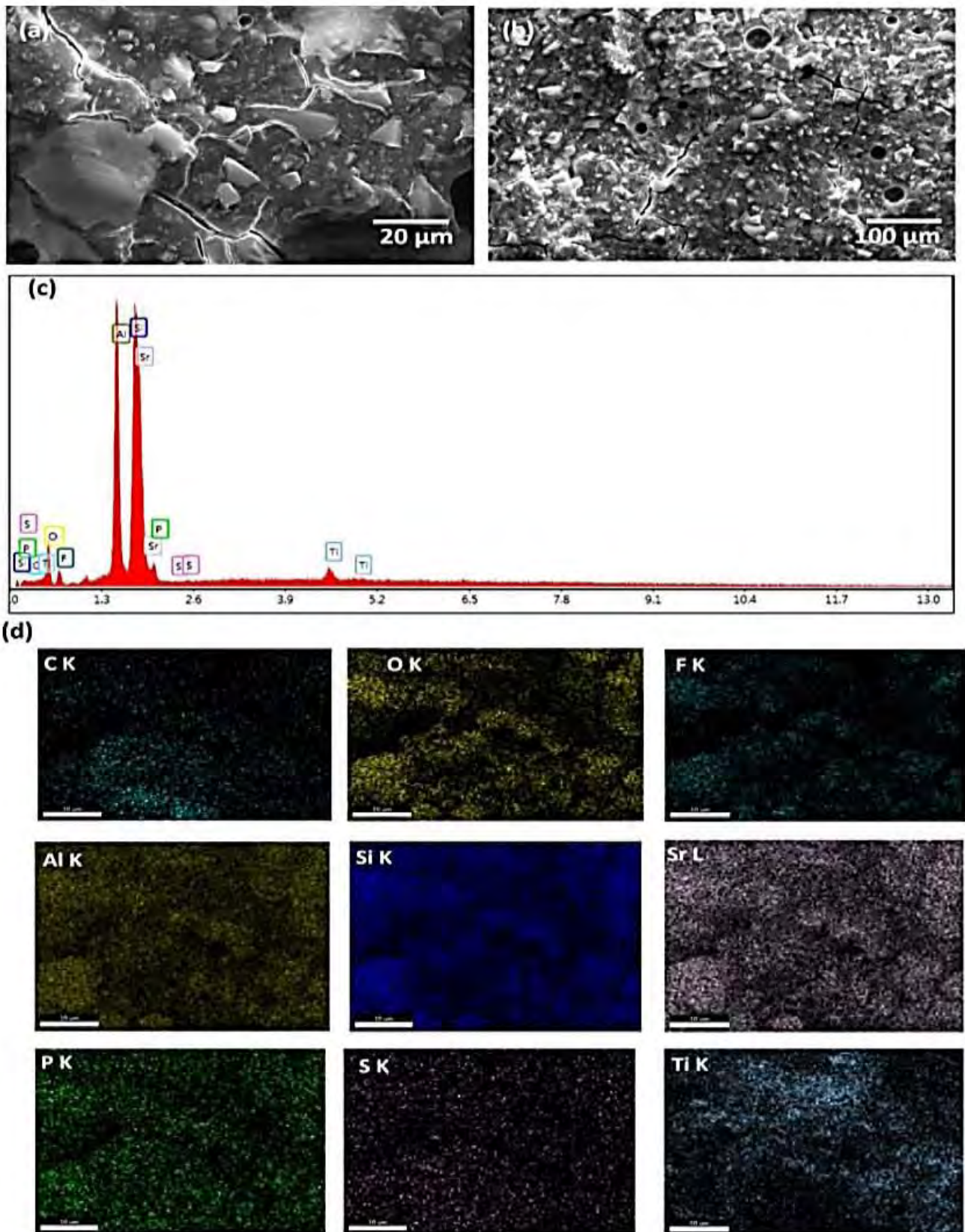
Figure 4.49: Spectrum mapping and Scanning electron microscopic analysis of Experimental group E-2 (3% TiO₂GIC) displaying: (a) glass particles having slightly declined reduction in disintegration sites with cracks and voids in its matrix with 7% Titania Nps in the SEM image, (c) atomic % composition of elements in the EDX scan and, (d) Exact quantity of different constituents present in the elemental spectrum.

4.5.2.6.5   *Experimental group E-5 (10% TiO$_2$GIC):*

The SEM scans of experimental group E-5 (10% TiO$_2$GIC)displayed glass particles having greatest quantity of Titania Nps at 50KX and 20KX magnifications with slightly more declined reduction in the voids of the glass matrix as compared to the experimental group E-2 (3% TiO$_2$GIC)**,** experimental group E-4 (7% TiO$_2$GIC)**,** andexperimental group E-5 (10% TiO$_2$GIC)(Figure-4.50a and b). The compositional analysis demonstrated the presence of C (13.02%), O (14.01%), F (10.34%), Al (20.62%), Si (19.71%), Sr (19.14%), P (0.59%), S (0.11%) and Ti (2.45%) in its composition by atomic %. The amounts of Al, Sr, Si, P, S and C were reduced in comparison to Conventional control group E-1 (0% TiO$_2$GIC), experimental group E-2 (3% TiO$_2$GIC) , and experimental group E-4 (7% TiO$_2$GIC) whereas F and Ti was increased further, when compared with Conventional control group E-1 (0% TiO$_2$GIC) , experimental group E-2 (3% TiO$_2$GIC), and experimental group E-4 (7% TiO$_2$GIC). The content of P, S, C and F in this group was greater than experimental group E-3 (5% TiO$_2$GIC)but O, Al, Sr, and Si were lesser comparatively (Figure-4.50c). The presence of carbon, oxygen, fluorine, aluminum, silicon, strontium, phosphorus, sulphur and titanium were confirmed in its composition by the elemental spectrum mapping (Figure-4.50d).
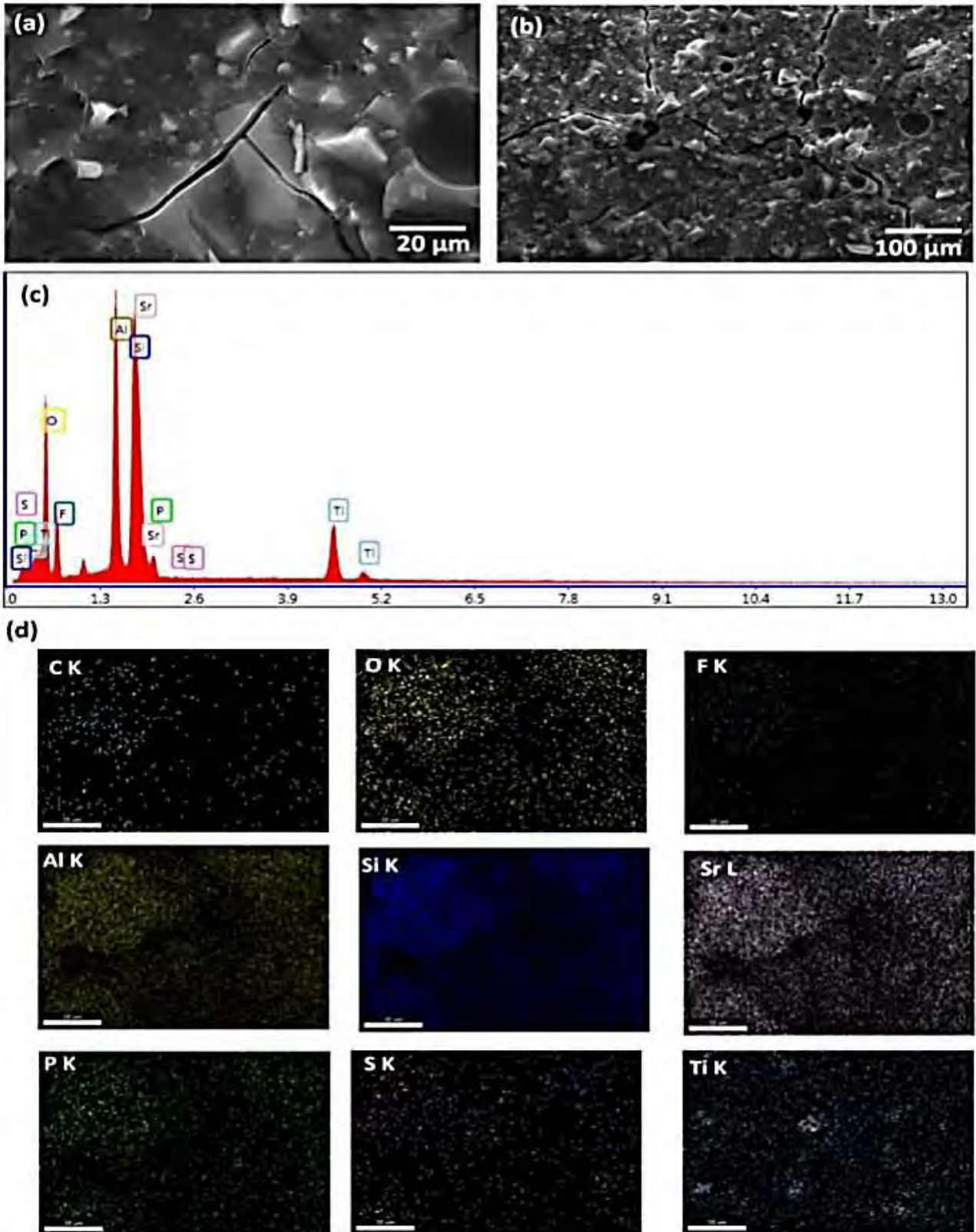
Figure 4.50: Spectrum mapping and Scanning electron microscopic analysis of Experimental group E-5 (10% TiO₂GIC) displaying: (a) glass particles having slightly more declined reduction in voids in its matrix with 10%Titania Nps in the SEM image, (c) atomic % composition of elements in the EDX scan and, (d) Exact quantity of different constituents present in the elemental spectrum .

Chapter-5

Discussion:

Nanotechnology has been gaining ample attraction in health care systems owing to its fascinating properties and broader implications in various technical domains [83]. The greater diversity in nanoparticles size, shape, surface morphology, chemical nature, phase form and above all synthesis methods have altered their biological, physical and chemical significance for advancing clinical diagnosis and treatment procedures [4]. The use of nanomaterials in the dentistry has been a comparatively neglected domain of the research. Compelling scientific data has been suggesting the future dominance of nanomaterials in designing drugs and composite materials for clinical dentistry. Considering the emerging role of Nps in future therapeutics, the current research was designed to prepare and Nps based innovative glass ionomer cement for its possible application in the dental filling materials.

5.1   *Phase-I: Synthesis of Titania (TiO$_2$ Nps):*

Titania (TiO$_2$ Nps) synthesis was carried out using *Bacillus coagulans* and *Mentha spicata* extract following ―green synthesis route" and under chemical laboratory conditions employing titanium tetrachloride solution. In flask containing *Bacillus coagulans* culture, the color was changed from creamy white to pure white after 24 hours (Figure -4.1) whereas, green to white color change was observed in *Mentha spicata* extract (Figure -4.2) and purple to white in titanium tetrachloride solution (Figure-4.3). These findings confirmed the synthesis of Titania (TiO$_2$ Nps) on the basis of results of some previous reports. The change of color has been suggested as the key indicator for synthesis of Nps [99]. The mechanism responsible for color change during Titania (TiO$_2$ Nps) might be oxidation process leading to Ti^{2+} cations and Ti^{2-} anions by reacting with water molecules entrapped in the precursor salts. The electron was released and taken up by Ti^{2+} cations along with water resulting in change of color from dark to lighter [202]. The scientific reason of the visibale color change has been explained in various previous works and was also a possible justification of color change as found in the present study.

5.2   *Phase-II   Standard Characterization Techniques:*

5.2.1   *XRD analysis and Raman spectroscopic analysis of Titania (TiO$_2$ Nps) for crystalline size and phase:*

The physico-chemical properties of the prepared Nps were determined via their characterization such as size, shape, phase, elemental composition, surface morphology, texture, topography, hydrodynamic size and functional compounds [203].

X-ray diffraction analysis and Raman spectroscopic analysis of Titania (TiO$_2$ Nps) was used to identify its phase and particle size. The Raman spectroscopic analysis depicted pure anatase peaks at the wave lengths of 243 cm^{-1} and 398 cm^{-1} for the innovative Titania (TiO$_2$ Nps) produced by *Bacillus coagulans* (Figure-4.32)and *Mentha spicata* (Figure -4.33) whereas Titania (TiO$_2$ Nps) prepared by *Conventional hydrothermal heating* (Figure-4.34) revealed pure anatase phase at the wave length of 243 cm^{-1} and rutile phase at 397 cm^{-1}. These peak formation at 243 cm^{-1} and 397 cm^{-1} are patent for anatase and rutile phases [204]. The raman peaks at higher intensity shows the smaller particle size and vice versa [191]. The innovative Titania (TiO$_2$ Nps) produced by *Bacillus coagulans*(Figure-4.32) demonstratedthe peak

intensities at 1,00,000 showing smaller particle size while Titania (TiO$_2$-Nps) synthesized by *Mentha spicata* (Figure-4.33) and *Conventional hydrothermal heating* (Figure-4.34) were observed at peak intensities of 98,000 and 97,000 showing medium and large size of these Nps. The innovative Titania (TiO$_2$-Nps) produced by *Bacillus coagulans*were found to be in 100% pure anatase phase (Figure-4.4,4.32 and Table-4.1)). Previous study conducted by S. Vijayakumar et al confirmed the pure anatase phase of Nps produced by *Bacillus subtilis* [205]. The Titania (TiO$_2$-Nps) synthesized by *Mentha spicata* were lying in 100% pure anatase phase (Figure-4.5, 4.33 and Table-4.2) which was in accordance with the previous study conducted by S. Babitha et al after utilizing green plant [206]. On the other hand, Titania (TiO$_2$-Nps) prepared by *Conventional hydrothermal heating* were lying in 82% pure anatase phase and 18% rutile phase (Figure-4.6, 4.34 and Table-4.3). The factors affecting phase form and particle size of Nps are temperature, pressure, pH and by-products produced during synthesis process [203]. The *Bacillus coagulans*culture used in the current study might have the highest pH that produced small sized Nps ranging between 5-30 nm [207], while *Mentha spicata* and C*onventionalhydrothermal* stock solution might have the lowest pH that resulted in slightly medium sized Nps between 31-40 nm and large sized Nps between 30-50 nm [208,209]. The large size of Nps produced by conventional methods is due to the utilization of the extra energy generated by the expensive toxic chemicals employed during their synthesis. These chemicals are not only responsible for the large size of the Nps but also making them unstable and more aggregated [210,211]. The plausible explanation for the aforementioned size of Nps via *Bacillus coagulans*culture might be the availability of very few NADH-dependent enzymes at high pH that might have prompted the particle aggregation quite slowly and gradually resulting in their small sizes. Secondly; natural capping and stabilizing agents might have caused a closely packed aggregation of Titania (TiO$_2$-Nps) producing spherical shape of these Nps synthesized by bacteria as compared to plant and *Conventional hydrothermal heating* that lacked these natural enzymes resulting in their mixed spherical and irregular shapes. The pure anatase phase of Titania (TiO$_2$-Nps) synthesized by *Bacillus coagulans* and *Mentha spicata* could be due to low process temperature without any pressure used in their preparation. On the other hand, Titania (TiO$_2$-Nps) prepared by *Conventional hydrothermal heating* might have undergone oxidation, reduction or corrosion in their composition at high temperature in the presence of toxic chemicals that might be responsible for producing different phases under similar circumstances. However, further research might be important to draw a conclusion regarding the appropriate mechanism for this phase behavior.

5.2.2 *DRS analysis of Titania (TiO$_2$-Nps) for confirmation of crystalline size:*

The UV-vis diffuse reflectance spectroscopic analysis was used to investigate the synthesis of Titania (TiO$_2$-Nps) in absorbance mode between 200-600 nm [212]. The absorbance mode of Titania (TiO$_2$-Nps) synthesized by *Bacillus coagulans, Mentha spicata* and *Conventional hydrothermal heating* was 337, 329 and 337 which matched the findings of the previous works [213,214]. The crystalline size, structure and aggregation of these Nps is calculated by band energy gap *P-value* in reflectance mode. The standard value of band gap energy for Titania (TiO$_2$-Nps) was 3.23eV. The band gap value verify particle size of synthesized Nps supporting the fact that smaller particle size constituted larger energy band gap and vice versa [212]. The band gap energy calculated for Titania (TiO$_2$-Nps) synthesized by *Bacillus coagulans* was found to be 3.5 eV (Figure-4.8) whereas for those synthesized by *Mentha spicata* and

Conventional hydrothermal heating it was 3.2eV and 2.9 eV (Figure-4.9, 4.10). These band gap energy values have confirmed that smallest Nps were produced by *Bacillus coagulans*in comparison to *Mentha spicata* and *Conventional hydrothermal heating* in the current study.

The concentration of solution (bacterial culture, plant extract and chemical) , type of catalyst, and size of raw materials used in fabrication of Nps have great effects on their particular properties including size, shape and phase distributions [215]. This showed that small sized Nps prepared by *Bacillus coagulans* imposed enhanced aggregation due to the presence of naturally potent biomolecules, enzymes, proteins and co-enzymes in them. The biomolecules might have been responsible for rapid capping of these Nps during initial nucleation and growth phases that could have closely packed these Nps together resulting in their spherical shape as well. Moreover, enzymes involved in microbial synthesis are devoid of any toxic chemical which could have enhanced particle aggregation and resulted in their well orderly arrangement of newly formed Nps resulting in their small sizes. The plants grow at different locations and at different times which might produce variations in the nature of their phytochemicals especially terpenoids that might generate impure substances. These impurities of phytochemicals might have assembled together inside these plant based Nps resulting in their size enhancement comparatively. The highly strong chemicals utilized by conventional methods may cause active polymerization reaction resulting in larger complex formation and further enlargement of Nps thereby, increasing their size.

5.2.3 *AFM analysis of Titania (TiO$_2$ Nps) for the size, shape and surface topography:*

The size, shape, surface roughness and texture of the prepared Nps was determined by AFM. The minimal surface roughness of about Rms=4.485 was observed by Titania (TiO$_2$ Nps) synthesized by *Bacillus coagulans* in comparison to *Mentha spicata* and *Conventional hydrothermal heating* where it was Rms = 5.693 and Rms=8.275 which was quite high.The Titania (TiO$_2$ Nps) synthesized by the bacteria revealed smooth surfaces which are in line with the reports of previous findings reported by Ladange et al [216]. The smooth surfaces imply that nano-architecture has been developed with high precision having no space in the lattice for the deposition of any other by product. The concatenation of these Nps was greater at the surfaces without any voids therefore, produced a smooth surface texture of the designed nanomaterials. Due to this property, Titania (TiO$_2$ Nps) have been considered as more active, chemically reactive and shows better performance when compared with the same particles synthesized by non-biological regimes [217]. Additionally, smoothness of Titania (TiO$_2$ Nps) might have occurred as a result of uniform capping during synthesis thereby, producing smaller size with spherical shape formation. The Titania (TiO$_2$ Nps) prepared by *Mentha spicata* displayed slightly greater surface roughness that might have been possible due to deposition of large amounts of plant phytochemicals in the voids left behind in the surfaces of these Nps during the synthesis. On the other hand, the Titania (TiO$_2$ Nps) prepared by *Conventional hydrothermal heating* confirmed the presence of mixed anatase-rutile phase with prominent surface roughness. These Nps possessed the anatase phase which had been considered as chemically reactive phase whereas rutile is inert and stable that might have prohibited them to get properly accumulated on the surfaces resulting in surface roughness.

5.2.4 *SEM analysis and DLS analysis of Titania (TiO₂ Nps) for particle size and shape:*

Scanning electron microscopic analysis and dynamic light scattering analysis was performed in order to observe the surface morphology including size and shape of the synthesized Titania (TiO₂ Nps) via three different routes. The Titania (TiO₂ Nps) synthesized by *Bacillus coagulans* displayed spherical shape having small particle size (Figure-4.16 and Figure-4.28) while those synthesized by *Mentha spicata* (Figure-4.17and Figure-4.29) and *Conventional hydrothermal heating* (Figure- 4.18 and Figure-4.30) revealed mixture of spherical and irregular shaped Titania (TiO₂ Nps) in medium and large sizes. A study performed by Kalishwaralal. et al reported small particle size of Titania (TiO₂ Nps) synthesized by bacteria [207] whereas medium particle size of Titania (TiO₂ Nps) using plant was obtained by Satishkumar, et. al., [208] and large particle size by conventional method was attained by Bekele, et. al.,[209]. The possible reasons for these results could be associated with reaction temperature, pressure, chemistry of reducing agents, nature of stabilizers and by-products produced. This assumption has been duly supported by the researchers who suggested that the chemical environment and temperature of the reaction are directly associated with size and shape based modifications of the Nps [218,219]. In case of the present research, lowest temperature and no pressure was used by *Bacillus coagulans* culture during the synthesis that produced spherical and small shaped Nps. Application of the microbial cultures generates small and spherical Nps suggested by some previous workers [207,220]. Although low temperature and pressure was used by *Mentha spicata* extract but some what mixture of spherical with slightly few irregularly shaped Nps were attained which might have been due to the prolonged heating in order to dissolve all biological components from plants in the substrate. The increased temperature and pressure used in *Conventional hydrothermal heating* produced large size having mixture of spherical with more irregularly shaped Nps [221]. The high temperature and pressure utilized by *Conventional hydrothermal heating* during the synthesis had adversely affected the size, shape and phase form of these Nps [99]. This might have occurred as a consequence of production of toxic by-products during their synthesis [222,223]. Another possible explanation of the aforementioned could be the prolonged incubation-time of reaction medium utilized by the microbial synthesis that could have reduced the availability of large amounts of reducing agents and metal salt precursors thus declining the secondary reduction of metallic ions on nuclei's surfaces after initial bonding of preformed nuclei on surface of metal ions resulting in spherically small sized Nps.b) presence of reduced amounts of reducing agents and precursors might have enhanced shrinkage among Nps, leading to loss of active aggregation between Nps by declining secondary reduction of metallic ions. These facts are also supported by the results of Patra, et. al., [224]. However, further research is required to understand the exact mechanism operating behind the size-shape relationship under varying reaction conditions, specifically using natural products.

5.2.5 *EDX analysis of Titania (TiO₂ Nps) for elemental composition in its spectrum:*

The true picture of elements present in composition of newly formed Np's was investigated by EDX/EDS [225]. These elements appear in EDS as a result of reducing agents and catalysts used during their synthesis. The energy dispersive x-ray spectroscopic analysis (EDS) of *Bacillus coagulans, Mentha spicata, and Conventional hydrothermal heating* derived Nps having pure titanium (Ti) and oxygen (O) peaks with no additional peaks of any impurity (Figure- 4.20,4.21,4.22). The presence of any impurity in EDS either detectable or non-

detectable in form of traces is responsible for producing cytotoxicity of Nps. The impurity leading to cytotoxicity of Nps is dependent on components used as reducing and stabilizing agents in their synthesis. The Titania (TiO_2 Nps) produced by *Bacillus coagulans* were declared safe and non-toxic as a result of their biomolecular synthesis [171,172]. The presence of naturally occurring biomolecules, enzymes, proteins, and co-enzymes inside microorganisms took part in the production of biocompatible *Bacillus coagulans* Nps. Based on these facts, it can be suggested that the presence of natural molecules facilitates high purity of the product owing target specific activity of cellular materials. However, different types of the microbial cells generate slightly different results due to difference in chemical environment of the cells. In general terms, application of microbial cultures generates similar type of the results with minor differences [226]. The Titania (TiO_2 Nps) formed by *Mentha spicata* used phytochemicals as reducing and stabilizing agents during synthesis. The phytochemicals named polyphenols, catechins, alkaloids, flavonoids, tannis and other functional group compounds are present inside the plants which are naturally toxic to some extent. These reducing and stabilizing agents are less safe due to their highly complex bioreduction process which promotes the formation of Nps but with traces of impurities [226]. Additionally, this complexity might have adversely affected size, shape and morphology of these Nps rendering them toxic in nature.

The Titania (TiO_2 Nps) synthesized by *Conventional hydrothermal heating* originated due to utilization of titanium tetrachloride as a reducing and stabilizing agent during synthesis. The titanium tetrachloride solution might have released traces of toxic byproducts from its composition. Previous studies have also confirmed that either usage of different chemicals as reducing and stabilizing agents during the synthesis or their byproducts released after the synthesis are equally responsible for inducing cytotoxic behavior in Nps [227]. Future investigations are required to confirm the effects of elemental compositions on the cytotoxic behavior of Nps.

5.2.6 *FTIR analysis of Titania (TiO_2 Nps) for the presence of functional groups:*

The Fourier transform infrared spectroscopic analysis was employed for presence of various functional groups in the Titania (TiO_2 Nps). The peaks observed between 600-400 cm^{-1} are characteristically patent peaks confirming the formation of Titania (TiO_2 Nps) synthesized by any route i.e bacteria, plant and conventional method as reported by A.Khadar et al (Figure-4.24,4.25,4.26 and table 4.4,4.5, 4.6) [228]. It was reported by V. Augugliaro et. al. that the peak of C-H stretching particularly at the wave length of 2900 cm^{-1} is the marker of presence of some kind of impurities [229]. The presence of O=C=O groups containing carbon dioxide at the wave length of 1499.01 cm^{-1} and 1445.7 cm^{-1} were demonstrated in Titania (TiO_2 Nps) synthesized by *Mentha spicata* and *Conventional hydrothermal heating* which were evident trace impurities reported previously between 1450 cm^{-1}-1400 cm^{-1}. [230]. The absence of any peak at 2900 cm^{-1} and 1450 cm^{-1}- 1400 cm^{-1} in the Titania (TiO_2-Nps) synthesized by *Bacillus coagulans*confirmedthe absence of any impurity while presence of this peak in Titania (TiO_2 Nps) synthesized by *Conventional hydrothermal heating* revealed the presence of some impurity. On the other hand, presence of trace impurities of carbon dioxide in Titania (TiO_2 Nps) synthesized by *Mentha spicata* and *Conventional hydrothermal heating* was confirmed in this study. The bacterial proteins and lipids present in the structure and function of *Bacillus coagulans* could be responsible for producing amine linkage chains that might have played an

essentially beneficial role in the synthesis of Nps. These amine linkage chains might have been produced in limited in numbers that could have generated small sized Titania (TiO$_2$ Nps) through adhesion of proteins with metallic ions. Thus, involvement of only bacterial protein and lipid chain as a functional group, during synthesis might have played a key role in declaring these Nps as biocompatible. The Titania (TiO$_2$ Nps) synthesized by *Mentha spicata* utilized phytochemicals which might have resulted in the repeated functional group chains that could have displayed their slightly less biocompatible behavior. The Titania (TiO$_2$ Nps) produced by *Conventional hydrothermal heating* have employed chemicals at high temperature and pressure during synthesis that might have resulted in production of large amounts of different functional group chains that could make them non-biocompatibile in the current study. Further studies are required to address the biocompatibility issues as its a genuine point of concern from medical point of view.

5.3 *Phase III: Antimicrobial Activity of Titania (TiO$_2$ Nps):*

The antimicrobial activity of synthesized Titania (TiO$_2$ Nps) was carried out via agar disc diffusion test. The Titania (TiO$_2$ Nps) synthesized by *Bacillus coagulans* displayed maximum antimicrobial activity against *E. coli followed by L .acidophilus*, *E. faecalis*, *E.faceium,S. aureus,*and *P. aeruginosa* as compared to those synthesized by *Mentha spicata* and *Conventional hydrothermal heating* (Figure-4.36 and Table 4.10). These findings were similar to some previous findings [136,231,]. The reason behind enhanced antimicrobial activity of Titania (TiO$_2$ Nps) synthesized by *Bacillus coagulans*againstboth the gram positive and gram negative caries promoting pathogens could be due to their exceptionally ideal small size, spherical shape, smooth surface, biomolecular based synthesis with pure anatse phase. Previous studies confirmed that Np's shape, size, surface morphology, synthesis methodology and phase forms are purely responsible for the increased antimicrobial activity of the Nps [232,233]. Furthermore, these microbially synthesized Titania (TiO$_2$ Nps) depicted excellent stability which enables the strong capping layer present on their surfaces to entrap large amount of pathogenic bacteria. This efficacy of the Nps is associated with the electrostatic interactions between negatively charged bacterial cell surfaces and positive charge of the Titania (TiO$_2$ Nps). Thus, it makes a practical sense to consider an antagonist relationship between the two. Mechanistically, this interaction leads to the rupture of bacterial cell envelopes in order to demonstrate the antimicrobial potential of these Nps. These results find reasonable agreement with the findings of the references [234,235]. Further, the enzymes, proteins, co-enzymes and biomolecules present in bacteria also releases large amounts of adsorbed Ti-ions which might have attacked the cell wall of pathogenic bacteria initially. This is followed by discharge of intracellular and proteinaceous components from bacteria. These released components destabilize the plasma and outer membranes of the cells due to the extensive reduction in intracellular ATP levels thus, prohibiting the release of Vitamin E responsible for the stability [130]. Then pits and pores of grave nature are developed on the cell wall surfaces of these pathogenic caries promoting bacteria exposed to Np's. This in turn, increases the permeability of cell wall surfaces to absorb and absorb large amounts of these Np's causing death of these pathogenic bacterial cells [236]. Besides, detail studies regarding the structure-function relationship and interactions of the Np's at cellular interfaces need further investigations.

The reason for the slightly lesser antimicrobial activity displayed by Titania (TiO$_2$.Nps) formed by *Mentha spicata* is that plants vary in the characteristics of the biomolecules produced by them due to the differences in their growth and development at certain geographical locations in different seasons. This variability in the characteristics of these plant biomolecules might occur as result of changes in the temperature, water, environment, soil, atmosphere and fertilizers. The most common plant biomolecules utilized in the synthesis of Titania (TiO$_2$-Nps) are phytochemicals, flavoids and terpenoids present in their composition. During syntheis of Nps, temperature variations might pose these plant biomolecules toxic that might become less capable of penetrating the pathogenic bacteria entirely. This in turn would hinder the absorption and adsorption of Titania (TiO$_2$.Nps) in bacterial cell surfaces as a result of toxic matter present in these Nps thus, reducing their deaths that could be hazardous [135]. The Titania (TiO$_2$.Nps) synthesized by *Conventional hydrothermal heating* displayed the least antimicrobial activity due to the reason that these methods utilize certain chemicals as capping, reducing and stabilizing agents during the synthesis process which produce toxic by-products. These toxic by-products gets attached on the surface of these Nps resulting in their instability. This instability altogether with toxic by-product formation are key factors responsible for their minimum antimicrobial activity against pathogenic bacteria [185]. Due to differences in the morphology of the gram positive and gram negative strains, there is a great deviation in the antimicrobial activity revealed by these Nps .Therefore, different results regarding antimicrobial activity were attained in the present investigation making a logic and reasonable justification of the present findings. The interaction of Nps with the membrane associated proteins and with the gram negative porins yet remain unexplained and invite further research.

5.4 *Phase -IV Biocompatibility (cell viability %) of Titania (TiO$_2$.Nps):*

The biocompatibility of Nps is the foremost requisite before their utilization at medical and dental platforms. The biocompatibility (non-cytotoxicity/cell viability %) of Nps is investigated by MTT assay testing [234]. The universally accepted standard used for detecting the cytotoxic response of Nps is characterized by following a standard protocol which describes Nps as Non cytotoxic (cell viability > 90%), mild cytotoxic (cell viability between 60-90 %), moderate cytotoxic (cell viability between 30-60%) and severe cytotoxic (between 30% - less) [197]. The cytotoxicity analysis of Titania (TiO$_2$.Nps) prepared with help of *Bacillus coagulans* and *Mentha spicata* demonstrated their non cytotoxic nature because of their greater cell viability > 90% at all the concentrations in comparison with the control group that showed 100% cell viability. The cytotoxicity analysis of Titania (TiO$_2$.Nps) prepared by *Conventional hydrothermal heating* revealed mild cytotoxicity at the end of investigation because their cell viability was in the range between 60-90 % as compared to the control group(*P-value* < 0.05) (Table-4.11 and 4.12).

The cytotoxicity of Nps is predominantly dependent on their mode of synthesis, physico-chemical properties, time-duration of exposure and concentration used [215]. The synthesis of Nps with the help of bacteria has been supported previously in the literature due to its enhanced advantages [91]. The advantages of bacteria include their outstanding biocompatibility, flexible nature, high growth rate, high yield, cost-effectiveness, easy culturing and manipulation [109, 237]. The biocompatible behavior of these Nps synthesized by bacteria might be due to presence of natural enzymes, proteins and co-enzymes [238]. Firstly, these natural products could have reduced and stabilized the Titania (TiO$_2$.Nps)

produced by *Bacillus coagulans* in the first step.Secondly, these natural products might have released non-toxic residues during the process of synthesis that might have rendered these Nps biocompatible with no toxicity. Thus, adverse effects of cytotoxicity might not have been observed in these Nps which commonly includes apoptosis, inflammation and oxidative stress.

The large variety of plant phytochemicals might have taken part in disrupting the biological functions of the cell lines that could have adversely affected their viability which might lead to future toxicity. There are seventy seven identified toxic plant phytochemicals present in different green species of which trepenoids, glycosides and alkaloids are the most common ones [239]. Further investigations are required to check the effects of these phytochemicals on the cell viability to ensure their biocompatible nature for future advanced biomedical applications.

The toxic and expensive chemicals were used in the synthesis of Nps by *Conventional hydrothermal heating.* The sodium hypochlorite used in the current study for reducing $TiCl_4$ salt to Titania (TiO_2 Nps) could have released hazardous byproducts which might have turned them in an unstable state. This unstable state of Titania (TiO_2 Nps) might have allowed their easy and increased penetration in the cells. This increased penetration might have lead to apoptosis, inflammation and oxidative stress in the fibroblast cell lines leading to rapid and excessive generation of ROS (reactive oxygen species) and free-radicals. These ROS and free-radicals inhibit the release of vitamin E and glutathione that play key role in maintaining the stability of Titania (TiO_2 Nps) [240].

The biocompatibility of Nps was also evaluated by their physico-chemical properties because there exists a direct relationship between these properties and cytotoxicity. The size, shape, phases, composition and surface area are the important characteristics of the Nps which can impart any negative effect. Although, small size and spherical shape of Nps exhibit large surface to volume ratio which means that small sized Nps can be easily adsorbed and absorbed in the cells and produce changes in their biological and metabolic functions [163]. These disruptions in the bacterial cell functions might lead to the reduction in their cell viability %. The Titania (TiO_2 Nps) synthesized by *Bacillus coagulans* displayed slight reduction in the cell viability % but within the range of non-cytotoxic in the current study. The plausable explanation for their non-cytotoxicity with larger surface area to volume ratio could be that small sized and spherical shaped Nps after coming in contact with cells might have easily and quickly penetrated the cell surfaces but couldn't release large quantities of toxic products such as reactive oxygen-species (ROS) and free-radicals because of the presence of their pure composition without any impurity. A study performed by Ganapathi, et. al., confirmed that excessive release of reactive oxygen-species (ROS) and free-radicals might serve as major contributors of cytotoxicity [156]. The Titania (TiO_2 Nps) synthesized by *Mentha spicata* and *Conventional hydrothermal heating* were comparatively larger and contained mixture of spherical with irregularly shape Nps. The large size of these Nps might have controlled their easy penetration in bacterial cell surfaces to some extent but their irregular shapes might have promoted their attachment with the cell surfaces. This attachment might help in releasing the toxic impurities present in the plant phytochemicals and toxic byproducts formed during the conventional methods. These released components might have reduced the cell viability % to greater extent eventually, inducing the well-defined cytotoxic effects.

The phases of Titania (TiO$_2$ Nps) also play a significant role in transforming these Nps from biocompatible to non-biocompatible by reducing their cell viability %. The anatase phase is chemically reactive and is somewhat unstable while mixed anatase-rutile phase is quite inert and stable [241]. The Titania (TiO$_2$-Nps) produced by *Bacillus coagulans* and *Mentha spicata* were having 100% pure anatase phase and those synthesized by *Conventional hydrothermal heating* fell in mixed anatase-rutile phase in this study. Although, cell viability % of fibroblasts against anatase Titania (TiO$_2$ Nps) synthesized by *Bacillus coagulans* and *Mentha spicata* in the current study was reduced as a result of strong reactivity and instability of these Nps that might have made these fibroblasts unstable leading to their deaths but not less than 90%. The pure composition and functional compounds of Titania (TiO$_2$ Nps) in the EDX and FTIR spectrum with no impurity might be the main factor responsible for upholding the cell viability% > 90%, hence, confirming their non-cytotoxic behavior. The Titania (TiO$_2$ Nps) synthesized by *Mentha spicata* possessed pure composition in their EDX scan but few traces of impurities in the form of nitrogen compounds and carbon dioxide in the FTIR spectrum that might have reduced their cell viability % but not less than 90% because of their anatse phase. The cell viability % of Titania (TiO$_2$ Nps) synthesized by *Bacillus coagulans* wasmaximum in comparison to Titania (TiO$_2$ Nps) synthesized by *Mentha spicata* but this difference between these two groups was insignificant. Still, future study regarding the cell viability % and biocompatibility in plant oriented Nps is required to get a justified scientific evidence regarding the safe nature of terpenoids, alkenoids, and alkoids present in the plants.

The compromised biocompatibility of Titania (TiO$_2$ Nps) synthesized by various conventional methods have been already reported in the literature [161,167]. The mixed anatase-rutile phase obtained by the Titania (TiO$_2$ Nps) synthesized by *Conventional hydrothermal heating* might have tried their level best to prevent the cell viability % from dropping beyond 90% against fibroblasts exposed to them because of the stable, inert nature of the rutile phase of these Nps but their toxic byproducts formed during the synthesis might have rendered them mildly toxic by reducing the cell viability% between 60-90% .The EDX scan of these Nps did not reveal any impurity but traces of impurities in the form of nitrogen compounds and carbon dioxide in the FTIR spectrum might have been responsible for reducing the cell viability < 90% thus, confirming their cytotoxic behavior.

The current study unveiled different concentrations of all the synthesized Nps to fibroblast cell lines to detect their cytotoxicity, where increased concentration exposure of Nps to cell lines results in death of cells [242]. The Nps synthesized by *Bacillus coagulans* and *Mentha spicata* exposed to fibroblast cell lines were non-cytotoxic whereas those synthesized by *Conventional hydrothermal heating* revealed mild cytotoxicity in greater concentrations. The reason may be the fact that Nps synthesized by *Bacillus coagulans* have attained a more stronger, stable, safe and uniform capping layer around their surfaces during redox reactions. This safe capping layer is formed from natural biomolecules such as proteins, enzymes and co-enzymes present in the bacteria. These Nps might have disintegrated the cells surfaces but without releasing any toxic product. Thus, this additional strong and stable capping layer around the Nps synthesized by *Bacillus coagulans* is responsible for their enhanced biocompatibility and non-cytotoxicity.

5.5 Phase - V: Mechanical strength and properties of TiO$_2$ Nps in GIC restorative material:

The GIC is till to date considered as the best restorative material in the dentistry because of its versatile qualities such as strong tooth adhesion, anti-cariogenic property, bio-compatibility, flouride release, dentin compatible elasticity and less co-efficient of thermal expansion but the only drawback lies in its reduced mechanical strength properties which needs improvement [243]. The conventional GIC is lacking in its mechanical properties due to the void formation in its structure during the mixing of powder and liquid as a result of entrapment of air in its structure. These voids vary in their size and number [244], which might develop stress concentration sites in the GIC restoration in the oral cavity that could have compromised the mechanical strength of this restorative material to the fullest.

The mechanical properties of the restorative materials are the key features responsible for their selection and utilization in the oral cavity. Multiple varieties of masticatory loads have been applied to the human dentition with in the oral cavity on regular basis. The restorative materials used in the oral cavity must possess adequate mechanical strength to bear such masticatory forces in order to enhance their shelf life and durability successfully in the clinical settings [245]. There exists a close association between mechanical strength properties of any restorative material and filler added to it particularly size and content of filler [246]. The incorporation of Nps enhances the mechanical strength and properties of restorative materials via provision of increased surface area and filler loadings because of its nanoscaled unique features [247]. Thus, the increased surface area and nano-size of the Titania (TiO$_2$ Nps) might have enhanced the mechanical interlocking between the GIC matrix and Nps by the close approximation of GIC powder particles and its liquid through these Nps [248]. Moreover, any change in the quantity, concentration, particle size distribution, cross-linking, chemical reaction and bonding between Nps and restorative materials also affect their mechanical strength and properties to a great extent [249]. Thus, commercial Titania (TiO$_2$ Nps) used as fillers in the GIC previously could possibly enhance the mechanical strength and properties of the restorative material but only up to a certain limit [181].

The mechanical properties of GIC with different concentrations of Titania (TiO$_2$ Nps) in the conventional control group E-1 (0% TiO$_2$GIC), experimental group E-2 (3% TiO$_2$GIC), experimental group E-3 (5% TiO$_2$GIC), experimental group E-4 (7% TiO$_2$GIC), and experimental group E-5 (10% TiO$_2$GIC), prepared by *Bacillus coagulans* were evaluated and compared utilizing Vicker's micro-hardness, compressive strength, flexural strength and shear bond strength tests on human tooth (enamel and dentin). The Titania (TiO$_2$ Nps) prepared by *Bacillus coagulans* were employed as a result of its natural biomolecular synthesis, highest level of stability, enhanced antimicrobial activity and biocompatibility with entirely pure and non-cytotoxic behavior. The experimental group E-3 (5% TiO$_2$GIC) displayed the maximum mechanical strength and properties in comparison to other groups used in this study.

The main test that contributes to the mechanical strength property of the restorative material is its surface hardness property due to its resistance to deformation [245]. The surface hardness of the restorative material is best investigated by Vicker's micro-hardness tester having pyramid shaped indent used for the specific time with a particular load [246]. The current study depicted the maximum surface hardness in the experimental group E-3 (5% TiO$_2$GIC) containing 5% Titania (TiO$_2$ Nps) in comparison to the conventional control group E-1 (0%

TiO$_2$GIC) having 0% Titania (TiO$_2$.Nps) and other experimental groups E-2 (3% TiO$_2$GIC) with 3% Titania (TiO$_2$.Nps), E-4 (7% TiO$_2$GIC) with 7% Titania (TiO$_2$.Nps), and E-5 (10% TiO$_2$GIC) with 10% Titania (TiO$_2$.Nps) (Figure-4.41 Table 4.13, 4.14). The findings in current study were similar to work done by Garcia, et. al., but only up to addition of 3% Titania (TiO$_2$. Nps) [181]. Another study performed by Ozge, et. al., also reported the same increase in the surface hardness up to the limit of 3% Titania (TiO$_2$.Nps) only which was insignificant [250]. The results of the addition of 5% Titania (TiO$_2$.Nps) in the experimental group E-3 in the current study did not match the literature and addition of 7% Titania (TiO$_2$.Nps) in the group E-4 and 10% Titania (TiO$_2$.Nps) in the group E-5 was not investigated previously [181, 250].

The filler's particle size, its density, and distribution plays a significant role in the surface micro-hardness of any restorative material [248]. Previously, mentioned studies utilized the commercially available Titania (TiO$_2$.Nps) [181, 250], whose biocompatibility was not evaluated that could have become the sole reason for the limited increase in their surface hardness. This might have been possible due to the entrance of impurities present in the Titania (TiO$_2$.Nps) into the GIC matrix that could have prevented the surface hardness from increasing with the increase in the concentration of these Nps. The biocompatibility of any material used in the oral cavity is the ultimate requirement in the clinical settings. The Titania (TiO$_2$.Nps) synthesized by *Bacillus coagulans* in our study were biocompatible enough that might have enhanced the surface hardness of this innovative glass ionomer restorative cement in the experimental group E-3 containing 5% Titania (TiO$_2$.Nps) only. The plausable explanation for this increase in surface hardness could be that these Titania (TiO$_2$.Nps) might have served the purpose of an ideal filler due to its pure composition, small size, spherical shape and adequate concentration that could have helped in establishing a strong mechanical interlocking between the GIC powder particles and liquid monomer eventually, resulting in the formation of a well-organized network between Nps and GIC. On the other hand, the increased percentage of Titania (TiO$_2$.Nps) in the experimental groups E-4 (7% TiO$_2$GIC), and E-5 (10% TiO$_2$GIC) might have prohibited their strong integration with GIC powder particles and liquid monomer. The excess content of these Nps that couldn't bind with GIC and its liquid monomer might have been left out freely unbounded in the matrix of GIC or on its surface thus, in turn resulting in its declined surface hardness in this study. Additionally, the purity of these Titania (TiO$_2$.Nps) up to 5% might have endorsed a dense surface texture by interacting more quickly with liquid monomer that might have prevented the indentation in their surface thus, improving their surface hardness.

The clinical performance of any restorative material in the oral cavity is assessed by the masticatory loads applied on it during biting and functioning purposes [251]. Therefore, compressive strength of the restorative material could play an immense role in enhancing their mechanical properties by contributing to their increased shelf life. The innovative experimental group E-3 (5% TiO$_2$GIC) containing 5% Titania (TiO$_2$.Nps) revealed maximum compressive strength in comparison to the control group E-1 and other experimental groups E-2, E-4 and E-5 (Figure-4.42 and Table-4.15, 4.16) which was in accordance with a study conducted by Abbas, et. al., [252]. The 5%Titania (TiO$_2$.Nps) in the experimental group E-3 (5% TiO$_2$GIC) synthesized by the *Bacillus coagulans* might have been stable enough at this concentration to intervene the polymer chain disruptions produced in the micro-structure of GIC powder particles during final mixing and placement. This might have been attained by the

entanglement of these Nps in the disruptions of GIC with the help of building strong cross-linking between them. The biological synthesis of these Nps could be the possible reason for their upgraded stability and sustainability that might also be helpful in improving their density at the tooth-restoration inter-junctions to prevent compression hence, magnifying its cross-linkings.

The restorative materials in the oral cavity are subjected to the twisting, bending and flexing forces on the regular basis that is dependent on the flexural strength [181], which is why an improvement in the fleural strength is essential. The innovative experimental group E-3 (5% TiO_2GIC) containing 5% Titania (TiO_2-Nps) depicted maximum flexural strength in comparison to the control group E-1 and other experimental groups E-2, E-4 and E-5 in the current study. The findings in the current study were similar to the work done by Garoushi, et. al.,[253]. Other researchers reported decrease in the flexural strength of commercial Nps added in different percentages to the GIC restorative material [181,254]. This decrease might have become possible due to much smaller Nps size used previously in comparison to the particle size used in the current study. Furthermore, pure elemental composition and functional groups of Titania (TiO_2-Nps) synthesized by *Bacillus coagulans* in 5% might have developed strong chemical bonding between the Nps in this concentration and free unbound metal ions present in the GIC powder which might have not been attained so easily in the commercially incorporated Titania (TiO_2-Nps). There might be possibility of trace impurities in these commercial Nps that could have been obtained as byproducts during their synthesis. These impurities might have prevented the chemical bonding between the surfaces of Nps and metal ions of GIC as a result of lack of attractive forces between them resulting in their deduced flexural strength.On the other hand, increased percentages of Titania (TiO_2-Nps) in the experimental groups E-4 and E-5 might have resulted in the weak chemical bonding between the Nps and free metal ions of GIC as a result of excessively increased amounts of Nps that might have reduced their flexural strength (Figure-4.443 and Table-4.17, 4.18).

Shear bond strength analysis for both the enamel and dentine portions of the tooth was being carried out by universal testing machine. The innovative experimental group E-3 (5% TiO_2GIC) containing 5% Titania (TiO_2-Nps) revealed maximum shear bond strength for both enamel and dentine as compared to control group E-1 and other experimental groups E-2, E-4 and E-5 (Figure-4.44, 4.45) [255]. The structure of human tooth enamel is homogeneous, having hydroxyapatite with high surface energy [183] while structure of human tooth dentin is heterogeneous, having organic and inorganic content with low surface energy [256]. On the other hand, the chemically active anatase phase of Titania (TiO_2-Nps) synthesized by *Bacillus coagulans* in the experimental group E-3 (5% TiO_2GIC) might have enabled these Nps in 5% to undergo a strong chemical reaction with both the enamel and dentin portions of the tooth as a result producing alterations in their structure architecture, composition and surface energy that might have supported the chemical reaction enhancing the shear bond strength to both enamel and dentin up to a certain limit. Beyond a certain specific limit, the chemical reaction would have become aggressive in an uncontrolled manner with the increase in the percentage of Titania (TiO_2-Nps) that might have produced adverse effects on the shear bond strength in the remaining experimental groups E-4 and E-5 in the current study respectively (Table-4.19-4.22).

The scanning electron microscopic analysis revealed presence of a highly porous structure with maximum voids, cracks and disintegration sites in the conventional control group E-1 (0% TiO_2GIC) without Titania (TiO_2.Nps) (Figure-4.46a,b) which decreased in the experimental group E-2 (3% TiO_2GIC) (Figure-4.47a,b). These pores, voids, cracks and disintegration sites became minimum in the experimental group E-3 (5% TiO_2GIC) (Figure-4.48a,b) but these pores, voids, cracks and disintegration sites again increased in the experimental group E-4 (7% TiO_2GIC) (Figure-4.49a,b) and became maximum in the experimental group E-5 (10% TiO_2GIC) (Figure-4.50a,b).

Smooth surface texture is the sole requirement of any ideal restorative material used in the clinical dentistry [257]. Various studies conducted by researchers concluded that smooth texture of a restorative material promotes the mechanical strength thus, inhibiting the caries progression [258,259]. The surface texture of GIC might be adversely affected by dehydration, moisture sensitivity, setting reaction time, and roughness [260,261]. Other factors contributing to the surface texture of GIC restoration includes their particle number and distribution, size, shape, particle-particle interfacial bonding, particle-matrix interfacial bonding, storage environment, powder particles, and its powder liquid ratio [258,259]. It was confirmed by researchers that during the mixing of GIC powder and liquid, air gets entrapped in the restoration matrices as a result of the large size of these powder particles. This large size of GIC powder particles hinder their accurate approximation leaving behind the air bubbles in the form of the voids in the set matrix of the GIC restoration thus adversely affecting its structural morphology and mechanical properties. Although, the set GIC matrix is stable in the aqueous environment of the oral cavity but these voids act as pathway for the entrance of various fluids and food particles that might allow the adherence of various micro-organisms to this set matrix of GIC [198]. Thus, it is concluded that restorative material's surface gets roughened through adherence of bacteria which causes the maturation of dental plaque in turn leading to the recurrent secondary caries [262]. This roughness in the restorative material's surface might be considered as the sole reason of discoloration, degradation and cracks in its texture [263]. The Titania Nps prepared in the current study were ideally small and pure enough to occupy the maximal larger gaps in the conventional GIC thereby, rendering its surface smooth in order to prevent the future bacterial adherence.

The spectrum mapping for compositional analysis revealed linear pattern decrease in Al, Si, Sr, P, C and S contents in all the experimental groups such as E-2 (3% TiO_2GIC) (Figure-4.47c,d), E-3 (5% TiO_2GIC) (Figure-4.48c,d), E-4 (7% TiO_2GIC) (Figure-4.49c,d) and E-5 (10% TiO_2GIC) (Figure-4.50c,d) in comparison to the conventional control group E-1 (0% TiO_2GIC) (Figure-4.46c,d).The linear pattern increase in F and Ti contents was attained from conventional control group E-1 (0% TiO_2GIC) (Figure-4.46c,d) to the experimental group E-5 (10% TiO_2GIC) (Figure-4.50c,d) .There was slight reduction seen in Al, Si and Sr contents in the experimental group E-3 (5% TiO_2GIC) with maximum declination in C ,P and S contents. On the other hand, maximum increase in the O content and intermediate increase in F content was depicted in this group ((Figure-4.48c,d) (Table-4.23).

The spectrum mapping gives the understanding of the any material utilized in clinical dentistry because it gives the accurate distribution of the elements on the material's outer surface which might come in contact with the oral tissues. The structural, biological, physical, chemical and mechanical properties of materials are greatly dependent on the presence of major components

in their composition [264,265]. The current study revealed the basic elemental composition of Carbon (C), Oxygen (O), Fluorine (F), Aluminum (Al), Silicon (Si), Strontium(Sr), Phosphorus (P), and Sulphur (S) in the conventional GIC (Gold GC universal restorative cement 2) which matched the literature where conventional GIC used was FAX-II [181]. Other studies confirmed the presence of Aluminium (12.820%), Silicon (13.180%) and Oxygen (66.750%) in the commercially prepared conventional Fuji-IX GP (Fast) whereas Aluminium (16.720%), Silicon (13.180%), and Oxygen (66.750%) in the commercially prepared conventional Fuji-IX GP as their main compositional elements as reported by Yapp. et., al [259]. In another study conducted by Zanata. et., al the presence of Aluminium (16.900%) ,Silicon (15.800%) , Fluoride (5.100%),Phosphorus (2.700%), Calcium (3.700%), Strontium (11.100%) and Potassium (1.100%) were confirmed as prime elements in the composition of GIC [266]. The difference in the amounts of these elements in the basic composition of the commercially prepared conventional GIC is according to the manufacture's instructions.

The commercial GIC has major components of aluminium and silicon in its composition which is responsible for its stability in set form [267]. The calcium and phosphorus content in GIC is responsible for imparting the mechanical strength to some extent. The increased quantity of these elements in GIC deteriorates not only their strength but also their aesthetics by diminishing their radiopacity which is the basic requirement of a clinically successful restorative material. Therefore, barium, strontium, and lanthanum could be induced in order to overcome this problem associated with commercially available GIC [268]. Barium is considered as the most suited optic modifier for enhancing the aesthetics but it might be responsible for causing genotoxicity and cytotoxicity [269]. The fluoride content in the GIC prevents the caries recurrent attack with the improvement in the handling and mechanical characteristics to some extent [270,271]. This fluoride release should be continued throughout the life in a controlled manner to prevent the caries [272]. The fluoride release is controlled by particle size, powder-liquid ratio, PH, handling and composition of GIC [273]. The reduction in the fluoride content of GIC after the clinical usage of ten years has been demonstrated in a study that could be responsible for initiating the secondary caries attack [266]. The increase in the fluoride content of GIC after the addition of Nps was reported by a researcher which might solve this problem of recurrent caries but up to a certain limit [274]. The experimental group E-5 (10% TiO_2GIC) in our study displayed reduction in the Al, Sr, Si, P and S but to the lesser extent with intermediate increase in F and Ti contents whereas maximum increase in the O content was observed. Additionally, maximum reduction in C content was observed in this group. The controlled release of F content from experimental group E-5 (10% TiO_2GIC)might play a significant role in preventing the demineralization of tooth's enamel surface hence, prohibiting the cavity formation in that structure.

The increase in the percentage of Ti and O contents in the spectrum mapping of current study matched with the work done by Garcia. et al., [181] but only up to 5% because Titania-Nps addition at 7% and 10% was not investigated. Previously, it was reported that addition of commercially available Titania Nps in the GIC reduces the content of C and increases the O in the spectrum of Titania induced GIC on small scale. This might have been possible due to the strong binding between glass particles matrix and Titania Nps [181]. The small size of these stable Titania Nps in adequate amounts produced through micro-organisms might have activated the interactive binding forces between the GIC- matrix and Nps in the absence of any

impurity or toxic by-product.Thus, these powerful binding interactive forces between large GIC glass powder particles matrix and small sized Titania might have improved their mechanical properties.

This suggests that addition of certain limit of Titania (TiO_2 Nps) to GIC powder might improve their mechanical properties by covering the stress concentration areas present in between GIC powder particles but in a calculative manner. This concludes that any change in the composition of GIC restorative material may affect its micro-hardness, flexural strength, compressive strength, shear bond strength and surface morphology but only to a certain level.

Conclusion:

The current study highlights the synthesis, characterization, antimicrobial activity and biocompatibility analysis of Titania (TiO$_2$ Nps) prepared by *Bacillus coagulans*, *Mentha spicata* and *Conventional hydrothermal heating*. Among them, the Titania (TiO$_2$ Nps) prepared by *Bacillus coagulans* provedto be having better antimicrobial activity and biocompatibility were incorporated in conventional glass ionomer cement (GIC) to produce most biosafe and biocompatible innovative TiO$_2$-GIC restorative material for the treatment of dental caries disease in the oral cavity. The Titania (TiO$_2$ Nps) synthesized by *Bacillus coagulans* were more stable, quick and sustainable without any toxic byproduct formation. Furthermore, different characterization techniques revealed small sized spherical shaped Titania (TiO$_2$ Nps) having diameter ranging between 20-30 nm. These newly formed Nps were found in 100% pure anatase phase. The Titania (TiO$_2$ Nps) synthesized by *Bacillus coagulans* were smooth with band gap energy of 3.5 eV that confirmed the small crystallite size of these Nps. The elemental composition depicted the formation of pure Titania (TiO$_2$Nps) because of only Ti and O peaks in its spectrum with natural functional groups of only O-H, C-H, C=O and Ti-O-Ti in *Bacillus coagulans* fabricated Titania (TiO$_2$ Nps).

The antimicrobial activity of Titania (TiO$_2$ Nps) synthesized by *Bacillus coagulans* revealed maximum activity against caries promoting bacteria:*E. coli*, *L .acidophilus*, *S. aureus*, *E. faecium*, *E. faecali* and *P. aeruginosa* as compared to other Titania (TiO$_2$ Nps) formed by *Mentha spicata* and *Conventional hydrothermal heating*. The biocompatibility analysis depicted that Titania (TiO$_2$ Nps) synthesized by *Bacillus coagulans* remained noncytotoxic during the whole experiment because of the cell viability of fibroblast cells exposed to them was > 90%. The mechanical properties of 5% innovative TiO$_2$GIC restorative material showed maximum hardness, compressive strength, flexural strength and shear bond strength (Enamel and Dentin) as compared to control group (conventional GIC) and other % of added Titania (TiO$_2$ Nps). Moreover, surface morphology of 5% innovative TiO$_2$GIC restorative material revealed minimum pores confirming the strength of restorative material to bear excessive masticatory stresses in the oral cavity without undergoing any distortion in order to increase the strength, durability and shelf life of the restorative material for the future applications in the dental sciences.

Future perspectives:

Current research highlighted the green synthesis and biomedical applications of Titania (TiO$_2$-Nps) for developing the innovative restorative materials for dental caries treatment. Materials were synthesized and evaluated for their mechanical strength and physico-chemical properties however, due to paucity of time and resources, some areas are left which needs absolute dire attention in the future research.

i.   Further research is required to understand the exact mechanism operating behind the size-shape relationship under varying reaction conditions, specifically using natural products.

ii. The crystallinity of nanoparticles in terms of their reactive anatase phase, inert rutile and brookite phases needs much more better understanding in order to declare them toxic or nontoxic in nature.

iii. The presence of natural molecules in *Bacillus coagulans* facilitates the high purity of product owing target specific activity of cellular materials which needs further investigations by utilizing other microorganisms.

iv. The structure-function relationship and interactions of the nanoparticles at cellular interfaces need further investigations.

v.   The biocompatibility of Titania (TiO$_2$-Nps) against different cell lines needs to be tested at more higher concentrations for longer duration in order to utilize them easily in the oral cavity.

vi. The mechanical strength of the innovative TiO$_2$GIC restorative material needs to be further investigated at more higher percentages so as to find out the most appropriate restorative material capable of bearing highest levels of masticatory loads.

References:-

1. Dye, B.; Thornton-Evans, G.; Li, X.; & Iafolla, T.; Dental caries and tooth loss in adults in the United States, 2011-2012. *NCHS data brief*, 2015, (197), 197.

2. Schwendicke, F.; Dörfer, C. E.; Schlattmann, P.; Foster Page, L.; Thomson, W. M.; & Paris, S.; Socioeconomic inequality and caries: a systematic review and meta-analysis. *Journal of dental research*, 2015, *94*(1), 10–18. https://doi.org/10.1177/0022034514557546.

3. Lohbauer U.; Dental glass ionomer cements as permanent filling materials?–properties, limitations and future trends. Materials. 2009;3(1):76-96.

4. Ching, H. S.; Luddin, N.; Kannan, T. P.; Ab Rahman, I.; & Abdul Ghani, N.; Modification of glass ionomer cements on their physical-mechanical and antimicrobial properties. *Journal of esthetic and restorative dentistry: official publication of the American Academy of Esthetic Dentistry ... [et al.]*, 2018, *30*(6), 557–571. https://doi.org/10.1111/jerd.12413.

5. Berg, J. H.; & Croll, T. P.; Glass ionomer restorative cement systems: an update. *Pediatric dentistry*, 2015. *37*(2), 116–124.

6. Najeeb, S.; Khurshid, Z.; Zafar, M.S.; Khan, A.S.; Zohaib, S.; Marti, J.M.; Sauro, S.; Matinlinna, J.P.; Rehman, I.U. Modifications in Glass Ionomer Cements: Nano-Sized Fillers and Bioactive Nanoceramics. Int. J. Mol. Sci. 2016, 17, 1134.

7. Lee Y.; Diagnosis and Prevention Strategies for Dental Caries. J Lifestyle Med. 2013; 3(2): 107-9.

8. Yadav, K.; & Prakash, S.; Dental Caries: A Microbiological Approach. *J. Clin. Infect. Dis. Pract.*02, 1–15 (2017)

9. Masoud, S.; Qazi, S.H.; Mumtaz, R.; Prevalence of Dental Caries and its Association with Risk Factors amongst Preschool Children of Bharakahu, Islamabad. *J Islam Med Dent Coll*. 2020;9(2):88-94. doi:10.35787/jimdc.v9i2.463

10. Kassebaum, N. J,; Bernabe, E,; Dahiya, M.; Bhandari, B.; Murray, C. J. L,; & Marcenes, W.; Global burden of untreated caries: a systematic review and metaregression. *Journal of Dental Research* 2015; **94**, 650– 658.

11. Balhaddad, A. A.; Kansara, A. A.; Hidan, D.; Weir, M. D.; Xu, H.; & Melo, M.; Toward dental caries: Exploring nanoparticle-based platforms and calcium phosphate compounds for dental restorative materials. *Bioactive materials*, 2018; *4*(1), 43–55. https://doi.org/10.1016/j.bioactmat.2018.12.002

12. Liu, C.; Niu, Y.; Zhou, X.; Zhang, K.; Cheng, L.; Li, M.; Li, Y.; et al. Hyperosmotic response of streptococcus mutans: from microscopic physiology to transcriptomic profile. *BMC microbiology*, 2013; *13*, 275. https://doi.org/10.1186/1471-2180-13-275

13. Nahsan, F. P.; Mondelli, R. F.; Franco, E. B.; Naufel, F. S.; Ueda, J. K.; Schmitt, V. L.; & Baseggio, W.; Clinical strategies for esthetic excellence in anterior tooth restorations: understanding color and composite resin selection. *Journal of applied oral science : revista FOB*, 2012; *20*(2), 151–156. https://doi.org/10.1590/s1678-77572012000200005.

14. Rosi, H.; Kalyanasundaram, S. 2018; Synthesis, characterization, structural and optical properties of titanium-dioxide Nps using Glycosmis cochinchinensis Leaf extract and its photocatalytic evaluation and antimicrobial properties. WNOFNS 17 (2018) 1-15.pdf. 2018;17(January):1-15

15. Sidhu SK, Nicholson JW. A review of glass-ionomer cements for clinical dentistry. *J Funct Biomater.* 2016;7:16.

16. Brzović Rajić V, Miletić I, Gurgan S, Peroš K, Verzak Ž, Ivanišević Malčić A. Fluoride Release from Glass Ionomer with Nano Filled Coat and Varnish.*Acta Stomatol Croat*. 2019. Jun;53(2):132–40.

17. Sidhu, S. K.; & Nicholson, J. W.; A Review of Glass-Ionomer Cements for Clinical Dentistry. *Journal of functional biomaterials*, 2016; *7*(3), 16. https://doi.org/10.3390/jfb7030016.

18. Sajjad,A.; Bakar,W.Z.W.; Mohamad, D.; Kannan, TP.; Various recent reinforcement phase incorporations and modifications in glass ionomer powder compositions: a comprehensive review. J Int Oral Health 2018;10(4):161–167

19. Mantri, S. S.; & Mantri, S. P.; The nano era in dentistry. *Journal of natural science, biology, and medicine*, 2013; *4*(1), 39–44. **https://doi.org/** 10.4103/ 0976-9668.107258.

20. Zhai, T.; Fang, X.; Liao, M.; Xu, X.; Zeng, H.; Yoshio, B.; Golberg, D.; A Comprehensive Review of One-Dimensional Metal-Oxide Nanostructure Photodetectors. Sensors, 2009; 9(8), 6504.

21. Niinomi M.; Mechanical biocompatibilities of titanium alloys for bio- medical applications. J Mech Behav Biomed Mater. 2008; Jan;1(1):30-42.

22. Besinis, A.; De Peralta, T.; & Handy, R. D.;. The antibacterial effects of silver, titanium dioxide and silica dioxide nanoparticles compared to the dental disinfectant chlorhexidine on Streptococcus mutans using a suite of bioassays. *Nanotoxicology*, 2014; *8*(1), 1–16. https://doi.org/10.3109/17435390.2012.742935

23. Long, M.; Wang, J.; Zhuang, H.; Zhang, Y.; Wu, H.; and Zhang, J.; 2014. ―Performance and mechanism of standard nano-TiO2 (P-25) in photocatalytic disinfection of food borne microorganisms - Salmonella typhimurium and Listeria monocytogenes," Food Control, vol. 39, no. 1, pp. 68–74.

24. Bai, W.; Chen, Y.; & Gao, A.; Cross talk between poly(ADP-ribose) polymerase 1 methylation and oxidative stress involved in the toxic effect of anatase titanium dioxide nanoparticles. *International journal of nanomedicine*, 2015; *10*, 5561–5569. https://doi.org/10.2147/IJN.S88059

25. Li, S.Q.; Zhu, R.R.; Zhu, H.; et al. Nanotoxicity of tio2 nanoparticles to erythrocyte in vivo. Food Chem Toxicol. 2008;46 (12):3626–3631. doi:10.1016/j.fct.2008.09.012

26. Baan R. A.; Carcinogenic hazards from inhaled carbon black, titanium dioxide, and talc not containng asbestos or asbestiform fibers: recent evaluations by an IARC Monographs Working Group. *Inhalation toxicology*, 2007; *19 Suppl 1*, 213–228. https://doi.org/10.1080/08958370701497903

27. Wang, Y.; Santos, A.; Evdokiou, A.; Losic, D.; An overview of nanotoxicity and nanomedicine research: principles, progress and implications for cancer therapy. J Mater Chem B.2015;3 (36):7153–7172. doi:10.1039/C5TB00956A

28. Tahir, A.; Moeen, F.; Mehmood, M.; Mansoor, A.; Abbas, Z.; Hussain, A.; Kashif, M. Compressive Strength and Flexural Strength of Titanium Nano-Enriched Gic at Different Percentages an in Vitro Study. *Ann. Dent. Spec.* 2019, *7*, 1–7.

29. Tahir, A.; Moeen, F.; Mehmood, M.; Mansoor, A.; Abbas, Z.; Shahzad, M.H.; Kashif, M. Evaluation of Shear Bond Strength to Human Teeth and Micro-hardness of GIC Containing Titanium Nano Particles: An In-Vitro Study. *Int. Med. J.* 2020, *25*, 1477–1488.

30. Wang, C.; Li, Y.; Interaction and nanotoxic effect of TiO(2) nanoparticle on fibrinogen by multi-spectroscopic method.*Sci Total Environ* 2012, 429: 156–160.

31. Andersson, P. O.; Lejon, C.; Ekstrand-Hammarström, B.; Akfur, C.; Ahlinder, L.; Bucht, A.; & Osterlund, L.; Polymorph- and size-dependent uptake and toxicity of TiO₂ nanoparticles in living lung epithelial cells. *Small (Weinheim an der Bergstrasse, Germany)*, 2011; *7*(4), 514–523. https://doi.org/10.1002/smll.201001832.

32. Shaffer,R.E.; Rengasamy, S.; Respiratory protection against airborne nanoparticles: a review. J Nanopar Res 2009;11: 1661-1672.

33. Nadeem, M.; Tungmunnithum, D.; Hano, C.; Abbasi, B.H.; Hashmi, S.S.; Ahmad, W.; The current trends in the green syntheses of titanium oxide nanoparticles and their applications. Green Chem. Lett. Rev. 2018; 11 (4), 492–502

34. Ingle, A.; Gade, A.; Pierrat, S.; Sonnichsen, C.; Rai, M. Mycosynthesis of silver nanoparticles using the fungus Fusarium acuminatum and its activity against some human pathogenic bacteria. Curr. Nanosci., 2008, 4, 141-144.

35. Chokriwal, A.; Madan, M. S.; & Abhijeet, S.; Biological Synthesis of Nanoparticles Using Bacteria and Their Applications. American Journal of PharmTech Research, 2014; 4(6), 38-61.

36. Li, X. Q.; Xu, H. Z.; Chen, Z. S.; & Chen, G. F.; Biosynthesis of nanoparticles by microorganisms and their applications. Journal of Nanomaterials. 2011. Sep 11, https://doi.org/10.1155/2011/270974

37. Abboud, Y.; Saffaj, T.; Chagraoui, A.; El Bouari, A.; Brouzi, K.; Tanane, O.; Ihssane, B. Biosynthesis, characterization and antimicrobial activity of copper oxide nanoparticles (CONPs) produced using brown alga extract (Bifurcaria bifurcata). *Applied Nanoscience (Switzerland)*, (2014); *4*(5), 571–576.

38. He, X. S.: & Shi, W. Y.; Oral microbiology: past, present and future. *International journal of oral science*, *1*(2), 2009; 47–58. https://doi.org/10.4248/ijos.09029.

39. Nyvad, B.; Crielaard, W.; Mira, A.; Takahashi, N.; & Beighton, D.; Dental caries from a molecular microbiological perspective. *Caries research*, 2013; *47*(2), 89–102. https://doi.org/10.1159/000345367.

40. Milgrom, P.; Riedy, C. A.; Weinstein, P.; Tanner, A. C.; Manibusan, L.; & Bruss, J.; Dental caries and its relationship to bacterial infection, hypoplasia, diet, and oral hygiene in 6- to 36-month-old children. *Community dentistry and oral epidemiology*, 2000; *28*(4), 295–306.

41. Berkowitz R.J.; Mutans streptococci acquisition and transmission. Pediatr. 2006; Dent. 2: 106–109.

42. Cephas K.D.; J. Kim, R.A.; Mathai, K.A.; Barry, S.E.; Dowd, B.; Meline and K.S.; Swanson.; Comparative analysis of salivary bacterial microbiome diversity in edentulous infants and their mothers or primary care givers using pyrosequencing. PLoS One 201; 6. 8

43. Mattos-Graner, R. O.; Li, Y., Caufield, P. W.; Duncan, M.; & Smith, D. J.; Genotypic diversity of mutans streptococci in Brazilian nursery children suggests horizontal transmission. *Journal of clinical microbiology*, 2001; *39*(6), 2313–2316. https://doi.org/10.1128/JCM.39.6.2313-2316.2001.

44. Horiuchi M.; Washio, J.; Mayanagi H.; Transient acid-impairment of growth ability of oral Streptococcus, Actinomyces and Lactobacillus: a possible ecological determinant in dental plaque. Oral. Microbiol. Immunol. 2009; 24: 319–324

45. Berkowitz R.J.; Acquisition and transmission of mutans steptococci. J. Calif. 2003; Dent. Assoc. 31: 135–138.

46. Duggal, M. S.; & van Loveren, C.; Dental considerations for dietary counselling. *International dental journal*, 2001; *51*(6 Suppl 1), 408–412. https://doi.org/10.1111/j.1875-595x.2001.tb00588.x.

47. FITZGERALD, R. J.; & KEYES, P. H.; Demonstration of the etiologic role of streptococci in experimental caries in the hamster. *Journal of the American Dental Association* 1960*; (1939)*, *61*, 9–19. https://doi.org/10.14219/jada.archive.1960.0138.

48. Nasidze, I.; Li, J.; Quinque, D.; Tang, K.; & Stoneking, M.; Global diversity in the human salivary microbiome. *Genome research*, 2009; *19* (4), 636–643. https://doi.org/10.1101/gr.084616.108.

49. Marsh, P. D.; Contemporary perspective on plaque control. *British dental journal*, 2012; *212*(12), 601–606. https://doi.org/10.1038/sj.bdj.2012.524.

50. Marsh, P. D.; Moter, A.; & Devine, D. A.; Dental plaque biofilms: communities, conflict and control. *Periodontology* 2011; *2000*, *55*(1), 16–35. https://doi.org/10.1111/j.1600-0757.2009.00339.x.

51. McLean, J. S.; Fansler, S. J.; Majors, P. D.; McAteer, K.; Allen, L. Z.; Shirtliff, M. E.; Lux, R.; & Shi, W.; Identifying low pH active and lactate-utilizing taxa within oral microbiome communities from healthy children using stable isotope probing techniques. *PloS one*, 2012; *7*(3), e32219. https://doi.org/10.1371/journal.pone.0032219

52. Takahashi N.; Microbial ecosystem in the oral cavity: Metabolic diversity in an ecological niche and its relationship with oral diseases. International Congress Series 2005;1284:103-112.

53. Yadav, K.; Prakash, S. (2015). Antibiogram profiles against polymicrobial pathogens among dental caries patients at Janaki Medical College teaching hospital, Nepal. Int J Applied Dental Sci 1: 156-162.

54. Yadav, K. (2016). Dental Caries: Bacterial profile of Dental caries. LAP LAMBERT Academic Publishing, OmniScriptum GmbH & Co. KG, Germany. Pp: 120.

55. Aas, J. A.; Griffen, A. L.; Dardis, S. R.; Lee, A. M.; Olsen, I.; Dewhirst, F. E.; Leys, E. J.; & Paster, B. J. (2008). Bacteria of dental caries in primary and permanent teeth in children and young adults. *Journal of clinical microbiology*, *46*(4), 1407–1417. https://doi.org/10.1128/JCM.01410-07

56. Marsh P. D. (2006). Dental plaque as a biofilm and a microbial community - implications for health and disease. *BMC oral health*, *6 Suppl 1*(Suppl 1), S14. https://doi.org/10.1186/1472-6831-6-S1-S14.

57. Becker, M. R.; Paster, B. J.; Leys, E. J.; Moeschberger, M. L.; Kenyon, S. G.; Galvin, J. L.; Boches, S. K.; Dewhirst, F. E.; & Griffen, A. L. (2002). Molecular analysis of bacterial species associated with childhood caries. *Journal of clinical microbiology*, *40*(3), 1001–1009. https://doi.org/10.1128/JCM.40.3.1001-1009.2002

58. Dufour, D.; & Lévesque, C. M.; Bacterial behaviors associated with the quorum-sensing peptide pheromone ('alarmone') in streptococci. *Future microbiology*, 2013; *8*(5), 593–605. https://doi.org/10.2217/fmb.13.23.

59. Abusleme, L.; Dupuy, A. K.; Dutzan, N.; Silva, N.; Burleson, J. A.; Strausbaugh, L. D.; Gamonal, J.; & Diaz, P. I.; The subgingival microbiome in health and periodontitis and its relationship with community biomass and inflammation. *The ISME journal*, 2013; *7*(5), 1016–1025. https://doi.org/10.1038/ismej.2012.174.

60. Kolenbrander, P. E.; Andersen, R. N.; Blehert, D. S.; Egland, P. G.; Foster, J. S.; & Palmer, R. J. Jr.; Communication among oral bacteria. *Microbiology and molecular biology reviews : MMBR*, 2002; *66*(3), 486–505. https://doi.org/10.1128/MMBR.66.3.486-505.2002

61. Irie, Y.; & Parsek, M. R.; Quorum sensing and microbial biofilms. *Current topics in microbiology and immunology*, 2008; *322*, 67–84. https://doi.org/10.1007/978-3-540-75418-3_4.

62. Sturme, M. H. J.; Kleerebezem, M.; Nakayama, J.; Akkermans, A. D. L.; Vaughan, E. E.; and de Vos, W. M.; Cell to cell communication by autoinducing peptides in gram-positive bacteria. *Antonie Van Leeuwenhoek* 2002; 81, 233–243. doi: 10.1023/A:1020522919555

63. Syvitski, R. T.; Tian, X. L.; Sampara, K.; Salman, A.; Lee, S. F.; Jakeman, D. L.; et al. Structure-activity analysis of quorum-sensing signaling peptides from *Streptococcus mutans*. *J. Bacteriol.* 2007; 189, 1441–1450. doi: 10.1128/JB.00832-06

64. Roberts, A. P.; & Mullany, P.; Oral biofilms: a reservoir of transferable, bacterial, antimicrobial resistance. *Expert review of anti-infective therapy*, 2010; *8*(12), 1441–1450. https://doi.org/10.1586/eri.10.106.

65. Que-Fue-2019

66. FRENCKEN, J.E.; PETERS, M.C.; MANTON, D.J. et al. ―Minimal intervention dentistry for managing dental caries - a review: report of a FDI task group." International Dental Journal, v. 62, n. 5, p. 223-243, 2012.

67. Saito, S.; Tosaki, S.; Hirota, K. Advances in Glass Ionomer Cements; Davidson C.L., Mjör I.A., Eds.; Quintessence Publishing Co: Berlin, Germany, 1999; pp. 15–50.

68. Singh, T.M.; Suresh, P.; hyarani, & Sravanthi, J.V.;. GLASS IONOMER CEMENTS (GIC) IN DENTISTRY: A REVIEW. *The International Journal of Plant, Animal and Environmental Sciences,* 2011; *1:1: 26-30*

69. Liu W.; Golshan N.H.; Deng, X.; et. al. Selenium nanoparticles incorporated into titania nanotubes inhibit bacterial growth and macrophage proliferation. Nanoscale. 2016;8:15783–15794.doi: 10.1039/C6NR04461A.

70. Sharma, A.; Singh, M.; Pandey, V.; Glass Ionomer Cement-A Phoenix and its new flight. Int J of Research in Health and Allied Sciences 2015:1:1:9-12.

71. Yadav, R.K.; Verma,U.P.; Tiwari, R.; Chaurasia, A.; Mercury or Mercury Free Restorations in Oral Cavity. Int J Public Heal Sci. 2018;7(3):201.

72. Chan, K.; Mai, Y.; Kim, H.; Tong, K.; Ng, D.; & Hsiao, J.; Review: Resin Composite Filling. *Materials*, 2010; *3*(2), 1228–1243. https://doi.org/10.3390/ma3021228.

73. Amin, F.; Rahman, S.; Khurshid, Z.; Zafar, M. S.; Sefat, F.; & Kumar, N.; Effect of Nanostructures on the Properties of Glass Ionomer Dental Restoratives/Cements: A Comprehensive Narrative Review. *Materials (Basel, Switzerland)*, 2021; *14*(21), 6260. https://doi.org/10.3390/ma14216260

74. Rashid, H.; Sheikh, Z.; Misbahuddin, S.; Kazmi, M. R.; Qureshi, S.; & Uddin, M. Z.; Advancements in all-ceramics for dental restorations and their effect on the wear of opposing dentition. *European journal of dentistry*, 2016; *10*(4), 583–588. https://doi.org/10.4103/1305-7456.195170.

75. Khademolhosseini, M.R.; Barounian, M.H.; Eskandari, A.; Aminzare, M.; Zahedi, A.; Ghahremani, D.; Development of new Al2O3/TiO2 reinforced glass-ionomer cements (GICs) nano-composites. J Basic Appl Sci Res. 2012;2:7526-9.

76. Khangura, S.D.; Seal, K.; Esfandiari, S.; et al. Composite Resin Versus Amalgam for Dental Restorations: A Health Technology Assessment [Internet]. Health Technology Assessment Report, No. 147, March 2018.

77. Griffin, S.G. H.R.; Influence of glass composition on the properties of glass polyalkenoate cements. Part I: influence of aluminium to silicon ratio. Biomaterials. 1999;20(17):1579-86.

78. Huang, Y.; Song, B.; Zhou, X.; Chen, H.; Wang, H.; Cheng, L.; Dental restorative materials for elderly populations. Polymers (Basel). 2021;13(5):1–14.

79. Prosser, H. J.; Powis, D. R.; & Wilson, A. D.; Glass-ionomer cements of improved flexural strength. *Journal of dental research*, 1986; *65* (2), 146–148. https://doi.org/10.1177/00220345860650021101.

80. Nicholson, J.W.; Sidhu, S.K.; Czarnecka, B. Enhancing the Mechanical Properties of Glass-Ionomer Dental Cements: A Review. *Materials* 2020, *13*, 2510. [CrossRef]

81. Palmer,G.;Anstice,H.M.; Pearson,G.J.; The effect of curing regime on the release of hydrox-ethyl meth acylate (HEMA) from resin-modified glass-ionomer cements. J. Dent. 1999, 27, 303–311

82. *Hamid, A.; Hume, W.R. Diffusion of resin monomers through human carious dentin in   vitro.   Endod.   Dent. Traumatol. 1997, 13, 1–5. [CrossRef] [PubMed]*

83. Atul, R, I.; Thakare. S,R.; Khati, N.T.; Wankhade, A.V.; Burghate, D. K.;   *"Green synthesis of selenium nanoparticles under ambient condition.".* Chalcogenide Letters, 2010. **7**: p. 485-489

84. Narducci D.; An introduction to nanotechnologies: what's in it for us?. *Veterinary research communications*, 2007; *31 Suppl 1*, 131–137. https://doi.org/10.1007/s11259-007-0082-8.

85. Ijaz, I.; Gilani, E.; Nazir, A.; Bukhari, A.; Detail review on chemical, physical and green synthesis, classification, characterizations and applications of nanoparticles. Green Chem Lett Rev. 2020;13(3):59–81.

86. WANG, W.N.; LENGGORO, I. W.; TERASHI, Y.; KIM, T. O.; & OKUYAMA, K.; One-step synthesis of titanium oxide nanoparticles by spray pyrolysis of organic
precursors. *Materials Science and Engineering:* 2005; *B,* 123**,** 194-202.

87. Razavi, H.; Darvishi, M.H.; Janfaza, S.; Silver sulfadiazine encapsulated in lipid-based nanocarriers for burn treatment. J Burn Care Res. 2018;39(3):319–325.

88. Hashemzadeh, H.; Allahverdi, A.; Ertl, P.; Naderi-Manesh, H.; Comparison between three-dimensional spheroid and two-dimensional monolayer in a549 lung cancer and pc9 normal cell lines under treatment of silver nanoparticles. Modares J Biotechnol. 2019;10(4):573–580.

89. Chang, H. P.; Tseng, Y. C.; Miniscrew implant applications in contemporary orthodontics. *The Kaohsiung journal of medical sciences*, (2014); *30* (3), 111–115. https://doi.org/10.1016/j.kjms.2013.11.002.

90. Hussain, I.; Singh, N. B.; Singh, A.; Singh, H.; & Singh, S. C.; Green synthesis of nanoparticles and its potential application. *Biotechnology letters*, 2016; *38*(4), 545–560. https://doi.org/10.1007/s10529-015-2026-7,"

91. Afifa Qidwai, A.; Pandey, R.; Kumar, S. K.; Shukla and A. Dikshit[*]Advances in Biogenic Nanoparticles and the Mechanisms of antimicrobial Effects, Indian J Pharm Sci 2018;80(4):592-603

92. Thekkae Padil, V. V.; & Černík, M.; Green synthesis of copper oxide nanoparticles using gum karaya as a biotemplate and their antibacterial application. *International journal of nanomedicine*, 2013; *8*, 889–898. https://doi.org/10.2147/IJN.S40599.

93. Singh, J.; Kumar, S.; Alok, A.; Upadhyay, S.K.; Rawat, M.; Tsang, D.C.; The potential of green synthesized zinc oxide nanoparticles as nutrient source for plant growth. J. Clean. Prod. 2019; 214, 1061–1070.

94. Joshi, D.R.; Adhikari, N.; An overview on common organic solvents and their toxicity. JPRI 2019; 1–18.

95. Ebnalwaled, A.A.; Essai, M.H.; Hasaneen, B.M.; Mansour, H.E.; Facile and surfactant-free hydrothermal synthesis of PbS nanoparticles: the role of hydrothermal reaction time. J. Mater. Sci. Mater. Electron. 2017; 28 (2), 1958–1965.

96. Parmar, S.; Kaur, H.; Singh, J.; Matharu, A. S.; Ramakrishna, S.; & Bechelany, M.; Recent Advances in Green Synthesis of Ag NPs for Extenuating Antimicrobial Resistance. *Nanomaterials (Basel, Switzerland)*, 2022; *12*(7), 1115. https://doi.org/10.3390/nano12071115.

97. Tschopp,M.A.; Murdoch, H.A.; Kecskes, L.J.; Darling, K.A.; Bulk nanocrystalline metals: Review of the current state of the art and future opportunities for copper and copper alloys. Journal of Metals. 2014;**66**(6):1000-1019

98. Nasirian, M.; Mehrvar, M.; Photocatalytic degradation of aqueous Methyl Orange using nitrogen-doped TiO2 photocatalyst prepared by innovative method of ultravioletassisted thermal synthesis. J. Environ. Sci. 2018; 66, 81–93.

99. Liu, N.; Chen, X.; Zhang, J.; & Schwank, J.W.; A review on TiO2-based nanotubes synthesized via hydrothermal method: Formation mechanism, structure modification, and photocatalytic applications. **Catalysis Today,** 2014;**225,** 34-51.DOI: 10.1016/j.cattod.2013.10.090

100. Kim, M.; Osone, S.; Kim, T.; Higashi, H.; Seto, T.; Synthesis of nanoparticles by laser ablation: A review. Kona Powder and Particle Journal. 2017;34:80-90

101. Reverberi, A.P.; Kuznetsov, N.T.; Meshalkin, V.P.; Salerno.; Fabiano, B.; Systematical analysis of chemical methods in metal nanoparticles synthesis. Theoretical Foundations of Chemical Engineering. 2016;50(1):59-66.

102. Patra, J.K.; Baek, K.H.; Green Nanobiotechnology: Factors Affecting Synthesis and Characterization Techniques. J Nanomater. 2014;2014.

103. Singh, A.; Singh, N.B.; Hussain, I.; Singh, H.; Singh, S.C.; Plant-nanoparticle interaction: An approach to improve agricultural practices and plant productivity. Int J Pharm Sci Invent 2015;4:25-40.

104. Gudikandula, K.; Maringanti, S.C.; Synthesis of silver nanoparticles by chemical and biological methods and their antimicrobial properties. J Exp Nanosci 2016;11(9):714-21.

105. Jameel, M.S.; Aziz, A.A.; Dheyab, M.A. (2020). Green synthesis: Proposed mechanism and factors influencing the synthesis of platinum nanoparticles. Green Process Synth. 2020;9(1):386–98. doi.org/10.1515/gps-2020-0041.

106. Ganesan, V., Deepa, B., Nima, P., & Astalakshmi, A. (2014). Bioinspired synthesis of silver nanoparticles using leaves of Millingtonia hortensis L.F. International Journal of Advanced Biotechnology and Research, 5, 93.

107. Sintubin, L., De Windt, W., Dick, J., Mast, J., Van der Ha, D., Verstarete, W., & Boon, N. (2009). Lactic acid bacteria as reducing and capping agent for the fast and efficient production of silver nanoparticles. Applied Microbiology and Biotechnology, 84, 741.

108. Hulkoti, N. I., & Taranath, T. C. (2014). Biosynthesis of nanoparticles using microbes—a review. Colloids and Surfaces B: Biointerfaces, 121, 474.

109. Faramarzi, M. A.; & Sadighi, A.; Insights into biogenic and chemical production of inorganic nanomaterials and nanostructures. *Advances in colloid and interface science*, 2013; *189-190*, 1–20. https://doi.org/10.1016/j.cis.2012.12.001

110. Olteanu, H.; Banerjee, R.; Human methionine synthase reductase, a soluble P-450 reductase-like dual flavoprotein, is sufficient for NADPH-dependent methionine synthase activation, J. Biol. Chem. 276 (2001) 35558–35563.

111. Iravani, S. (2014). Bacteria in Nanoparticle Synthesis: Current Status and Future Prospects. *International scholarly research notices*, 2014; 359316. https://doi.org/10.1155/2014/359316.

112. Palza, H.; Antimicrobial Polymers with Metal Nanoparticles. *International Journal of Molecular Sciences,* 2015; *16*, 2099 - 2116.

113. A'gçeli, G.K.; Hammachi, H.; Kodal, S.P.; Cihangir, N.; Aksu, Z.; A innovative approach to synthesize TiO2 nanoparticles: biosynthesis by using Streptomyces sp. J. Inorg. Organomet. Polym. 2020; Mater. 1–9, HC1.

114. Fulekar, J.; Dutta, D.P.; Pathak, B.; Fulekar, M.H.;Innovative microbial and root mediated green synthesis of TiO2 nanoparticles and its application in wastewater remediation. J. Chem. Technol. Biotechnol. 2018; 93 (3), 736–743.

115. Sinica, D.P.; Annadurai, G. (2013). Pelagia research library innovative eco-friendly synthesis of titanium oxide nanoparticles by using Planomicrobium sp. and its antimicrobial evaluation. Der Pharmacia. 2013;4:59-66

116. Verdier, T.; Coutand, M.; Bertron, A.; Roques, C. (2014). Antibacterial activity of TiO$_2$ photocatalyst alone or in coatings on E. coli: The influence of methodological aspects. Coatings. 2014;4:670-686. DOI: 10.3390/coatings4030670

117. Xie, J.; Hung, Y.C. (2019). Methodology to evaluate the antimicrobial effectiveness of UV-activated TiO$_2$ nanoparticle-embedded cellulose acetate film. Food Control. 2019;106:106690. DOI: 10.1016/j.foodcont.2019.06.016

118. Podporska-Carroll, J.; Panaitescu, E.; Quilty, B.; Wang, L.; Menon, L.; Pillai, S.C. (2015). Antimicrobial properties of highly efficient photocatalytic TiO2 nanotubes. Applied Catalysis B: Environmental. 2015;176-177:70-75. DOI: 10.1016/j.apcatb.2015.03.029.

119. Dhandapani, P.; Maruthamuthu, S.; Rajagopal, G. Bio mediated Synthesis of TiO2 Nanoparticles and its Photocatalytic Effffect on Aquatic Biofifilm. J. Photochem. Photobiol., B 2012, 110, 43–49.

120. Shah, M.; Fawcett, D.; Sharma, S.; Tripathy, S. K.; & Poinern, G.; Green Synthesis of Metallic Nanoparticles via Biological Entities. *Materials (Basel, Switzerland)*, 2015; *8*(11), 7278–7308. https://doi.org/10.3390/ma8115377

121. Nasrollahzadeh, M.; and Sajadi, S. M.; ─Synthesis and characterization of titanium dioxide nanoparticles using Euphorbia heteradena Jaub root extract and evaluation of their stability," Ceram. Int., vol. 41, no. 10, pp. 14435–14439, 2015.

122. Saif, S.; Tahir, A.; & Chen, Y.; Green Synthesis of Iron Nanoparticles and Their Environmental Applications and Implications. *Nanomaterials (Basel, Switzerland)*, 2016; *6*(11), 209. https://doi.org/10.3390/nano6110209.

123. Abisharani, J.M.; Devikala, S.; Kumar, R.D.; Arthanareeswari, M.; Kamaraj, P.; Green synthesis of TiO2 nanoparticles using Cucurbita pepo seeds extract. Mater. Today Proc. 2019; 14, 302–307.

124. Thakur, B.K.; Kumar, A.; Kumar, D. (2019). Green synthesis of titanium dioxide nanoparticles using Azadirachta indica leaf extract and evaluation of their antibacterial activity. South African Journal of Botany. 2019;124:223-227. DOI: 10.1016/j.sajb.2019.05.024.

125. Santhoshkumar, T.; Rahuman, A.A.; Jayaseelan, C.; Rajakumar, G.; Marimuthu, S.; Kirthi, A.V.; et al. (2014). Green synthesis of titanium dioxide nanoparticles using Psidium guajava extract and its antibacterial and antioxidant properties. Asian Pacific Journal of Tropical Medicine. 2014;7:968-976. DOI: 10.1016/S1995-7645(14)60171-1.

126. Ambika, S.; Sundrarajan, M. (2016). [EMIM] BF 4 ionic liquid-mediated synthesis of TiO$_2$ nanoparticles using Vitex negundo Linn extract and its antibacterial activity. Journal of Molecular Liquids. 2016;221:986-992. DOI: 10.1016/j.molliq.2016.06.079.

127. Hunagund, S.M.; Desai, V.R.; Kadadevarmath, J.S.; Barretto, D.A.; Vootla, S.; Sidarai, A.H. Biogenic and Chemogenic Synthesis of TiO 2 NPs via Hydrothermal Route and Their Antibacterial Activities. RSC Adv. 2016, 6 (99), 97438–97444.

128. Amanulla, A. M.; Sundaram, R. (2019). Green synthesis of TiO2 nanoparticles using orange peel extract for antibacterial, cytotoxicity and humidity sensor applications. Materials Today Proceedings. 2019;8:323-331. DOI: 10.1016/j.matpr.2019.02.118.

129. Mukunthan, K.S.; Balaji, S.; Cashew apple juice (*Anacardium occidentale* L.) speeds up the synthesis of silver nanoparticles. Int J Green Nanotech- nol. 2012;4:71–9. https://doi.org/10.1080/19430892.2012.676900.

130. Sundrarajan, M.; Bama, K.; Bhavani, M.; Jegatheeswaran, S.; Ambika, S.; Sangili, A.; Sumathi, R.; Journal of Photochemistry and Photobiology B: Biology, 2017, 171(April), 117–124

131. Parveen, S.; Sharma, G.; Sharma, S.B.; A Review on Synthesis and Biological Evaluation of Plants Based Metallic Nanoparticles. Glob J Res Rev 2021; Vol.8 No.S1: 002..

132. Naika, H.R.; Lingaraju, K.; Manjunath, K.; Kumar, D.; Nagaraju, G.; Suresh, D.; *et al*. Green synthesis of CuO nanoparticles using *Gloriosa superba* L. extract and their antibacterial activity. J Taibah Univ Sci 2015;9:7-12.

133. Foster, H.A.; Ditta, I.B.; Varghese, S.; Steele, A.; Photocatalytic disinfection using titanium dioxide: spectrum and mechanism of antimicrobial activity. Appl Microbiol Biotechnol. 2011;90(6):1847–1868.

134. Gahlawat, G.; & Choudhury, A. R.; A review on the biosynthesis of metal and metal salt nanoparticles by microbes. *RSC advances*, 2019; *9*(23), 12944–12967. https://doi.org/10.1039/c8ra10483b

135. Anirudh, K.V.S.; Bottu,M.M.V.; Sarvamangala, D.; Production of TiO2 nanoparticles by green and chemical synthesis-A short review: Volume 9, Issue 11, November-2018.

136. Priyanka, K. P.; Sukirtha, T. H.; Balakrishna, K. M.; & Varghese, T. (2016). Microbicidal activity of TiO2 nanoparticles synthesised by sol-gel method. *IET nanobiotechnology*, *10*(2), 81–86. https://doi.org/10.1049/iet-nbt.2015.0038

137. Slavin, Y.N.; Asnis, J.; Häfeli, U.O.; *et al.* Metal nanoparticles: understanding the mechanisms behind antibacterial activity. *J Nanobiotechnol* 15, 65 (2017). https://doi.org/10.1186/s12951-017-0308-z

138. Podporska-Carroll, J.; Panaitescu, E.; Quilty, B.; Wang, L.; Menon, L.; Pillai, S.C.; Antimicrobial properties of highly efficient photocatalytic TiO2 nanotubes. Applied Catalysis B: Environmental. 2015;176-177:70-75. DOI: 10.1016/j.apcatb.2015.03.029.

139. Dicastillo, C.L.; De, Correa, M.G.; We are IntechOpen , the world ' s leading publisher of Open Access books Built by scientists , for scientists TOP 1 % Antimicrobial Effect of Titanium Dioxide Nanoparticles.

140. Samavati, A.; Ismail, A.F.; Antibacterial properties of copper-substituted cobalt ferrite nanoparticles synthesized by co-precipitation method. Particuology 2016;30:158-63.

141. Mirzajani, F.; Ghassempour, A.; Aliahmadi, A.; & Esmaeili, M. A.; Antibacterial effect of silver nanoparticles on Staphylococcus aureus. *Research in microbiology*, 2011; *162*(5), 542–549. https://doi.org/10.1016/j.resmic.2011.04.009.

142. Saito, T.; Iwase, T.; Horie, J.; & Morioka, T.; Mode of photocatalytic bactericidal action of powdered semiconductor TiO2 on mutans streptococci. *Journal of photochemistry and photobiology. B, Biology*, 1992; *14*(4), 369–379. https://doi.org/10.1016/1011-1344(92)85115-b

143. Huang, Z.; Zheng, X.; Yan, D.; Yin, G.; Liao, X.; Kang, Y.; Yao, Y.; Huang, D.; & Hao, B.; Toxicological effect of ZnO nanoparticles based on bacteria. *Langmuir : the ACS journal of surfaces and colloids*, 2008; *24*(8), 4140–4144. https://doi.org/10.1021/la7035949.

144. Liu, P.; Duan, W.; Wang, Q.; & Li, X.;. The damage of outer membrane of Escherichia coli in the presence of TiO2 combined with UV light. *Colloids and surfaces. B, Biointerfaces*, 2010; *78*(2), 171–176. https://doi.org/10.1016/j.colsurfb.2010.02.024.

145. Marimuthu, S.; Rahuman, A.A.; Jayaseelan, C.; Kirthi, A.V.; Santhoshkumar, T.; Velayutham, K.; Bagavan, A.; Kamaraj, C.; Elango, G.; Iyappan, M. Acaricidal Activity of Synthesized Titanium Dioxide Nanoparticles Using Calotropis Gigantea Against *Rhipicephalus microplus* and *Haemaphysalis bispinosa*. *Asian Pacific J. Trop. Med.* 2013,*6* (9), 682–688. doi: 10.1016/S1995-7645(13)60118-2

146. Bouwmeester, H.; van der Zande, M.; & Jepson, M. A.; Effects of food-borne nanomaterials on gastrointestinal tissues and microbiota. *Wiley interdisciplinary reviews. Nanomedicine and nanobiotechnology*, 2018; *10* (1), e1481. https://doi.org/10.1002/wnan.1481.

147. Patil, S.; Chandrasekaran, R.; Biogenic nanoparticles: a comprehensive perspective in synthesis, characterization, application and its challenges. *J Genet Eng Biotechnol* **18,** 67 (2020). https://doi.org/10.1186/s43141-020-00081-3.

148. Subbarayan, P.V.; Athinarayanan, J.; Al-Hadi, A. M.; Juhaimi, F. Y. A.; Mahmoud, M.; and Alshatwi, A.; ‖Identification of titanium dioxide nanoparticles in food products: induce intracellular oxidative stress mediated by TNF and CYP1A genes in human lung fi broblast cells.‖ Environ Toxicol Pharmacol 2015; 39(1): 176-186

149. Shah, P.; Kaushik, A.; Zhu, X.; Zhang, C.; Li, C.Z.; Chip based single cell   analysis for   nanotoxicity assessment. *Analyst.* 2014;139:2088.

150. Sava, S.; Moldovan, M.; Saroşi, C.; Mesaroş, A.Ş.; Dudea, D.; Alb, C.; & Bolyai, B.; Effects of Graphene Addition on the Mechanical Properties of Composites for Dental Restoration. 2015;52:90–92.

151. Asadpour, E.; Sadeghnia, H.R.; Ghorbani, A.; Sedaghat, M.; Boroushaki, M.T.; Oxidative stress-mediated cytotoxicity of zirconia nanoparticles on PC12 and N2a cells. J Nanoparticle Res. 2016;18:14.

152. Murugadoss S.; Lison D.; Godderis L.; Toxicology of silica nanoparticles: an update. Arc Toxicol. 2017:1–44.

153. Katsumiti, A.; Gilliland, D.; Arostegui, I.; Cajaraville, M.P.; Mechanisms of toxicity of ag nanoparticles in comparison to bulk and ionic ag on mussel hemocytes and gill   cells. PloS One. 2015;10:e0129039.

154. otu E.E.; Nechifor A.C.; Poly (methyl methacrylate) with TiO2 nanoparticles inclusion for stereolitographic complete denture manufacturing—The fututre in dental care for elderly edentulous patients? J. Dent. 2017; 59:68–77. doi: 10.1016/j.jdent.2017.02.012.

155. Ammendolia, M.G.; Iosi, F, Maranghi, F.; et al. Short-term oral exposure to low doses of nano-sized TiO$_2$ and potential modulatory effects on intestinal cells. Food and Chemical Toxicology : an International Journal Published for the British Industrial Biological Research Association. 2017 Apr;102:63-75. DOI: 10.1016/j.fct.2017.01.031. PMID: 28159593.

156. Ganapathi, A.; Devaki, R.; Thuniki, N.; Manna, J.; Tirumuru, B.; Gopu ,C.; et al. In vitro assessment of Ag and TiO2 nanoparticles cytotoxicity. Int J Res Med Sci. 2014;2(4):1360.

157. Louro, H.; Saruga, A.; Santos, J.; Pinhão, M.; Silva, M.J. Biological impact of metal nanomaterials in relation to their physicochemical characteristics. Toxicol. Vitr. 2019, 56, 172–183.

158. Louro, H.; Relevance of Physicochemical Characterization of Nanomaterials for Understanding Nano-cellular Interactions. *Advances in experimental medicine and biology*, 2018; *1048*, 123–142. https://doi.org/10.1007/978-3-319-72041-8_8.

159. Setyawati, M. I.; Khoo, P. K.; Eng, B. H.; Xiong, S.; Zhao, X.; Das, G. K.; Tan, T. T.; Loo, J. S.; Leong, D. T.; & Ng, K. W. (2013). Cytotoxic and genotoxic characterization of titanium dioxide, gadolinium oxide, and poly(lactic-co-glycolic acid) nanoparticles in human fibroblasts. *Journal of biomedical materials research. Part A*, *101*(3), 633–640.https://doi.org/10.1002/jbm.a.34363

160. Chen, J.; Dong, X.; Zhao, J.; & Tang, G. (2009). In vivo acute toxicity of titanium dioxide nanoparticles to mice after intraperitioneal injection. *Journal of applied toxicology : JAT*, *29*(4), 330–337. https://doi.org/10.1002/jat.1414

161. Savi, M.; Rossi, S.; Bocchi, L.; Gennaccaro, L.; Cacciani, F.; Perotti, A.; Amidani, D.; Alinovi, R.; Goldoni, M.; Aliatis, I.; Lottici, P. P.; Bersani, D.; Campanini, M.; Pinelli, S.; Petyx, M.; Frati, C.; Gervasi, A.; Urbanek, K.; Quaini, F.; Buschini, A.; Zaniboni, M. (2014). Titanium dioxide nanoparticles promote arrhythmias via a direct interaction with rat cardiac tissue. *Particle and fibre toxicology*, *11*, 63. https://doi.org/10.1186/s12989-014-0063-3

162. Fabian, E.; Landsiedel, R.; Ma-Hock, L.; Wiench, K.; Wohlleben, W.; & van Ravenzwaay, B. (2008). Tissue distribution and toxicity of intravenously administered titanium dioxide nanoparticles in rats. *Archives of toxicology*, *82*(3), 151–157. https://doi.org/10.1007/s00204-007-0253-y

163. Braydich-Stolle, L.K.; Schaeublin, N.M.; Murdock, R.C. *et al.* Crystal structure mediates mode of cell death in TiO$_2$ nanotoxicity. *J Nanopart Res* **11**, 1361–1374 (2009). https://doi.org/10.1007/s11051-008-9523-8

164. Xia, T.; Kovochich, M.; Brant, J.; Hotze, M.; Sempf, J.; Oberley, T.; Sioutas, C.; Yeh, J. I.; Wiesner, M. R.; & Nel, A. E.; Comparison of the abilities of ambient and manufactured nanoparticles to induce cellular toxicity according to an oxidative stress paradigm. *Nano letters*, 2006; *6*(8), 1794–1807. https://doi.org/10.1021/nl061025k

165. Gratton, S.E.; Ropp, P.A.; Pohlhaus, P.D.; et al. The effect of particle design on cellular internalization pathways. *Proc Natl Acad Sci U S A*. 11618;105(33):11613–11618.

166. Sayes, C.M.; Wahi, R.; Kurian, P.A.; Liu, Y.; West, J.L.; Ausman, K.D.; Warheit, D.B.; Colvin, V.L.; Correlating nanoscale titania structure with toxicity: a cytotoxicity and inflammatory response study with human dermal fibroblasts and human lung epithelial cells.Toxicol Sci 2006, 92: 174–185. 10.1093/toxsci/kfj197

167. Mohamed, H.R. (2015). Estimation of TiO2 nanoparticle-induced genotoxicity persistence and possible chronic gastritis-induction in mice. Food Chem Toxicol 83:76–83. **https://doi.org/10.1016/j. fct.2015.05.018.**

168. Duan, Y.; Liu, J.; Ma, L.; Li, N.; Liu, H.; Wang, J.; Zheng, L.; Liu, C.; Wang, X.; Zhao, X.; Yan, J.; Wang, S.; Wang, H.; Zhang, X.; & Hong, F. (2010). Toxicological characteristics of nanoparticulate anatase titanium dioxide in mice. *Biomaterials*, *31*(5), 894–899. https://doi.org/10.1016/j.biomaterials.2009.10.003

169. Setyawati, M. I.; Khoo, P. K.; Eng, B. H.; Xiong, S.; Zhao, X.; Das, G. K.; Tan, T. T.; Loo, J. S.; Leong, D. T.; & Ng, K. W.; Cytotoxic and genotoxic characterization of titanium dioxide, gadolinium oxide, and poly(lactic-co-glycolic acid) nanoparticles in human fibroblasts. *Journal of biomedical materials research. Part A*, 2013; *101*(3), 633–640. https://doi.org/10.1002/jbm.a.34363

170. Yin, H.; Too, H. P.; & Chow, G. M.;. The effects of particle size and surface coating on the cytotoxicity of nickel ferrite. *Biomaterials*, 2005; *26*(29), 5818–5826. https://doi.org/10.1016/ j.biomaterials.2005.02.036.

171. Khade, G.V.; Suwarnkar,M.B.; Gavade, N. L.; Garadkar, K.M.; Green synthesis of TiO2 and its photocatalytic activity. J Mater Sci Mater Electron 2015; 26: 3309

172. Maddinedi, S.B.; Mandal, B. K.; Vankayala, R.; Kalluru, P.; Pamanj, S.R.; Bioinspired reduced graphene oxide nanosheets using Terminalia chebula seeds extract. Spectrochim. Acta Mol. Biomol. Spectrosc. 2015; 145: 117-124.

173. Sohal, I.S.; Cho, Y.K.; O'Fallon, K.S.; Gaines, P.; Demokritou, P.; Bello, D. Dissolution Behavior and Biodurability of Ingested Engineered Nanomaterials in the Gastrointestinal Environment. ACS Nano **2018**, 12, 8115–8128.

174. Garcia-Contreras, R.; Scougall-Vilchis, R. J.; Contreras-Bulnes, R.; Kanda, Y.; Nakajima, H.; & Sakagami, H.; Effects of TiO2 nano glass ionomer cements against normal and cancer oral cells. *In vivo (Athens, Greece)*, 2014; *28*(5), 895–907..

175. Vanajassun, P.P.; Nivedhitha M.S.; Nishad N.T.; Soman, D.; Effects of zinc oxide nanoparticles in combination with conventional glass ionomer cement: In vitro study. *Adv. Hum. Biol.* 2014;14:31.

176. Panahandeh, N.; Torabzadeh, H.; Aghaee, M.; Hasani, E.; & Safa, S.; Effect of incorporation of zinc oxide nanoparticles on mechanical properties of conventional glass ionomer cements. *Journal of conservative dentistry : JCD*, 2018; *21*(2), 130–135. https://doi.org/10.4103/JCD.JCD_170_17

177. Nonomura, Y.; Powders and Inorganic Materials. Theoretical Principles and Applications. *Int. J. Cosmet. Sci.* 2017;7:223–229.

178. Haghshenas, L.; Amini, A.; Bahati, A.B.; Rahimi, G.; In vitro Antibacterial Biofilm effect of Magnesium Oxide Nanoparticles on Streptococcus mutans. *Micro Nano Biomed.* 2016;1:21–27. doi: 10.15412/J.MNB.05010104

179. Hook, E.R.; Owen, O.J.; Bellis, C.A.; Holder, J.A.; O'Sullivan, D.J.; Barbour, M.E.; Development of a innovative antimicrobial-releasing glass ionomer cement functionalized with chlorhexidine hexametaphosphate nanoparticles. *J. Nanobiotechnol.* 2014;12:3. doi: 10.1186/1477-3155-12-3.

180. Wang, L.; D'Alpino, P. H.; Lopes, L. G.; & Pereira, J. C.; Mechanical properties of dental restorative materials: relative contribution of laboratory tests. *Journal of applied oral science : revista FOB*, 2003; *11*(3), 162–167. https://doi.org/10.1590/s1678-77572003000300002.

181. Garcia-Contreras, R.; Scougall-Vilchis, R. J.; Contreras-Bulnes, R.; Sakagami, H.; Morales-Luckie, R. A.; & Nakajima, H.; Mechanical, antibacterial and bond strength properties of nano-titanium-enriched glass ionomer cement. *Journal of applied oral science : revista FOB*, 2015; *23*(3), 321–328. https://doi.org/10.1590/1678-775720140496

182. Haghshenas, L.; Amini, A.; Bahati, A.B.; Rahimi, G.; In vitro Antibacterial Biofilm effect of Magnesium Oxide Nanoparticles on Streptococcus mutans. *Micro Nano Biomed.* 2016;1:21–27. doi: 10.15412/J.MNB.05010104.

183. Magni, E.; Ferrari, M.; Hickel, R.; & Ilie, N.; Evaluation of the mechanical properties of dental adhesives and glass-ionomer cements. *Clinical oral investigations*, 2010; *14*(1), 79–87. https://doi.org/10.1007/s00784-009-0259-3.

184. Tay, F. R.; Carvalho, R. M.; & Pashley, D. H.; Water movement across bonded dentin - too much of a good thing. *Journal of applied oral science : revista FOB*, 2004; *12*(spe), 12–25. https://doi.org/10.1590/s1678-77572004000500003.

185. Ahn, S. J.; Lee, S. J.; Kook, J. K.; & Lim, B. S.; Experimental antimicrobial orthodontic adhesives using nanofillers and silver nanoparticles. *Dental materials : official publication of the Academy of Dental Materials*, 2009; *25*(2), 206–213. https://doi.org/10.1016/j.dental.2008.06.002.

186. Vishnu Kirthi, A.; Abdul Rahuman, A.; Rajakumar, G.; et al. Biosynthesis of titanium dioxide nanoparticles using bacterium Bacillus subtilis. *Mater Lett.* 2011;65(17-18):2745-2747. doi:10.1016/j.matlet.2011.05.077

187. Swathi, N.; Sandhiya,; Rajeshkumar,S.; Lakshmi,T.; Green synthesis of titanium dioxide nanoparticles using Mulberry and its antibacterial activity. Int J Res Pharm Sci. 2019;10(2):856-860

188. Hameed, H.G.; Abdulrahman, N.A. (2023). Synthesis of TiO2 nanoparticles by hydrothermal method and characterization of their antibacterial activity: Investigation of the impact of magnetism on the photocatalytic properties of the nanoparticles. Phys Chem Res J. 2023; 11(4): 771–782. doi: https://doi.org/10.22036/pcr.2022.351688.2137.

189. ISO. ISO 9917-1: (2007). Dentistry - Water Based Cements - Part 1: Powder/Liquid Acid-Base Cements 2007 [Available from: https://www.iso.org/standard/45818.html.

190. Iliev, M.N.; Hadjiev, V.G.; Litvinchuk, A.P. Raman and infrared spectra of brookite (TiO2): Experiment and theory. *Vib. Spectrosc.* 2013, *64*, 148–152.

191. Ohsaka, T. (1980). Temperature Dependence of the Raman Spectrum in Anantase TiO2. J Phys Soc Japan. 1980;48(5):1661–1668.

192. Kwon, J. S.; Illeperuma, R. P.; Kim, J.; Kim, K. M.; & Kim, K. N.; Cytotoxicity evaluation of zinc oxide-eugenol and non-eugenol cements using different fibroblast cell lines. *Acta odontologica Scandinavica*, 2014; *72* (1), 64–70. https://doi.org/ 10.3109/00016357.2013.798871.

193. Suker,D.K.; and Albadran, R.M.; Cytotoxic Effects of Titanium Dioxide anoparticles on Rat Embryo Fibroblast REF-3 Cell Line in vitro. 2013;3(1):354-363

194. Wendt, S.L.; Ziemiecki, T.L.; Spångberg, L.S.; Indirect cytotoxic evaluation of dental materials. Oral Surgery, Oral Med Oral Pathol. 1993;75(3):353–6.

195. Fresheny, R.I.; Culture of animal cells. Amanual of Basic Technique,3rd ed. A John Wiley & sons. Ins .New York.1994.

196. Marczuk-Kolada, G.; Łuczaj-Cepowicz, E.; Pawińska, M.; Hołownia, A.; Evaluation of the cytotoxicity of selected conventional glass ionomer cements on human gingival fibroblasts. Adv Clin Exp Med 2017; 26(7):1041–5.

197. Colombo, M.; Poggio, C.; Dagna, A.; Meravini, M. V.; Riva, P.; Trovati, F.; & Pietrocola, G.; Biological and physico-chemical properties of new root canal sealers. *Journal of clinical and experimental dentistry*, 2018; *10*(2), e120–e126. https://doi.org/10.4317/jced.54548.

198. Gjorgievska, E.; Nicholson, J.W.; Iljovska, S.; Slipper, I.J.; A preliminary study of the water movement across dentin bonded to glass-ionomer cements. Acta stomatologica Croatica. 2008;42(4):326-34.

199. Reddy, K.M.; Manorama, S.V.; & Reddy, A.R.; Bandgap studies on anatase titanium dioxide nanoparticles. *Materials Chemistry and Physics,* 2003; *78*, 239-245..

200. Li, X.; Zhu, D.; & Wang, X. 2007; Evaluation on dispersion behavior of the aqueous copper nano-suspensions. *Journal of colloid and interface science*, *310*(2), 456–463. https://doi.org/10.1016/j.jcis.2007.02.067

201. Benehkohal, N.; Innovations in Electrophoretic Deposition of Nanotitania-Based Photoanodes for Use in Dyesensitizedolar Cells [PhD Thesis]. McGill University; 2013

202. Mansoor, A.; Khurshid, Z.; Khan, M.T.; Mansoor, E.; Butt, F.A.; Jamal, A.; Palma, P.J. Medical and Dental Applications of Titania Nanoparticles: An Overview. Nanomaterials2022, 12, 3670. https://doi.org/10.3390/nano12203670

203. Ingale, A. G.; and Chaudhari, A. N.; ―Biogenic synthesis of nanoparticles and potential applications: an eco-friendly approach," *Journal of Nanomedicine and Nanotechnology*, vol. 4, no. 2, 2013.

204. Khalameida, S., Skwarek, E., Janusz, W., Sydorchuk, V. & Leboda, R. Electokinetic and adsorption properties of different titanium dioxides at the solid / solution interface. **12**, (2014). doi:10.2478/s11532-014-0568-5.

205. Vijayakumar, S.; Malaikozhundan, B.; Shanthi, S.; Vaseeharan, B.; Thajuddin, N.; Control of biofilm forming clinically important bacteria by green synthesized ZnO nanoparticles and its ecotoxicity on Ceriodaphnia cornuta. Microbial Pathogenesis. 2017 Jun;107:88-97. DOI: 10.1016/j.micpath.2017.03.019. PMID: 28330748.

206. Babitha, S.; & Korrapati, P.S.; Biosynthesis of titanium dioxide nanoparticles using a probiotic from coal fly ash effluent. *Materials Research Bulletin,* 2013; *48*, 4738-4742..

207. Shahaverdi, A.R.; Fakhimi, A.; Shahaverdi, H.R.; Manaian, S. Synthesis and effect of silver nanoparticles on the antibacterial activity of different antibiotics against S. aureus and E. coli. Nanomedicine, 2007, 3(2), 168-171.

208. Patil, S.; & Chandrasekaran, R. (2020). Biogenic nanoparticles: a comprehensive perspective in synthesis, characterization, application and its challenges. *Journal, genetic engineering & biotechnology*, *18*(1), 67. https://doi.org/10.1186/s43141-020-00081-3

209. Bulcha, B.; Tesfaye, J. L.; Anatol, D.; et al. (2021). Synthesis of Zinc Oxide Nanoparticles by Hydrothermal Methods and Spectroscopic Investigation of Ultraviolet Radiation Protective Properties. *Journal of Nanomaterials.* Vol. 2021:1-10. DOI: 10.1155/2021/8617290.

210. Rajakumar, G.; Rahuman, A. A.; Jayaseelan, C.; Santhoshkumar, T.; Marimuthu, S.; Kamaraj, C.; Bagavan, A.; Zahir, A. A.; Kirthi, A. V.; Elango, G.; Arora, P.; Karthikeyan, R.; Manikandan, S.; & Jose, S. (2014). Solanum trilobatum extract-mediated synthesis of titanium dioxide nanoparticles to control Pediculus humanus capitis, Hyalomma anatolicum anatolicum and Anopheles subpictus. *Parasitology research*, *113*(2), 469–479. https://doi.org/10.1007/s00436-013-3676-9

211. Tilahun Bekele, E.; Gonfa, B. A.; & Sabir, F. K. (2021). Use of Different Natural Products to Control Growth of Titanium Oxide Nanoparticles in Green Solvent Emulsion, Characterization, and Their Photocatalytic Application. *Bioinorganic chemistry and applications*, *2021*, 6626313. https://doi.org/10.1155/2021/6626313.

212. Vijayalakshmi, R.; and Rajendran, V.; 2012. Synthesis and characterization of nano titanium dioxide via different methods. Arch. Appl. Sci., 4 (2):1183-1190.

213. Ba-Abbad, M. M.; Kadhum, A. A. H.; Mohamad, A. B.; Takriff, M. S.; Sopian, K., Synthesis and catalytic activity of TiO2 nanoparticles for photochemical oxidation of concentrated chlorophenols under direct solar radiation, *Int. J. Electrochem. Sci.* 2012, *7*, 4871- 4888.

214. Hasan, N.; Wu, H. F.; Li, Y. -H.; Nawaz, M., Two-step on-particle ionization/enrichment *via* a washing-and-separation-free approach: multifunctional TiO2 nanoparticles as desalting, accelerating, and affinity probes for microwave-assisted tryptic digestion of phosphoproteins in ESI-MS and MALDI-MS: comparison with microscale TiO2, *Anal. Bioanal. Chem.,* 2010, *396*, 2909-2919, DOI: 10.1007/s00216- 010-3573-3.

215. Roy, A.; Bulut, O.; Some, S.; Mandal, A.K.; Yilmaz, M.D.; (2019). Green synthesis of silver nanoparticles: biomolecule-nanoparticle organizations targeting antimicrobial activity. RSC Adv 9:2673–2702. https://doi.org/10.1039/ c8ra08982e

216. Landage, K. S,; Gajanan, K. A.; Khanna,P.; Bhongale, C.J.; Biological approach to synthesize TiO2 nanoparticles using Staphylococcus aureus for antibacterial and antibiofilm applications, 2020;8(1):36–43

217. Velayutham, K.; Rahuman, A. A.; Rajakumar, G.; Santhoshkumar, T.; Marimuthu, S.; Jayaseelan, C.; Bagavan, A.; Kirthi, A. V.; Kamaraj, C.; Zahir, A. A.; & Elango, G.;. Evaluation of Catharanthus roseus leaf extract-mediated biosynthesis of titanium dioxide nanoparticles against Hippobosca maculata and Bovicola ovis. *Parasitology research*, 2012; *111*(6), 2329–2337. https://doi.org/10.1007/s00436-011-2676-x.

218. Kredy, H.M. (2018). The effect of pH, temperature on the green synthesis and biochemical activities of silver nanoparticles from Lawsonia inermis extract. J Pharm Sci Res 10(2018):7–12.

219. Moosa, A.A.; Ridha, A.M.; Al-kaser M. (2015). process parameters for green synthesis of silver nanoparticles using leaves extract of aloe vera plant process parameters for green synthesis of silver nanoparticles using leaves extract of aloe vera plant. Int J Multidiscipl Curr Res 3:966–975.

220. Pugazhenthiran, N.; Anandan, S.; Kathiravan, G.; Udayprakash, N.K.; Crawford, S.; Ashokkumar, M. Microbial synthesis of silver nanoparticles by Bacillus sp. J. Nanopart. Res., 2009, 11(7), 1811-1815.

221. Gupta, R.; and Xie, H.; Nanoparticles in daily life: applications, toxicity and regulations. *J. Environ. Pathol. Toxicol. Oncol*. 2018; 37, 209–230. doi: 10.1615/JEnvironPatholToxicolOncol.2018026009

222. Parasharu K, S.a.S.A.; *"Bioinspired Synthesis of Silver Nanoparticles"*. Digest Journal of Nanomaterials and Biostructures, 2009; 4: p. 159-166.

223. Parashar, V.; Parashar, R.; Sharma, B.; and Pandey, A. C.; ―Partenium leaf extract mediated synthesis of silver nanoparticles: a innovative approach towards weed utilization," *Digest Journal of Nanomaterials and Biostructures*, vol. 4, no. 1, pp. 45–50, 2009.

224. Patra, J.K.; Baek, K. (2014). Green nanobiotechnology : factors affecting synthesis and characterization techniques, Journal of Nanomaterials Synthesis (2014). https://doi.org/https://doi.org/10.1155/(2014)/417305

225. Mubarak Ali, D.; Sasikala, M. ; Gunasekaran, M.; and Tha juddin, N. (2011). ―Biosynthesis and characterization of silver nanoparticles using marine cyanobacterium, *Oscillatoria willei* ntdm01," *Digest Journal of Nanomaterials and Biostructures*, vol. 6, no. 2, pp. 385–390.

226. Mukunthan K.S.; Balaji, S.; Cashew apple juice (*Anacardium occidentale* L.) speeds up the synthesis of silver nanoparticles. Int J Green Nanotechnol 2012;4:71-9.

227. Burda, C.; Chen, X.; Narayanan, R.; & El-Sayed, M. A.; Chemistry and properties of nanocrystals of different shapes. *Chemical reviews*, 2005; *105*(4), 1025–1102. https://doi.org/10.1021/cr030063a.

228. Khadar,A.; Behara,D.K.; Kumar,M.K.; Synthesis and Characterization of Controlled Size TiO2 Nanoparticles via Green Route using Aloe vera Extract, International Journal of Science and Research, Volume 5 Issue 11, November 2016, 1913-1916.

229. Augugliaro, V.; Coluccia, S.; Loddo, V.; Marchese, L.; Martra, G.; Palmisano, L.; & Schiavello, M. 1999; Photocatalytic oxidation of gaseous toluene on anatase TiO_2 catalyst: mechanistic aspects and FT-IR investigation. *Applied Catalysis B-environmental, 20*, 15-27.

230. Khalameida, S., Skwarek, E., Janusz, W., Sydorchuk, V., Leboda, R. & Skubiszewska-Zięba, J. (2014). Electokinetic and adsorption properties of different titanium dioxides at the solid/solution interface. *Open Chemistry*, *12*(11), 1194-1205. https://doi.org/10.2478/s11532-014-0568-5

231. Aravind, M., Amalanathan, M. & Mary, M.S.M. Synthesis of TiO_2 nanoparticles by chemical and green synthesis methods and their multifaceted properties. *SN Appl. Sci.*3, 409 (2021). https://doi.org/10.1007/s42452-021-04281-5

232. Bindhu, M.R.; Rekha, P.V.; Umamaheswari, T.; Umadevi, M. (2014). Antibacterial activities of Hibiscus cannabinus stem-assisted silver and gold nanoparticles. Mater Lett 131:194–197

233. Fattahi, F.S.; Zamani, T. (2020). Synthesis of polylactic acid nanoparticles for the innovative biomedical applications: a scientifc perspective. Nanochem Res 5(1):1–13

234. Abbai, R.; Mathiyalagan,R.; Markus,.; et al. Green synthesis of multifunctional silver and gold nanoparticles from the oriental herbal adaptogen: Siberian ginseng. Int. J. Nanomedicine. 2016;11:3131-3143

235. Khatoon, N.; Ahmad, R.; Sardar, M. (2015). Robust and fluorescent silver nanoparticles using Artemisia annua: biosynthesis, characterization and antibacterial activity. Biochem Eng J. 2015;102:91–97.

236. Senapati, S.; Ahmad, A.; Khan, M. I.; Sastry, M.; & Kumar, R.; Extracellular biosynthesis of bimetallic Au-Ag alloy nanoparticles. *Small (Weinheim an der Bergstrasse, Germany)*, 2005; *1*(5), 517–520. https://doi.org/10.1002/smll.200400053.

237. Kharissova, O.V.; Dias, H.V.; Kharisov, B.I.; Pérez, B.O.; Pérez, V.M.; The greener synthesis of nanoparticles. Trends in Biotechnology. 2013 Apr;31(4):240-248. DOI: 10.1016/j.tibtech.2013.01.003. PMID: 23434153..

238. Kharissova, O. V.; Dias, H. V.; Kharisov, B. I.; Pérez, B. O.; & Pérez, V. M.; The greener synthesis of nanoparticles. *Trends in biotechnology*, 2013; *31*(4), 240–248. https://doi.org/10.1016/j.tibtech.2013.01.003

239. Günthardt, B. F., Hollender, J., Hungerbühler, K., Scheringer, M. & Bucheli, T. D. Comprehensive Toxic Plants-Phytotoxins Database and Its Application in Assessing Aquatic Micropollution Potential. *J. Agric. Food Chem.***66**, 7577–7588 (2018).

240. Wang, J.; Zhou, G.; Chen, C.; Yu, H.; Wang, T.; Ma, Y.; Jia, G.; Gao, Y.; Li, B.; Sun, J.; Li, Y.; Jiao, F.; Zhao, Y.; & Chai, Z.; Acute toxicity and biodistribution of different sized titanium dioxide particles in mice after oral administration. *Toxicology letters*, 2007; *168* (2), 176–185. https://doi.org/10.1016/j.toxlet.2006.12.001

241. Nemmar, A.; Holme, J. A.; Rosas, I.; Schwarze, P. E.; & Alfaro-Moreno, E.; Recent advances in particulate matter and nanoparticle toxicology: a review of the in vivo and in vitro studies. *BioMed research international*, 2013; 279371. https://doi.org/ 10.1155/2013/279371.

242. Kukia, N.R.; Rasmi, Y.; Abbasi, A.; Koshoridze, N.; Shirpoor, A.; Burjanadze, G.; Saboory, E. Bio-effffects of TiO2 nanoparticles on human colorectal cancer and umbilical vein endothelial cell lines. *Asian Pac. J. Cancer Prev.* 2018, *19*, 2821–2829.

243. Ching, H. S.; Luddin, N.; Kannan, T. P.; Ab Rahman, I.; & Abdul Ghani, N. R. N. (2018). Modification of glass ionomer cements on their physical-mechanical and antimicrobial properties. *Journal of esthetic and restorative dentistry : official publication of the American Academy of Esthetic Dentistry ... [et al.]*, *30*(6), 557–571. https://doi.org/10.1111/jerd.12413

244. Topaloglu-Ak, A.; Çoğulu, D.; Ersin, N.K.; & Şen, B.H. (2012). Microhardness and surface roughness of glass ionomer cements after APF and TiF4 applications. *The Journal of clinical pediatric dentistry, 37 1*, 45-51. DOI:10.17796/JCPD.37.1.UU24059V066508G4

245. Allam, G.; & Abd El-Geleel, O. (2018). Evaluating the Mechanical Properties, and Calcium and Fluoride Release of Glass-Ionomer Cement Modified with Chicken Eggshell Powder. *Dentistry journal*, *6*(3), 40. https://doi.org/10.3390/dj6030040.

246. Buldur, M.; Sirin Karaarslan, E. (2019). Microhardness of glass carbomer and high-viscous glass Ionomer cement in different thickness and thermo-light curing durations after thermocycling aging. *BMC Oral Health* 19, 273.https://doi.org/10.1186/s12903-019-0973-4

247. Najeeb, S.; Khurshid, Z.; Zafar, M. S.; Khan, A. S.; Zohaib, S.; Martí, J. M.; Sauro, S.; Matinlinna, J. P.; & Rehman, I. U. (2016). Modifications in Glass Ionomer Cements: Nano-Sized Fillers and Bioactive Nanoceramics. *International journal of molecular sciences*, *17*(7), 1134. https://doi.org/10.3390/ijms17071134

248. Moharam, L. M.; El-Hoshy, A. Z.; & Abou-Elenein, K. (2017). The effect of different insertion techniques on the depth of cure and vickers surface micro-hardness of two bulk-fill resin composite materials. *Journal of clinical and experimental dentistry*, *9*(2), e266–e271. https://doi.org/10.4317/jced.53356.

249. Gu, Y. W.; Yap, A. U.; Cheang, P.; & Khor, K. A. (2005). Effects of incorporation of HA/ZrO(2) into glass ionomer cement (GIC). *Biomaterials*, *26*(7), 713–720. https://doi.org/10.1016/j.biomaterials.2004.03.019

250. Hepdeniz, O.K.; & Osman, G. (2021). The Effect of Titanium Dioxide Nanoparticles On Micro-hardness and SEM-EDS Analysis of Glass Ionomer Cement and Amalgomer. *Selcuk Dent. J.*628, 623–628 (2021).

251. Sakaguchi, R.; Powers, J. (2012). Craig′s restorative dental materials. 13ᵗʰ ed. Philadelphia: Elsevier Inc 2012.

252. Abbas, H.M.A.; Alhamaoy, A.R.; Salman, R.D.; Mechanical and Energy Engineering The effect of titanium oxide microparticles on mechanical properties, absorption and solubility processes of a glass ionomer cement. *J Eng*. 2020;26 (3):160-173. doi:10.31026/j.eng.2020.03.13.

253. Garoushi, S. K.; He, J.; Vallittu, P. K.; & Lassila, L. V. J.; Effect of discontinuous glass fibers on mechanical properties of glass ionomer cement. *Acta Biomaterialia Odontologica Scandinavica,* 2018; 4(1), p. 72–80.

254. Jowkar, Z.; Jowkar, M.; & Shafiei, F. (2019). Mechanical and dentin bond strength properties of the nanosilver enriched glass ionomer cement. *Journal of clinical and experimental dentistry*, *11*(3), e275–e281. https://doi.org/10.4317/jced.55522

255. Gjorgievska, E.; Van Tendeloo, G.; Nicholson, J. W.; Coleman, N. J.; Slipper, I. J.; & Booth, S.; The incorporation of nanoparticles into conventional glass-ionomer dental restorative cements. *Microscopy and microanalysis : the official journal of Microscopy Society of America, Microbeam Analysis Society, Microscopical Society of Canada*, 2015; *21*(2), 392–406. https://doi.org/10.1017/S1431927615000057

256. Lohbauer, U. (2009). Dental Glass Ionomer Cements as Permanent Filling Materials? —Properties, Limitations Future Trends. *Materials*, *3*(1), 76–96. https://doi.org/10.3390/ma3010076.

257. Smales, R.; & Joyce, K. (1978). Finished surface texture, abrasion resistance, and porosity of Aspa glass-ionomer cement. *The Journal of prosthetic dentistry*, *40*(5), 549–553. https://doi.org/10.1016/0022-3913(78)90091-4

258. Gladys, S.; Van Meerbeek, B.; Braem, M.; Lambrechts, P.; & Vanherle, G. (1997). Comparative physico-mechanical characterization of new hybrid restorative materials with conventional glass-ionomer and resin composite restorative materials. *Journal of dental research*, *76*(4), 883–894. https://doi.org/10.1177/00220345970760041001

259. Yap, A. U.; Pek, Y. S.; & Cheang, P. (2003). Physico-mechanical properties of a fast-set highly viscous GIC restorative. *Journal of oral rehabilitation*, *30*(1), 1–8. https://doi.org/10.1046/j.1365-2842.2003.01006.x

260. Kramer, P. F.; Pires, L. A.; Tovo, M. F.: Kersting, T. C.: & Guerra, S. (2003). Grau de infiltração marginal de duas técnicas restauradoras com cimento de ionômero de vidro em molares decíduos: estudo comparativo " in vitro [Microleakage between two filling restorative techniques using glass ionomer cement in primary molars: comparative "in vitro " study]. *Journal of applied oral science : revista FOB*, *11*(2), 114–119. https://doi.org/10.1590/s1678-77572003000200006.

261. Pereira, L. C.; Nunes, M. C.; Dibb, R. G.; Powers, J. M.; Roulet, J. F.; & Navarro, M. F. (2002). Mechanical properties and bond strength of glass-ionomer cements. *The journal of adhesive dentistry*, *4*(1), 73–80.

262. Bala, O., Arisu, H. D., Yikilgan, I., Arslan, S., & Gullu, A. (2012). Evaluation of surface roughness and hardness of different glass ionomer cements. *European journal of dentistry*, *6*(1), 79–86.

263. Goenka, S., Balu, R., & Sampath Kumar, T. S. (2012). Effects of nanocrystalline calcium deficient hydroxyapatite incorporation in glass ionomer cements. *Journal of the mechanical behavior of biomedical materials*, *7*, 69–76. https://doi.org/10.1016/j.jmbbm.2011.08.002.

264. Islam, I.; Chng, H. K.; & Yap, A. U. (2006). X-ray diffraction analysis of mineral trioxide aggregate and Portland cement. *International endodontic journal*, *39*(3), 220–225. https://doi.org/10.1111/j.1365-2591.2006.01077.x

265. Souza, P. P.; Aranha, A. M.; Hebling, J.; Giro, E. M.; & Costa, C. A. (2006). In vitro cytotoxicity and in vivo biocompatibility of contemporary resin-modified glass-ionomer cements. *Dental materials : official publication of the Academy of Dental Materials*, *22*(9), 838–844. https://doi.org/10.1016/j.dental.2005.10.002

266. Zanata, R. L.; Magalhães, A. C.; Lauris, J. R.; Atta, M. T.; Wang, L.; & Navarro, M. F. (2011). Microhardness and chemical analysis of high-viscous glass-ionomer cement after 10 years of clinical service as ART restorations. *Journal of dentistry*, *39*(12), 834–840. https://doi.org/10.1016/j.jdent.2011.09.003.

267. Wilson, A.D.; McLean, J.W. (1988). Glass-ionomer cements. Chicago, IL, USA: Quintessence Publishing Co. Inc., 1988.

268. Crowley, C. M.; Doyle, J.; Towler, M. R.; Rushe, N.; & Hampshire, S. (2007). Influence of acid washing on the surface morphology of ionomer glasses and handling properties of glass ionomer cements. *Journal of materials science. Materials in medicine*, *18*(8), 1497–1506. https://doi.org/10.1007/s10856-007-0128-z

269. Witten, M.L.; Shepparel, P.R.; Witten, B.L. (2012). Tungsten toxicity. Chem Bio Interact 2012 Apr 5;196(3):87–88.doi:10.1016/j.cbi.2011.12.002

270. De Barra, E.; & Hill, R. G. (2000). Influence of glass composition on the properties of glass polyalkenoate cements. Part III: influence of fluorite content. *Biomaterials*, *21*(6), 563–569. https://doi.org/10.1016/s0142-9612(99)00215-x.

271. Griffin, S. G.; & Hill, R. G. (2000). Influence of glass composition on the properties of glass polyalkenoate cements. Part II: influence of phosphate content. *Biomaterials*, *21*(4), 399–403. https://doi.org/10.1016/s0142-9612(99)00202-1.

272. Dionysopoulos, P.; Kotsanos, N.; & Pataridou, A. (2003). Fluoride release and uptake by four new fluoride releasing restorative materials. *Journal of oral rehabilitation*, *30* (9), 866–872. https://doi.org/10.1046/j.1365-2842.2003.00993.x

273. Williams, J. A.; Billington, R. W.; & Pearson, G. J. (1999). The influence of sample dimensions on fluoride ion release from a glass ionomer restorative cement. *Biomaterials*, *20*(14), 1327–1337. https://doi.org/10.1016/s0142-9612(99)00035-6.

274. Guedes, O. A., Borges, Á. H., Bandeca, M. C., Nakatani, M. K., de Araújo Estrela, C. R., de Alencar, A. H., & Estrela, C. (2015). Chemical and structural characterization of glass ionomer cements indicated for atraumatic restorative treatment. *The journal of contemporary dental practice*, *16*(1), 61–67. https://doi.org/10.5005/jp-journals-10024-1636.